THE EXTRACTION OF POWER AND FRESH WATER FROM THE OCEAN OFF THE COAST OF KZN UTILISING OCEAN THERMAL ENERGY CONVERSION (OTEC) TECHNIQUES

by

Makhosonke Gumede

A dissertation submitted in fulfilment of the requirements for
the degree of

Doctor of Engineering (Electrical Power)

(Ocean Energy Studies)

In the Faculty of Engineering and the Built Environment

Durban University of Technology

Supervisor: Dr. P. Naidoo

Technical Supervisor: Mr. F. D'Almaine

February 2021

ABSTRACT

Ocean thermal energy conversion (OTEC) is an electric power generation system which uses the temperature difference between warm water at the surface (26 ^{o}C) and cold water from the depths (5 ^{o}C) of the ocean. Generating electricity is not the only function of OTEC as it can also produce significant amounts of fresh water. This can be very important, for example on islands and in some regions, such as Port Edward, where fresh water is limited.

This thesis sets out to harness this fluidic energy, thus generating significant amounts of useful electric power for insertion into the national grid, as well as fresh water in Port Edward on the KwaZulu-Natal (KZN), South Coast. The site of Port Edward is naturally suited to the establishment of alternate energy collection sources such as OTEC; the geographical location of this region is additionally suited to the development of Open Cycle - Ocean Thermal Energy Conversion (OC-OTEC).

Port Edward lies just beneath the tropic of cancer and on the shore of the Indian Ocean thus two important elements needed for OTEC namely constant sunlight and large coastal areas can easily be found in this region. More importantly, the steep drop in water depth down to 3000 meters makes this an ideal research site for ocean thermal energy conversion in KwaZulu-Natal (KZN). If the proposed theories are correct, this can possibly be used for base generated energy capacity and fresh water.

The results are presented with reference to the temperature difference between the sea surface and the sea bottom because it is an important parameter in choosing an actual plant site and system design of OC-OTEC.

This research is mainly laboratory based concentrating on design, calculations, modelling and simulation of OC-OTEC. The thermodynamic fluid calculations were undertaken with a view to design the main mechanical components of an OC-OTEC system, i.e. flash evaporator, condenser and steam turbine. SOLID EDGE software was utilized to design OC-OTEC plant and ASPEN PLUS V8.6 software was used to simulate and model the experiment. An OC-OTEC demonstration plant was designed and constructed in an Electrical Power Laboratory at Durban University of

Technology (DUT). The experimental study was carried out on the demonstration plant with consideration given to water temperature, mass flow rate of fluid, and pressure. The measurements were taken before and after each component.

The selection of a good process modelling and simulation tool was of extreme importance for the success of this work. Throughout the measurements, we found that the thermal efficiency (%) and the power output increased with increasing temperature difference $\Delta t = t_w - t_c$. The power output was produced when the total temperature difference was sufficient to allow heat transfer within the evaporator and provide a pressure drop across the turbine.

There was more heat transfer (steam produced) in the flash evaporator at a constant flow rate because the warm water continuously supplied heat energy to the evaporator without losing much energy through the process, therefore continuous feed to the turbine improved constant power output. The thermal efficiencies were increased with increasing pressure across the turbine. The increase of pressure drops across the steam turbine caused the output power to increase. The larger flow rates of the warm water lead to higher amounts fresh water produced from the condenser.

The final step in this process was the design of the main components of a practical plant to be used as a pilot plant at a selected location on the KwaZulu-Natal South coast. This will address the problem of lack of water in the region.

DEDICATION

This Dissertation is dedicated to my sons, Lethokuhle Gumede, Zanokuhle Gumede, Khethokuhle Gumede and my parents, Mbuso Gumede and Thembi Ngidi.

I thank my parents for their support through my study years, and for the sacrifices they had to make to ensure that I achieved my dream of pursuing a career in Electrical Engineering.

God bless you all!

DECLARATION OF ORIGINAL AUTHORSHIP

I hereby declare that this dissertation represents original work by the author and has not been submitted in any form at another university. Where use has been made of the work of others, it has been duly acknowledged in the text and included in the list of references.

Makhosonke Gumede**,**

Durban, South Africa 2021

ACKNOWLEDGEMENTS

Firstly, the writer would like to thank the Lord who provided the intensity level and confidence to initiate this investigation and the ability to finish it.

"Everything is possible for him who believes. Mark 9:23"

I would wish to convey my earnest gratitude to my research supervisors, Mr. G. Frederick D'Almaine and Dr. Pat Naidoo of Durban University of Technology for monitoring progress and verifying that this research was caused in a satisfactory manner, certifying that the work was finished, and the final document completed.

I also wish to acknowledge Mr. Bussy for proof reading my thesis.

I would also like to express my appreciation to Mr. Elly Obwaka from UKZN (University of KwaZulu-Natal) for his invaluable help on ASPEN PLUS software.

Lastly, the generous financial support of this task through the channels provided by Durban University of Technology (DUT) is greatly valued.

PUBLICATIONS

1. **Gumede M**, D'Almaine F**.** Experimental Design of Possible Open Cycle OTEC Plant in KwaZulu Natal-South Coast. International Journal of Renewable Energy, Elsevier. (Under review).

2. **Gumede M**, D'Almaine F**.** Application and Design Calculation of 200kW OC- OTEC Plant in KwaZulu Natal (KZN) - South Coast. International Journal of Renewable Energy, Elsevier. (Under review).

3. **Gumede M**, D'Almaine F. The Extraction of Power and Fresh Water from the Ocean off the Coast of KZN utilizing Ocean Thermal Energy Conversion (OTEC) Techniques. 24th Southern African Universities Power Engineering Conference, 26 - 28 January 2016, Vereeniging, South Africa.

4. **Gumede M**, D'Almaine F**.** Proposal of Open Cycle-Ocean Thermal Energy Conversion (OTEC) Plant from Ocean off The Coast of KZN. International Journal of Electrical Engineering, 30 March 2017 (Under review).

5. **Gumede M**, D'Almaine F**.** Proposal of Open Cycle-Ocean Thermal Energy Conversion (OTEC) Plant from Ocean off The Coast of KZN. South Africa Institution Electrical Engineers, Eskom, Central University of Technology, Free States. Engineering Conference Proceedings, 2016.

QUANTITIES AND UNITS

A	Area for heat transfer
A_a	Area for fluid in annulus
A_F	Cross section area of coil
C	Inside diameter of the cylinder (shell)
C_p	Specific Heat Capacity of water at constant pressure
CO_2	Carbon Dioxide
D	Inside diameter of coil
D_E	Shell side equivalent diameter of coil
D_H	Average diameter of helix
d_o	Outside diameter of coil
f_{st}	Ratio of steam to warm surface seawater flow rate
G_s	Mass velocity of fluid
H	Height of the helix
H	Enthalpy
h_i	Heat transfer coefficient inside a straight tube
h_{io}	Heat transfer coefficient outside tube
J	Flux
J_H	Colburn factor for heat transfer
k	Thermal conductivity of fluid
K_c	Thermal conductivity of coil
L	Length of helical coil needed to form N turns
M	Mass flowrate of warm surface seawater
m	Mass flowrate of steam
N	Number of turns of helical coil
W	Power generation rate
N_{pr}	Prandtl number

N_{RE}	Reynolds number
Q	Heat load
R_a	Shell side fouling factor
R_t	Tube fouling factor
τ_c	Corrected log mean temperature difference
τ_{lm}	Log mean temperature difference
u	Fluid velocity
U	Overall heat transfer coefficient
P	Pressure
V	Volume
V_a	Volume of annulus
V_c	Volume occupied by N coils
V_f	Volume available for fluid flow
μ	Fluid viscosity,
μ_w	Fluid viscosity kinematic
T	Degree Celsius
L_{hev}	Specific heat of water for evaporation
α	Fraction of cold deep seawater to the turbine or condensers
β	Recycled fraction of cool seawater from C_1 condenser
ε	Efficiency
η	Dynamic viscosity
ν	Kinematic viscosity
ρ	Density
τ	Temperature of cold deep seawater

ABBREVIATIONS

DCC	Direct Contact Condenser
DoE	Department of Energy
DWA	Department of Water Affairs and Forestry
GW	Giga Watt
kW	Kilo Watt
KZN	KwaZulu Natal
MD	Membrane Distillation
MED	Multi-Effect Distillation
MSF	Multi-Stage Flash
NO_x	Nitric Oxide
NODC	National Oceanographic Data Centre
OC	Open Cycle
OTEC	Ocean Thermal Energy Conversion
OC-OTEC	Open Cycle Ocean Thermal Energy Conversion
PEM	Polymer Electrolyte Membrane
RO	Reverse Osmosis
SST	Sea Surface Temperature

TABLE OF CONTENTS

LIST OF FIGURES

LIST OF TABLES

CHAPTER 1

INTRODUCTION AND RESEARCH OVERVIEW

1. INTRODUCTION

There is a rapidly developing problem in South Africa concerning its ability to supply sufficient power and water to cover the country's ever increasing needs. This is being exacerbated by rapid expansion of local manufacturing industries, and by the broader program to supply domestic electricity to the entire population. In this research, a novel design of a thermal energy plant, for supplying fresh water and power in the south coast region of KwaZulu-Natal is proposed.

- This project is unique because it has never been implemented in Southern Africa.
- It is a unique application to generate electric power and simultaneously harvest a fresh water. It is, in effect a self-powered desalination plant.

At present, a steady provision of power and water is an important aspect of human aliveness. Currently, almost generated energy is dependent on fossil fuels and nuclear power [1], [2]. Even so, the world population is increasing at an explosive rate – and as a result, energy and water consumed by mankind are also increasing explosively [3].

Through seeing future economic growth and environmental problems, it is obvious that in the 21st century, current mainstream resources, such as petroleum, coal, and uranium cannot be relied on, for the world's energy supply [4], [5]. This is a worldwide issue, and is a serious problem when considering the repercussions such as global warming and air pollution through great carbon dioxide (CO_2) increase [6]. Therefore, the crucial problem of developing an alternative energy source to fossil and nuclear fuel must be faced:

"Energy is essential for growth; yet two billion people currently go without, condemning them to persist in the poverty trap. It is required to make clean energy supplies accessible and low-cost. It is also required to increase the role of renewable energy sources and better energy efficiency. And the issue of over consumption must be addressed - the fact that people in the developed countries use far more energy per capita than those in the emerging world" (Kofi Annan).

For alternative energy, sources such as, wind, solar and geothermal power could easily be considered. Still, Ocean thermal energy (OTEC) is an alternative that can produce substantial contributions to a solution for a sustained supply of fresh potable water, and power [7], [8], [9].

OTEC has the potential to significantly improve the techno-economic viability of regions facing a scarcity of water and high energy costs [10], [11]. Because large quantities of seawater pump through an OTEC system to generate what could be used as base load power, the proximity of the voluminous energy and water supplies allows OTEC to function efficiently and economically with typical thermal desalination processes, as well as those driven solely by electricity.

The environmental impact of desalinating seawater is quite high when using fossil fuels. Replacing the energy supply with a renewable energy source, such as OTEC, eliminates the pollution caused by fossil fuels and other problems associated with the use of fossil fuels to produce potable water.

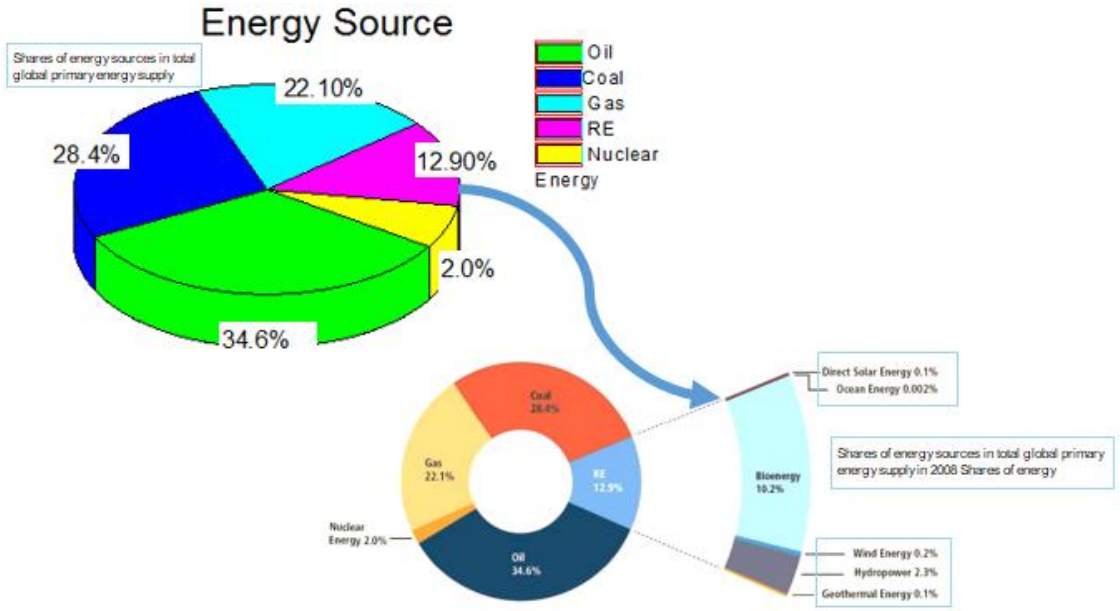

Figure 1: Shares of energy sources in total global primary energy supply in 2008 Shares of energy total and global primary energy supply [4], [12].

1.1. WATER CHALLENGES

Rapid industrial expansion and the world-wide population explosion have resulted in significant contamination of streams and lakes by industrial waste and the great amounts of sewage discharged. On a worldwide scale, man-made

pollution of natural sources of water is becoming the single largest cause of the current fresh water shortage. Water is as valuable a resource as electricity.

Deprived of fresh water, no society can function. Water is a critical element in sustainable development, and is at the core of all economies in the context of sustainable socioeconomic development and poverty eradication. The only nearly inexhaustible sources of water being the oceans and seas.

South Africa is the 30th driest country in the world [14]. Water viability has been under stress in many parts of KwaZulu-Natal (KZN) including Port Edward, as reported by the Department of Water Affairs and Forestry (DWA) [14]. Water holds a decisive function in the South African economic system where it contributes 60 % towards agriculture and irrigation. Survey 2011 recognized that 91 % of the population have admission to enhanced water sources, while 79% has access to improved sanitation (see Fig 2). Of all the global water, a mere 0.5 -1% is fresh water available for the demands of all flora, beast and human life. About 97% of water in the world is in the oceans [14].

Figure 2: Water drought in KZN [14].

To solve this water problem, desalination of water is important. Figure 3 shows the open cycle OTEC plant diagram that is proposed for South Africa on the KZN-South coast.

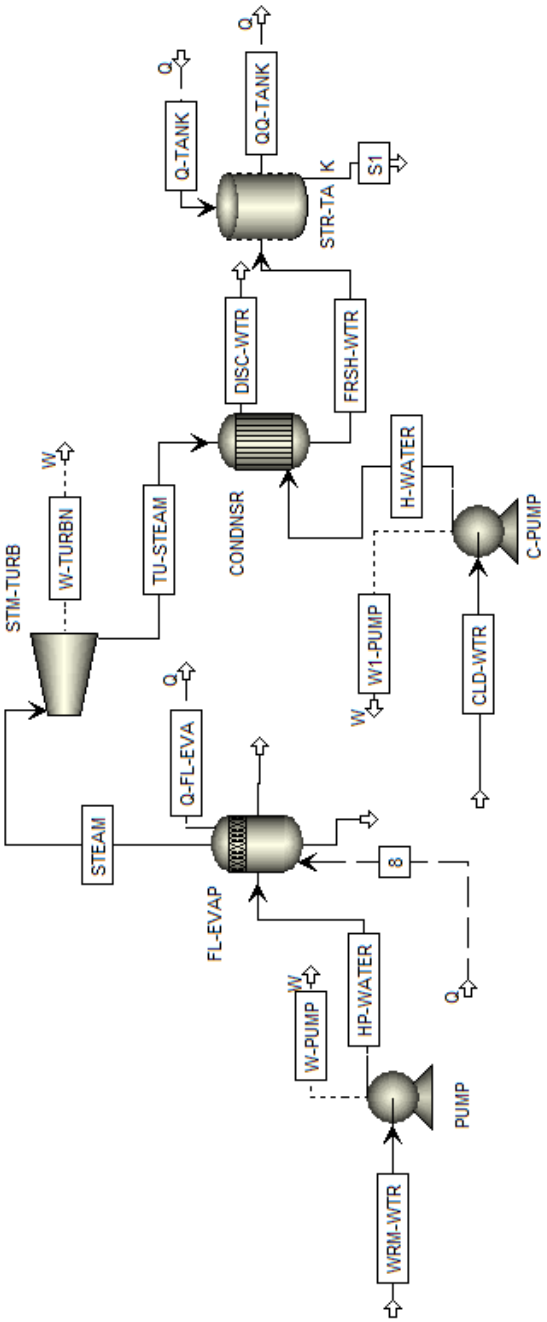

Figure 3: Design of Open cycle OTEC plant.

1.2. OPEN CYCLE OCEAN THERMAL ENERGY CONVERSION (OC-OTEC) OVERVIEW

Open cycle thermal energy conversion was initiated in 1930 by George Claude [10]. This system utilized steam evaporated directly from seawater to power a turbine. Since the seawater pressure was sub atmospheric, the steam temperature was less than the normal boiling point at atmospheric pressure. Research

conducted by Florida Solar Energy Center (FSEC) has delivered data and approaches used in a recent system study of OC-OTEC [11].

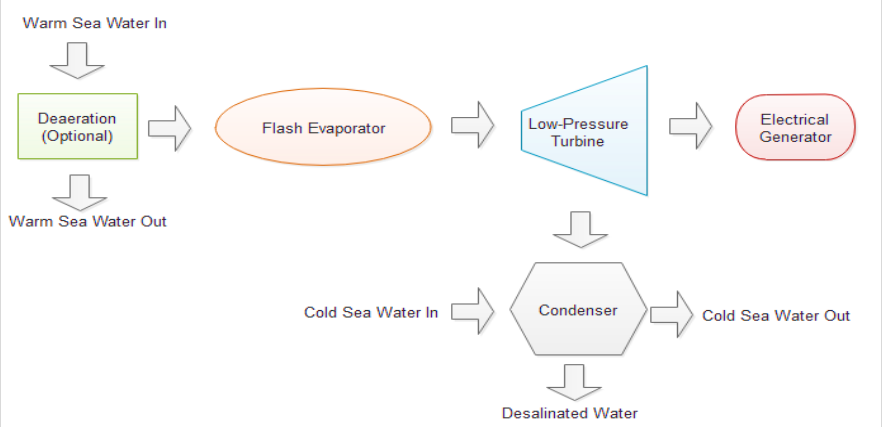

Figure 4: OC-OTEC Plant [12].

Open cycle OTEC has a distinct advantage over closed cycle OTEC systems owing to the use of a direct contact (flash) evaporator which is cheaper, smaller and more efficient than the conventional or surface evaporator required for closed cycle systems.

If fresh water is not a requirement, then direct contact condensers can also be used [13]. If fresh water is a requirement, then a surface condenser can be used in this system since the evaporator acts as a distillation unit. In this case studies have shown that the value of fresh water produced could offset the extra cost and possible performance degradation associated with its use.

Studies have shown that the most cost-effective operation utilizes a direct contact condenser in the system shown below in fig 5 [13].

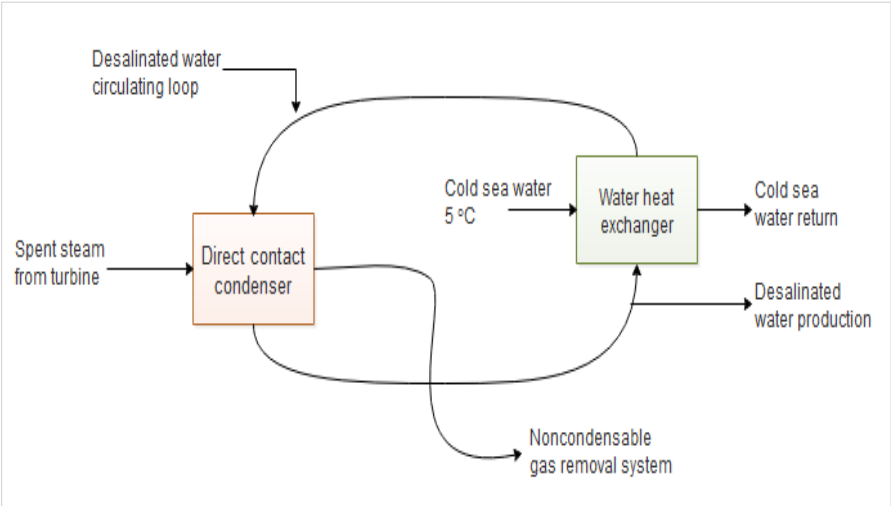

Figure 5: Purified water production scheme using condenser [13].

CHAPTER 2

LITERATURE REVIEW

2. INTRODUCTION

In the current literature, there have been numerous research and development studies conducted to investigate the performance and feasibility of the OC-OTEC system. However, an integrated system of desalination, and water production is lacking in the current literature. This research proposes an OC-OTEC system that can extract fresh water, and generate electrical supply simultaneously using an OC-OTEC system.

In this chapter, recent studies regarding different types of OTEC are presented. Thermodynamic processes of an OTEC open cycle, desalination technology, and cost of water generated by distillation plant are reviewed. The literature has been categorised based on thermal energy, previous related studies, open cycle system components, thermodynamic and economic feasibility analysis, and recent open-cycle power system studies. These are discussed and summarised.

2.1. RESEARCH DEVELOPMENTS

A suitable location for an OTEC plant location should be in a stable environment with suitable parameters for effective operation. The most important parameter is the temperature difference (Δt) at the location which has to be Δt a minimum of 20 ºC between the sea surface and the sea bed. Even if the surface temperature is very warm. OTEC might not be viable if there is a lack of a cold water heat sink.

The most suitable resources can be found in the area between 30° South and 30° North, i.e. in tropical oceans [14]. Fig 6 indicates the ∆t between water at depths of 20 m and 1km, and the locations with a temperature gradient of more than 20° C. The data presented below is for global assessments of potential OTEC resources indicating the global distribution of ∆T using data archived at the National Oceanographic Data Center. From this it is shown that the east coast of South Africa could be suitable for such a plant.

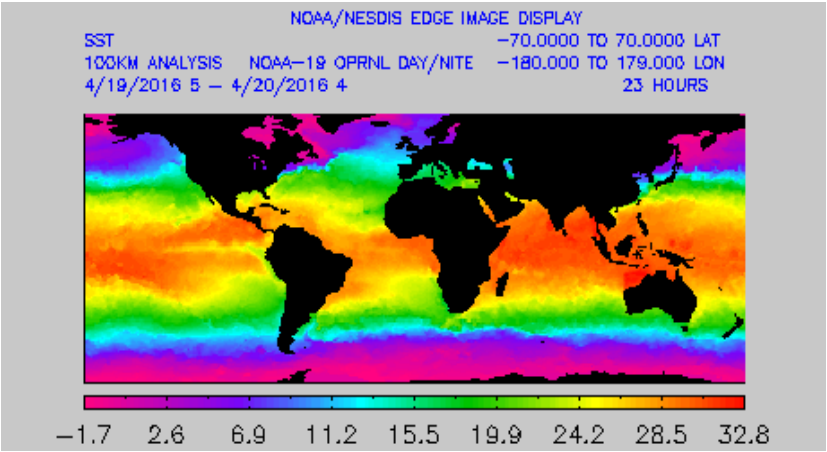

Figure 6: Global sea surface temperatures SST (Available at:http://www.ospo.noaa.gov/data/sst/fields/FS_km10000.gif. [15].

Compared to other ocean energy technologies, OTEC has certain advantages: It can provide continuous base-load power, and it can also provide fresh water for irrigation or drinking water, and cold water for refrigeration [20], [21]. Resources for ocean thermal energy conversion are more abundant than for any other type of ocean energy. It is estimated that between 30,000 and 90,000 terawatt hours (TWh)/year of power are extractable without having negative impacts on the thermal characteristics of the oceans [22], [23], and [24].

In 2011, Etemadi et al. reported that an OTEC plant works with the alteration in the middle of surface seawater and a point at a depth of one km. In the tropical countries, this temperature gradient is around of 20º C. This difference comes because the seawater temperature drops as the depth increases [27], [28], [29]. Fig 7 shows the variation of the seawater temperature with depth, where there is a temperature difference of about 20º C between the surface and a depth of 3,000 m, as is expected at Port Edward.

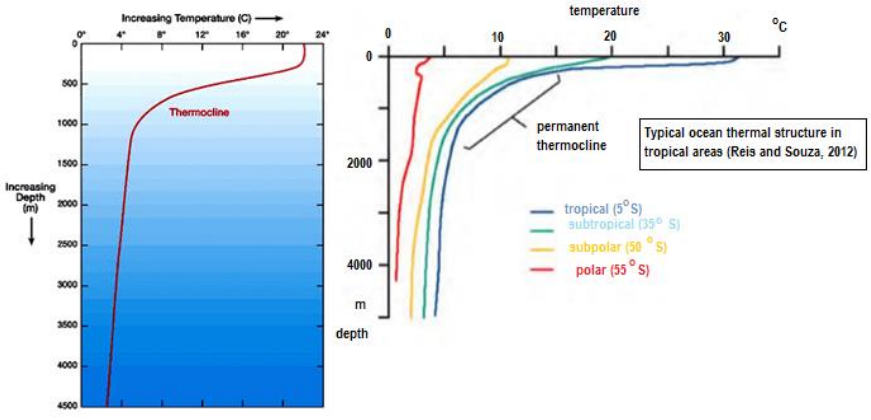

Figure 7: The temperature profile of ocean water [30], [31].

2.2. AVAILABLE OCEAN POWER ALONG THE KZN SOUTH COAST

The proposed site in KwaZulu natal (Port Shepstone to Port Edward) is naturally suited for the establishment of alternate energy collection sources such as OTEC. Since Port Shepstone is located at the coast of KZN just below the southern Tropic the two elements required: near constant sunlight and the Δt needed are present, hence its selection for this study.

OTEC sites are abundant in the southern parts of the case-study region. Off the coast of Southern KwaZulu Natal, the continental shelf is fairly close to the shore, approaching to within a few km in some places. Further, the shelf is steep dropping to a depth up to 3000 metres making this area suitable for investigation for OTEC in KZN. Maritime maps of the coast of KZN indicate possible sites where the continental shelf is suitably close the shore.

The University of Hawaii has tested this technology and obtained a significant volume of desalinated water [18] which can help the countries that have a problem with water such as South Africa. The figure 8 below shows the proposed site for Open Cycle OTEC.

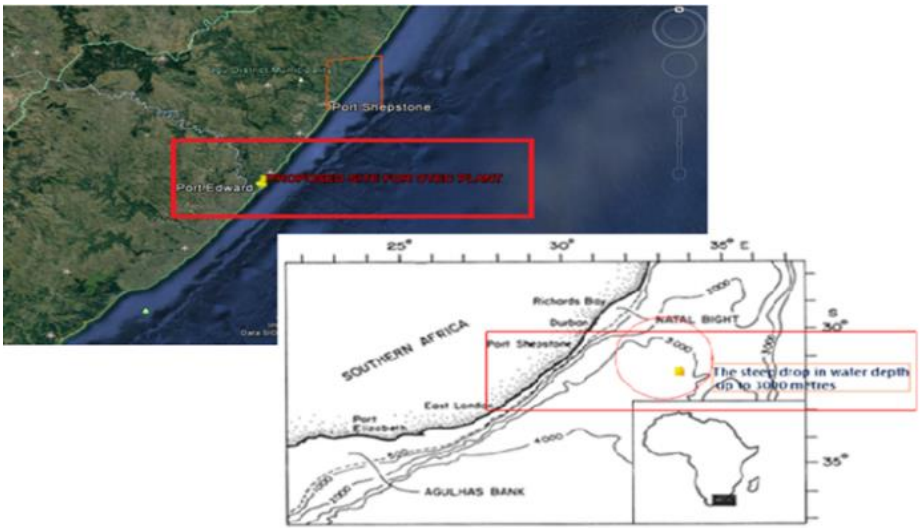

Figure 8: The propose site for Open Cycle OTEC.

TABLE 1: TEMPORAL VARIABILITY, PREDICTABILITY AND RANKING CRITERIA OF THE OCEAN ENERGY RESOURCES [38]

	Wave power	**OTEC**	**Tidal barrages**	**Tidal current turbines**	**Ocean current power**	**Solar PV**	**Wind power**
Temporal variability	Daily &seasonal	Seasonal	Hourly & weekly	Hourly & weekly	seasonal	Hourly & weekly	Hourly & weekly
Predictability	Moderate	High	High	High	High	Moderate	Low
Ranking criteria high	≥ 25kWm^{-1}	≥20∆T, ≤ 5km	≥5m mean tidal range	≥2ms^{-1} peak speed	≥1.5m^{s-1} seasonal average speed	≥5.5kWh m^{-2} d^{-1}	≥5.5ms^{-1}
Conditional	15-25 5kWhm^{-}	≥20∆T, ≤ 10km	24-5m mean tidal range	≥1.5ms^{-1} peak speed	1-1.5 ms^{-1} seasonal average speed	3-5.5kWh m^{-2} d^{-1}	4-5. 5ms^{-1}

2.3. LAND BASED ELECTRICAL INFRASTRUCTURE

Any offshore generating station will require a land based substation to collect the energy, transform it into a form suitable for insertion into the grid, and then connect it to the grid. This substation must take into consideration any sensitivities concerning the local habitat and population. A substation could be camouflaged relatively easily to blend in with the area, but injection of the harnessed energy to the grid would have to be either by overhead line (unsightly) or by underground cable (expensive), so this would have to be factored into a final design. It is also essential for Eskom's existing and planned infrastructure to be considered when identifying a suitable site for an offshore generating station. The figures below indicate present and future planned Eskom transmission lines for KwaZulu-Natal.

In the Durban area, transmission extends southward to Illovo on the coast and in the south of the province; there is also a planned line extending to the coast at St Faiths. There are, however, rural networks up and down the coast of KZN, and further investigations could be undertaken into the possibility of strengthening or adapting these for use on this project.

Cognisance must also be taken of the fact that the south coast from Durban down to Port Shepstone and beyond is a built-up area, and suitable sites for a substation could prove difficult to identify.

Fig 9 shows the existing (2012) electrical infrastructure in KZN [39] where it can be seen that an 88-kV transmission line runs down the coast to past Marina Beach. This line, if it is electrically strong enough, could be ideal for connecting to the OC-Cycle OTEC generating station.

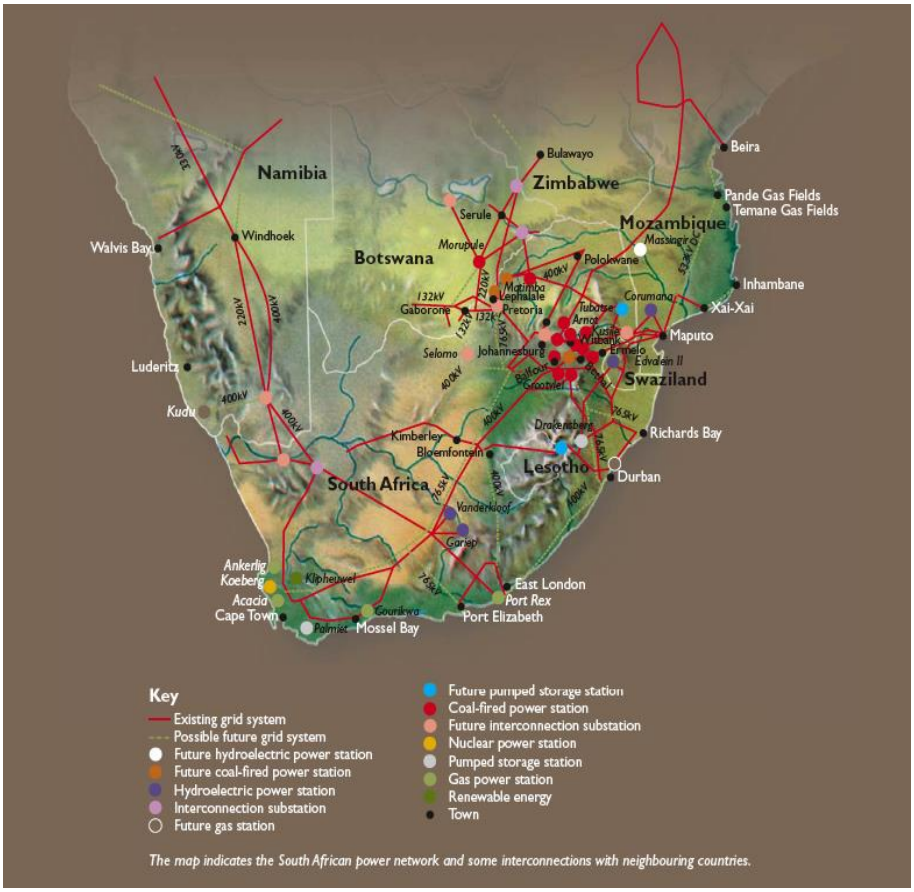

Figure 9: Eskom's existing infrastructure in SA [39].

It is also essential for Eskom's existing and planned infrastructure to be considered when identifying a suitable site for an offshore generating station. Figure 10 below indicates Eskom's present and future planned transmission lines for KwaZulu-Natal.

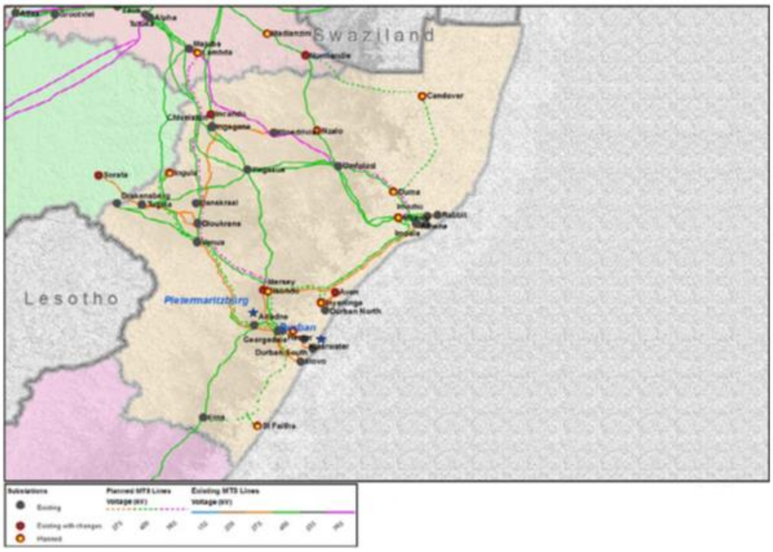

Figure 10: Eskom's future development plans for KZN [40].

2.4. Assessment Of Oc-Otec Resources In South Coast

The accessible OTEC temperature difference between surface and deep ocean waters, ΔT is distributed between the foremost components of a power plant: one half across a power generating turbine, as recommended from modest optimization measures, and the balance to permit surface seawater to cool down in an evaporator and deep seawater to warm up in a condenser.

Figs 11 and 12 illustrate a minimum approach (pinch) temperature $\Delta T/16$ (of the order of 1 °C) in either evaporator or condenser. This is imposed to maintain the exchange of heat. The thermodynamic efficiency of such a typical OTEC power cycle is $\varepsilon_{tg}\Delta T/(2T)$, where T is the surface water temperature and ε_{tg} thturbogenerator efficiency possibly as high as 0.85 [28], [41].

Figs 15 and 16 illustrate a minimum approach (pinch) temperature $\Delta T/16$ (of the order of 1 °C) in either evaporator or condenser. This is imposed to maintain the exchange of heat. The thermodynamic efficiency of such a typical OTEC power cycle is $\varepsilon_{tg}\Delta T/(2T)$, where T is the surface water temperature and ε_{tg} thturbogenerator efficiency possibly as high as 0.85 [28], [41].

The tiny amount of energy lost through the OTEC process can be considered negligible, e.g., when defining the OTEC temperature ladder in an overall enthalpy balance of the seawater currents. The information shown below is for global assessments of potential OTEC resources showing the worldwide distribution of ΔT using data archived at the National Oceanographic Data Center (NODC) [28].

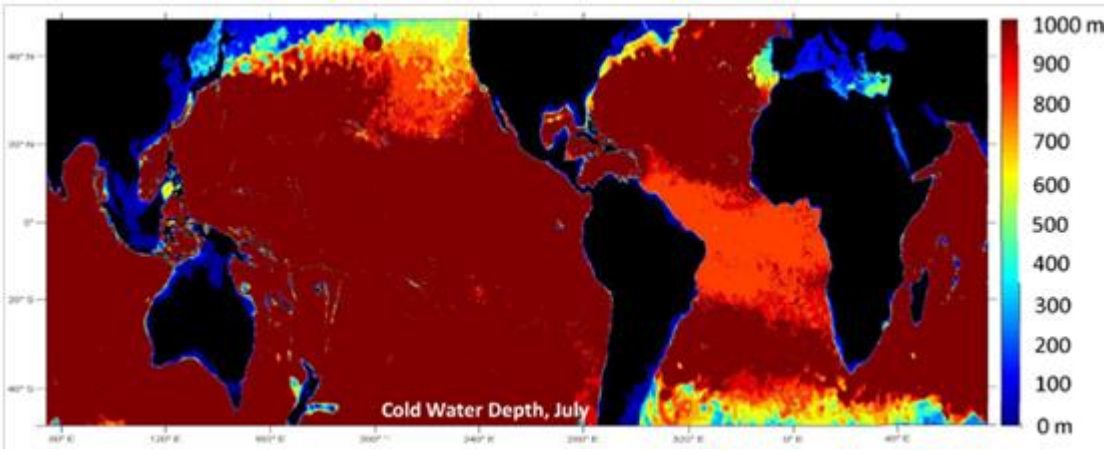

Figure 11: Cold water depth based on HYCOM data [28], [30].

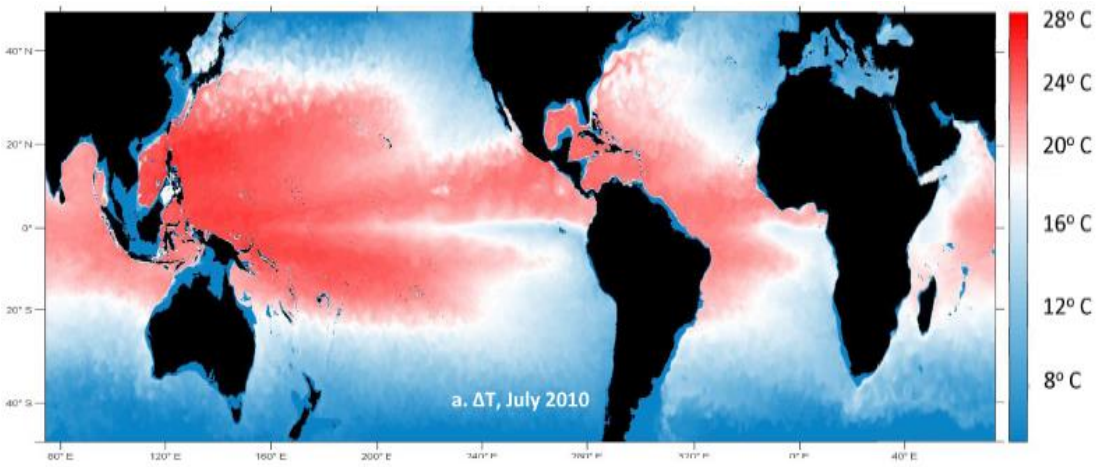

Figure 12: Cold water depth based on HYCOM data [28], [30].

2.5. OC-OTEC: EFFICIENCY

The overall efficiency of an OC-OTEC system is given by the following equation:

$$\eta = \frac{P_{in}}{\dot{Q}_{in}} \tag{2.1}$$

where P_n is the net power and $\dot{Q}_{in}$ is the rate of heat transfer into the system [20]. The potential efficiency of an OC-OTEC is higher than close cycle since a greater portion of the temperature change is available to produce power. In addition, it can also be used to provide drinking water. According to a system analysis done in 1985, the condenser surface area of a plant producing 2 MWe of net power can generate approximately 4300 cubic meters of purified water each day [21].

Whilst OC-OTEC does have a higher efficiency potential, the technology required is not yet established. That is, OC-OTEC systems are not yet economically feasible. Todd Taniguchi reported that the Research and Development of OC-OTEC systems have been stalled because of foreseeable problems with developing the technology on a commercial scale. As mentioned above, no OC-OTEC system has been designed or built because of the large turbine sizes required [22]. This project mitigates against these constraints by concentration mainly on water production this reducing the size of generator required if used for pure energy production.

2.6. OTEC RESEARCH OVERVIEW

Novel technologies for the extraction of valuable ocean resources have become significant following the increasing scarcity of other relatively cheap sources, i.e. oil [51], [52]. Furthermore, global warming has shown the disadvantage of using other fossil fuels such as coal [53], [54], [55]. Any alternative to coal fired power stations in South Africa would lead to a large saving in carbon based pollution.

A white paper, circulated by Department of Minerals and Energy, indicates that the South African Government is committed to ensuring that renewable energy, including wind, solar, and ocean energy becomes a significant part of its energy portfolio.

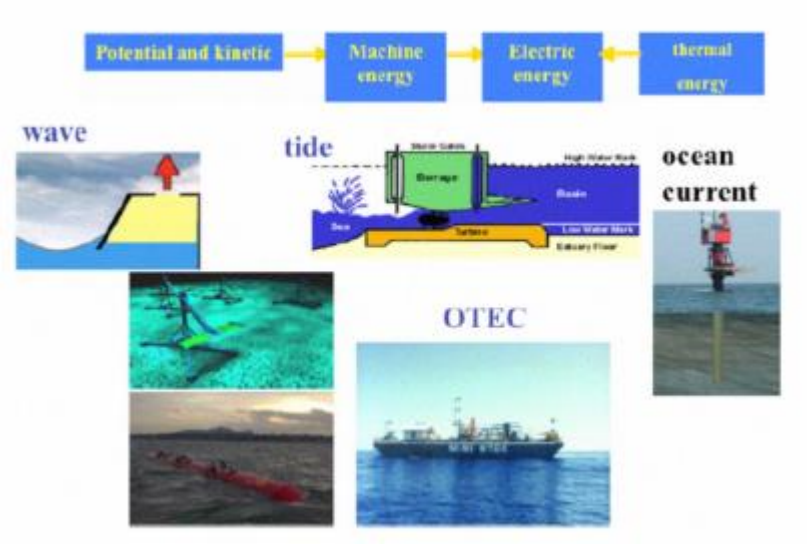

Figure 13: Ocean energy power system diagram [55].

Figure 13 further categorises ocean energy into its component parts such as ocean currents, tidal currents, wave energy, thermal energy, and energy derived from differences in salinity.

2.7. Related Research

2.7.1. Tidal Currents

Tides are created by the sun and the moon in mixture with Earth's rotation. They interact via gravitational forces. This is what tidal energy generators use to produce energy.

It is well known that if the water level is higher and/or tidal currents are faster, the potential will be greater to obtain a larger amount of energy.

Tidal energy, also called tidal power, is considered a clean, renewable energy because during its transformation no pollutant substances are produced [56], [57]. It is a form of hydropower that uses an alternator to transform tidal energy into electricity [58]. This is not an option for South Africa as the local tidal range is only in the region of 1 to 2 M.

2.7.2. Wave Energy

The renewable energy system of power generated by sea waves has the most concentrated energy potential. These systems are based on the kinetic energy of the sea waves [59]. The wind generated by the sun transmits its energy to the

waves which is then gathered, stored, and transmitted along the oceans [60], [61]. Once created, wind waves can travel extremely far (thousands of kilometers) with very little energy losses. This happens if they don't encounter head winds, which will make them lose energy due to friction. Also, it must be noted that near the coast, the wave energy intensity decreases because of the interaction with the seabed, although this fact can be compensated for by phenomena such as refraction or reflection. This system of energy harvesting, while suitable for the Cape, is not optimal for the KZN South Coast as the average wave height is not high enough for commercial energy production.

2.7.3. OCEAN CURRENT

An ocean current is the constant flow of oceanic water in a relatively fixed direction. In KwaZulu-Natal the Agulhas Current flows relatively close to the coastline. It has been identified as one of the five Major Ocean Currents in the world based on the power, speed, and consistency at which they flow. The current energy can be calculated using the formula of kinetic energy of flowing bodies:

$$KE = 0.5.\rho V^3 \tag{2.2}$$

Where the kinetic energy KE, is proportional to the density ρ, and proportional to the cube of the velocity V. [62]. The velocities of ocean currents around the world are typically more than five knots or 2.5m/s (1 knot=0.50 m/s) and current energy has been estimated greater than 5,000 GW, with power densities of up to 15 kW/m² [63].

The power that can be extracted from a flowing mass depends on the interaction between the devices used to extract the energy. The following rearrangement of the formula for kinetic energy is shown above [64]:

$$\left(\frac{P}{A}\right) = \frac{1}{2}\rho V^3 \tag{2.3}$$

The power flux from ocean currents depends on the cross-sectional area of the flow intercepted by a device A (in m^2). Additionally, this depends on P (the water density) and V (the current speed measured in meters per second) [65].

This technology is very suitable for the Coast of KZN and is presently being explored by d'Almaine and Gumede. Although the technology does not yet exist for dedicated ocean current turbines, Tidal turbines can be adapted to this use. The fundamental difference between tidal and ocean currents, apart from the fact that a tidal current reverses every 6 hours, is the depth of the seafloor at which these systems operate. A tidal system typically operates at depths between 20 and 40M whilst ocean current systems will typically be operated at seafloor depths of 100 to 200m. This poses interesting engineering challenges which can be overcome using technology developed for the offshore oil industry.

2.7.4. OCEAN THERMAL ENERGY CONVERSION (OTEC)

Considering the above, this thesis examines the thermal energy resource and, more specifically, the Ocean Thermal Energy Conversion off the coast of KwaZulu-Natal.

OTEC development has been dormant for a long time, given that it was first proposed in 1881 [66]. However, it has now regained recognition worldwide as a realistic solution to our world energy issue. Ocean Thermal Energy Conversion alone can meet the world energy demands, as observed from the world energy used in the year 2010. In 2003, Vega stated that the amount of solar energy absorbed by the oceans in a year is equivalent to at least 4000 times the amount currently consumed on Earth [67], [68], [69]. From an OTEC efficiency of 3% in converting ocean thermal energy to electricity, we would need less than 1% of this renewable energy to satisfy the world demand [70].

Since OTEC uses natural energy from the oceans, no greenhouse gases are emitted and other pollution is minimal. Furthermore, OTEC is an environment-friendly and semi-permanent energy source [71], [72]. Conversely, a steady output is difficult to obtain because of the change in water temperature through the days and seasons. Hence, the thermal efficiency of the OTEC is rather low (about 5-6%) compared with commercial thermal plants (about 40-50%) [73].

Figure 14: 210 kW OC-OTEC experimental apparatus (1993–1998) [101].

The attractiveness of OTEC is the seemingly limitless energy of the hot surface water in relation to the cold deep water and its potential for constant, base load, extraction [75]. Even for heating, warm seawater cannot be utilised on land due to its high salt content. Moreover, large volumes of seawater need to be pumped, so reducing the net energy generated and requiring large pipes and heat exchangers.

Winter reported that OTEC has the least environmental impact and is capable enough to provide thousands of megawatts of power, which are urgently required in developing countries [78]. OTEC usually incorporates a low- temperature Rankine cycle engine which boils a working fluid such as ammonia to generate a vapour, which turns the turbine to generate electricity, and then is condensed back into a liquid in a continuous process [79], [80].

OTEC can produce fuels by using electricity to produce hydrogen, which can be used in hydrogen fueled cars as well as in the development of synthetic fuels [81], [82], [83], [84]. For a small city, millions of tons of carbon dioxide are generated annually through fossil fuel use - while with OTEC, this value is zero [84].

Hoffert reported that OTEC has the potential to replace some fossil fuel use [85]. An OTEC system utilizes low-grade energy and has a low energy efficiency (approximately $(3 \text{ to } 5\%)$ [86]. Therefore, achieving a high electricity generating capacity with OTEC requires the use of large quantities of seawater, and a

correspondingly, a large amount of pumping power. Although OTEC has a low energy density, the thermal energy in the ocean is extremely abundant.

2.8. OPEN CYCLE OTEC OVERVIEW

D'Arsonval produced the concept that was presented in 1879 when the state of Hawaii and a pool of U.S. companies raised more than 50 kW of gross power, with a net output of upwards to 18 kW from a small OTEC plant mounted on a barge off Hawaii [87], [88], [89]. Subsequently, a 100-kW gross power, land-based plant was operated in the island country of Nauru by a syndicate of Japanese companies [90], [91].

These plants were operated for a few months to demonstrate the concept. They were too minor to be scaled to commercial-size organizations. Since then, the US Department of Energy [100], [101], [102], [103] and researchers at Saga University in Japan have done extensive testing of heat exchangers and have conducted research using ammonium hydroxide-water mixture as the working fluid [104], [105].

Decades after D'Arsonval, Georges Claude, another French inventor, proposed to use the ocean water as the working fluid [100], [106]. [107]. In Claude's cycle, the surface water is flash-evaporated in a vacuum chamber [108]. The resulting low-pressure steam is used to drive a turbine-generator, and the relatively colder deep seawater is used to condense the steam after it has passed through the turbine.

This cycle can, therefore, be configured to produce desalinated water as well as electricity [100]. Claude's cycle is also referred to as open cycle OTEC (OC-OTEC) because the working fluid flows once through the system. In 1930, Claude demonstrated this cycle in Cuba with a small land-based plant making use of a direct contact condenser (DCC). Therefore, desalinated water was not a by-product.

The plant failed to achieve net power production because of poor site selection (thermal resource) and a mismatch of the power and seawater systems. However, the plant operated for several weeks [100], [102], [109], [110] [111].

Claude, subsequently, designed a 2.2 MW floating plant for the production of up to 2,000 t of ice (this was prior to the wide availability of household refrigerators)

for the city of Rio de Janeiro in Brazil. Claude housed his power plant in a ship (i.e., a plantship), about 100 km offshore [100], [112].

Unfortunately, he failed in his numerous attempts to install the long vertical cold water pipe (CWP) required to transport the deep ocean water to the ship and had to abandon his enterprise in 1935 [101], [113]. His failure can be attributed to the absence of the offshore industry, and ocean engineering expertise presently available. His biggest technological challenge was the at-sea installation of a CWP.

This situation is markedly different now that there is a proven record of the installation of several pipes during experimental operations [100], [114]. The next step toward answering questions related to the operation of OTEC plants was the installation of a small OC-OTEC land-based experimental facility in Hawaii (Fig. 22).

The turbine-generator was designed for an output of 210 kW for 26°C warm surface water and a deep-water temperature of 6°C. 10 %. A small fraction of the steam produced was diverted to a surface condenser, for the production of desalinated water. The experimental plant successfully operated for 6 years (1993-1998), during which time the highest production rates achieved were 255 kW (gross) with a corresponding net power of 103 kW and 0.4 L/s of desalinated water. These are world records for OTEC [100], [101], [114].

A two-stage OTEC hybrid cycle, where electricity is produced in a closed cycle first-stage followed by water production in an open cycle second-stage, has been proposed in order to maximise the use of the thermal resources available to produce water and electricity [115], [116]. In the second stage, the temperature difference available in the seawater effluents from an OTEC plant is used to produce desalinated water through a system consisting of a flash evaporator and a surface condenser (in simple terms, an open cycle without a turbine-generator) [117], [118]. In the case of an open cycle plant, the addition of a second stage results in doubling water production.

The use of the cold deep water as the chiller fluid in air conditioning (AC) systems was proposed and implemented by Vega [119]. It has been demonstrated that these systems can provide significant energy conservation independent of OTEC [7].

OTEC energy could be transported via chemical, thermal, and electrochemical carriers. The technical evaluation of nonelectrical carriers leads, for example, to the consideration of hydrogen produced using electricity and desalinated water generated with OTEC technology. The product would be transported from the OTEC plantship located at distances of about 1,500 km offshore [39], [100], [120], [121], [122].

A 100 MW-net plantship can be configured to use electrolysis to yield 1,300 kg/h of liquid hydrogen [119], [123], [124]. Unfortunately, the production cost of liquid hydrogen delivered to the harbour would be equivalent to at least $300 per barrel of crude oil (approximately four times present cost).

2.8.1. THE OC-OTEC EXPERIMENTAL APPARATUS

The relationships between power production and the system control parameters were established experimentally. From the perspective of the overall system, the control parameters are the flow rate of warm water, the flow rate of cold water, and the compressor subsystem setting as given, for example, by the inlet pressure. The other control parameters are set by seasonal variations of seawater temperature and cannot be set by the operator [125], [126].

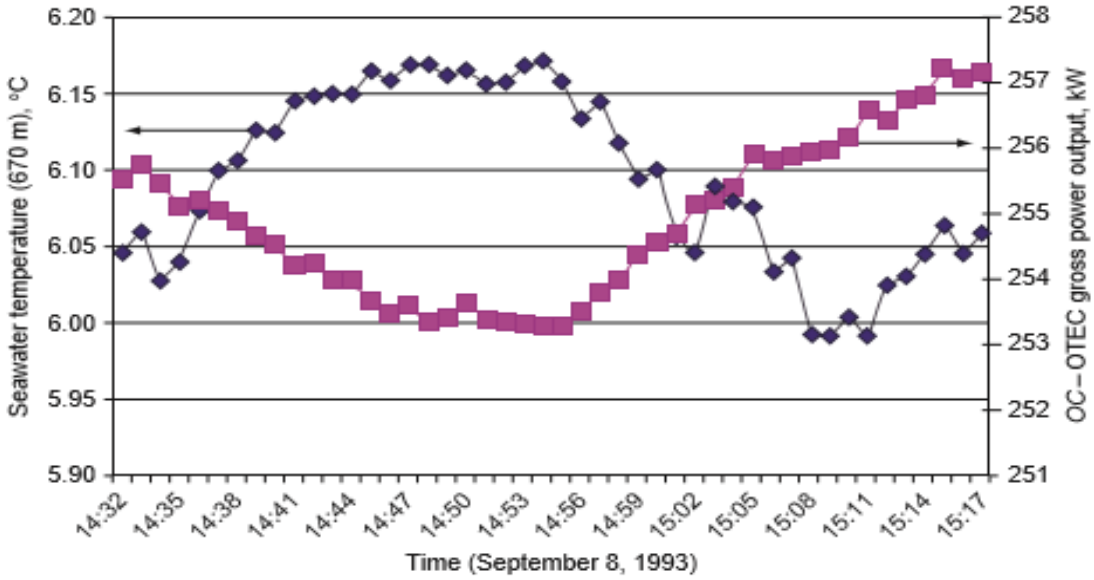

Figure 15: 210 kW OC-OTEC experimental apparatus: power output varies as a function cold-water temperature [100], [101].

Figure 15 depicts the effect in gross power output as the cold-water temperature varies. The power increases as the temperature decreases with all other control

parameters constant. The unexpected oscillation in cold-water temperature depicted in Figure 15 is induced by internal waves of periods in the order of 1 hour with corresponding wave lengths of approximately 3,500 m, and 50 m height [102]. The power output as a function of warm-water temperature, with all other control parameters constant is shown in Figure 16.

The relationship depicted in Figure 16 is clear; it is interesting to note that the temperature variations shown, by means of the 1 min averages of surface water temperature (20 m depth) sampled once per second, are apparently caused by a warmer water mass intrusion that could have been driven by an ocean gyre of the kind observed in coastal regions close to channels (in this case the Alenuihaha Channel between Maui and the Big Island of Hawaii). Data records like these were used to establish that the variation of power output with seawater temperature is approximately 34 kW/°C at power levels of about 200 kW [90], [100].

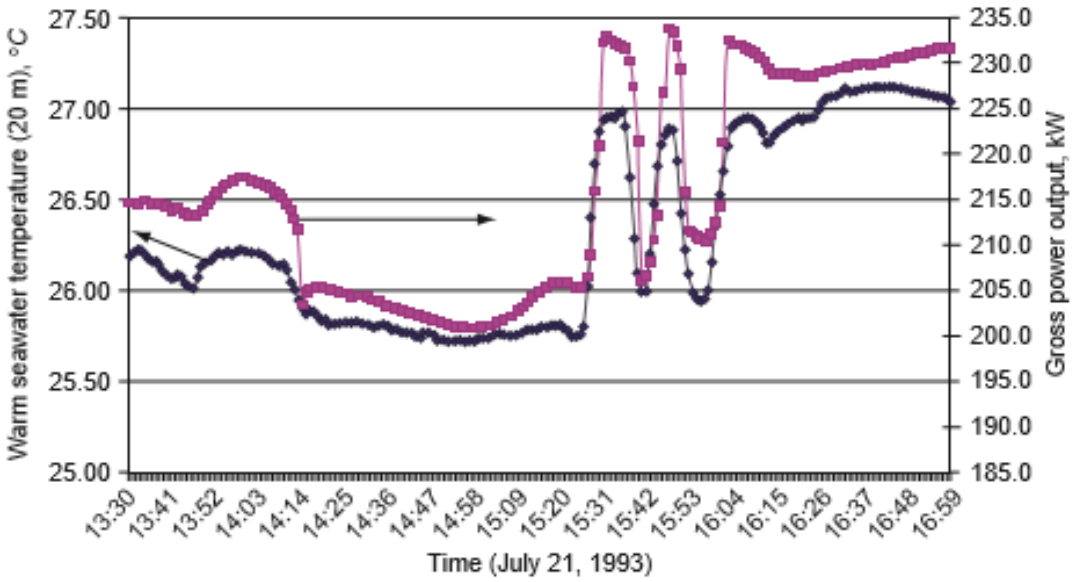

Figure 16: 210 kW OC-OTEC experimental apparatus: Power output variation as a function warm-water temperature [100], [101].

2.8.2. OPEN CYCLE OTEC DESCRIPTION

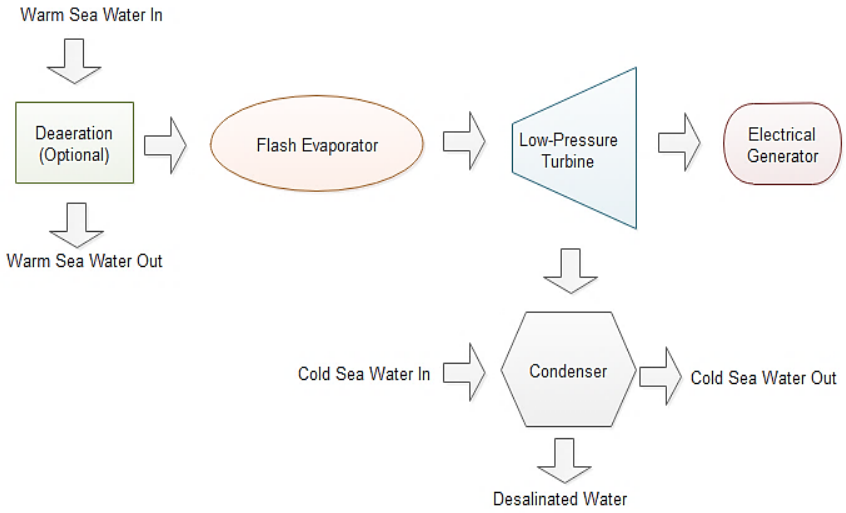

Figure 17: OC-OTEC layout.

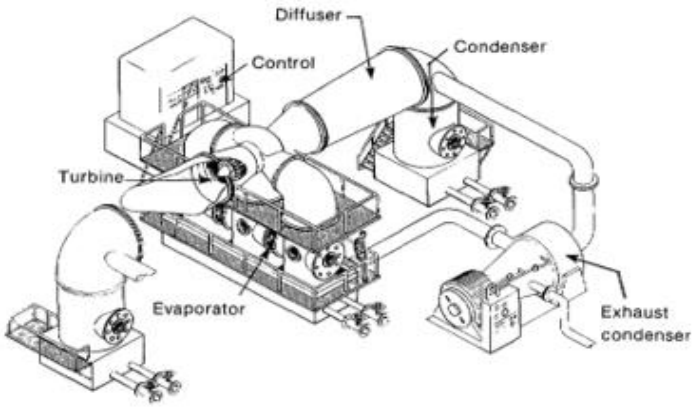

Figure 18: Conceptual layout of a 165kW experiment [127].

The open cycle consists of the following steps [127], [128], and [129]:

- Flash evaporation of a fraction of the warm seawater by reduction of pressure below the saturation value corresponding to its temperature. The evaporator determines the warm seawater flowrate from the steam temperature, water inlet temperature, and the evaporator effectiveness, defined as:

The steam temperature is slightly higher than the turbine inlet temperature due to the pressure drop through a mist removal from evaporator. The pressure drop is calculated from an input pressure loss coefficient [129]. Heat addition at the evaporator is equal to the heat lost by warm seawater. Overall heat transfer

coefficient and effective surface area of the evaporator is correlated with the heat addition rate.

where ΔT is the logarithmic mean temperature difference across the evaporator. expansion of the vapor through a turbine to generate power;

- heat transfer to the cold seawater thermal sink resulting in condensation of the working fluid; and
- compression of the non-condensable gases (air released from the seawater streams at the lowest operating pressure) to pressures required to discharge them from the system.

These steps are depicted in Figure 18 above. In the case of a surface condenser, the condensate, or desalinated water, must be compressed to pressures required to discharge it from the power generating system [74], [130]. Vega reported that the evaporator, turbine, and condenser operates in partial vacuum ranging from 3% to 1% atmospheric pressure.

This poses several practical concerns that must be addressed which are [74]:

- The system must be carefully sealed to prevent the ingress of atmospheric air that can severely degrade or shut down operation.
- The specific volume of the low-pressure steam is very large compared to that of the pressurized working fluid used in closed cycle OTEC.

Vega reported that components must have large flow areas to ensure that steam velocities do not attain excessively high values. Finally, gases such as oxygen, nitrogen and carbon dioxide that are dissolved in seawater (essentially air) come out of solution in a vacuum [74], [101], [103].

These gases are uncondensable and must be exhausted from the system. Despite complications, the Claude cycle provides certain benefits from the selection of water as the working fluid [103]: Water, unlike ammonia, is non-toxic and environmentally benign. Moreover, since the evaporator produces desalinated steam, the condenser can be designed to yield fresh water [74], [131]. In 2013, Luis reported that many potential sites in the tropics, potable water is a highly-desired

commodity that can be marketed to offset the price of OTEC-generated electricity [15], [101].

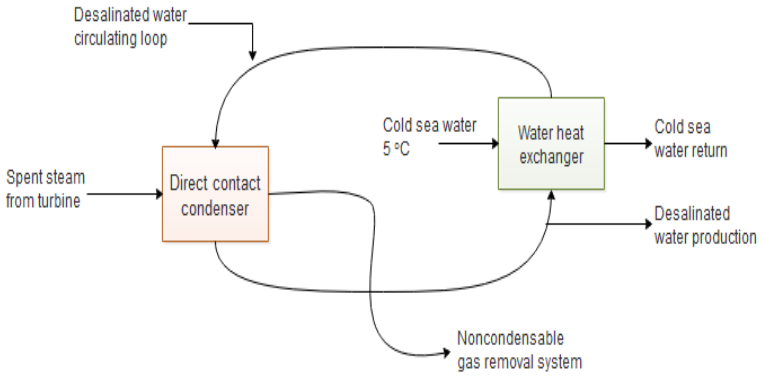

Figure 19: Desalinated water production scheme using direct contact condenser [15].

Bharathan stated that the flash evaporation is a distinguishing feature of open cycle OTEC. Flash evaporation involves complex heat and mass transfer processes [132], [133], [134], [135], [136]. Figure 20 depicts the results of the configuration tested by a team lead by the Vega where warm seawater was pumped into a chamber through spouts designed to maximise the heat and-mass-transfer surface area by producing a spray of the liquid [101].

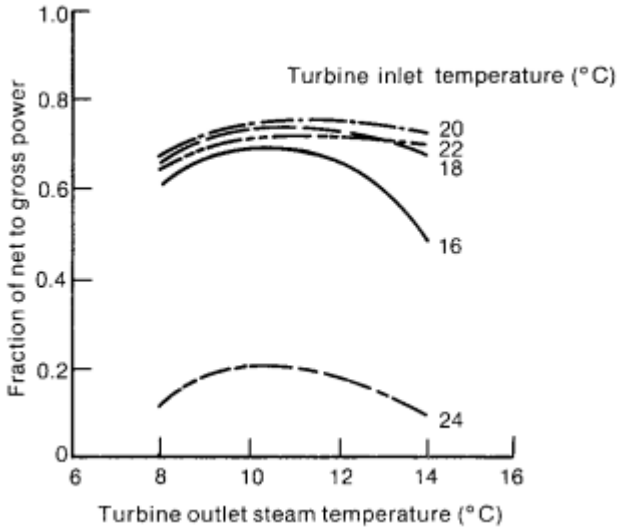

Figure 20: Difference of Net power fraction with turbine inlet and outlet steam temperatures of 5MW shore base system [137].

Here the pressure in the chamber (2.6% of atmospheric) was less than the saturation pressure of the warm seawater [130], [137]. Exposed to this low-pressure environment, water in the spray began to boil. As in thermal desalination plants, the

vapor produced was relatively pure steam [138]. As steam is generated, it carries away with it its heat of vaporization [137].

This energy comes from the liquid phase and results in a lowering of the liquid temperature and the cessation of boiling. Thus, as mentioned above, flash evaporation may be a transfer of thermal energy from the bulk of the warm seawater to the small fraction of the mass that is vaporized to become the working fluid. Approximately 0.5% of the mass of warm seawater entering the evaporator is converted into steam. A large turbine is required to accommodate the huge volumetric flow rates of low-pressure steam needed to generate any practical amount of electrical power [137].

Vega and Luis stated that although the last stages of turbines used in conventional steam power plants can be adapted to OC-OTEC operating conditions, existing technology limits the power that can be generated by a single turbine module, comprising a pair of rotors, to about $2.5\ \mathrm{MW}$ [101]. Unless significant effort is invested to develop new, specialised turbines (which may employ fiber-reinforced plastic blades in rotors having diameters more than 100m), increasing the gross power generating capacity of a Claude cycle plant above $2.5\ \mathrm{MW}$ will require multiple modules and incur an increased associated equipment cost [101], [103].

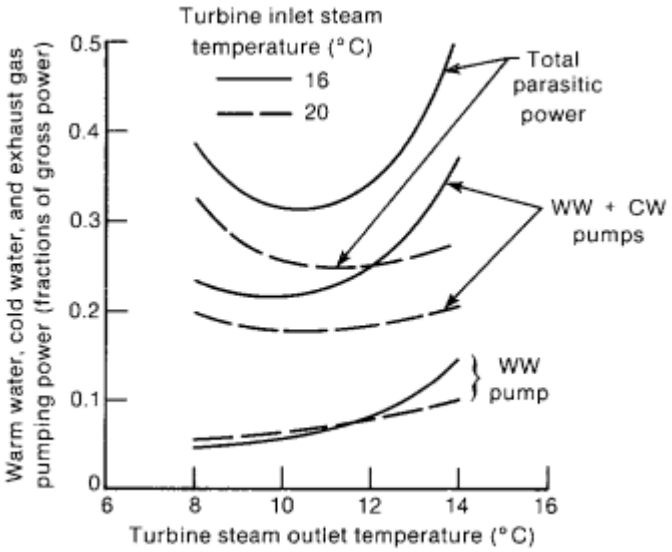

Figure 21: Breakdown of pumping power in warm water, Coldwater, and exhaust gas with turbine inlet and outlet steam temperature for a 5MW shore-based system [137].

2.8.2.1. CONDENSATION

In 1977, Smith reported that the condensation of the low-pressure working fluid leaving the turbine occurs by heat transfer to the cold seawater [139], [140]. This heat transfer may occur in a Direct Contact Condenser (DCC), in which the seawater is sprayed directly over the vapor, or in a surface condenser that does not allow contact between the coolant and the condensate [90], [138], [141], [142].

DCCs are relatively inexpensive and have good heat transfer characteristics due to the lack of a solid thermal boundary between the warm and cool fluids [90], [100], [143]. Although surface condensers for OTEC applications are relatively expensive to fabricate, they permit the production of desalinated water [102], [145].

2.8.2.2. DESALINATION

Vega reported that desalinated water production with a DCC requires the use of fresh water as the coolant. In such an arrangement, the cold seawater sink is used to chill the fresh water coolant supply using a liquid-to-liquid heat exchanger [101], [103]. Effluent from the low-pressure condenser must be returned to the environment. Liquid can be pressurised to ambient conditions at the point of discharge by means of a pump or, if the elevation of the condenser is suitably high, it can be compressed hydrostatically [101].

Figure 22: Surface condenser for desalinated water production (1994-1998) [103].

2.9. PREVIOUS RESEARCH

Large-scale experimental research on OTEC materials and fouling issues has, since 1981, been carried out at the Natural Energy Laboratory of Hawaii [146], [147], [148], and [149]. The open-cycle experiment that produced fresh water at the rate of 350 G/h was built there in 1987 and is called the Heat and Mass Transfer Scoping Test Apparatus (HMTSTA) [147], [150].

The purpose of the experiment was to gather data on the performance of evaporators and condensers operating under open-cycle OTEC conditions [147]. Parsons stated that this information is needed for the design of a planned systems experiment; one that will produce 200 kW gross electrical output, and establish the technical feasibility of the Open-Cycle process to produce more electrical power than it consumes [151], [152]. Although fresh water has long been produced from seawater by the application of an external energy source, this was the first time the energy source has come from the seawater itself [153], [154].

While an external source of electrical power is used to run the pumps in this experiment, an actual OTEC plant would produce more than enough power with its own turbo generator [147], [155].

TABLE 2: THREE PREVIOUS DESIGN CASES, SPECIFICALLY FOR THE FLASH EVAPORATION, MIN [KG], TIN [OC], PST [KPA] AND MST [KG/S] ARE REPORTED IN EACH REFERENCE, PIN [KPA] AND TST [OC]. [161].

Power	M_{in}[kg]	T_{in}[°C]	P_{st}[kPa]	m_{st}[kg/s]	P_{in}[kPa]	t_{st}[°C]	f_{st}[%]	B_{st}[K/kPa]	t_{in}[°C]
250	620	26	2.61	3.5	3.3639	21.780	0.564	2.35676	6.1
1.8	6000	26	2.76	33.4	3.3639	22.2692	0.556	2.90579	4.5
50	127.4	26	2.76	15.000	3.3639	22.2692	0.554	2.89570	4.5

Similarly, DoE initiated research on the extraction and conversion of the ocean thermal energy resource using an open-cycle process late in 1978 with the funding of a task to assess the feasibility of this technology [156] to produce cost-effective electrical power [157].

Link and Parsons reported that the original SERI (Solar Energy Research Institute) studies supported by the results of subcontracted studies at the Colorado School of Mines Westinghouse Corporation, and University of Massachusetts, concluded that large scale plants based on this technology could be economically viable if the main assumptions in the studies were valid [156]. A research program to develop data and analytical methods to refine and support these assumptions was initiated in 1980 [157], [158], [159].

Research conducted over the last 6 years has provided data and methods that were recently applied to a new systematic study of the open-cycle technology [157].

The Florida Solar Energy Center (FSEC) concluded that all the major assumptions made in the early feasibility studies had been conservative. Thus, Open-Cycle OTEC is even more encouraging than first anticipated. Their results indicated that smaller plants (5-15 MW) are nearly as economical to build as larger plants. This result is promising since many tropical-island communities do not require large power-generating facilities [157]. Although laboratory tests have verified many of the data and analysis methods used by the FSEC/Creare analysis, experiments to date have only been conducted on individual components, primarily in fresh water [159], [160].

The fundamentals of OC-OTEC in terms of detailed transport mechanisms are lacking in the current OTEC literature [161], [162], and [163]. Although OC-OTEC can produce electric power and desalinated water at the same time, their relative production rate is rigidly fixed because the turbine and condenser are connected in series. If a direct condenser is used (as proposed by the original conceptual design [161], [164], [165]), the condensed water is simply mixed with cold deep seawater (taken in) and then discharged onto the ocean surface.

2.9.1. SURFACE CONDENSER

If a surface condenser is used, the condensed fresh water is collected into a reservoir as one of the final products. In both cases, a condenser generates fresh water from the steam gas generated by the flash evaporator and then used by the turbine. Therefore, the conventional OC-OTEC design is restricted by the fixed ratios of power generation to desalination and desalination to discharge.

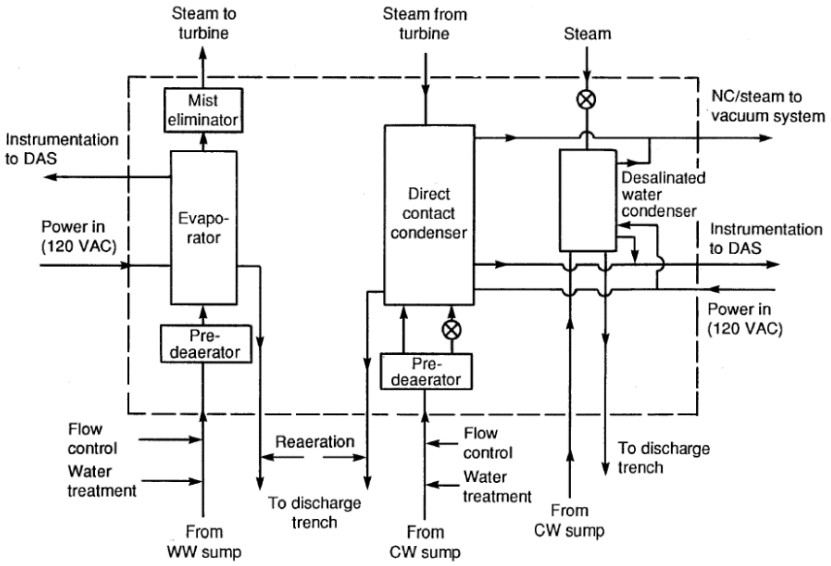

Figure 23: Surface condenser for desalinated water production (1994-1998) [161].

TABLE 3: COMPARISONS OF FOUR OPERATION MODES WITH 207 KW AND 1000 KW SCALES. *FOR PUMPING POWER CALCULATION, WE USED $D_{P,WW}$ =0.7M AND $D_{P,CW}$ = 1.0M FOR 207 KW AND $D_{P,WW}$ = $D_{P,CW}$ =1.5M FOR 1000 KW OTEC. FOR BOTH CASES, PIPE LENGTHS ARE $L_{P,WW}$ = 200 M AND $L_{P,CW}$ =100 [161].

Parameters [Units]	Scale (KW)	Power Gen.	Desalination	Only Half And Half With	Only Half And Half With
W_{gen} [kW]	1000kW	206.72	0	103.36	103.36
	206 kW	1000	0	500	500
M_{in} [kg/s]	1000kW	620	620	620	620
	206 kW	2432.64	2432.64	2432.64	2432.64

μ_{in} [kg/s]	1000kW	420	113.05	178.15	202.48
	206 kW	1759.7	473.65	746.4	865.7
Wp.ww [kW]	1000kW	4,759	4,759	4,759	4,759
	206 kW	3.929	3.929	3.929	3.929
Wp.w [kW]	1000kW	1,283	0.0325	0.1156	0.1655
	206 kW	10,430	0.258	0.9267	1,407
M_{in}/μ_{in} [-]	1000kW	1,476	5,484	3,480	3,062
	206 kW	1,382	5,136	3,259	2,810
W_{gen}/μ_{in} [kj/kg]	1000kW	0.493	0	0.58	0.51
	206 kW	0.568	0	0.67	0.578
m_{st} [kg/s]	1000kW	3.5	3.5	3.5	3.5
	206 kW	16.93	16.93	16.93	16.93
m_{pw} [kg/s]	1000kW	0	3.5	3.5	3.5
	206 kW	0	16.93	16.93	16.93
m_{dw} [kg/s]	1000kW	423.5	113.05	178.15	202.48
	206 kW	1,283	1,283	746.4	865.7

Albert and Hyeont demonstrated the production rates versus K_{tb} of 207 kW and 1000 kW plants as indicated above, the relative power generation rate, i.e., the power generation rate per cold water intake flowrate in the half and- half mode is higher than that of the power-only mode (see Table 3.2). This infers that the entire system can be optimised for the best (relative) performance by controlling the stream fraction to the turbine, K_{tb} (=1-K_{ec}).

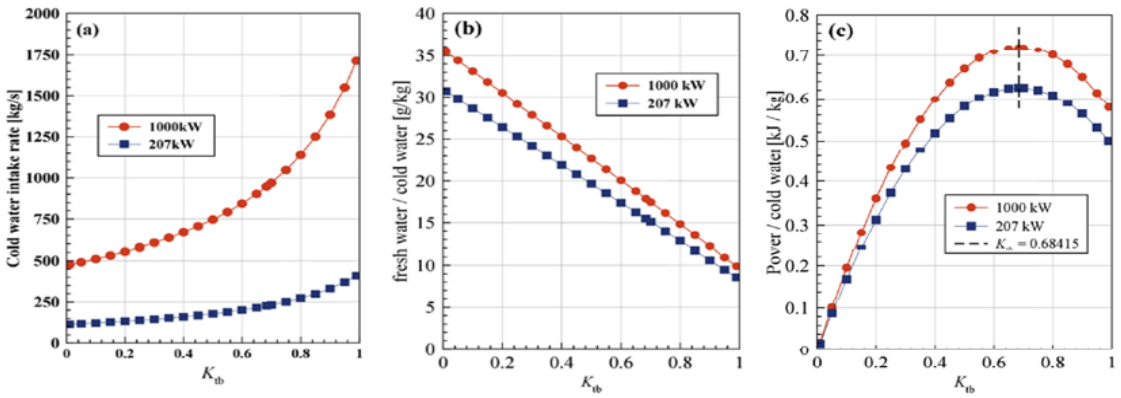

Figure 24: Dependence of (a) cold water intake [kg/s], (b) relative desalination [g/kg], (c) relative power generation rate [kJ/kg] rates with respect to Ktb for 207 kW (Min = 620 kg/s) and 1000 kW (Min =2432:64 kg/s) scale operations. For 207 kW, Bst = 2.357 K/K [161].

As K_{tb} increases from zero, the (absolute and relative) power generation rate must increase with respect to K_{tb}. It is questionable whether this linear relationship continues until K_{tb} reaches 1 because the temperature difference between C-condenser exit and cold water is about three times that between the turbine exit and the cold stream. The amount of the cold water, when used partially for the turbine

and condenser, must vary non-linearly with respect to K_{tb}. Figure 24 shows how the cold-water intake, and relative production of power and fresh water vary with K_{tb}.

2.10. FEASIBILITY STUDIES

The feasibility studies of an open-cycle power plant are reported and discussed in [167] and [168] and an extensive conceptual design study of open cycle are presented in [169], in which a computer cost optimisation analysis is performed [170].

Zabihian states that the open cycle thermodynamics is the governing principle of any thermal power system, and is of importance for the power system development. While advanced component design analyses and complex cost optimisation schemes in these studies have advanced the open-cycle technology, they tend to mask the thermodynamic interrelationship among different power components in the system [171], [172].

2.11. THERMODYNAMIC PROCESS OF AN OTEC OPEN CYCLE

An open-cycle power system consists of power components such as a flash evaporator, vapour, expansion turbine and generator, steam condenser, noncondensibles removing equipment, and deaerator [172], [173], [174].

Figure 25 present , warm surface water at around 27 °C enters an evaporator at pressure slightly below the saturation pressures causing it to vaporize. Where H_f is enthalpy of liquid water at the inlet temperature, T_1.

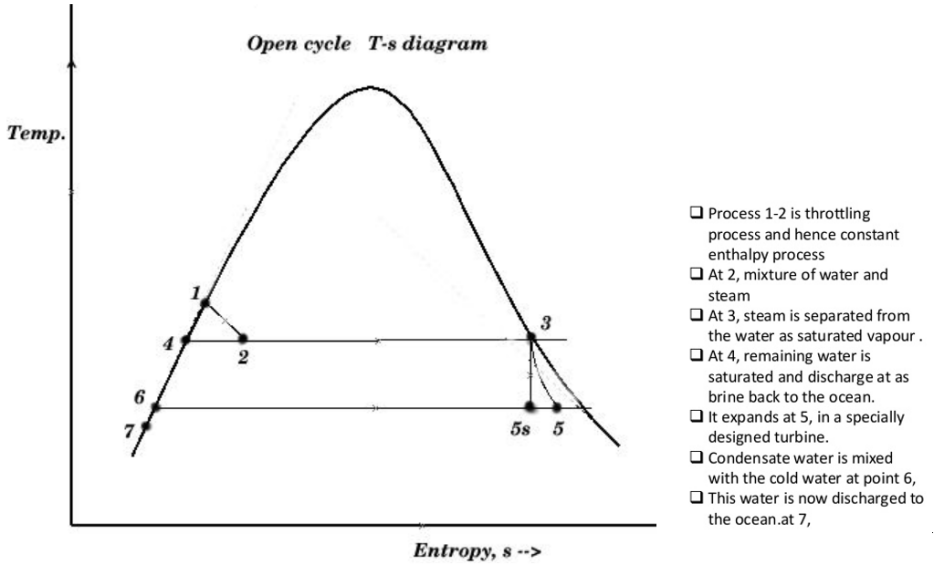

Figure 25: Open cycle -OTEC T-s diagram.

This temporarily superheated water undergoes volume boiling as opposed to pool boiling in conventional boilers where the heating surface is in contact. Thus the water partially flashes to steam with two-phase equilibrium prevailing. Suppose that the pressure inside the evaporator is maintained at the saturation pressure, T_2. Figure 26 is a representative schematic of an open-cycle OTEC power- system.

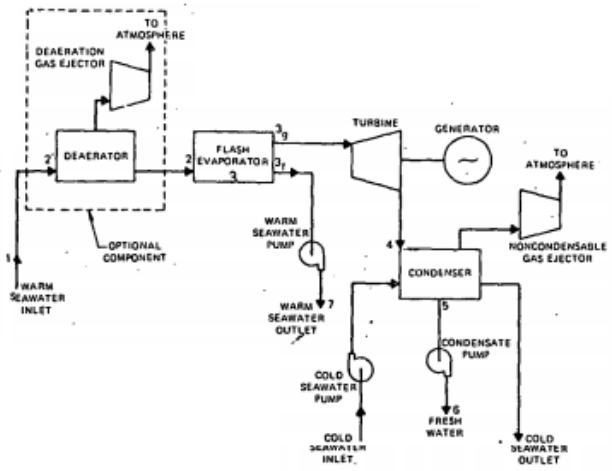

Figure 26: Schematic of an open-cycle power system [176].

The fundamental thermodynamic principle of the open-cycle OTEC power generation is no different from fossil or nuclear power generation [173], [176]. In theory, all one needs for power generation is a heat source, a heat sink, and a suitable working fluid capable of performing cyclic motion between the temperature

bounds of the heat source and the heat sink [174]. A thermodynamic temperature-entropy (T-S) diagram of the open cycle is shown in Figure 16 [175], [176], [177].

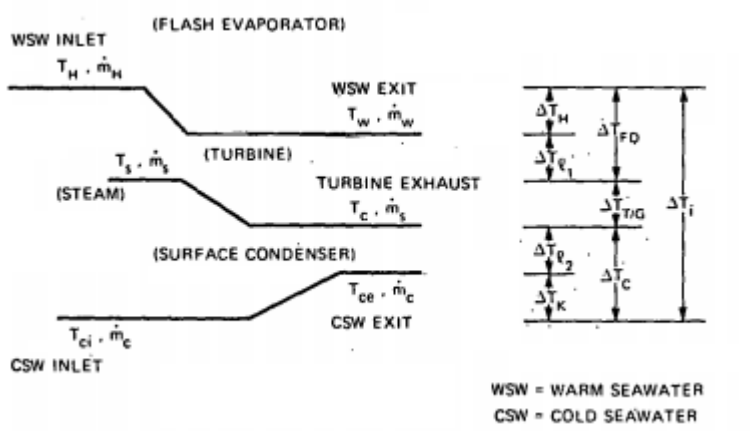

Figure 27: System temperature (T) and mass flow (m) distribution [176], [178].

2.12. DESALINATION TECHNOLOGIES

In the last decade, significant research has been done in the field of applicability and reliability of desalination methods using renewable energy sources [179], [180], and [181]. Furthermore, the results of relative research programs [182], [183] demonstrated that the implementation of such desalination schemes can contribute successfully to current water shortage problems. Many reports referring to the assessment of the RES (Renewable Energy Source) potential have also been presented [184], [185]. Twidell [186] and Stone [187] provide information on RES technologies.

The technology proposed in the literature [188], [189] for desalination plants powered by RES are listed in Fig. 28. When several alternative RES desalination schemes are applicable to a specific case, the final decision concerning the most prominent combination should be based on criteria such as:

- Commercial maturity of technology
- Availability of local support
- Simplicity of operation and maintenance of the system

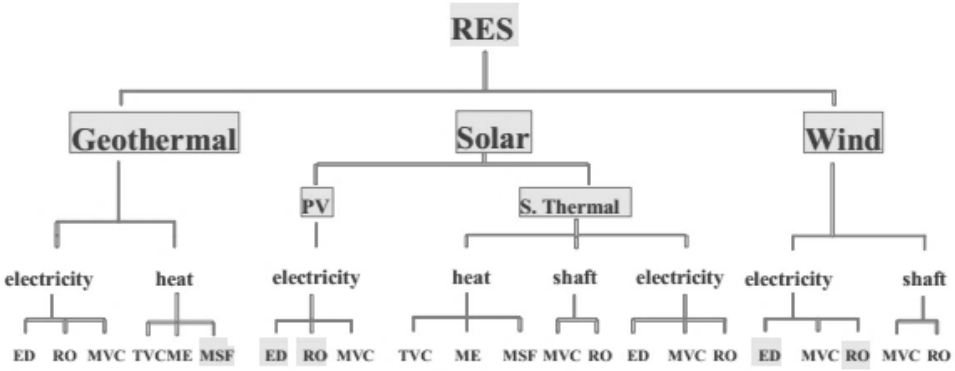

Figure 28: Renewable energy schemes for desalination [189].

Water concern is a serious problem world-wide because of rapid increase in population, global warming, and climate change. Many sectors have a keen interest in desalination technology, which produces fresh water from almost inexhaustible seawater [190], [191] and [192].

About 97.5% of the earth is covered with water, out of which only 2.5% is fresh water that can be used by humans [193], [194], [195], [196].

Locke, Bogart and Schultz point out that the areas of greatest potential water shortages tend to be regions with high population density, or high wealth density [199], [200].

Regions such as those in South Africa, KwaZulu-Natal are also regions with shortages [201], [202]. The water footprint network was founded in 2008 to promote the sharing of water equitably. The problem has also been studied by Hoekstra (2008) in the context of globalization [203], [204].

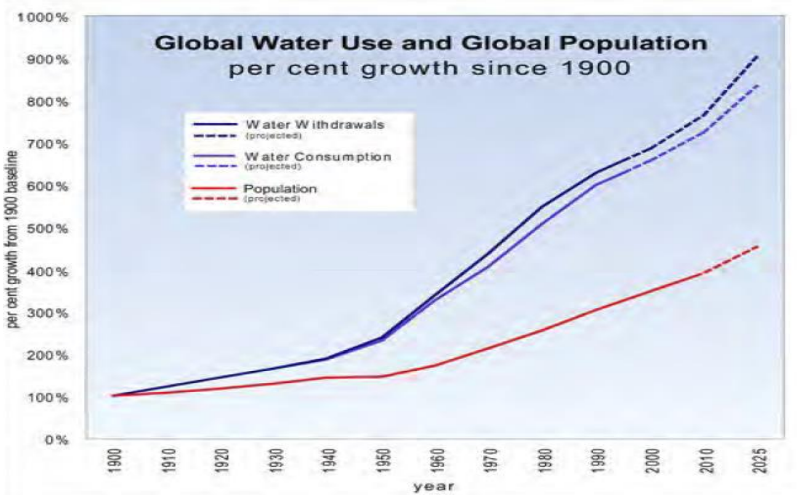

Figure 29: The demand for water has grown twice as fast population [205], [206].

Li reported that all desalination process uses chemical engineering technology in which a stream of saline water is fed through the process equipment; energy in the form of heat, water pressure or electricity is applied [207], [208], and two outlet streams are produced; a stream of desalinated (fresh) water and a stream of concentrated brine which must be disposed of [209], [210]. This is shown in Figure 30.

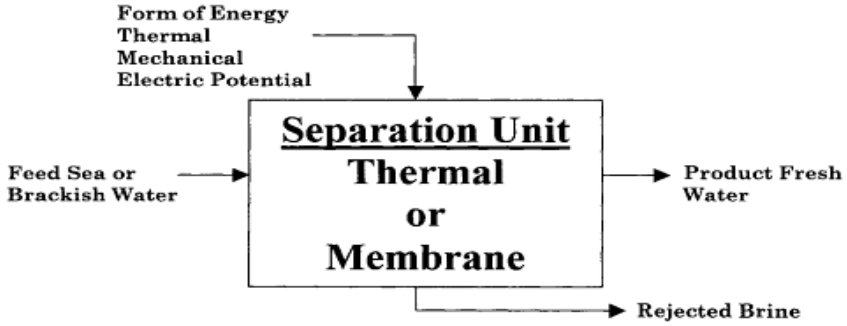

Figure 30: Basic principle of desalination [211].

Muralidharan reported that the capital costs estimates are a function of four parameters. First, the scale of the project has an important impact on the cost projections. Due to the large overhead costs, small scale OTEC plants in the range of 1-10MW have relatively high installation costs of around $16 400–35,400/kW.

However, combined with the production of fresh water, they become economically viable for small island states or isolated communities (up to 100,000 residents), especially if OTEC resources are within 10 km of the shore [224]. OTEC plants in the 10-100 MW range are estimated to cost between $ 15000/kW and $ 5000/kW when installed (Muralidharan, 2012; Vega, 2012).

Larger OTEC plants built on moored ships could have costs as low as $ 2650/kW [222], [223], [225]. The capital costs of the individual components themselves are relatively predictable as most components are commercially available for other offshore applications. For OTEC plant components these would include vertical pipes ($ 500/m), pumps ($ 700-2000/kW), heat exchangers ($ 200-800/m^2) and components for thermodynamic cycles, such as the Rankine cycle $ 1000/kW) among others. Based on the same studies, recent estimates suggest the following levelised costs of electricity production (LCOE).

TABLE 4: COST ESTIMATE FOR OTEC [224].

	Source of LCOE ($/kWh)[2]				
Size (MW)	**Vega (2007;2012)[3]**	**Energy and Environment Council (2011)**	**Straatman Environment Council (2011)**	**Upshaw (2012)**	**Muralldharan (2012)**
1-1.35	0.60-0.94	0.51-0.77			
5[4]	0.35-0.65				
10	0.25-0.45	0.19-0.33			
				0.13-0.65	
28					
50	0.08-0.20	0.10-0.16	0.11-0.65		
50 (Combined with offshore solar pond)	0.03-0.05				
100	0.07-0.18				0.19
200					0.16
400					0.12

CHAPTER 3

OCEAN THERMAL ENERGY CONVERISON RESEARCH METHODOLOGY

3. INTRODUCTION

In order to meet the objective of this research, the following steps have been undertaken:

- A site suitable for OTEC has been broadly identified.
- Surface and sub-surface temperatures at this site will be measured over a period.
- A computer model of a suitable OTEC plant has been developed and simulated at DUT.
- A physical small-scale model has been built in the DUT laboratory and measurements have been compared with the simulation. A next step will be a pilot plant near Port Shepstone.

The model developed was used to assess the feasibility of OTEC based on fundamental principles. The analysis of the plant was conducted numerically with the help of ASPEN PLUS. ASPEN PLUS software was used as the main software to simulate all parts of the combined plant system. Each sub-system has its own governing equations, which were simplified to provide a reasonable approximation of how the sub-system would operate.

When modelling a typical system, the design of the major components comprises a large part of the design process.

these major components are;

- The steam generation system (flash evaporator)
- The Turbine for driving the generator
- The condenser for producing fresh water
- The cold water pipe for drawing cold water in and piping.to the system
- All the pumps including the vacuum pump

For the laboratory model the pumps have been sourced commercially so the design has concentrated on the flash evaporator, turbine and collector vessel.

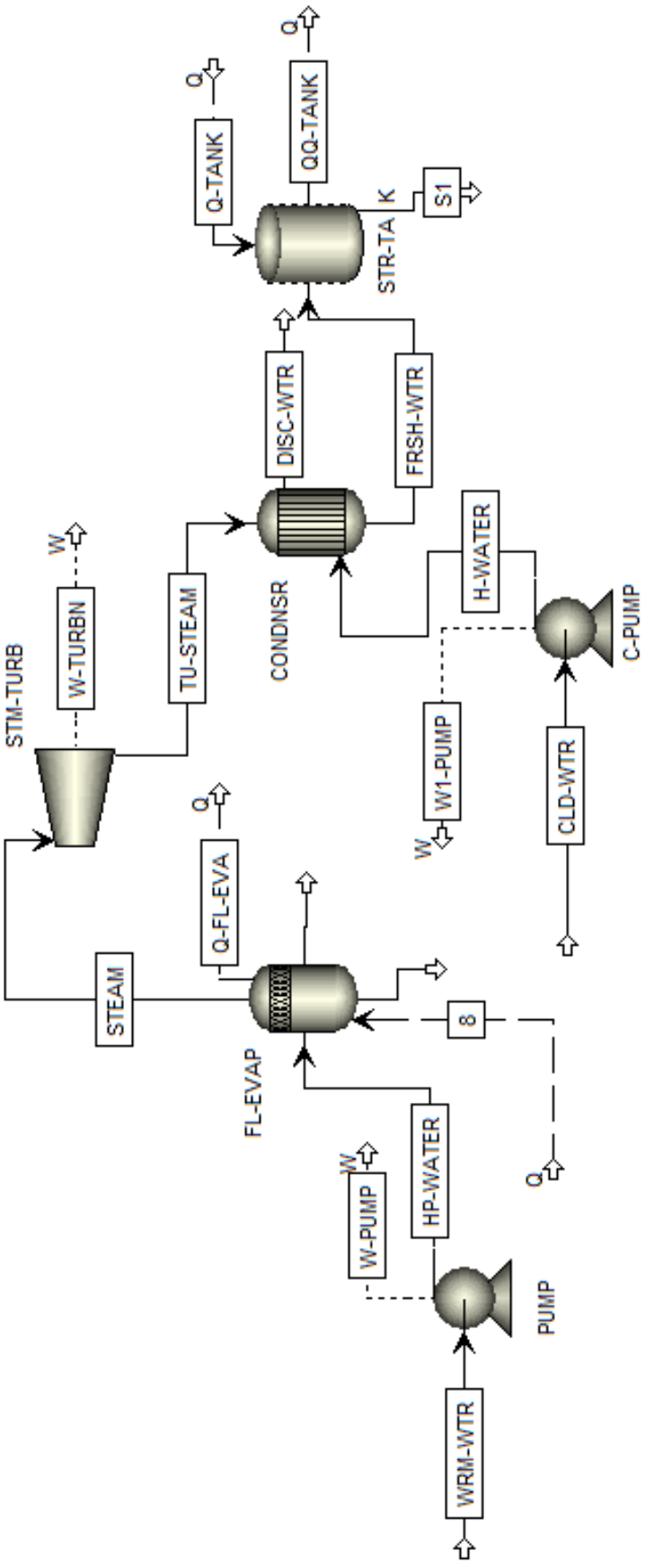

Figure 31: Open Cycle OTEC plant with condenser [author].

3.1. MECHANICAL DESIGN AND ANALYSIS OF THE FLASH EVAPORATOR

In order to design a pressure vessel or flash evaporator, the selection of code is very important as a reference guide to achieve the safety of the pressure vessel. Pressure and temperature are two important factors that affect the mechanical design of evaporator systems. Factors like startup, shutdown, upset, external loading from supports, pulsating pressure, wind loading, and earthquake load also significantly affect the evaporator operation. Various factors are considered that affect the mechanical design of equipment, and their effect is detailed in heat exchanger design.

It is important to determine both minimum and maximum anticipated operating temperatures and pressures, to obtain the design temperature and pressure; the design pressure being the sum of the maximum allowable pressure and the static head of the fluid in the pressure vessel refer to equation (3.1). The combination of temperature and pressure affect the mechanical design of the equipment. Many of the design considerations are also related pressure design too.

3.1.1. SHELL DESIGN

It is recommended that the minimum thickness or maximum allowable working pressure of cylindrical shells shall be the greater thickness or lesser pressure as given by equation (3.2).

Circumferential stress when the thickness does not exceed one- half of the inside radius, or P does not exceed 0.385SE, the following formulas shall apply:

$$P = \frac{SEt}{R - 0.6t} \tag{3.1}$$

If the thickness does not exceed one-half of the inside radius, or P does not exceed 1.25SE, the following formulas shall apply:

$$t = \frac{PR}{2SE - 0.4P} \tag{3.2}$$

3.1.2. ELLIPSOIDAL HEAD DESIGN FOR FLASH EVAPORATOR

The thickness that is crucial to design a dished head of semi elliptical form, in which half the minor axis equal one-fourth of the inside diameter of the head skirt, is determined by:

$$t = \frac{PD}{2SE - 0.2P} \text{ or } P = \frac{2SEt}{R - 0.2t} \tag{3.3}$$

The semi-elliptical head is the most commonly used head type. Half of its minor axis (i.e. the inside depth of the head minus the length of the straight flange section) equals one fourth of the inside diameter of the head. The thickness of this type of head is normally equal to the thickness of the cylinder to which it is attached.

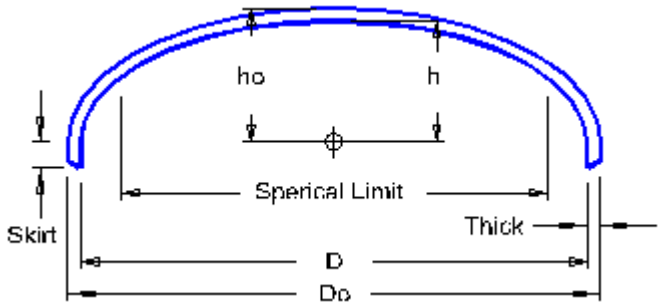

Figure 32:Semi-Elliptical of Flash evaporator [228].

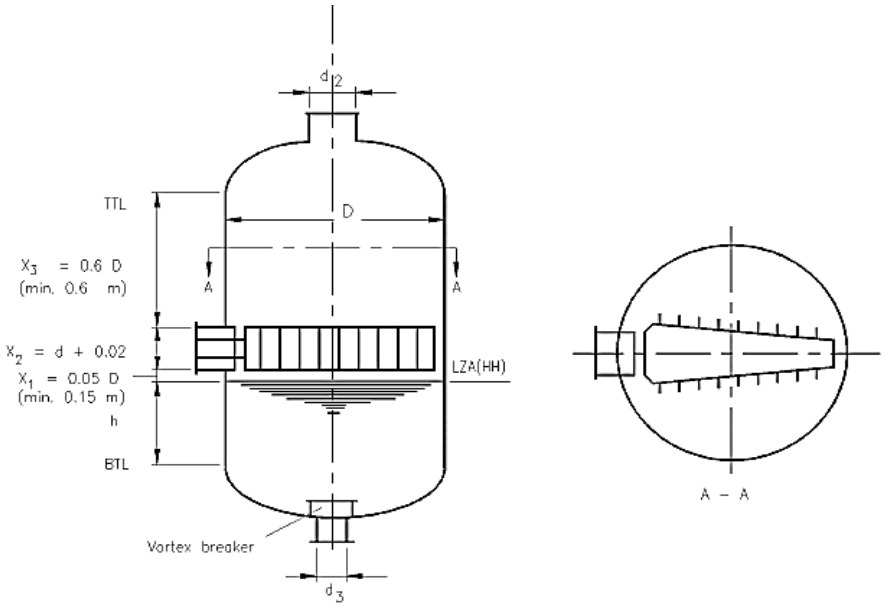

Figure 33: Vessel and Diffuser of Flash Evaporator [229].

3.1.3. MIST ELIMINATOR DESIGNER FOR FLASH EVAPORATOR

The mist elimination of the flash evaporator is made of knitted wire formed to give the correct shape, and not cut to leave raw edges and or loose pieces of wire which could become detached.

Mist eliminators are normally stainless steel. The mist mat must have a free volume of at least 97% (ε = 0.97) a wire thickness of dw, between 0.23 mm and 0.28 mm. The thickness of a horizontal mat in a vertical vessel is normally 0.1 m.

3.1.4. LIQUID REMOVAL EFFICIENCY

The liquid removal efficiency of a wire mesh separator is highly dependent on the liquid droplet size distribution and liquid load at the demister mat. Figure 48 demonstrates the effect of average droplet size on efficiency. For design purposes, an overall liquid removal efficiency of greater than 98% can be assumed for a correctly sized vertical demisting vessel (this includes the pre-separation by the feed inlet device).

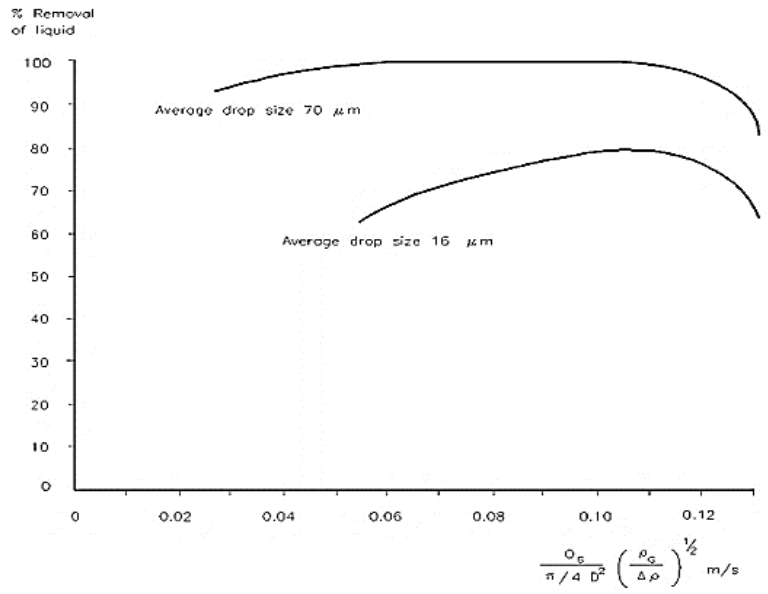

Figure 34: Typical efficiency curves for demister mats. System: Air/ spindle oil (kin, viscosity=13 x 〖10〗^(-6) m^2/s). ρ (G)= density, ∆ρ = density change, Q_G = flow [230].

3.1.5. DIAMETER OF FLASH EVAPORATOR

The vessel diameter D, is designed to make sure that it handles the capacity of the gases produce inside the vassel of the flash evaporator

$$\lambda_{max} = \frac{Q_{max}}{\pi D_{min}^2 / 4} = 0.105 f_\eta f_\varphi [m/s] \quad (3.4)$$

$$D \approx \sqrt{\frac{4}{\pi}} A_D \quad (3.5)$$

$$D \approx \sqrt{\frac{4}{\pi}} \frac{V}{v_{perm} P_v} \quad (3.6)$$

or

$$D \geq 3.348 \sqrt{Q_{max} / (f_\eta f_\varphi)} [m] \quad (3.7)$$

where f_η is the derating factor allowing for the viscosity of the liquid phase, and f_ϕ is the derating factor related to the flow parameter at the face of the wiremesh ϕ_{wm}, $f_\phi = 1/(1 + 10\phi_{wm})$, if $\phi_{wm} \leq 0.1$, ϕ_{wm}in practice, will not exceed 0.1.

The allowable stress of the shell is calculated as follows, note that t = 0.0016 cm and S =193MPa.

$$S = \frac{P(D + 0.2t)}{2t} = \frac{P(0.12 + (0.2 \times 0.0016) + 0.2t)}{2(0.0016)} = P = 0.513kP \quad (3.8)$$

3.1.6. NOZZLE OF FLASH EVAPORATOR

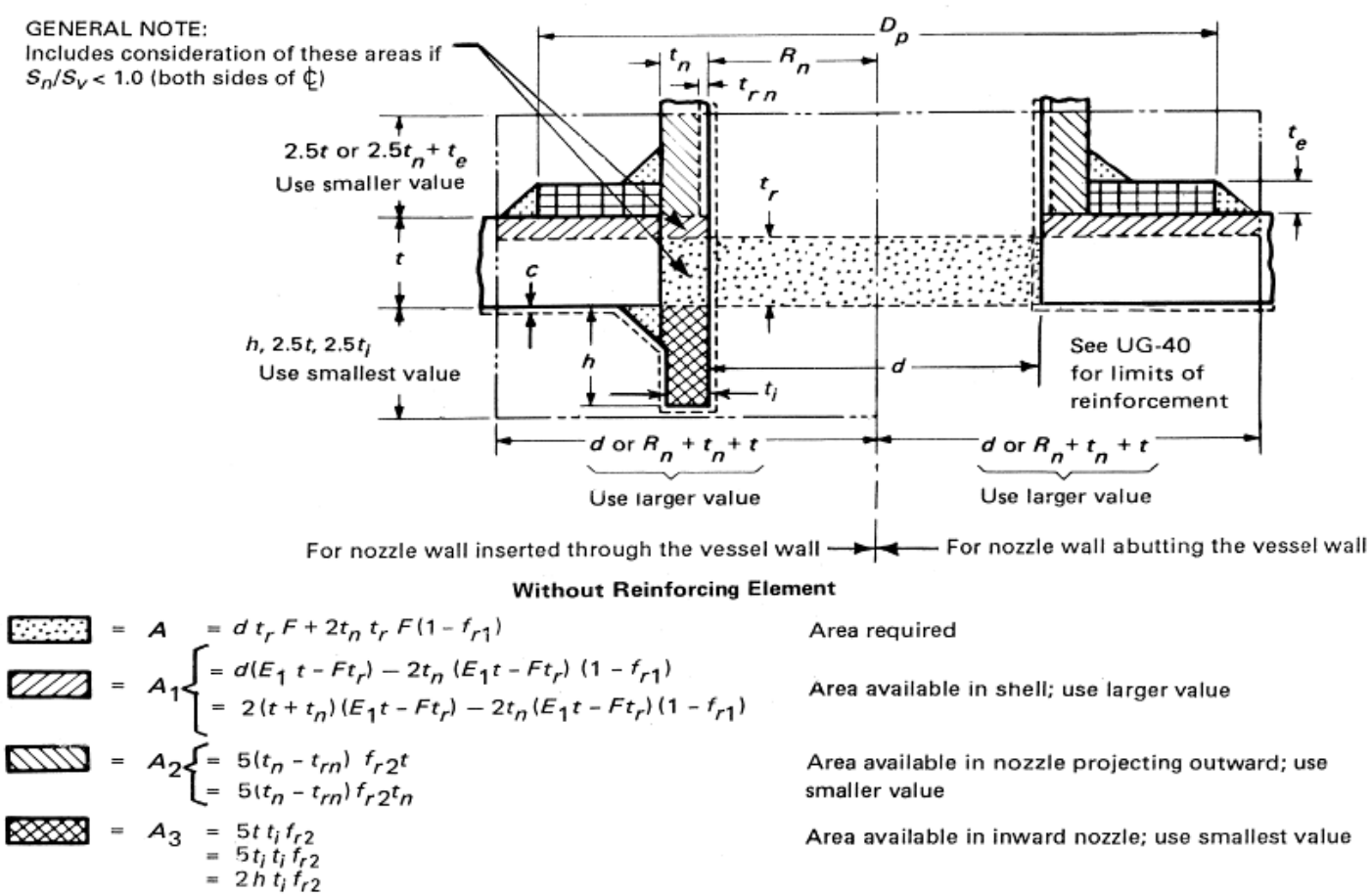

Figure 35: Reinforcement design of nozzle [231].

Total nozzle available area is greater than the required area; the reinforcement and nozzle are safe in design [232].

3.1.7. VESSEL HEIGHT CONDENSER

This refers to the height H of the vessel required for liquid hold up. The total tangent-to-tangent vessel height is:

$$H = h + X_1 + X_2 + X_3 + t_{wm} + X_3 [m] \quad (3.9)$$

Where,

t_{wm} = Thickness of demister mat, usually 0.1 m

X_1 = 0.05 D with a minimum of 0.15 m

$X_2 = d_1 + 0.02 m$ with d_1 = internal diameter of inlet nozzle

$X_3 = d_1$ with a minimum of 0.3 m

$X_4 = 0.15 D$ with a minimum of 0.15 m

3.2. FLASH EVAPORATOR DESIGN CALCULATIONS

This section focuses on calculations for the mechanical design of the flash evaporator and their properties, and thermodynamics of the fluid. The mass flowrate within the flash evaporator and pressures were calculated.

3.2.1. MATERIAL STAINLESS STEEL

TABLE 5: PHYSICAL PROPERTIES FLASH EVAPORATOR [234].

Parameters	Values
Density (g/cm^3)	8000

3.2.2. MECHANICAL PROPERTIES FLASH EVAPORATOR

Table 6 and 7 show the standard parameters that were utilised to design the flash evaporator.

TABLE 6: PHYSICAL PROPERTIES FLASH EVAPORATOR [234].

Parameters	Values
Hardness, Rockwell, B (Kgf)	82
Tensile strength, Ultimate (%) (Pa)	564
Tensile strength, Yield (Pa)	210
Elongation at break (at 50mm)	58%
Modulus of Elasticity (Nm^{-2})	200

3.2.2.1. THERMAL PROPERTIES

TABLE 7: THERMAL PROPERTIES OF FLASH EVAPORATOR [234].

Parameters	Values
Specific Heat Capacity (J/kg ^{o}C)	2093.4
Melting point (^{o}C)	1400 – 1450

The flash evaporator receives water of mass flowrate ($\dot{M}_{in}$) from the pump at a certain temperature and pressure (T_{in} and P_{in}), as illustrated by

$$f_{st} = \frac{\dot{m}_{st}}{\dot{M}_{in}} \tag{3.10}$$

where it uses a low vacuum pressure (P_{ev}) to evaporate warm water. Steam pressure (P_{st}) is expected to be equivalent to the vacuum pressure, $P_{ev} = (P_{st})$. Mass flowrate of steam $(\dot{m}_{st})$ is only a small fraction of ($\dot{M}_{in}$), which is 0.565%.

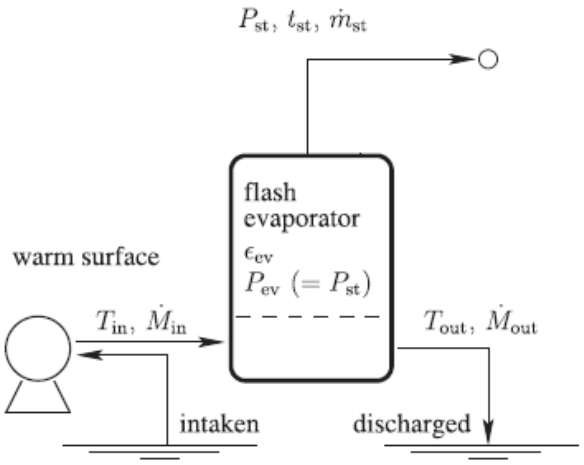

Figure 36: Mass flowrate balance [235].

The mass flowrate balance can be understood by discharged mass flowrate from the evaporator, which is the received mass flowrate ($\dot{\mathrm{M}}_{\mathrm{in}}$) minus the steam flowrate $\Delta Q_{ww} = \mathrm{C}_{\mathrm{cp}}\left(\mathrm{T}_{\mathrm{in}}\dot{\mathrm{M}}_{\mathrm{in}} - \mathrm{T}_{\mathrm{out}}\dot{\mathrm{M}}_{\mathrm{out}}\right)$ The thermal energy difference between the in intake and discharged warm water is calculated by:

$$\Delta \mathrm{Q}_{\mathrm{ww}} = \mathrm{C}_{\mathrm{cp}}\left(\mathrm{T}_{\mathrm{in}}\ \mathrm{M}_{\mathrm{in}} - \mathrm{T}_{\mathrm{out}}\ \dot{\mathrm{M}}_{\mathrm{out}}\right) \tag{3.11}$$

$\Delta \mathrm{Q}_{\mathrm{ww}}$ is used to change phase from liquid to vapour. Latent heat ($\mathrm{L}_{\mathrm{nev}}$) is the required heat to evaporate water (specific heat of evaporation). Maximum flowrate passing the pump, before the evaporator, is given equation (A1).

3.2.3. MASS FLOWRATE OF WARM WATER

The mass flow rate of surface-warm ocean water is calculated by heat-balancing the evaporator knowing the inlet and outlet conditions of water equation (A2), Fraction of vapour in the Flash Evaporator (%).

3.2.4. STEAM MASS FLOWRATE, $\dot{m}_{st}$

The mass flowrate of the steam was calculated using the formula of the flash evaporator which utilise the low vacuum pressure as a driving force to evaporate the surface warm water from the ocean. the pump takes in the surface seawater of temperature T_{in} = 30°C and sends it to the flash evaporator with mass flow rate of $\dot{M}_{in}$. Mass flow rate of the produced steam gas, $\dot{m}_{st}$, is only a small fraction of $\dot{M}_{in}$, calculated equation (A3).

3.2.5. THE MASS FLOWRATE BALANCE

It is often presumed that the flash evaporator is in a thermodynamic state close to a phase transformation equilibrium between warm seawater and vapor gas so that steam temperature, (tst), can be calculated using the Clausius-Clapeyron equation. This gas flow includes a very small amount of non-condensable gases, whose mass flow rate is denoted $\dot{m}_{ncg}$. Because f_{st} is small, a majority of warm water is discharged back onto the open ocean with $\dot{M}_{out}$. The mass flowrate balance was calculated equation (A4).

3.2.6. VELOCITY AND FLOWRATE OF DISCHARGED WATER

The name ‘open cycle’ comes from the fact that the working fluid (steam) is discharged after a single pass and has different initial and final thermodynamic states; hence, the flow path and process are ‘open.’ The discharge water velocity is calculated utilising the formula of the mass flowrate of the warm water from the OC-OTEC plant. Equation (A5) presents the equation for velocity discharge fluid from the OC-OTEC plant.

The $\mathrm{Q_{ww}}$ is utilised to change phase from liquid to vapour and it is proportional to the latent heat. As latent heat $\mathrm{L_{nev}}$ is the required heat to evaporate water (specific heat of evaporation) refer to equation (A7) for detailed calculation. Maximum flowrate passing the pump fed to the evaporator. The calculation of the flowrate of discharge water is presented on equation (A6).

The thermal energy difference between the intake and discharged warm water is calculated using temperature at intake T_{in} = 30^{o}C, and assumed temperature at the discharge is T_{out} = 20^{o}C. Specific heat capacity at T_{in} is, C_p = 4.182 kJ/kgK, see A7.

3.2.7. LOW VACUUM PRESSURE IS 3.5 KPa, THEREFORE $P_{ev} = P_{st}$ = 3.5kpa.

The Estimation of $\dot{m}_{st}$ is a key design process, which is governed by physical conditions of the warm water and vacuum pressure. the vapor pressure at saturation equilibrium of the warm seawater temperature, and is a proportionality, depending on the specific evaporator type, size, and structure. Evaporation occurs at liquid gas interfaces. Calculated steam temperature by interpolation see equation (A9).

3.2.8. THE FLASH STEAM GENERATED (%).

The OTEC (OC) flash evaporation involves complex heat and mass transfer processes. In the configuration pilot plant, warm seawater was pumped into a chamber through spouts designed to maximize the heat-and-mass- transfer surface area by producing a spray of the liquid.

The pressure in the chamber (2.6 percent of atmospheric) was less than the saturation pressure of the warm seawater. Exposed to this low-pressure environment, water in the

spray began to boil. the vapor produced was relatively pure steam. As steam is generated from the Flash evaporator, it carries away with it its heat of vaporization, and it is pushed to the generator. It calculated as 1.7% refer to equation (A10).

3.2.9. CONDENSATE VOLUME

The condensate volume is derived from the steam volume of the OTEC system produced from the flash evaporator. It was calculated as c_v is 0.00099 m^3/Kg. (Eq. A11).

3.2.10. STEAM VOLUME

The specific volume of vapor at the OC-OTEC plant was calculated Eq. A12 the volume of the steam was calculated asV_{steam} is 0.78 m^3/Kg. With the aim of finding some relation which would make possible a reliable extrapolation to the OTEC system. the volumetric data at the steam volume, and the absolute temperature were examined.

One formula was found to be particularly useful on account of its simplicity and close representation of the observed data at lower pressures. this formula employs a function of the deviation of the saturated steam from the behaviour of an ideal gas. The calculation was done using the volume of the condensate c_v is 0.00099 m^3/Kg multiple by flash generated steam (%).

3.2.11. CALCULATION STEAM SPEED INSIDE A PIPE

The speed inside the pipe was calculated as shown in, Eq. A13. The formulate to calculate the *v* was derived from m_{st} equation was $m_{st} = pAv$, where *p* is the density of the steam, *v* is the average velocity in the pipe and *A* is the area of the pipe.

3.3. VESSEL DESIGN CALCULATION

Fig 37 below present the design of the flash evaporate tha was used for the OC-OTEC plant. The design formulas used in the design by rule method were based on the principal stress theory and calculate the average hoop stress. The principal stress theory of failure states that failure occurs when one of the three principal stresses reaches the yield strength of the material. Assuming that the radial stress is negligible, the other two

principal stresses can be determined by simple formulas based on engineering mechanics.

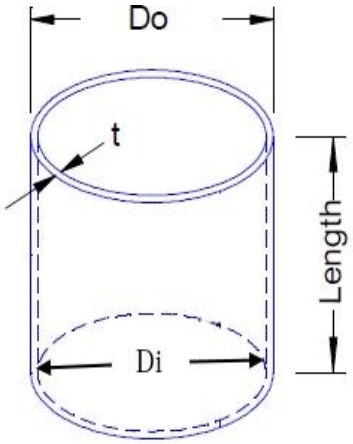

Figure 37: Flash Evaporate tank [author].

TABLE 8: DESIGN PARAMETER.

Parameters	Length[mm]
Outside diameter of the vessel, D_o	203
Inside diameter of the vessel, D_i	200
Thickness of the vessel, t	1.6
Height (length) of the vessel, H	300

$$V = \pi\left(r_o^2 - r_o^2\right)$$
$$= \pi\left(0.1016^2 - 0.1^2\right)0.3$$
$$= 304\times10^{-6}\ m^3$$

3.3.1. MASS OF THE STAINLESS STEEL MATERIAL

$$M_m = V\rho_m$$
$$= 304\times10^{-6}\times8000$$
$$= 2.43 Kg$$

TABLE 9: PROPERTIES OF STAINLESS STEEL.

Parameters	Units
Design pressure, P	3.5 kPa
Corrosion allowance, cr	0.01%
Nominal wall thickness, nt	1.6mm
Allowable stress, σ_s	210MPa
Elongation efficiency, Ee	70%
Circle efficiency, Ce	85%
Under tolerance allowance, UT	0.0%

3.3.2. VARIABLES

$$UT = t(UTP)$$
$$= 0.0016 \times 0$$
$$= 0$$

3.3.3. NOMINAL THICKNESS

$$nt = t - Corr - UT$$
$$= 0.0016 - 0.001 - 0$$
$$= 0.0006\,m$$

$$R_i = \frac{D_o}{2} - nt$$
$$= \frac{203.2}{2} - 0.0006$$
$$= 0.101$$

3.3.4. THICKNESS BEFORE FORMING

$$t_b = \frac{PR_i}{2_{\sigma s} C_e + P}$$
$$= \frac{3500 \times 0.101}{2 \times 210 \times 10^6 \times 0.85 + 3500}$$
$$= 0.99 \times 10^{-6}\,m$$

3.3.5. THICKNESS BEFORE FORMING

$$t_b = \frac{PR_i}{\sigma s E_e + P}$$
$$= \frac{3500 \times 0.101}{210 \times 10^6 \times 0.7 + 3500}$$
$$= 2.405 \times 10^{-6}\ \mathrm{m}$$

3.3.6. REQUIRED THICKNESS

$$t_{re} = t_b t_a + corr$$
$$= 0.99 \times 10^{-6} \times 2.405 \times 10^{-6} + 0.001$$
$$= 1 \times 10^{-3}\ \mathrm{m}$$

1mm < 1.6mm is acceptable

3.3.7. MAXIMUM PRESSURE

$$P_{max} = \frac{\sigma s E_{ent}}{R_i + nt}$$
$$= \frac{210 \times 10^6 \times 0.7 \times 0.0006}{0.101 + 0.0006}$$
$$= 868.11\,\mathrm{kP}\,a$$

3.3.8. THE HYDROSTATIC PRESSURE CAUSES STRESSES IN THREE DIMENSIONS

- Longitudinal stress (axial) σ_L
- Radial stress $\sigma_{r,}$ (neglect)
- Hoop stress σ_h

3.3.8.1. ALL OF THEM ARE NORMAL STRESSES

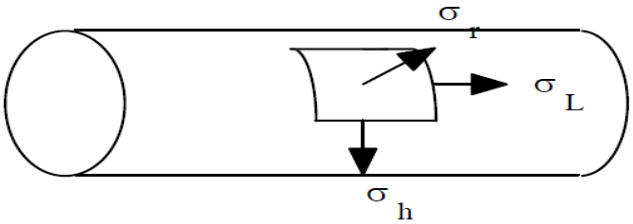

Figure 38: The stresses in three dimensions [author].

3.3.8.2. THE LONGITUDINAL STRESS σ_L

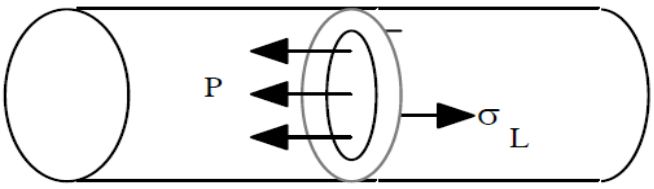

Figure 39: The longitudinal stress σ_L.

$$\sigma_L = \frac{PD}{4t}$$
$$= \frac{3500 \times 0.2}{4 \times 0.0016}$$
$$= 109.375 \text{kPa}$$

3.3.8.3. The hoop stress $\sigma_{h,}$

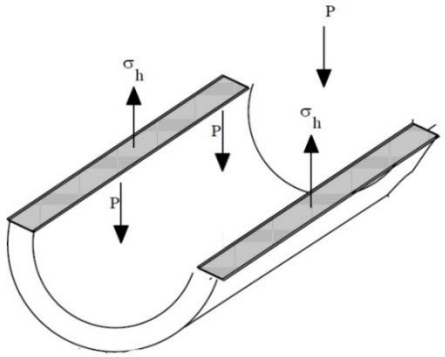

Figure 40: The hoop stress σh.

$$\sigma_L = \frac{PD}{4t}$$
$$= \frac{3500 \times 0.2}{2 \times 0.0016}$$
$$= 218.5 \text{kP} a$$

3.4. CALCULATED HEAD PROPERTIES

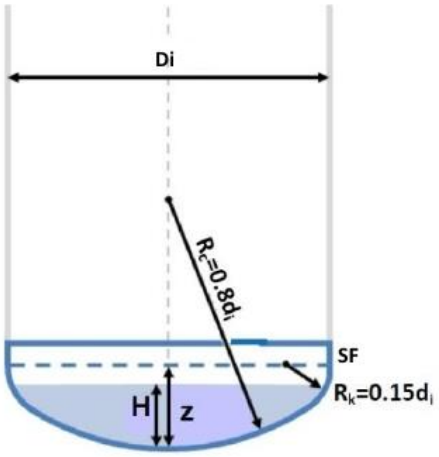

Figure 41: Head properties.

$$Rk = 0.8D_1$$
$$= 0.8 \times 0.2$$
$$= 0.16\text{m}$$

$$R_k = 0.2\,D_1$$
$$= 0.15 \times 0.2$$
$$= 0.03\text{m}$$

$$Z = 0.25\,D_1$$
$$= 0.25 \times 0.2$$
$$= 0.05\,\text{m}$$

3.4.1. HEAD VOLUME, V_{head}

STRAIGHT FLANGE IS 30 mm

$$V_1 = \frac{\pi D_i^3}{24} + \frac{\pi D_i^2 SF}{4}$$
$$= \frac{\pi \times 0.2^3}{24} + \frac{\pi \times 0.2 \times 0.03}{4}$$
$$= 1.99 \times 10^{-3}\,\text{m}^3$$

$$V_2 = \frac{\pi D_o^3}{24} + \frac{\pi D_o^2 SF}{4}$$
$$= \frac{\pi \times 0.2032^3}{24} + \frac{\pi \times 0.2032 \times 0.03}{4}$$
$$= 2.07 \times 10^{-3}\ m^3$$

$$V_{Tot} = V_2 - V_1$$
$$= 2.07 \times 10^{-3} - 1.99 \times 10^{-3}$$
$$= 0.08 \times 10^{-3}\ m^3$$

3.4.2. MASS OF THE STAINLESS STEEL MATERIAL

$$M_m = V \rho_m$$
$$= 0.08 \times 10^{-3} \times 8000$$
$$= 0.65\ Kg$$

Therefore, the approximate total mass of the vessel: 2.43 + 0.65 = 3.08 kg, 3.08 kg ≤ x kg≤ 6 kg acceptable.

3.4.3. THICKNESS BEFORE FORMING, t_b

$$t_b = \frac{PD_i}{(2\sigma s E_e - 0.2P)}$$
$$= \frac{3500 \times 0.2}{2 \times 210 \times 10^6 \times 0.7 \times 0.2 + 3500}$$
$$= 2.38 \times 10^{-6}\ m$$

3.4.4. THICKNESS AFTER FORMING, t_a

$$t_a = \frac{PD_i}{(2\sigma s C_e - 0.2P)}$$
$$= \frac{3500 \times 0.2}{2 \times 210 \times 10^6 \times 0.7 - 0.2 + 3500}$$
$$= 1.96 \times 10^{-6}\ m$$

6.1.18. NOMINAL THICKNESS, nt

$$nt = t - Corr - UT$$
$$= 0.0016 - 0.001 - 0$$
$$= 0.0006\,m$$

3.4.5. REQUIRED THICKNESS, t_{req}

$$t_{re} = t_b t_a + corr$$
$$= 0.99 \times 10^{-6} \times 2.405 \times 10^{-6} + 0.001$$
$$= 1 \times 10^{-3}\,m$$

1mm < 1.6mm is acceptable

3.4.6. MAXIMUM PRESSURE, P_{max}

$$P_{max} = \frac{\sigma s E_{ent}}{R_i + 0.2\,nt}$$
$$= \frac{2 \times 210 \times 10^6 \times 0.7 \times 0.0006}{0.2 + 0.2 + 0.0006}$$
$$= 881.47\,kPa$$

881.47kPa > 3.5kPa acceptable

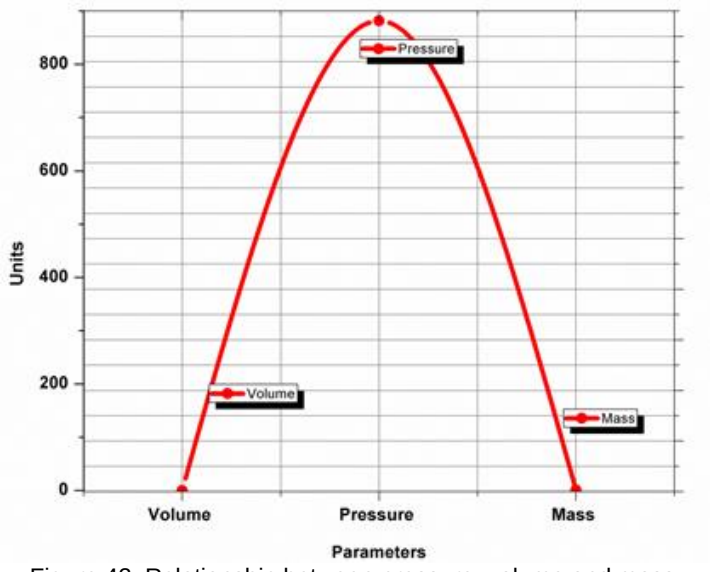

Figure 42: Relationship between pressure, volume and mass.

3.4.7. THE HOOP STRESS, σ_h

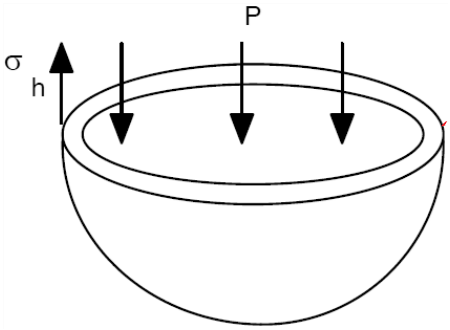

Figure 43: The hoop stress σ_h.

$$\sigma_L = \frac{PD}{4t}$$
$$= \frac{3500 \times 0.2}{4 \times 0.001}$$
$$= 175\text{kPa}$$

3.5. MESH WIRE DESIGN

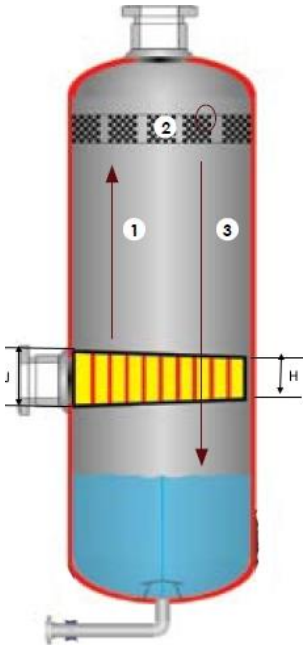

Figure 44: Demister mist eliminator to separate dry steam and saturated steam.

3.5.1. OPERATION OF A DEMISTER MIST ELIMINATOR

As demonstrated in Figure 44 above, a Demister Mist Eliminator operates according to the following 3 steps:

1. A vapour stream carrying entrained liquid vapour droplets passes through a demister pad. The vapour moves freely through the knitted mesh.
2. The inertia of the droplets causes them to contact the wire surfaces and coalesce.
3. The large, coalesced droplets formed in the mesh ultimately drain and drop to the vessel bottom. Suitable design velocities occur at a K – factor of 0.11 m/s for velocity flow, V_s. Actual vapour velocity, m/s ρ_v vapour density, kg/m^3, ρ_l water density, kg/m^3.

$$V_s = K\left(\frac{\rho_1 - \rho_V}{\rho_V}\right)^{0.5}$$

$$= 0.11\left(\frac{1000 - 1.12083}{1.12083}\right)^{0.5}$$

$$= 3.28\,\text{m/s}$$

3.5.1.1. ALLOWABLE STEAM SPEED THROUGH THE MESH WIRE

The mist mat shall have:

- A free volume of at least 97 % (ε = 0.97)
- A wire thickness, d_w, between 0.23 mm and 0.28 mm.

An approximate pressure drop ΔP within the mesh wire pad. Wet is $\Delta P = C(\rho_1 - \rho_v)K^2 t$,

Factor C=0.2 for a general purpose (GP) style mesh demister. T is the pad thickness; note that the dry pressure drop is 0.5ΔP of wet pressure drop. Thus, the following dimensions are required:

Grid depth is 5mm.

Pad depth is 30mm.

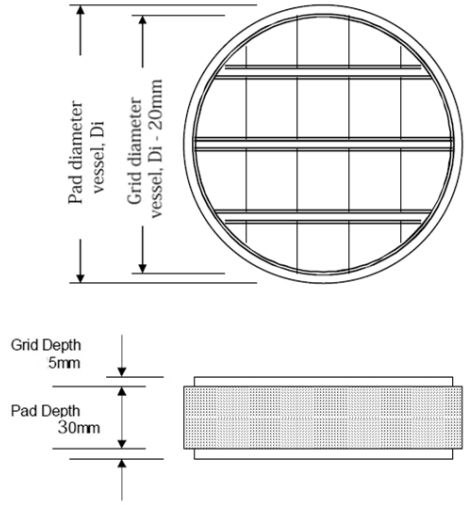

Figure 45: Mesh wire of a flash evaporator.

$$\Delta P = C(\rho_1 - \rho_v)K^2 t$$
$$= 0.2(1000 - 1.12083) \times 0.11^2 \times 0.03$$
$$= 0.073\,\text{Pa}$$

3.5.1.2. DRY PRESSURE DROP

$$= \frac{0.073}{2}$$
$$= 0.036\,\text{Pa}$$

3.6. DIFFUSER DIMENSIONS

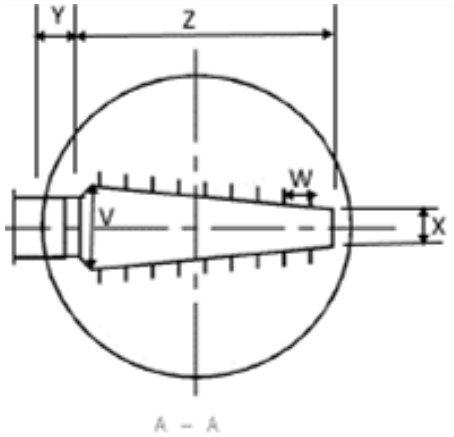

Figure 46: Diffuser dimensions.

$Y = 50\,mm$

$Z = 130\,mm$

$W = 10\,mm$

$V = 80\,mm$

$X = 15\,mm$

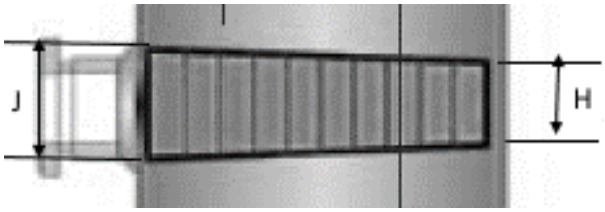

Figure 47: Diffuser dimensions.

$J = 50\,mm$

$H = 30\,mm$

3.6.1. BLADE DIMENSIONS

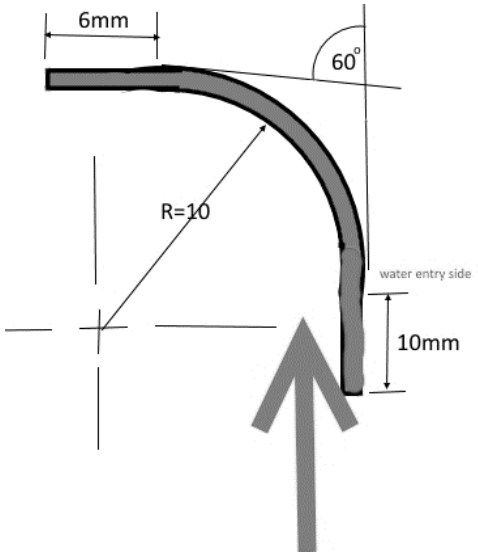

Figure 48: Diffuser blade.

3.6.2. DIMENSIONS

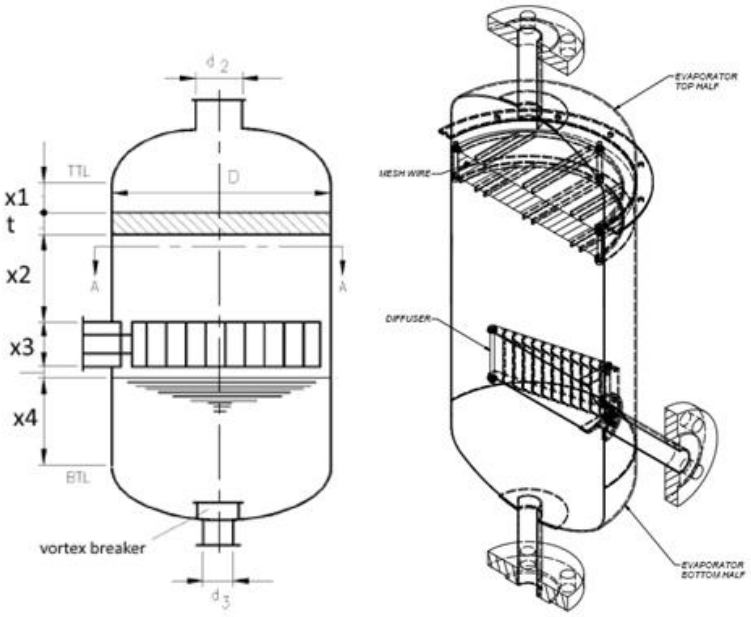

Figure 49: Positions of the Diffuser and Mesh wire.

$$x_1 = 0.15 D_i$$
$$= 0.15 \times 0.2$$
$$= 30\,\text{mm}$$

$$T = 30mm$$
$$x_2 = 0.6 D_i$$
$$= 0.6 \times 0.2$$
$$= 120\,\text{mm}$$

$$x_3 = d_1 0.02$$
$$= 0.022 \times 0.02$$
$$= 42\text{mm}$$

$$x_4 = 0.3 D_i$$
$$= 0.3 \times 0.2$$
$$= 60\text{mm}$$

3.7. WATER CLEARANCE BETWEEN THE DIFFUSER AND WATER LEVEL 18 mm

Figure 50 below shows the mass flowrate process from stages 1 to 6 of the fluid. The temperature of the fluid, steam properties including enthalpy (kJ/kg) and entropy (kJ/kg. K) of the steam are demonstrated.

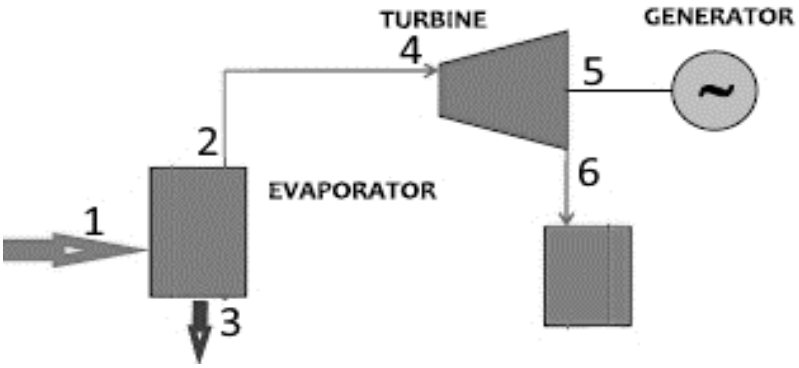

Figure 50: Process layout of OTEC open cycle plant.

3.7.1. STATE 2-4 PROPERTIES

$T_{st4} = 26.52\ ℃$

$P_{st4} = 3.5\text{kPa}$

$h_4 = \cdots$

$$\frac{30-26.52}{30-25} = \frac{2555.5-h_4}{2555.5-2546.5}$$

$$\therefore h_4 = 2549.236\ \text{kJ/k}$$

$$S_4 = S_5$$

$$\frac{30-26.52}{30-25} = \frac{8.4520-S_4}{8.4520-8.5566}$$

$$S_4 = 8.5248\ \text{kJ/kgK}$$

3.7.2. STATE 5 PROPERTIES

$$\frac{25-24}{25-20} = \frac{0.3672-S_{f5}}{0.3672-0.2965}$$

$S_{f5} = 0.35306\ \text{kJ/kgK}$

$\frac{25-24}{25-24} = \frac{8.1894-S_{fg5}}{8.1894-8.3695}$

$S_{fg5} = 8.22542\ \text{kJ/kgK}$

$S_5 = S_{f5} + X_5 S_{fg5}$ at 24℃

$8.5248 = 0.35306 + X_5 \times 8.22542$

$\therefore X_5 = 0.99$

$\frac{25-24}{25-24} = \frac{104.8-h_{f5}}{104.8-83.9}$

$h_{f5} = 100.62\ \text{kJ/kgK}$

$\frac{25-24}{25-24} = \frac{2441.7-h_{fg5}}{2441.7-2453.5}$

$h_{fg5} = 2444.06\ \text{kJ/kgK}$

$h_5 = h_{f5} + X_5 h_{fg5}$

$= 100.62 + 0.99 \times 2444.06$

$h_5 = 2520.2394\ \text{kJ/kg}$

Figure 51 illustrates the OTEC process, where the mass flowrate, temperature and the velocity of the fluid has been simulated. If the pressure is decreasing on the OTEC plant process, the mass flowrate of the fluid increased with the temperature. This clearly demonstrates that if the temperature of the OTEC plant can increase, the amount of energy obtained will also increase.

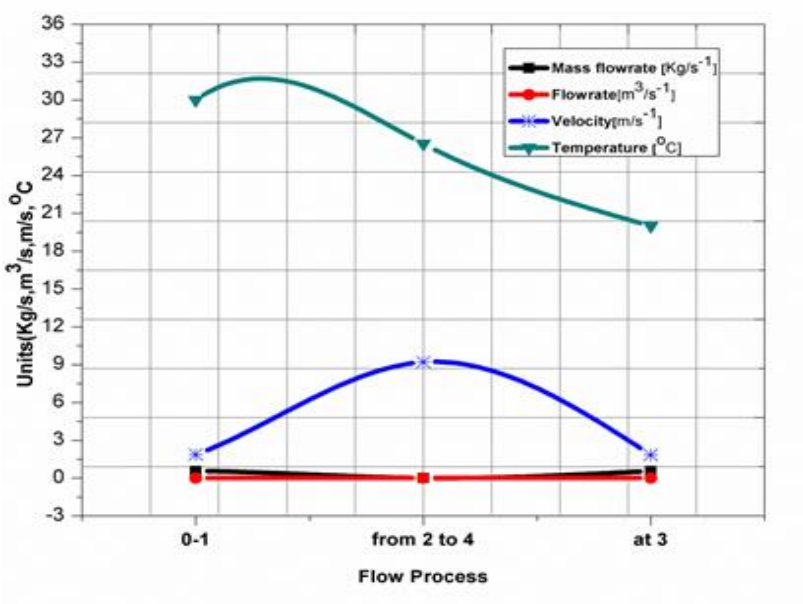

Figure 51: OTEC plant process graph.

Table 10 below tabulates the process parameters that were calculated to simulate the OTEC Plant. These parameters such as mass flowrate, velocity and temperature were calculated on the different process stages.

TABLE 10: PROCESS PARAMETERS.

Process	Mass flowrate	Flowrate	Velocity	Temp
0-1	0.573 Kg/s	0.000583 m^3/s^{-1}	1.857 m/s^{-1}	30 ^oC
from 2 to 4	0.003238 Kg/s	0.00299 m^3/s^{-1}	9.2 m/s^{-1}	26.52 ^oC
at 3	0.5698 Kg/s	0.00058 m^3/s^{-1}	1.845 m/s^{-1}	20 ^oC

3.7.3. PIPE AREA REDUCTION

$$\dot{m}_{st,a} = \dot{m}_{st,b}$$

$$\rho A_a v_a = \rho A_a v_a$$

$$\frac{\pi}{4} \times 0.02^2 \times 9.2 = \frac{\pi}{4} \times 0.015^2 \, v_a$$

$$v_a = 16.35 \, m/s$$

Therefore, speed Nozzle V_a = 16.35 m/s

3.7.4. PARAMETRIC ANALYSIS

The effect of flow rate($\dot{Q}$), temperature (T), number of turns on effectiveness and overall heat transfer coefficient (U) on the functioning of the OTEC plant are discussed below.

3.7.4.1. EFFECT OF FLOWRATE ON EFFECTIVENESS

As the flow increases in the flow configuration of helical copper pipe, effectiveness increases slightly to a certain temperature, and starts decreasing gradually after the maximum temperature is reached. As flowrate of cold water increases, there is less contact time (period) with hot water or steam. Therefore, effectiveness begins to decrease.

3.7.4.2. EFFECT OF FLOWRATE ON OVERALL HEAT TRANSFER COEFFICIENT

As the flowrate increases in the flow configuration, overall heat transfer coefficient increases slightly to a certain temperature then after that point it decreases.

3.7.4.3. EFFECT OF TEMPERATURE ON OVERALL HEAT TRANSFER COEFFICIENT

In the flow configuration of the helical copper pipe, as temperature increases the overall heat transfer coefficient increases sharply, then begins to decrease, until finally maintaining a constant overall heat transfer coefficient.

TABLE 11: OPERATING PARAMETERS OF THE HELICAL COIL HEAT EXCHANGER [239].

Parameters	**Cold Water (chilled)**		**Saturated Steam**	
Mass flowrate ($\dot{m}$)	19.8kg/s		0.01636kg/s	
Inlet temperature (t_i)	5^{o}C	278.15K	131 ^{o}C	404.15K
Outlet temperature (t_o)	40 ^{o}C	313.15K	71 ^{o}C	344.15K
Specific heat capacity (Cp)	4.202 kj/kg. K		2.18099kj/kg. K	
Parental Number (Pr)	6.0816		1.82	
Pressure (kPa)	101.325kPa		176.871kPa	
Thermal conductivity (K)	0.60932W/m. K		0.016W/m. K	

Viscosity (μ)	0.001520kg/m. s	13.3349×10^{-6} kg/m. s
Density (ρ)	1000kg/m^3	1.53778kg/m^3
Velocity (υ)	1.5m/s	28m/s

TABLE 12: PHYSICAL PROPERTIES OF COPPER [240].

Properties	**Matrix**	
	Values	**Units**
Density	8.92	g/cm^3
Melting point	1083	℃
Boiling point	2595	℃
Latent heat of fusion	205	J/g
Specific Heat Capacity @ 100℃	0.393	J/g℃
Linear Coefficient of Thermal Expansion @ (25°C - 100°C)	16.8 x 10^{-6}	cm/cm°C
Thermal Conductivity @ 100℃	3.85	Wcm/cm^2 °C
Electrical Conductivity (Volume) @ (20°C) Fully Cold Worked	56.3	MS/m(mΩmm^2)
Electrical Resistivity (Volume) @ (20°C) Fully Cold Worked	1.78	μΩ·cm
Modulus of Elasticity (Tension) @ (20°C) Annealed	118,000	MPa

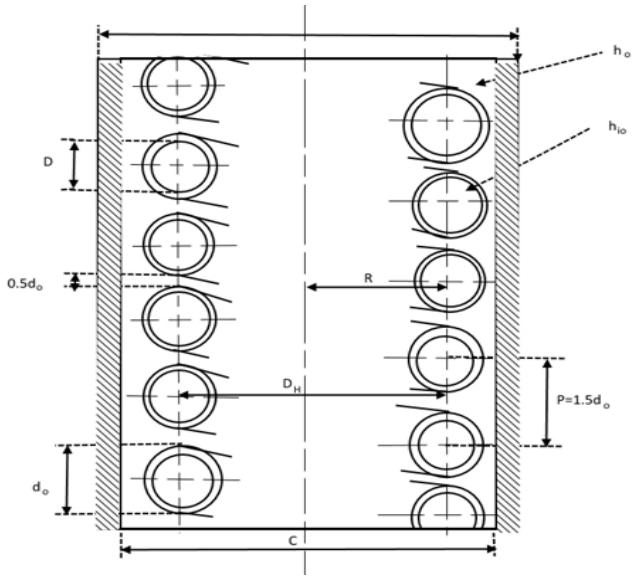

Figure 52: Schematic drawing Helical Coil Tube Heat Exchanger [241].

The geometry considered and the systems of the coordinates are illustrated in Fig. 42 (where, $d_{i,inner}$ is the diameter of the inner coiled tube; R_c is the coil radius; H is the distance between the two turns; and $d_{o,inner}$ is the inner diameter of the outer tube).

In the present study, the Cartesian coordinate system (x, y, and z) are used to represent flow in numerical simulation. The flow and heat transfer develop simultaneously down-stream in the helical pipe.

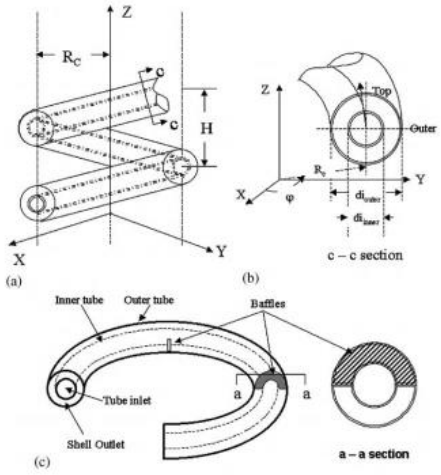

Figure 53: Tube-in-tube helical heat exchanger [242].

3.7.5. DESIGN PROCEDURE FOR HELICAL COIL HEAT EXCHANGER CONDENSOR

The height of the shell/cylinder is 500mm. The minimum height of the cylinder required to accommodate several turns of coils is 400mm, P is the pipe size in diameter, therefore number of turns, N is;

$$H = NP + d_o$$
$$0.4 = N \times 0.0225 + 0.015$$
$$N = 17.11 \approx 17$$

3.7.5.1. CONDENSOR COIL DESIGN

$$P_r = \frac{\mu C_p}{K}$$
$$= \frac{12.9553 \times 10^{-6} \times 2125.54}{K} = 1.72$$

$$x_1 = 0.5 d_o$$
$$= 0.5 \times 0.015$$
$$= 7.5\,mm$$

$$x_2 = 0.5 d_o$$
$$= 0.5 \times 0.015$$
$$= 7.5\,mm$$

$$P = 1.5 d_o$$
$$= 1.5 \times 0.015$$
$$= 22.5\,mm$$

$$D_H = C - 2 d_o$$
$$= 0.2 - 2 \times 0.015$$
$$= 170\,mm$$

$$r = 0.5 D_H$$
$$= 0.5 \times 0.17$$
$$= 85\,mm$$

3.7.5.2. HEAT TRANSFER COEFFICIENT OUTSIDE THE COIL (H_o)

Length of the coil (L)

$$L = N\sqrt{(2\pi(A))^2 + P^2}$$
$$= 17.11\sqrt{(2\pi \times 0.085)^2 + (0.0225)^2}$$
$$= 9.15\,m \approx 9\,m$$

3.7.5.3. VOLUME OCCUPIED BY THE COIL (V_c)

$$V_c = \left(\frac{\pi}{4}\right) d_o{}^2 L$$

$$= \left(\frac{\pi}{4}\right)(0.015)^2(9.15)$$

$$= 1.62 \times 10^{-3}\ \mathrm{m}^3$$

3.7.5.4. VOLUME OF THE ANNULUS (V_a)

$$V_a = \left(\frac{\pi}{4}\right) C^{\ 2} PN$$

$$= \left(\frac{\pi}{4}\right)(0.2)^2(0.0225)17.11$$

$$= 12.09 \times 10^{-3}\ \mathrm{m}^3$$

3.7.5.5. VOLUME AVAILABLE FOR THE FLOW OF THE FLUID IN THE ANNULUS (V_f)

$$V_f = V_a - V_c$$

$$= 12.09 \times 10^{-3} - 1.62 \times 10^{-3}$$

$$= 10.47 \times 10^{-3}\ \mathrm{m}^3$$

3.7.5.6. SHELL SIDE EQUIVALENT DIAMETER OF THE COILED TUBE (D_e)

$$D_e = \frac{4V_f}{\pi d_o L}$$

$$= \frac{4\left(10.4 \times 10^{-3}\right)}{\pi(0.015)(9.15)}$$

$$= 97.13\mathrm{mm}$$

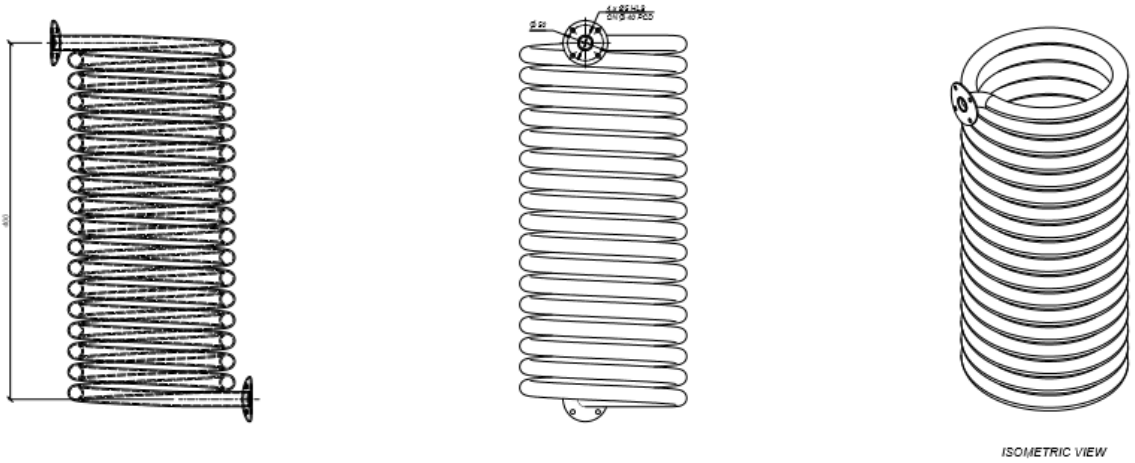

Figure 54: Shell-side equivalent diameter of the coiled tube.

3.7.5.7. STEAM CALCULATIONS

Steam flowrate $(\dot{Q}_s)$

$$\dot{Q}_s = vA$$

$$= 28 \times \frac{\pi}{4}(0.022)^2$$

$$= 10.64 \times 10^{-3}\ m^3/s^{-1}$$

3.7.5.8. MASS FLOWRATE OF THE STEAM $(\dot{m}_s)$

$$\dot{Q}_s = \frac{\dot{m}_s}{\rho} = 10.64 \times 10^{-3}$$

$$= \frac{\dot{m}_s}{1.12083}$$

$$\dot{m}_s = 11.93 \times 10^{-3} Kg/s^{-1}$$

3.7.5.9. MASS VELOCITY OF FLUID (G_s)

$$\dot{Q}_s = \frac{\dot{m}_s}{\frac{\pi}{4}C^2}$$

$$= \frac{11.93\times10^{-3}}{\frac{\pi}{4}(0.2)^2}$$

$$= 0.37960\,\text{Kg/m}^2\text{s}$$

3.7.5.10. REYNOLDS NUMBER (N_{Re})

$$N_{Re} = \frac{D_e G_s}{\mu_s}$$

$$= \frac{97.13\times10^{-3}\times0.3796}{12.9553\times10^{-6}}$$

$$= 2845.96$$

Heat transfer coefficient outside the coil (h_o), For Reynolds Number, N_{Re}, in the range of 50 > N_{Re} >10 000.

$$\frac{h_o D_e}{k} = 0.6\,N_{Re}^{0.5} N_{Pr}^{0.31}$$

$$= \frac{h_o\times0.09713}{0.016} = 0.6\times2845.96^{0.5}\times1.72^{0.31}$$

$$= h_o = 6.238\,\text{W/m}^2\text{K}$$

3.7.5.11. HEAT TRANSFER COEFFIENT INSIDE THE COIL (h_i)

Reynolds Number (N_{Re})

$$N_{Re} = \frac{\rho_c v D}{\mu_c}$$

$$= \frac{1000\times1.5\times0.013}{0.001520}$$

$$= 12828.95$$

3.7.5.12. TURBULENT FLOW N_{re}>10000

$$N_{up} = \frac{h_i D_p}{k_p} = 0.023 N_{Rep}^{4/5} N_{pr_p}^{n}$$

$$n = 0.4. \text{if .fluid..is..being..heated.}$$

$$\therefore N_{up} = 0.023 N_{Rep}^{4/5} N_{pr_p}^{n}$$

$$= 0.23(12828.95)^{4/5}(6.0816)^{0.4}$$

$$= 91.6$$

$$N_{up} = \frac{h_i D_p}{k_p}$$

$$91.6 = \frac{h_i \times 0.013}{0.60932}$$

$$h_i = 4293.36 \, W/m^2K$$

3.7.5.13. HEAT TRANSFER COEFFICIENT BASED ON THE OUTSIDE DIAMETER (h_{io})

$$h_{io} = h_i \frac{D}{d_o}$$

$$= 4293.36 \times \frac{0.013}{0.015}$$

$$= 3720.91 W/m^2K$$

3.7.5.14. OVERALL HEAT TRANSFER COEFFICIENT (U)

The fouling factors, R_t depend on the nature of the fluids – namely, the presence of suspended matter in the fluids, the operating temperature and the velocities of the fluids. For water R_t and R_a are 0.0002m^2 K/W. Thermal conductivity of Copper is $K_{coppert}$ = 385 W/MK.

$$\frac{1}{U} = \frac{1}{h_o} + \frac{1}{h_{io}} + \frac{t_{coil}}{K_{cu}} + R_t + R_a$$

$$\frac{1}{U} = \frac{1}{h_o} + \frac{1}{h_{io}} + \frac{t_{coil}}{K_{cu}} + 0.0002 + 0.0002$$

$$\frac{1}{U} = 0.1610562727$$

$$\therefore U = 6.209\,W/m^2K$$

3.7.5.15. DETERMINE THE REQUIRED AREA (m^2)

The log-mean temperature difference, (^oC)

$$\Delta t_{1m} = \frac{\left[\left(t_s - t_w\right)_{inlet} - \left(t_s - t_w\right)_{outlet}\right]}{\ln\left[\frac{\left(t_s - t_w\right)_{inlet}}{\left(t_s - t_w\right)_{outlet}}\right]}$$

$$= \frac{\left[\left(120-5\right) - \left(43-40\right)\right]}{\ln\left[\frac{\left(120-5\right)}{\left(43-40\right)}\right]}$$

$$= 30.72\,°C$$

3.7.5.16. CORRECTION FACTOR IS 99%

$$\Delta t_c = 0.99\,\Delta t_{1m}$$

$$= 0.99 \times 30.72$$

$$= 30.41^o\,C$$

$$\Delta T_c = t + 273.15$$

$$= 30.41 + 273.15$$

$$= 303.56\,K$$

3.7.5.17. THE HEAT LOAD (Q)

$$Q = \dot{m}_s C_p \Delta t_s$$
$$= 11.93\times10^{-3} \times 2125.54(393.15-316.15)$$
$$= 1952.54\,W$$

3.7.5.18. THE REQUIRED AREA

$$A = \frac{Q}{U\Delta t_c}$$
$$= \frac{1952.54}{6.209\times303.56}$$
$$= 1.04\,m^2$$

3.8. TURBINE OVERVIEW

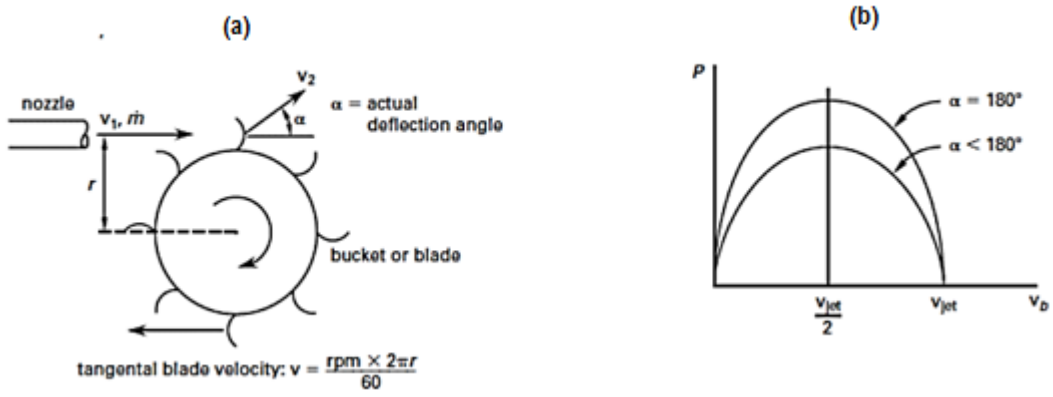

Figure 55: Deflector and characteristics [243].

The total pressure head h of the steam in the nozzle causes the steam to be discharged with a velocity V_1 from the nozzle [244].

If the velocity coefficient of the nozzle is C_v, then

$$V_1 = C_v\sqrt{2gh} \tag{3.12}$$

If the wheel is turning at a speed of $N\,r/\min$ or $\omega\,\frac{rad}{s}$. then the velocity of the case on a pitch circle diameter is D.

$$u = \frac{D}{2}\omega = \frac{\pi N}{60} \tag{3.13}$$

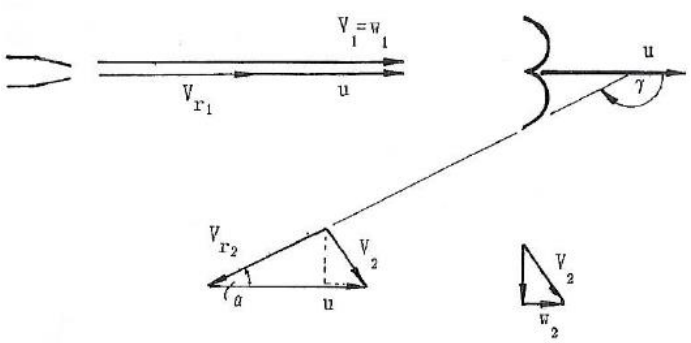

Figure 56: Velocity diagram of a Pelton wheel [245].

The velocity with the steam strikes the case is;

$$V_{r1} = V_1 - u \tag{3.14}$$

3.8.1. TURBINE DESIGN

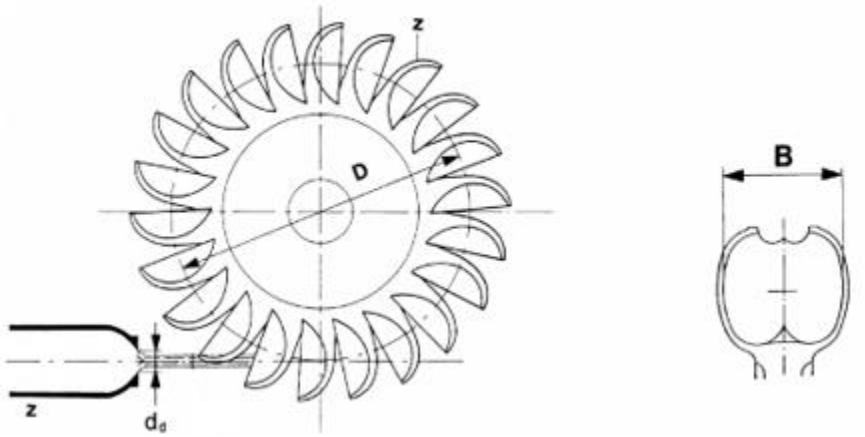

Figure 57: Velocity diagram of a Pelton wheel [263].

The velocity with which the steam strikes the case is;

$$V_{r1} = V_1 - u$$
$$= 16.35 - 8.175$$
$$= 8.175 \frac{m}{s}$$

The steam slides along the wall of the case and is deflected through an angle γ deflection angle, and leaves the case with a relative velocity v_{r2} which is usually less than v_{r1} due to friction losses. This is calculated using $v_{r2} = nv_{r1}$, n being a constant which represents the losses. Usually the value of n is about 90% - the velocity of the steam is reduced by 10% while flowing across the case.

$$v_{r2} = nv_{r1}$$
$$= 0.9 \times 8.175$$
$$= 7.36 \text{m/s}^{-1}$$

Hydraulic efficiency is 96%

3.8.2. BUCKETS WIDTH DIMENSION

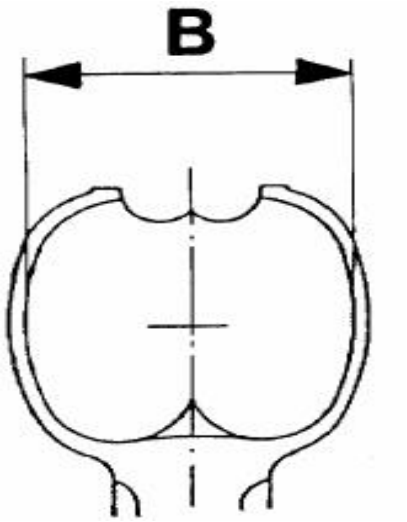

Figure 58: Buckets' width dimension.

3.8.3. RULES OF THUMB

$$B = 3{,}1.d_s \; 1 \text{nozzle}$$
$$B = 3{,}2.d_s \; 2 \text{nozzles}$$
$$B = 3{,}3.d_s \; 4-5 \text{nozzles}$$
$$B > 3{,}3.d_s \; 6 \text{nozzles}$$

$$B = 3.1d_s$$
$$= 3.1 \times 0.015$$
$$= 0.0465\text{m} = 46.5\text{mm}$$

3.8.3.1. BUCKET WIDTH

$$B = 3.1d_s$$

$$= 3.1 \times 0.008$$

$$= 0.0248\text{m} = 24.8\text{mm}$$

3.8.3.2. BUCKET HEIGHT

$$h = 2.7d$$

$$= 2.7 \times 0.008$$

$$= 0.0216\ \text{m} = 21.6\ \text{mm}$$

3.8.3.3. CAVITY LENGTH

$$h_1 = 0.35d$$

$$= 0.35 \times 0.008$$

$$= 0.0028 = 2.8\ \text{mm}$$

3.8.3.4. LENGTH TO IMPACT POINT

$$h_2 = 1.5d$$

$$= 1.5 \times 0.008$$

$$= 0.012 = 12\ \text{mm}$$

3.8.3.5. BUCKET DEPTH

$$t = 0.9d$$

$$= 0.0072 = 7.2\ \text{mm}$$

3.8.3.6. CAVITY WIDTH

$$a = 1.2d$$

$= 1.2 \times 0.008$

$= 0.0096\ \text{m} = 09.6\ \text{mm}$

3.8.3.7. OFFSET OF BUCKET

$k = 0.17d$

$= 0.17 \times 0.008$

$= 0.00136 = 1.36\text{mm}$

3.8.4. RUNNER DIAMETER

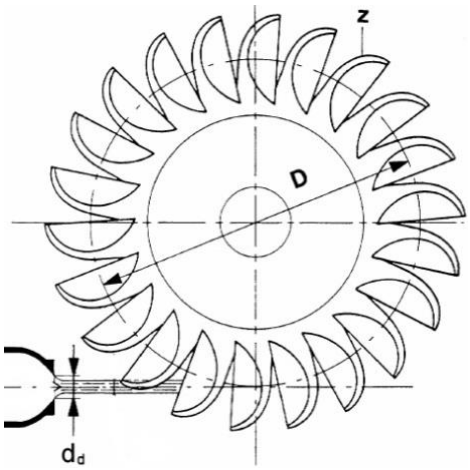

Figure 59: Runner diameter.

3.8.5. RULES OF THUMB

$D = 10.d_s$

$= 10 \times 0.015$

$= 0.15\,\text{m} = 150\,\text{mm}$

BUCKET VELOCITY

Bucket velocity, U_1 is half velocity of the Nozzle jet, V_1

$U_1 = 0.5V_1$

$= 0.5 \times 16.35$

$= 8.175\,\text{m/s}^{-1}$

3.8.6. TURBINE SPEED

$$n = \frac{60\,U_1}{\pi D}$$
$$= \frac{60 \times 8.175}{\pi \times 0.15}$$
$$= 1040.87\,\text{r/min}$$

Choose the number of poles on the generator, the speed of the runner is given by the generator and the net frequency:

$$n = \frac{3000}{z_p}$$

where, Z_p is the number of poles on the generator.

3.8.7. THE NUMBER OF POLES WILL BE;

$$Z_p = \frac{3000}{n}$$
$$= \frac{3000}{1040.87}$$
$$= 2.88$$

The number of poles is approximately 3, therefore recalculate the other parameters:

3.8.8. RECALCULATE THE SPEED RUNNER

$$n = \frac{3000}{z_p}$$
$$= \frac{3000}{3}$$
$$= 1000\,\text{rpm}$$

3.8.9. RECALCULATE RUNNER DIAMETER

$$n = \frac{60\,U_1}{\pi D}$$
$$= \frac{60 \times 8.175}{\pi \times 1000}$$
$$= 0.156\,\text{rpm}$$

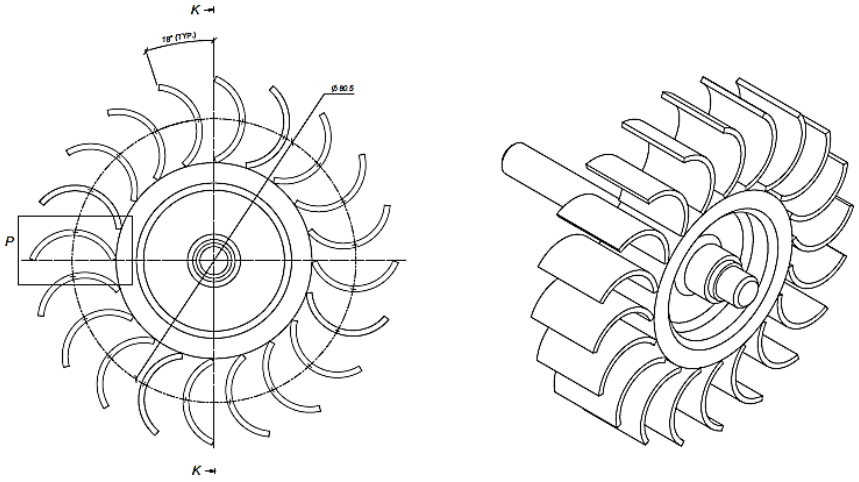

Figure 60: Runner diameter.

Number of buckets is Z ≥ 17.

Choose 22 buckets for this design.

The angle between buckets is $\frac{360}{22} = 16.36^{o}\,C$

The runner with blades must fit the Turbine housing.

The maximum speed number for a Pelton turbine

3.8.10. Nozzle

$$\underline{\omega} = \frac{d_s}{D}\sqrt{\frac{\pi z}{4}}$$
$$= \frac{0.015}{0.15}\sqrt{\frac{\pi \times 1}{4}}$$
$$= 0.089$$

$$\dot{M}_{st,tb} = \rho A v$$

$$= 1.12083 \times \frac{\pi}{4}(0.02)^2 \times 7.36$$

$$= 0.00259\,\text{Kg/s}^{-1}$$

$$Q_{ww} = Av$$

$$= \frac{\pi}{4}(0.02)^2 \times 7.36$$

$$= 0.0023\,\text{m}^3/\text{s}^{-1}$$

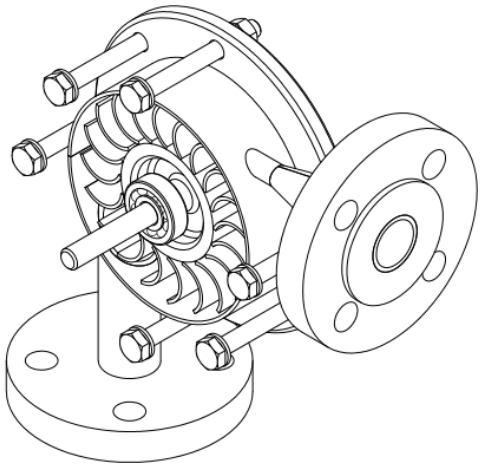

Figure 61: Structural design of a turbine.

3.8.11. NOZZLE DESIGN

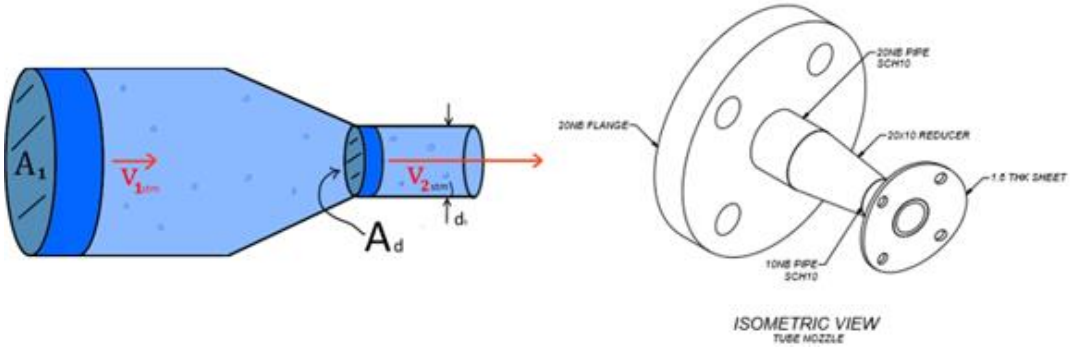

Figure 62: Structural design of a nozzle.

3.8.12. PIPE AREA REDUCTION

Operating Nozzle diameter: 8 mm

$\dot{m}_{st,1} = \dot{m}_{st,2}$

$\rho A_1 \upsilon_1 = \rho A_2 \upsilon_2$

$0.02^2 \times 9.2 = 0.008^2 \upsilon_2$

$V_2 = 57.5\ m/s^{-1}$

Therefore, speed nozzle is $\upsilon_a = 57.5\ m/s^{-1}$

3.8.13. FLOWRATE IN THE NOZZLE

$\dot{Q} = AV$

$= \frac{\pi \times 0.008^2}{4} \times 57.5$

$= 0.00289\ m^3/s^{-1}$

3.8.14. BUCKET VELOCITY

Bucket velocity, U_1 is the half velocity of the Nozzle jet, $V_2 = V_1$

$U_1 = 0.5V_1$

$= 0.5 \times 57.5$

$= 28.75 m/s^{-1}$

3.8.15. WATER DIAMETER IN THE JET

$d_s = \sqrt{\frac{4\dot{Q}}{z\pi V_1}}$

$= \sqrt{\frac{4 \times 0.00289}{1 \times \pi \times 57.5}}$

$= 8\ mm$

3.9. TANK DESIGN (HOT WATER RESERVOIR)

$400 \times 300 \times 300\ mm$, Water temperature is $30^\circ C$ at pressure $= 101.325 kPa$.

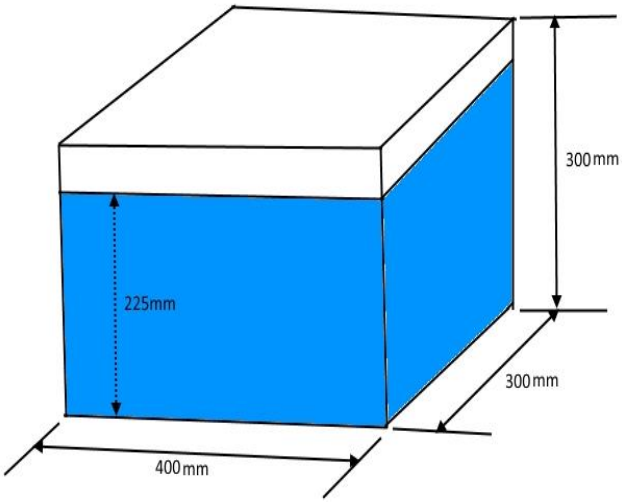

Figure 63: Water storage.

3.9.1. TANK VOLUME

$$= 0.4 \times 0.3 \times 0.3$$
$$= 0.036\,\mathrm{m}^3$$

3.9.2. WATER VOLUME

$$= 0.4 \times 0.3 \times 0.23$$
$$= 0.027 m^3$$

3.9.3. WATER HEIGHT

$$= \frac{0.027}{0.4 \times 0.3}$$
$$= 0.225\,\mathrm{m}$$

3.9.4. Litres of water

$$= 27.6\,\mathrm{l}$$

3.9.5. MASS OF WATER

$$m_w = \rho V$$
$$= 995.71 \times 0.0276$$
$$= 27.48\,\text{Kg}$$

3.10. PUMP DESIGN SELECTION

TABLE 13: HPE60 PERIPHERAL PUMP.

Parameters	Values
Power, P	0.37 kW
Flow rate, Q	35 l/min
Head max, H	35 m
Speed, N	2850 rpm

It must be noted that the pump requirements appear to be parger than the turbogenerator output. This is a scaling problem caused by financial and technical restraints imposed when designing the model. When designing practical systems this discrepancy will fall away as the larger the system, the more efficient it becomes and the less relative power is required for the vacuum pump.

TABLE 14: INPUTS AND CONSTRAINTS OF THERMODYNAMIC ANALYSIS.

Parameter	Symbol	Value
HPE60 Peripheral Pump		
Power	P	0.37 kW
Head max,	H	35 m
Flow rate	Q	35 l/min
Speed	N	2850 rpm
Flash Evaporator design		
Density	d	8000 kg/m^3
Hardness		564 MPa
Tensile strength	T_s	564 MPa
Tensile strength		210 MPa
Elongation at break		58%
Modulus of Elasticity		200 GPa
Specific Heat Capacity		2093.4 J/kgK
Melting point		1400 – 1450 ^{0}C
Temperature at intake	T_{in}	30^{o}C = 303.15 K
Specific heat capacity at T_{in}	Cp	4.182 kJ/kgK.
temperature at the discharge	T_{out}	20^{o}C = 293.15 K
	υ	$1.857\ \mathrm{m/s}$
Maximum flowrate passing the pump is, before evaporator.		
Mass flowrate of warm water	$\dot{M}_{in}$	$0.573\ \mathrm{kg/s}$
Steam mass flowrate	$\dot{m}_{st}$	$0.003409\ \mathrm{kg/s}$
The mass flowrate balance	$\dot{M}_{out}$	$0.5696\ \mathrm{kg/s}$
Velocity of discharged water	υ	$1.816\mathrm{m/s}$
Flowrate of discharged water	Q_{ww}	$0.00057\ \mathrm{m^3/s}$
	ΔQ_{ww}	$28.131\ \mathrm{kW}$
Latent heat (L_{nev}), (specific heat of evaporation).	$L_{h,ev}$	$8252.0097\ \mathrm{kJ/kg}$
Low vacuum pressure	$P_{ev} = P_{st}$	3.5 kPa
steam temperature by interpolation	T_{st}	$26.52℃ = 299.67\mathrm{l}$
steam speed inside a pipe	υ	$426.04\mathrm{m/s}$
	$A\upsilon$	$0.1338\ \mathrm{m^3/s}$
State 2 – 4 properties		
	T_{st4}	$26.52℃$
	P_{st4}	$3.5\mathrm{kPa}$
	h_4	$2549.236\ \mathrm{kJ/kg}$
	S_4	$8.5248\ \mathrm{kJ/kgK}$
State 5 properties		
	S_{f5}	$0.35306\ \mathrm{kJ/kgK}$
	S_{fg5}	$8.22542\ \mathrm{kJ/kgK}$
	h_{f5}	$100.62\ \mathrm{kJ/kgK}$
	h_{fg5}	$2444.06\ \mathrm{kJ/kgK}$
	h_5	$2520.2394\ \mathrm{kJ/kg}$
Vessel design		
Outside diameter of the vessel	Do	203.2mm
Inside diameter of the vessel	Di	200mm
Thickness of the vessel	t	1.6mm
Height (length) of the vessel	H	300mm
Volume	V	$304 \times 10^{-6}\mathrm{m^3}$

Mass	M_m	2.43 kg
Properties for calculations		
Design pressure	P	3.5 kPa
Corrosion allowance	cr	0.01%
Nominal wall thickness	nt	1.6mm
Allowable stress	σ_s	210MPa
Elongation efficiency	Ee	70%
Circl efficiency	Ce	85%
Under tolerance allowance	UT	0.0%
Nominal thickness	nt	0.0006 m
	R_i	0.101 m
Thickness before forming	t_b	0.99×10^{-6}m
Thickness after forming	t_a	2.405×10^{-6}m
Required thickness	t_{re}	1×10^{-3}m 1mm<1.6mm
Maximum pressure	P_{max}	868.11 kPa 868.11 kPa >
Mesh wire design		
Allowable steam speed through the mesh wire	V_s	21.75 m/s
mist mat	ε	0.97
wire thickness	dw	between 0.23 mm and 0.28 mm.
Grid depth		5mm
Pad depth		30mm
pressure drop	ΔP	0.072Pa
Dry pressure drop		0.036Pa
Nozzle design		
Pipe area reduction		
Operating Nozzle diameter		8 mm
Speed Nozzle	υ_a	57.5 m/s
Flowrate in the Nozzle	$\dot{Q}$	0.00289 m^3/s
Bucket velocity	U_1	28.75m/s
Water diameter in the jet	d_s	8 mm
velocity with the steam strikes	v_{r1}	28.75 m/s
	v_{r2}	25.875 m/s
Hydraulic efficiency		96%
Turbine speed		6863.56 rpm
Speed runner		7200 pm
Runner diameter		76 mm
Design procedure for helical coil heat exchanger		
PARANDL number	Pr	1.72
Heat transfer coefficient outside the coil (h_o)		
Length of the coil	L	9.15m ≈ 9m
Volume occupied by the coil	V_c	$1.62 \times 10^{-3}m^3$
Volume of the annulus	V_a	$12.09 \times 10^{-3}m^3$

Volume available for the flow of the fluid in the annulus	V_f	$10.47 \times 10^{-3} m^3$
Shell-side equivalent diameter of the coiled tube	D_e	$97.13mm$
Steam calculations		
Steam velocity	υ	$9.2m/s$
Steam flow rate	$\dot{Q}_s$	$0.00289\ m^3/s$
Mass velocity of fluid	G_s	$0.103\ kg/m^2s$
Reynolds Number	N_{Re}	772.78
Heat transfer coefficient outside the coil	h_o	$3.251\ W/m^2K$
Reynolds Number	N_{Re}	$12\ 828.95$
	Nu_p	91.6
	h_i	$4293.36\ W/m^2K$
Heat transfer coefficient based on the outside diameter of the coil	h_{io}	$3720.91\ W/m^2K$
Overall heat transfer coefficient	U	$3.244\ W/m^2K$
Determine the required area		
log-mean temperature difference	Δt_{lm}	$30.72℃$
	Δt_c	$30.41℃$
	ΔT_c	$303.56K$
Heat load	Q	$529.917W$
Required area	A	$538117mm^2$

3.11. TURBINE LAYOUT DESIGN

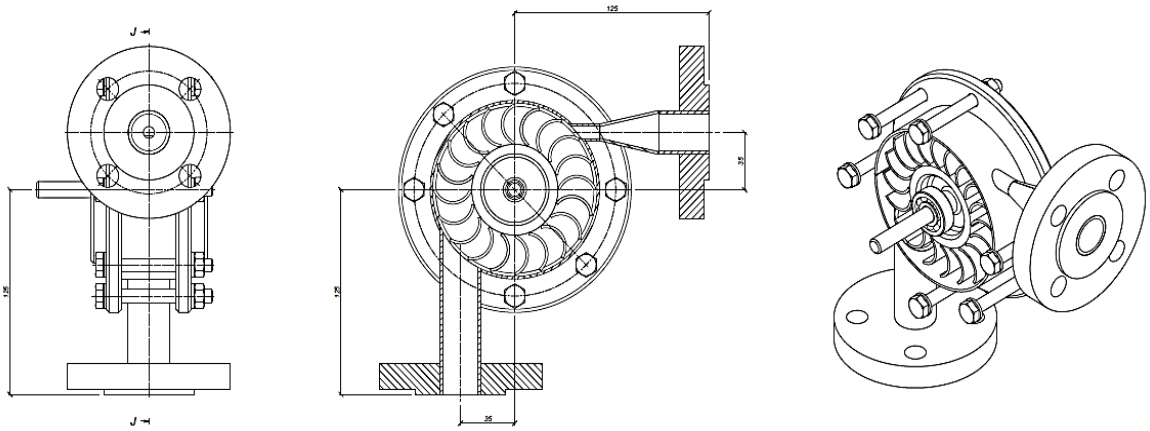

Figure 64: Dimension designs of turbine.

3.12. EVAPORATOR DIFFUSER

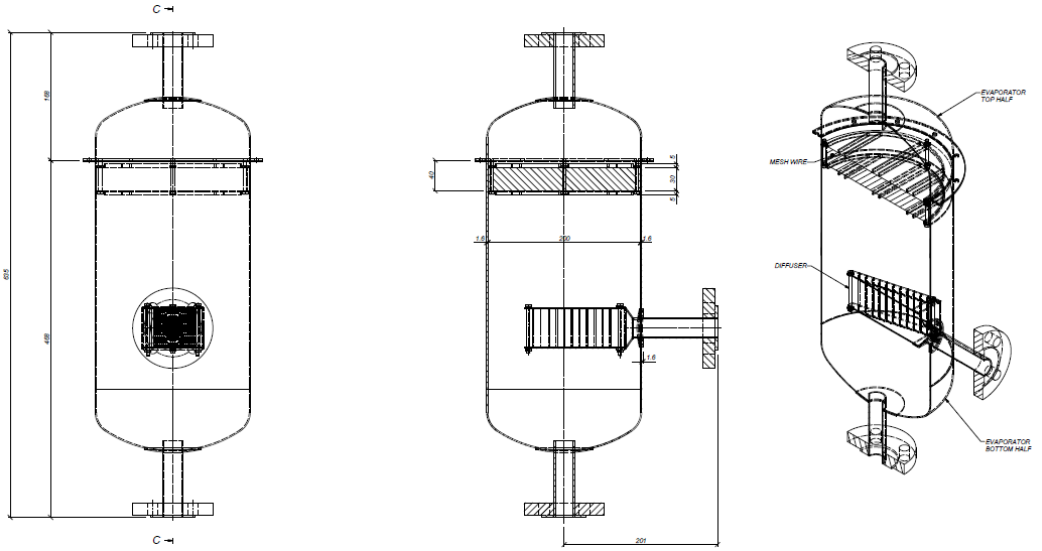

Figure 65: Designs of evaporator.

3.13. OC- OTEC CONDENSER

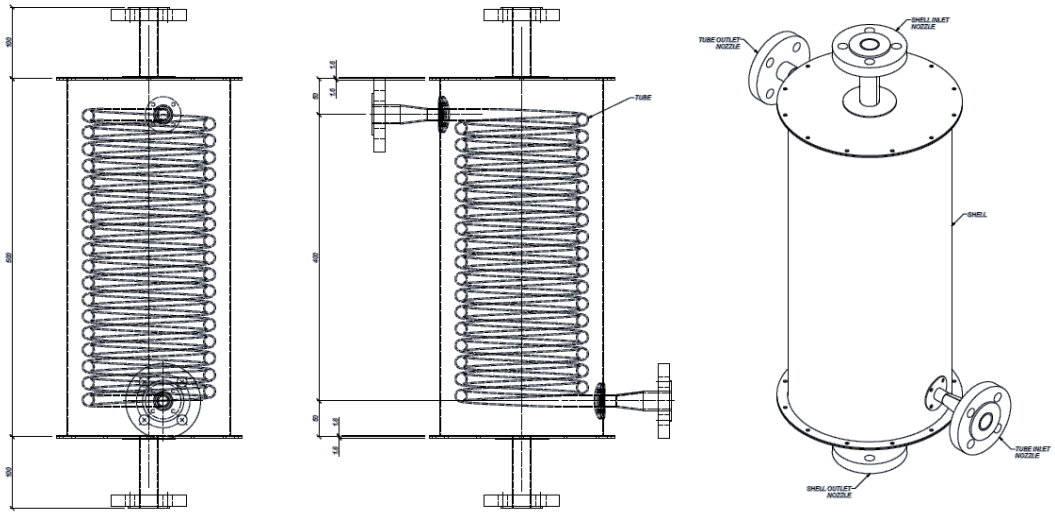

Figure 66: Designs of condenser.

3.14. OC-OTEC EXPERIMENTAL SYSTEM AND PROCEDURE FOR A 5W

A study was carried out on a newly designed OC-OTEC laboratory demonstration system where temperature, mass flowrate and pressure readings were taken before and after each component. The flash evaporator was used in this plant to produce low pressure steam for the steam turbine. The exhausted steam from the turbine was lead to the condenser. Fig. 67 shows a photograph of the OC-OTEC experimental setup.

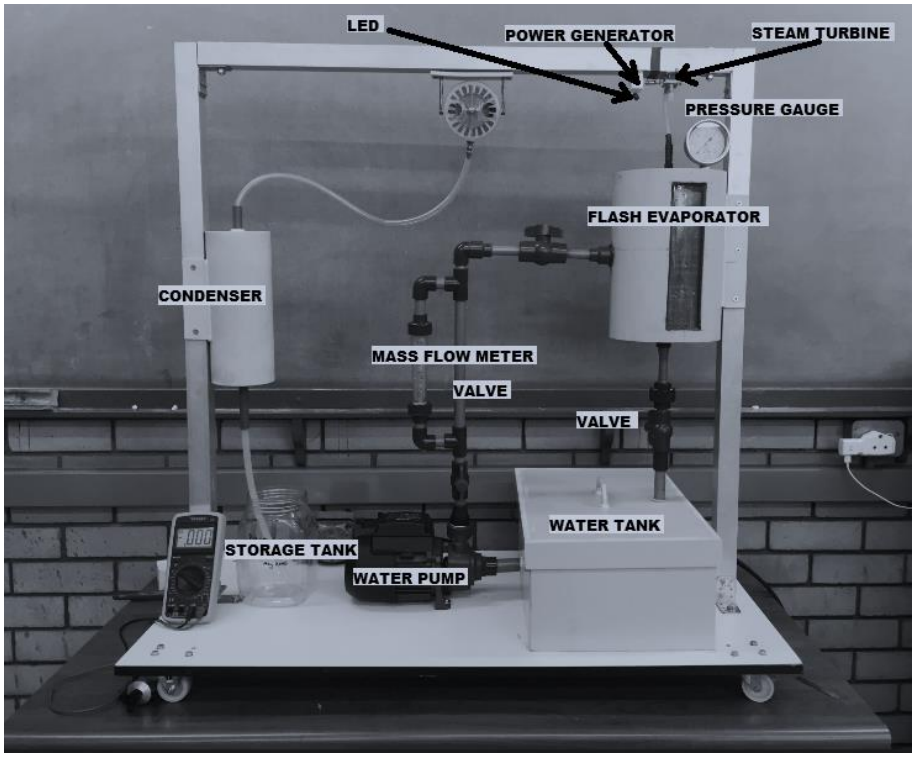

Figure 67: A photograph of the OC-OTEC investigational system.

Outside diameter of the flash evaporator, D_0 has a wall thickness 91,5 mm, with an inside diameter of 20mm and height (H) of 300mm. The design pressure is 3,5kPa and allowable stress σ_s. Mini turbine steam engine, is designed with two universal brass connecting rods with micro power generator. The length is 90mm, width 45mm, high 40mm, and inlet diameter. The Bourdon tube pressure gauge filled with liquid is utilised, with nominal size of 63mm and scale range is 0 – 60kPa. It also contains plastic flow meters for gases & liquids, using trogamid and polysulfone technology. Scaled directly is l/h, m3/h, %.

3.14.1. FLASH EVAPORATOR

This flash evaporator produces steam by dropping the pressure of water at the saturation temperature. The excess heat flashes part of the water into steam. A vertical flash evaporator for introducing a super-heated liquid into flash evaporator chamber includes a vertical inlet tube with a diffuser.

The method of using the flash evaporator for this concept includes flowing liquid upward through the vertical tube into the diffuse chamber where initial expansion and boiling occurs. Un-vaporised liquid sheets and drops collide with each other to enhance surface renewal and evaporation properties, with liquid flowing over the outlet end of the diffuser.

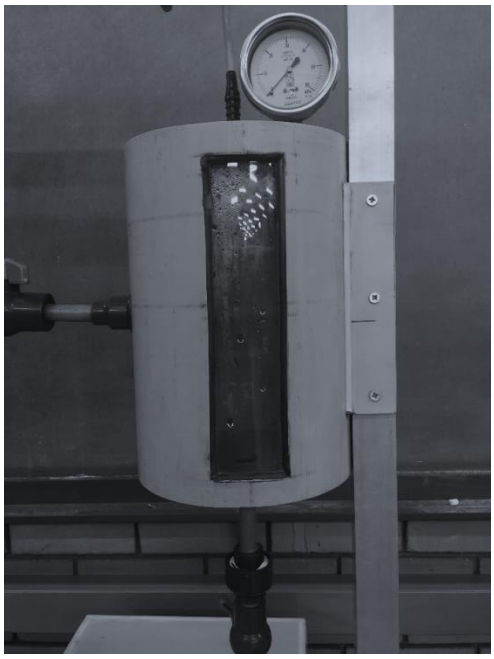

Figure 68: Photo of Flash evaporator.

3.14.2. DIFFUSER

The diffuser increases the residence time of liquid in the flash chamber; the diffuser being a portion of the outlet having a diverging cross–sectional area that is larger than the cross – sectional area of the remaining portion of the cylinder.

Figure 69: Flash Evaporator with a Diffuser.

The vacuum lowers the boiling point of the warm water, to produce the steam that is required to turn the turbine.

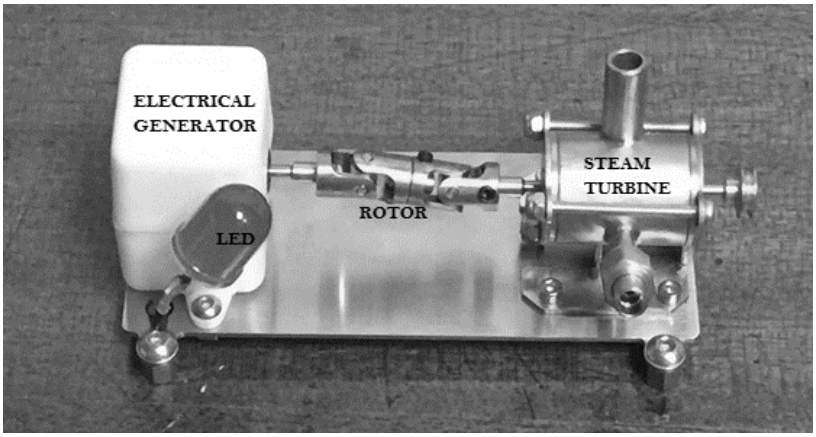

Figure 70: Mini turbine steam engine.

This engine is a mini turbine steam engine, designed with two universal brass connecting rods with micro power generator. When the engine is running, it will power on the LED light, - this is perfectly suited to demonstrate electricity generator theory. The dimensions are as follows: length 90mm, width 45mm, height 40mm, inlet diameter 4mm, outlet diameter 6mm, and output shaft diameter 1.95mm

3.14.3. FLOW METER

The fluid flows up through the tapered tube forcing the float to a position with sufficient free area to enable the flow to pass. This free area is related to the flow rate, the weight of the float, and the density and viscosity of the fluid.

Figure 71: Flow rate meter.

The pressure drop across the flow meter remains constant over the entire flow range. This occurs because the pressure drop is related to the fluid velocity and area of flow; the area of flow increases as the flow rate increases.

3.14.4. VACUUM PUMP OPERATION

Edwards vacuum pump was utilised for experience. The dual-voltage, dual-frequency motor is designed for a single-phase electrical supply and is suitable for 50 Hz or 60 Hz operation. The motor can be manually switched between nominal supply voltages of 110–120 V and 220–240 V.

As we know that the vacuum pump converts the mechanical input energy of a rotating shaft into air-filled energy by evacuating the air contained within a system. The internal pressure level thus becomes lower than that of the outside atmosphere.

The amount of energy produced depends on the volume evacuated and the pressure difference produced. Mechanical vacuum pumps use the same pumping mechanism as

air compressors, except that the unit is installed so that air is drawn from a closed volume and exhausted to the atmosphere.

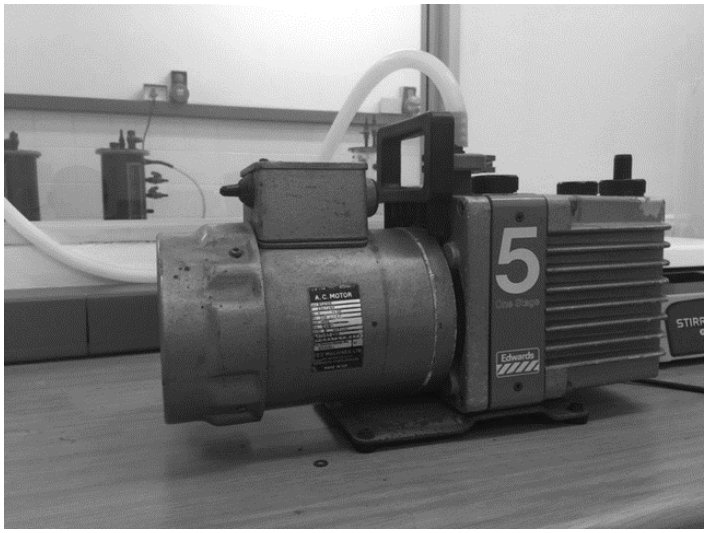

Figure 72: Single phase vacuum pump.

It must be noted that for this model the vacuum pump consumed excessive power w.r.t. the output of the turbogenerator set. This is due to the size of the model and to the fact that a commercial vacuum pump was employed for the model.

CHAPTER 4

LABORATORY MODEL SIMULATIONS

4. LABORATORY MODEL FOR 5W

Since this work is purely based on simulation, the selection of a good process modelling and simulation tool is of extreme importance for its success. The Aspen plus V8.6 software was utilised to simulate and design the OTEC plant. The system consists of steam side with a steam turbine, steam condenser, condensate pump, and steam side of the flash evaporate.

To endorse the simulation model design, specification and different standards are used to calculate the required parameters. The results obtained were compared with the calculated design results. The inputs and constraints used in the model development are listed in the previous chapter.

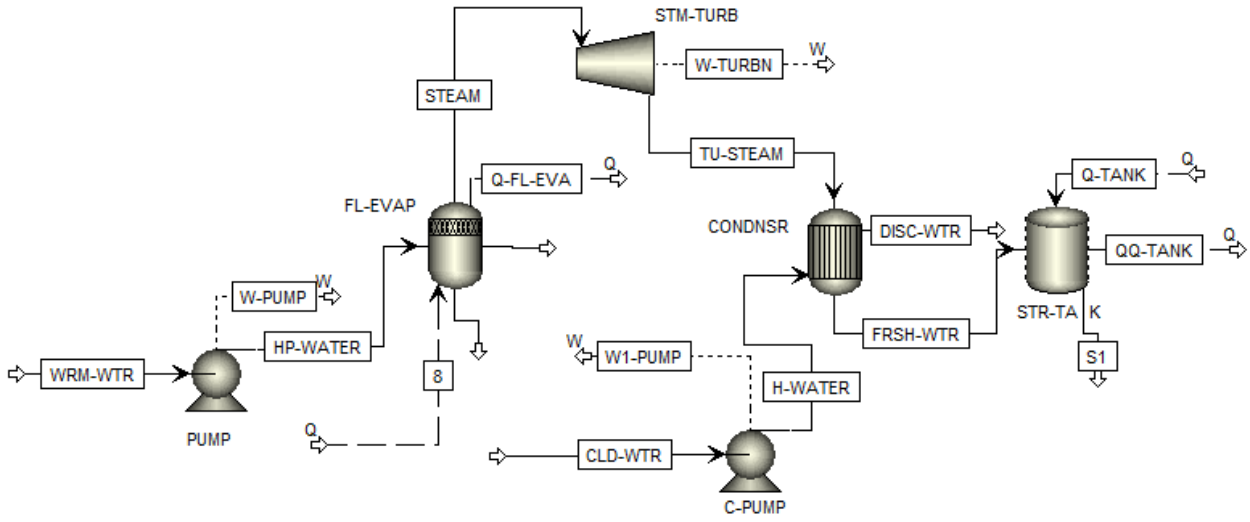

Figure 73: Schematic diagram of OTEC plant simulation [author].

The higher the percentage of the steam phase in this flow, more steam will be extracted by the flash evaporator. Therefore, the amount of mass flow of the stream (steam) is higher and because of that, more electricity generated by the turbine. Hence, the temperature of the hot outlet stream of the steam turbine flow is reduced to 21 ^{o}C until

the maximum thermal exchange between the two (hot and cold streams) are reached, thus creating the maximum steam phase in the condenser.

The operational temperature of the flash evaporator affects the temperature of cold water produced during power generation. It also affects the amount of power generated. These effects are presented in Figure 73. According to these graphs, a higher temperature can produce more electricity and lower cold water temperature which means more benefit. Figure 68 relates to the designed open cycle and signifies the total duty amount based on temperature and pressure in the flash evaporator and the condenser.

The pump is also a vital piece of equipment for the cycle, and the simulation results for it are illustrated in Figure 74. The summarised results of OC-OTEC application to produce electrical power and fresh water are presented in Table 15.

Figure 74 below shows the warm water pump, flash evaporator and steam turbine, between flash evaporator the temperature of the steam is (22.5 ^{o}C), mass flowrate (0.907 kg/s^{-1}) and a pressure of 0.1 kPa. These results are obtained during the optimisation process of an open cycle OTEC plant. The T, m_s and P are utilised to calculate the power generated in the experiment plant.

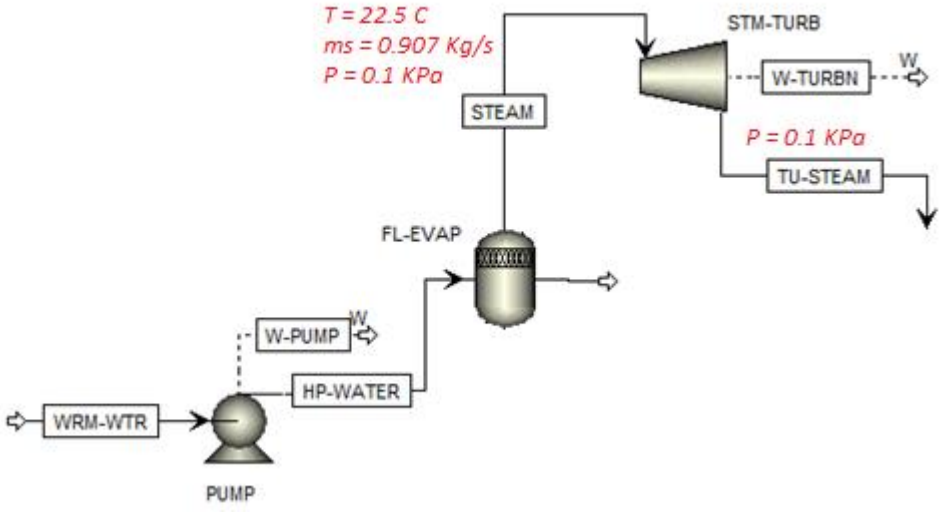

Figure 74: Schematic diagram of OTEC plant simulation [author].

The total calculation of electrical efficiency:

$$\text{Turbine efficiency} = \frac{3.6\text{xP}}{\text{mx}\Delta\text{hs}'} = 0.96 \text{ pu}$$

Table 15 below shows the parameters and unit of experiment OC-OTEC plant. The mechanical efficiency turbine (0.96 pu), efficiency of generator (0.96 pu), isentropic efficiency (0.75 pu).

TABLE 15: STREAM PROPERTIES OF OTEC PLANT.

Parameters	Unit
Mechanical efficiency turbine	0.96
Isentropic efficiency	0.75

4.1. TURBINE CALCULATIONS

Since the expansion is isentropic, then $s_2 = s_3 = 6.586\ \text{kJ/kgK}$. The enthalpy h_2 can be found, as we know the isentropic efficiency of the turbine, as follows:

$$s_3 = 6.586 = S_f + X_3\, S_{fg} \text{ at } 0.099\ \text{kPa}$$

$$6.586 = 0.1050 + X_3\,(8.8690)$$

$$X_3 = 0.7307$$

$$h_3 = h_f + X_3\, h_{fg} \text{ at } 0.099\ \text{kPa}$$

$$h_3 = 29.303 + 0.7307(2484.4)$$

$$= 1845\text{kJ/kg}$$

The power delivered by the turbine to an external load, such as an electrical generator, is calculated below:

4.2. EVAPORATOR

$$\emptyset_m = m_s\,(h_2 - h_1)$$

$$= 1(2675.58 - 419.107)$$

$$= 5\ \text{kW}$$

4.3. POWER OUTPUT FROM THE TURBINE

$P_{(output)} = 5W$

TABLE 16 SIMULATION RESULTS FOR OC CYCLE OTEC.

Parameters	Stream	Production rate
Fresh water	1	1.056 (kg/s)
Electricity	2	5 (kW)

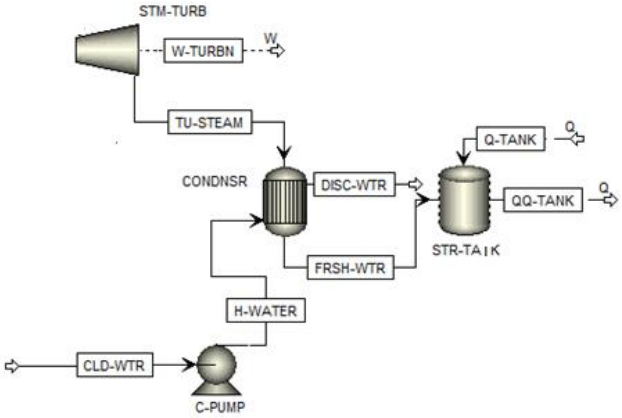

Figure 75: Schematic diagram of OTEC plant simulation [author]

Table 17 lists the thermodynamic specifications of the OC-OTEC plant, plus evaporator, condenser electricity generated by the turbines, pumps, mass flow rate, cold water mass flow rate, hot water mass flowrate, and cost of environmental impact.

TABLE 17: STREAM THERMODYNAMIC PROPERTIES.

Parameters	Units	Values
TEMP	^{0}C	22.5
PRESS	bar	0.001
VFRAC		1
MOLE FLOW	MMscmh	0.0044
MASS FLOW	Tonne/hr	3.6
VOLUME LMX	Cum/hr	4912
VLSTDMX	Cum/hr	3.360
MWMX		18.015
HMX ETHALPY-FLO	Gcal/hr	-11.5456
HMX MASS –ENTHALPY	Kcal/Kg	-57.777
SMX MOLE-ENTROPY	Cal/mol-K	-3207.12
SMX MASS –ENTROPY	Cal/gm-K	3.0650
CPMX MOLE -HEAT-CA	Cal/mol-K	0.17013
CPMX MASS- HEAT-CA	Cal/gm-K	8.0175
RHOMX MOLE - DENSITY	Kmol/cum	0.4450
RHOMX MASS- DENSITY	Kg/cum	4.07E-05
RHOLSTD MOLE – DENSITY	Kmol/cum	0.00073
RHOLSTD MASS-DENSITY	Kg/cum	55.40166

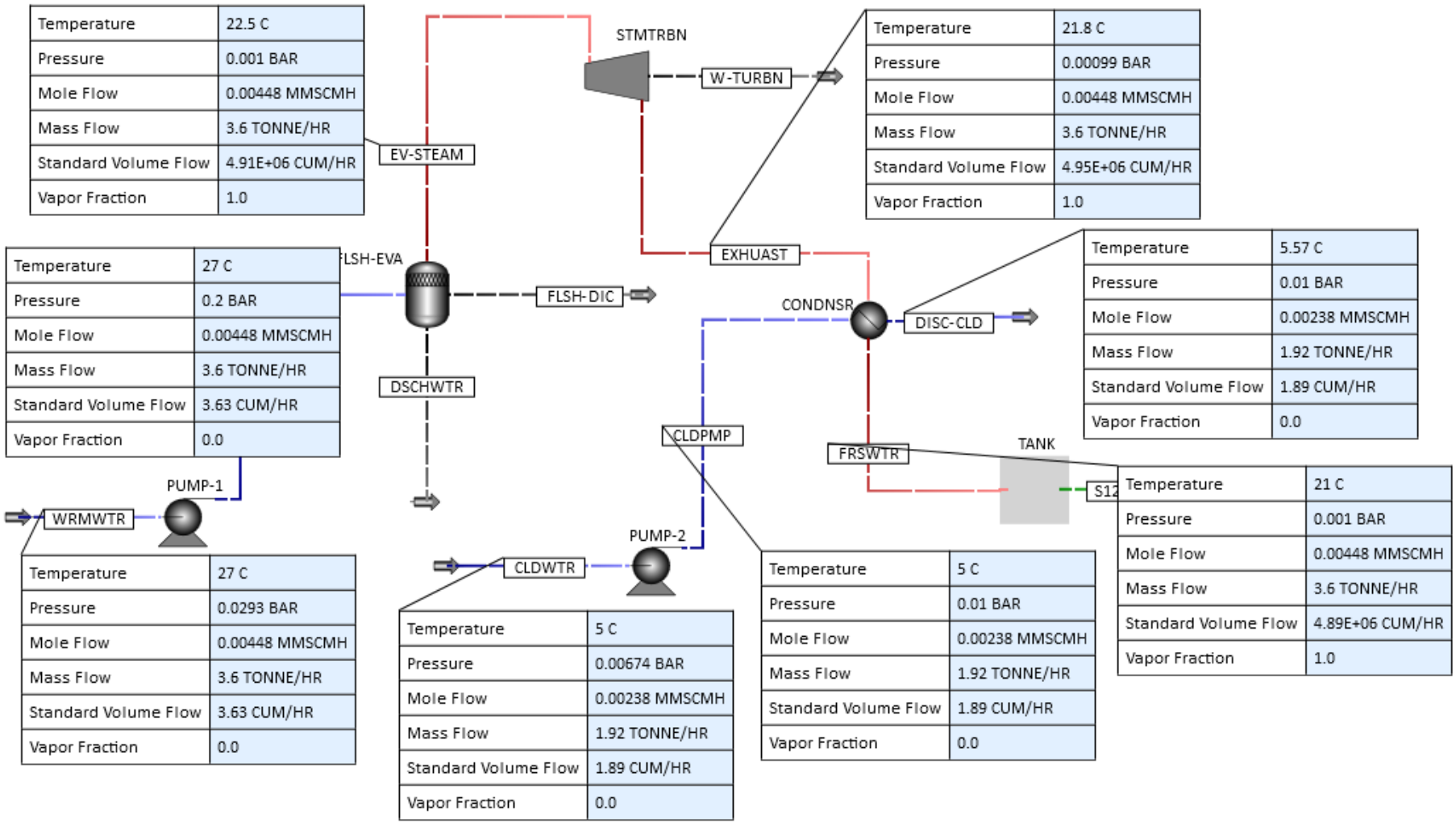

Figure 76: OTEC power plant view [author].

4.4. THE OUTCOME OF WARM WATER TEMPERATURE (°C)

Figure 77 shows how the power generation and cold water intake rates increase with respect to the warm water temperature Tin. Henceforth, analysis is restricted to the performance analysis of the large (2-5 kW) scale plant in the half mode. The warm water intake rate is set to be Min = 4.95kg/s-1, and the generated steam is divided into the turbine and condenser with equal fractions of 50%.

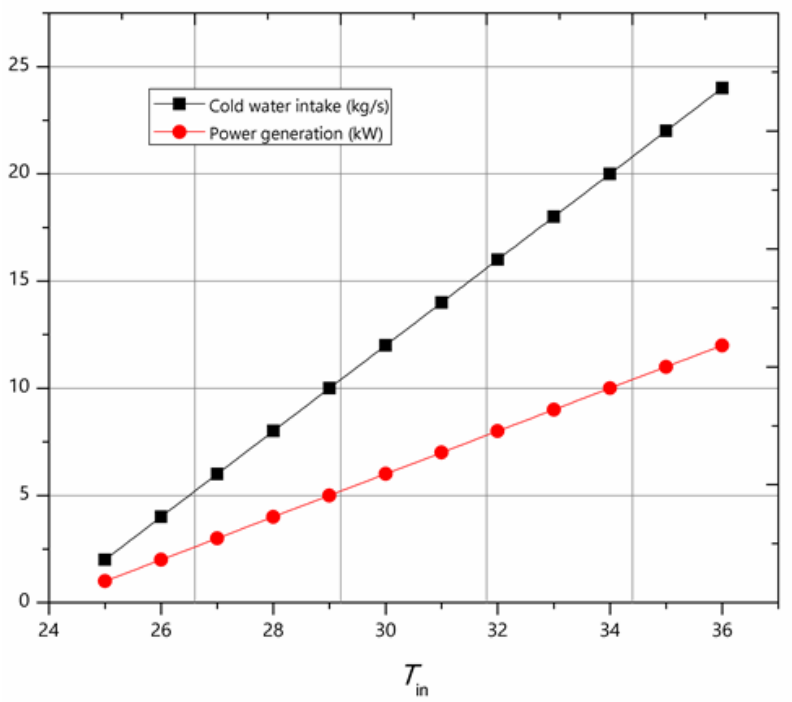

Figure 77: Difference of the cold-water intake and power generation rates with respect to the warm water intake temperature.

The higher the temperature of warm water, the higher the capacity of electrical power generated. Figure 78 illustrates the deviation of the cold intake and power generation rates with respect to the warm intake temperature. The hot stream transfers its heat to the cold stream; thus the flow direction of the hot stream is towards lower temperature and the flow direction of the cold stream is towards higher temperatures.

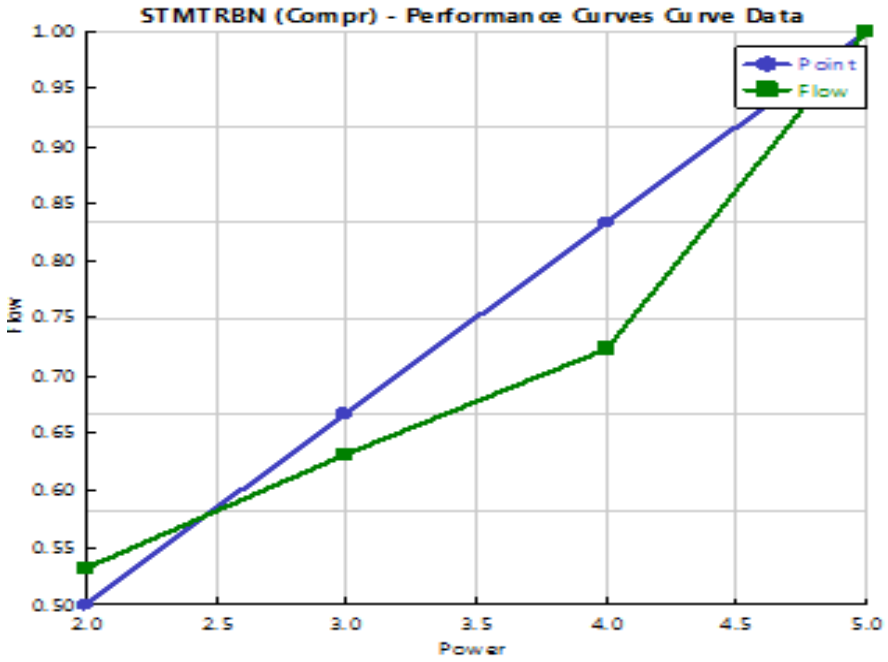

Figure 78: Performance curve of the turbine; mass flowrate vs. power generated.

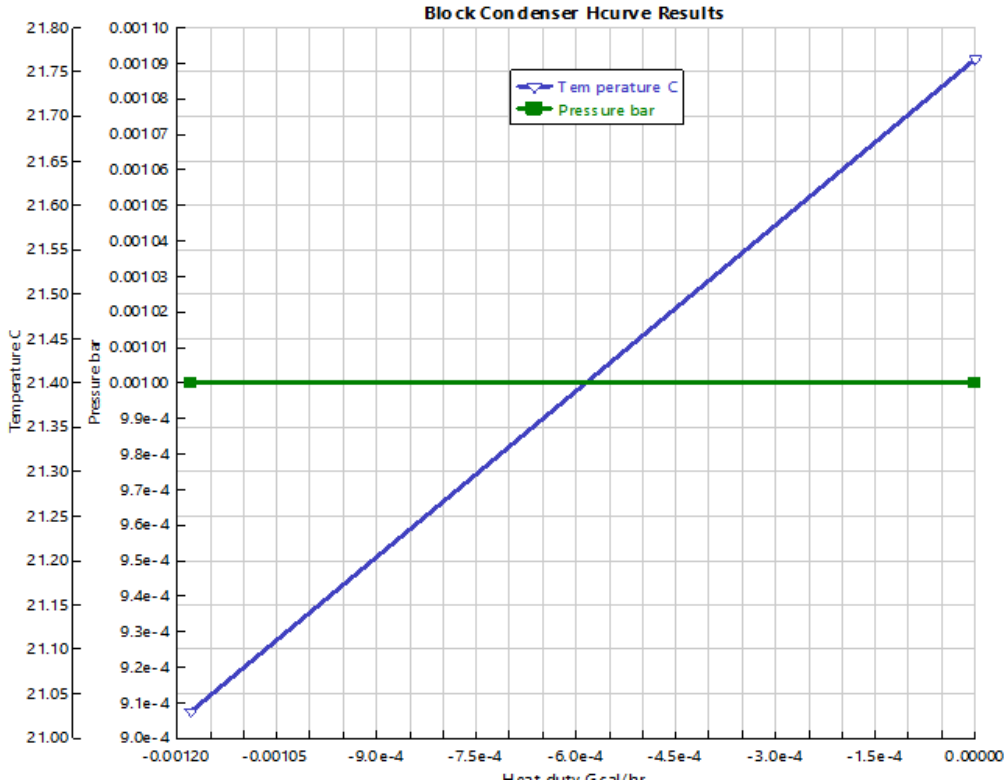

Figure 79: Temperature and pressure of process fluid in a condenser vs. Heat duty.

Figure 79 presents the amount of energy the heat exchange transferred during the process to heat/cool it to the desired temperature, $\dot{m}C_p\Delta TA$. The input temperature of the condenser from the steam turbine is increasing gradually with temperature increase.

At a temperature of 21 ^{0}C, the pressure is 0.000009 bar and heat duty is -0, 0012. The pressure of the condenser is 0.001 bar. Pressure is constant irrespective of increasing heat duty (G/hr) of the heat exchange.

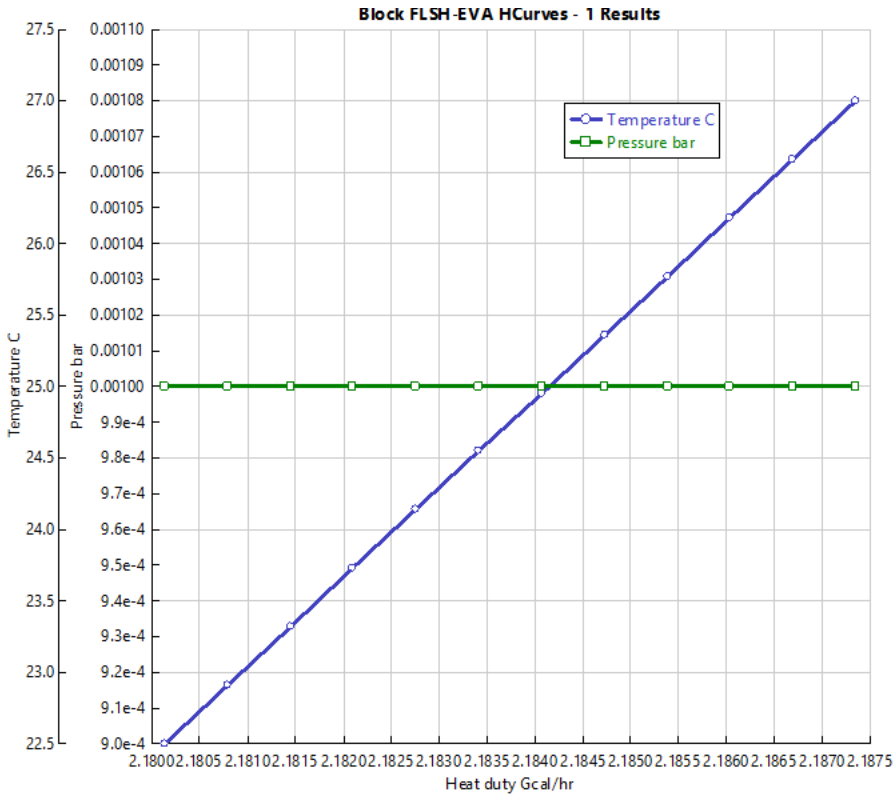

Figure 80: Temperature and pressure of process fluid in a flash evaporator vs. Heat duty.

The evaporator pressure drop inside the barrel does not impress the pressure loss of the main stream flow through the evaporator. This tells us that saturated steam departure the steam evaporator has the similar pressure as the supply water inflowing the steam evaporator. The pressure loss of the evaporator overcome using the driving force (natural circulation) or circulation pump (forced circulation).

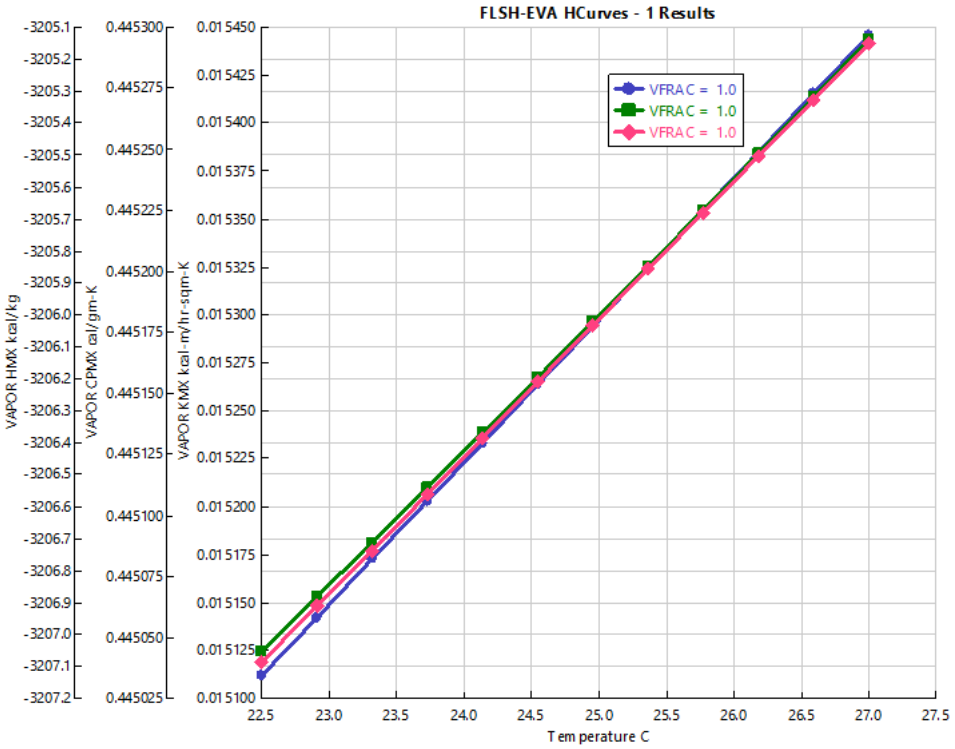

Figure 81: Vapor HMX, CPMX and KMX of process fluid in a flash evaporator vs. temperature.

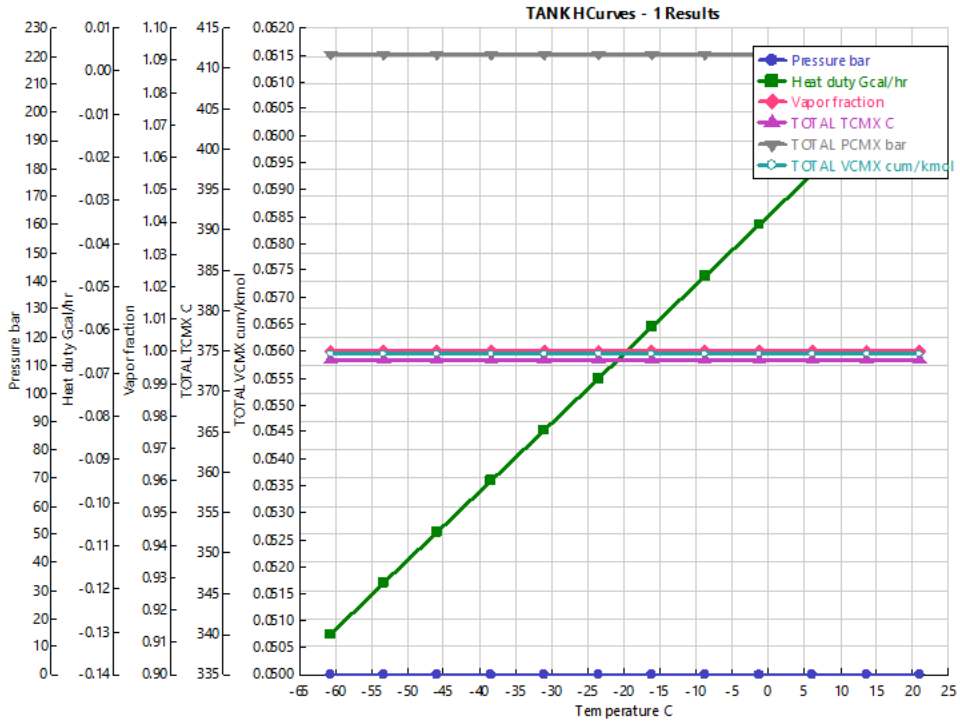

Figure 82: Performance curve of the turbine; mass flowrate vs. power generated.

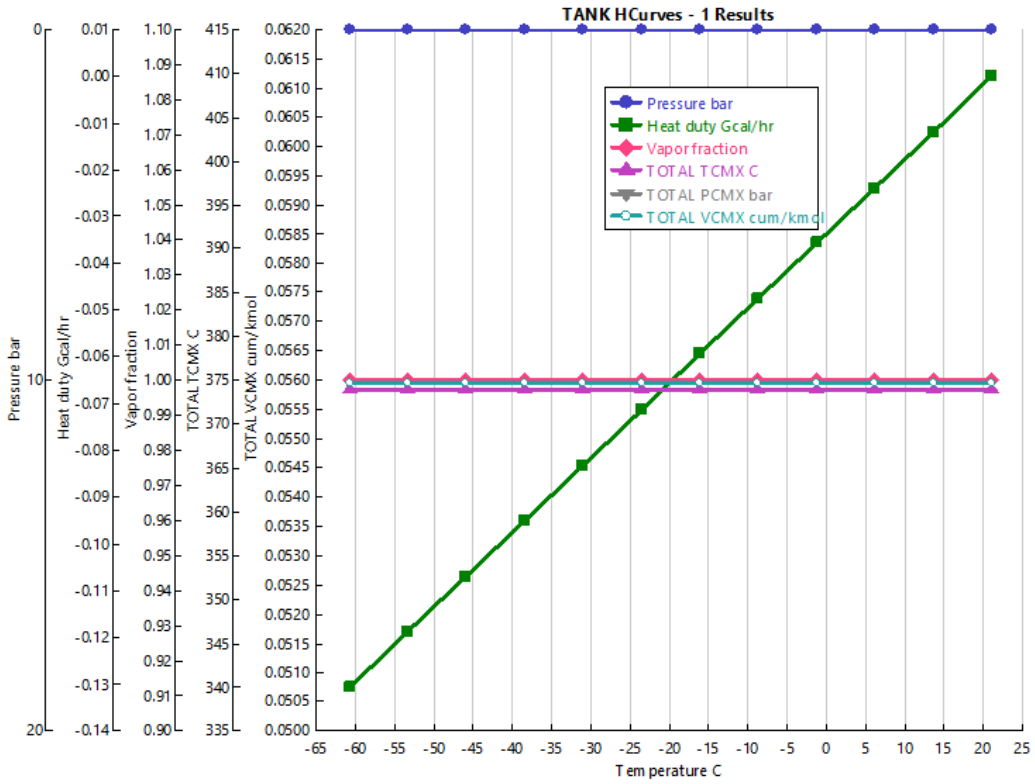

Figure 83: Performance curve of the turbine; mass flowrate vs. power generated.

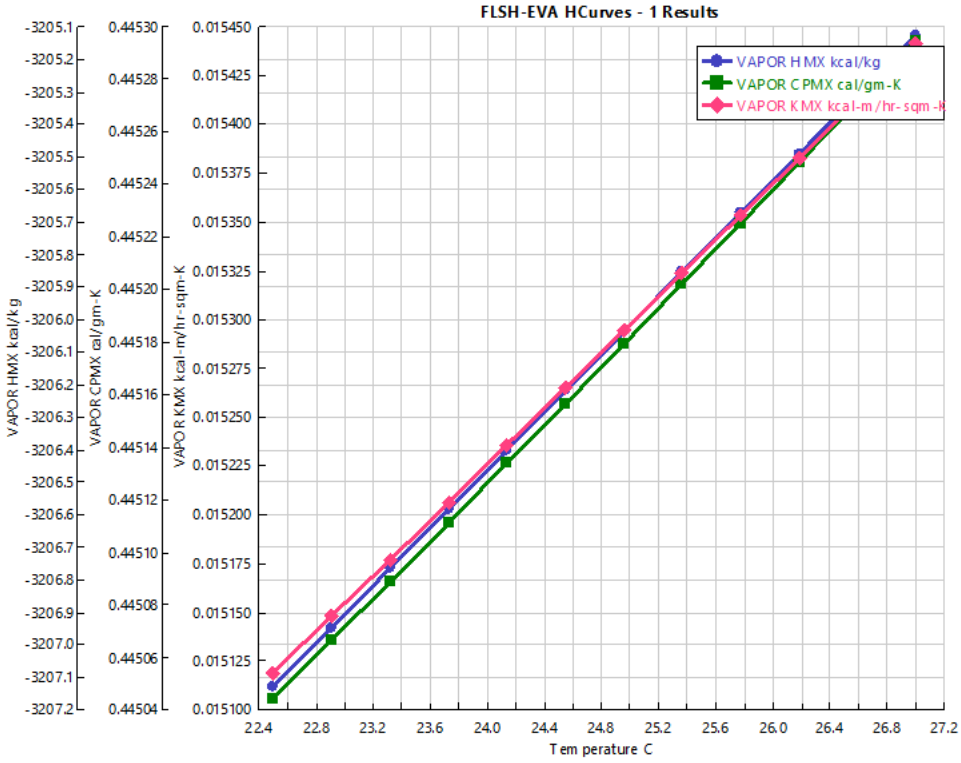

Figure 84: Vapor HMX, CPMX and KMX of process fluid in a flash evaporator vs. temperature.

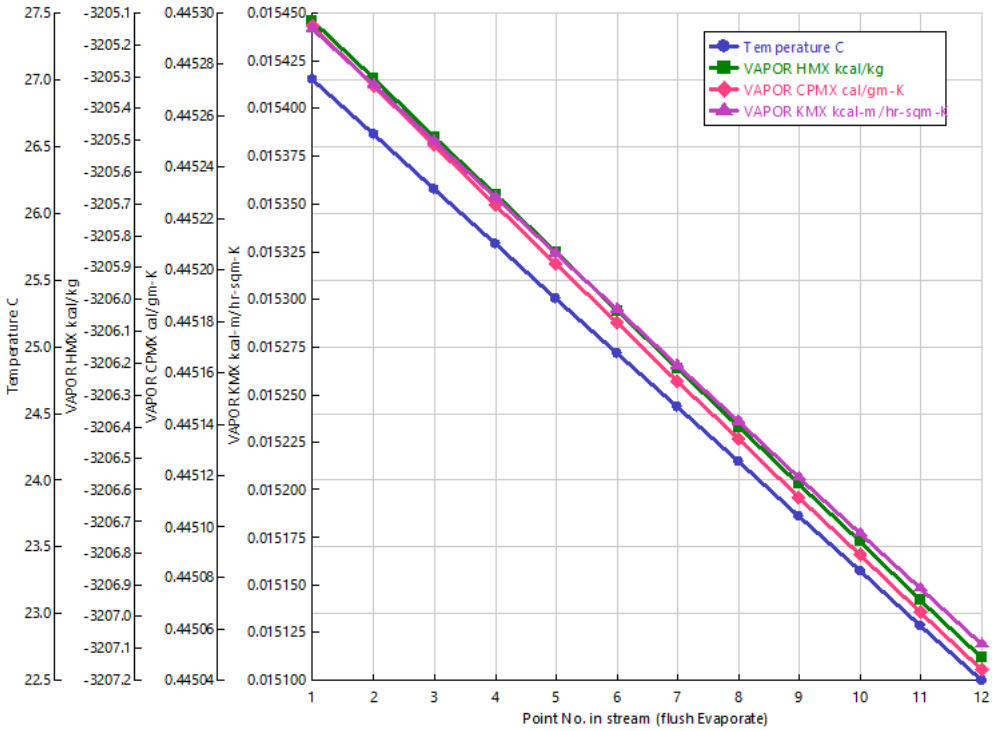

Figure 85: Temperature, Vapour HMX, CPMX and KMX of process fluid in a flash evaporator.

TABLE 18:SIMULATION RESULT FOR PUMP IN ASPEN SOFTWARE

Parameters	Values	Unit
Fluid power	0.0172	kW
Brake power	0.0172	kW
Electricity	0.0172	kW
Volumetric flow rate	3.6289	Cum/hr
Pressure change	0.1706	Bar
NPSH available	0	Meter
NPSH required		
Head developed	1.7546	Meter
Pump efficiency used	1	
Net work required	0.0172	kW
Outlet pressure	0.2	Bar

TABLE 19: OC-OTEC PLANT STREAM PROPERTIES.

	Units	CLDPMP	CLWTR	DISC-CLD	DSCHWTR	EV-STEAM	EXHUAST	FLSH-DIC	FRSWRT	S12	WRMPMP	WRMWTR
From		**PUMP-2**		**CONDNSR**	**FLSH-EVA**	**FLSH-EVA**	**STMTRBN**	**FLSH-EVA**	**CONDNSR**	**TANK**	**PUMP-1**	
To		**CONDNSR**	**PUMP-2**			**STMTRBN**	**CONDNSR**		**Tank**		**FLSH-EVA**	**PUMP-1**
Phase:		Liquid	Liquid	Liquid		Vapor	Vapor		Vapor	Mixed	Liquid	Liquid
Water	MMSCMH	0.00238	0.00238	0.00238	0	0.00447899	0.00447899	0	0.00447899	0.004479	0.004479	0.00447899
Mole flow	MMSCHM	0.00238	0.00238	0.00238	0	0.00447899	0.00447899	0	0.00447899	0.004479	0.004479	0.00447899
Mass flow	TONNE/HR	1.9152	1.9152	1.9152	0	3.6	3.6	0	3.6	3.6	3.6	3.6
Volume flow	CUMHR	1.890533	1.890533	1.890534	0	4912020	4949300	0	4887590	35286800	3.628939	3.628938
temperature	C	5	5	5.567481		22.5	21.7649		21.02977	-60.7652	27.00024	27
Pressure	BAR	0.01	0.00673	0.01	0.01	0.01	0.00099	0.001	0.001	1.00E-05	0.2	0.0293039
Vapor fraction		0	0	0		1	1		1	0.1	0	0
Liquid fraction		1	1	1		0	0		0	0.9	1	1
Solid fraction		0	0	0		0	0		0	0	0	0
Molar Enthalpy	KCAL/MOL	-69.11605	-96.1160	-69.10497		-57.77731	-57.77731		-57.78909	-69.2194	-68.68725	-68.68732
Mass enthalpy	KCAL/KG	-3836.524	-3836.52	-3835.909		-3207.128	-3207.455		-3207.782	-3842.26	-3812.721	-3812.726
Enthalpy flow	GCAL/HR	-7.34771	-7.34771	-7.346533		-11.54566	-11.54684		-11.54802	-13.8321	-13.7258	-13.72581
Molar entropy	CAL/MOL-K	-41.47283	-41.4728	-41.43305		3.065014	3.065014		3.025048	-41.1742	-39.98944	-39.9839
Mass entropy	CAL/GMK	-2.302092	-2.30209	-2.998841		0.1701341	0.1701341		0.1679157	-2.28552	-2.219751	-2.219749
Molar density	KMOL/CUM	56.2327	56.2327	56.20294		4.07E-05	4.04E-05		4.09E-05	5.66E-06	55.06578	55.06579
Mass density	KG/CUM	1013.048	1013.048	1012.512		0.000732897	0.000727376		0.00073656	0.000102	992.0255	992.0257
Average molecular weight		18.01528	18.01528	18.01528		18.01528	18.01528		18.01528	18.01528	18.01528	18.01528
Phase vapor Compressibility factor, mixture						0.9999844	0.9999845		0.9999842	1		
Molar volume, mixture	CUM/HR					4912020	4949300		4887590	35286800		
Molar flowrate, mixture	MMSCMH					0.00447899	0.00447899		0.00447899	0.000448		
Ratio Cp/Cv for mixture						1.32969	1.329729		1.329768	1.332133		

4.5. RESULTS AND DISCUSSIONS

In this section, compare performance of an OC - OTEC system by controlling the mass flow rates of inlet warm water and inlet cold water. Two cases are considered for ultimate studies: power generated by the steam turbine and desalinated water produced in the condenser. The efficiency and power output of an OC-Cycle plant is calculated using the enthalpy values.

The properties to be calculated are saturation temperature, and fresh water generated.

The power output is then calculated using the enthalpy drop across the turbine ($h_1 - h_2$) multiplied by the steam flowrate.

The thermal efficiency is calculated by dividing the enthalpy drop across the turbine by the enthalpy difference between the output and inlet of the evaporator.

4.5.1. THERMAL EFFICIENCY AND POWER OUTPUT

Figs. 86 and 87 illustrations the thermal efficiency and power output of the system plotted against δt, change in the temperature difference between the warm water (T_w) and cold water (T_c). In Fig. 86, the thermal efficiency increased from 0.16 to 0.28 % and the power output increased from 0.83 to 1.53 W within a 5 ^oC increase in temperature deference for average of $\dot{m}_{ws}$=0.0372 l/s. The power output is produced when the total change in temperature is large enough to allow heat transfer within the evaporator and thus lowers the pressure across the turbine.

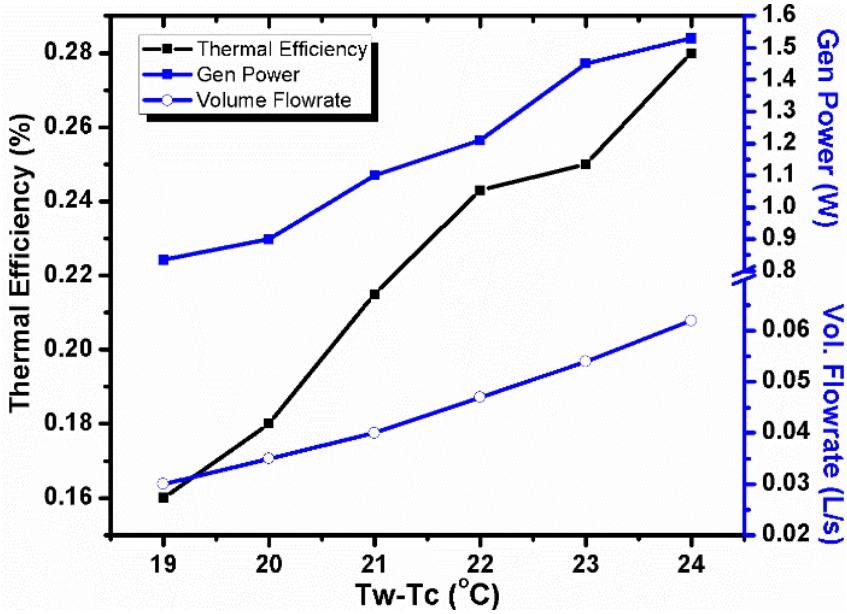

Figure 86: Thermal efficiency and power output of the system against operating temperature difference, for average of $\dot{m}_{ws}$=0.0372 l/s.

A similar trend was observed in Fig. 87, where the thermal efficiency increased from 0.14 to 0.33 % and the power output increased from 0.37 to 2.25 W within a temperature range 19 to 24 ºC for average $\dot{m}_{ws}$=0.0098 l/s.

Heat transfer (steam produced) in the evaporator increases when the flow rate is constant as energy loss in the process is minimized therefore providing the turbine with a better constant power output.

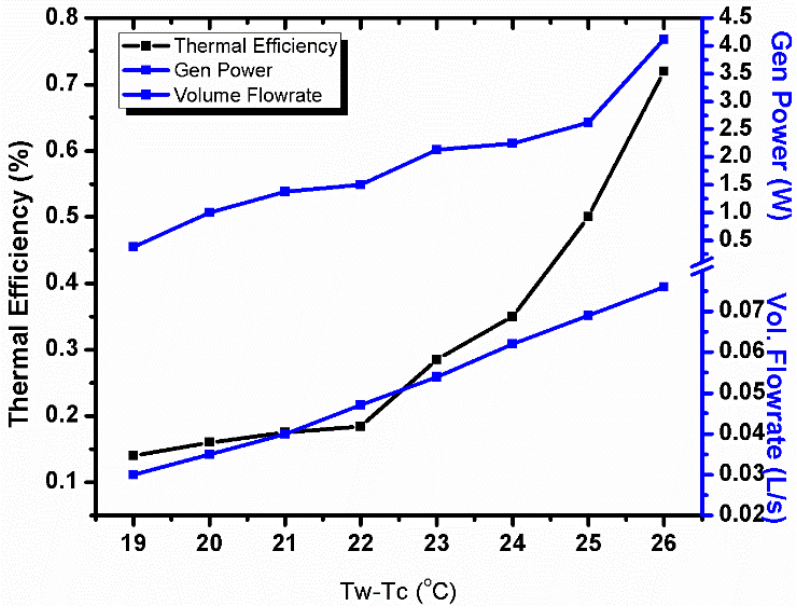

Figure 87: Thermal efficiency and power output of the system against operating temperature difference, for average of $\dot{m}_{ws}$=0.0098 l/s.

The efficiencies for the average of $\dot{m}_{ws} = 0.0372\,l/s$ are approximately equal to the efficiencies of the average of $\dot{m}_{ws} = 0.0098\,l/s$. The work done by the turbine for both values of $\dot{m}_{ws}$ increases with increasing operating δt. The turbine uses the energy from the steam to do work, hence enthalpy drop observed is due the significant temperature drop across the turbine.

Fig. 88 indicates the thermal efficiencies and power output of the turbine vs the pressure drops across the turbine for an average of $\dot{m}_{ws} = 0.0372\,l/s$.

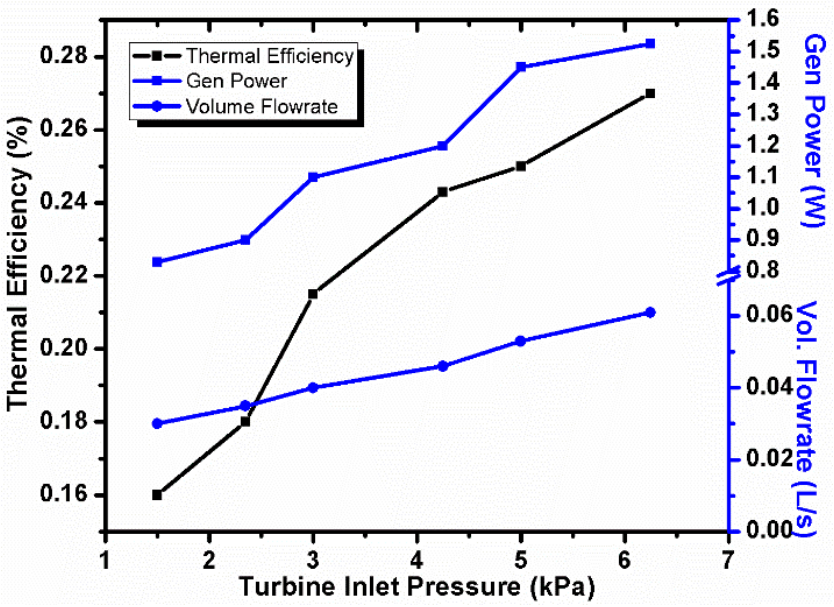

Figure 88: Thermal efficiency and power output of the system against the pressure drop across the turbine, for average of m ̇_ws=0.0372l/s.

According to the graph, it evident that the thermal efficiencies increases as the pressure drop increases from 1.5 to 6.5 kPa across the turbine. Ultimately as the pressure drops increases, leading to the power output increase from 0.83 to 1.53 W.

Figs. 88 and 89 show minimum efficiency of 0.16 % and power output of 0.85 W, at $19\,^{o}C$ and 1.5 kPa. The maximum efficiency is 0.26 % with power output of 1.55 W, at $24\,^{o}C$ and 6.25 kPa for both. Fig. 89 shows the thermal efficiencies and power output vs the pressure drops across the turbine for the average of $\dot{m}_{ws} = 0.0098\,l/s$. The pressure drops obtained from this experiment are between 2 and 11 kPa.

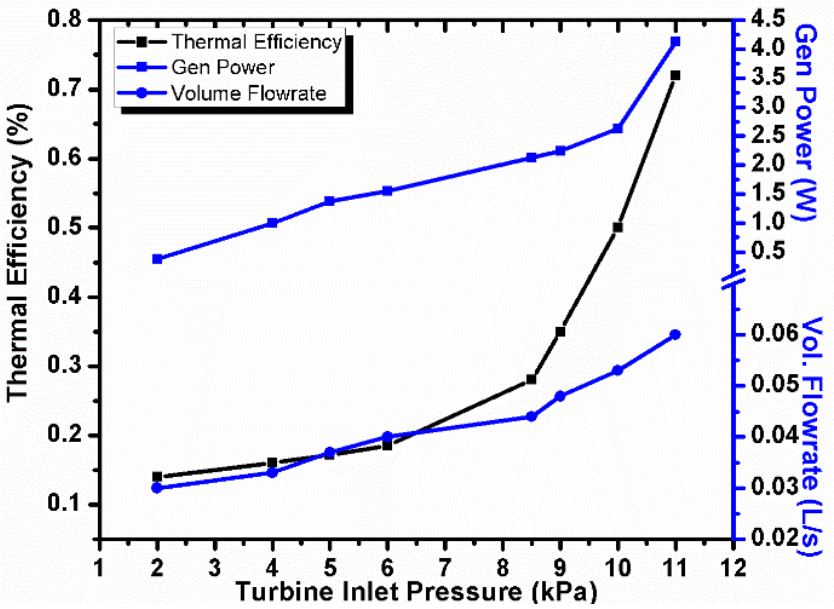

Figure 89: Thermal efficiency and power output of the system against the pressure drop across the turbine, for average of $\dot{m}$_ws=0.0098l/s.

According to the graph, thermal efficiencies increases as the pressure drop across the turbine increases. An increase in pressure drop leads to a power output increase 4.5 W.

4.5.2. Steam and Power Output

Comparing Figs. 90 and 91, it is clear to see that power output of Fig. 90 is influenced by the increase in flowrate $0.0372\ \mathrm{l/s}$. of a steam produced in an evaporator, thus increasing the thermal efficiency of plant.

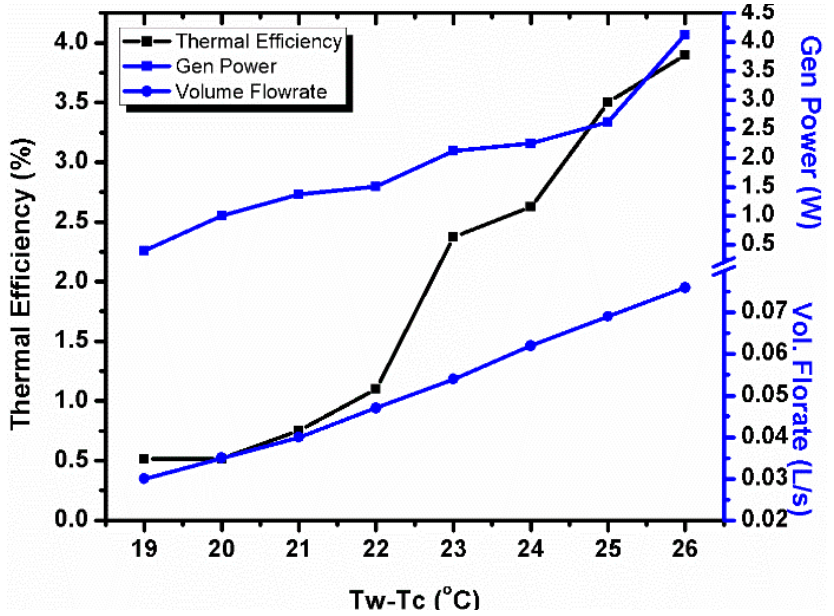

Figure 90: Steam and power output of the system against operating temperature difference, for average of $\dot{m}$_ws=0.0372l/s.

Fig. 91 shows the steam and power output vs the volume of the flowrate across the turbine for the average of $\dot{m}_{ws} = 0.0098\,\mathrm{l/s}$.

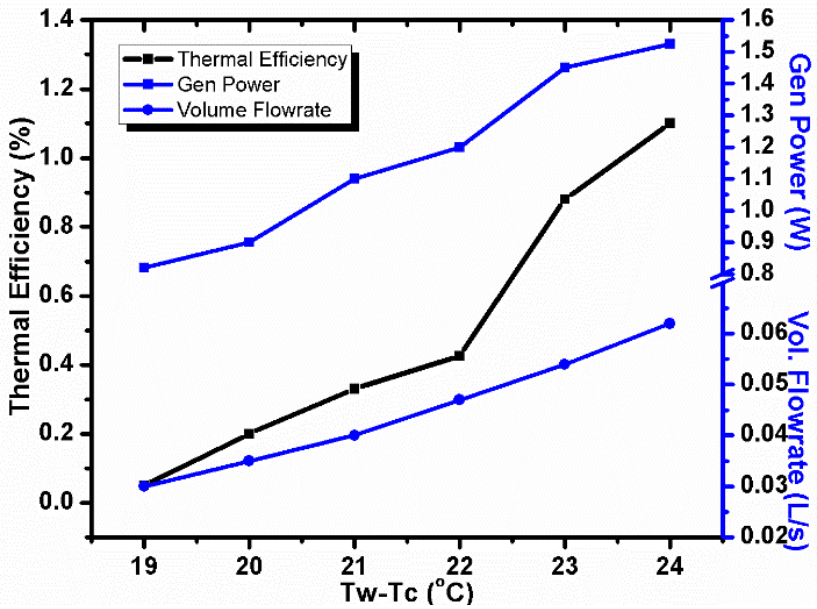

Figure 91: Steam and power output of the system against operating temperature difference, for average of m ̇_ws=0.0098l/s.

Fig. 91 shows the steam and power output vs the pressure drops across the turbine for the average of $\dot{m}_{ws} = 0.0098\,\mathrm{l/s}$. Minimum steam mass flow rate of 0.05 kg/s at $19\,^{o}\mathrm{C}$ and maximum of 1.03 kg/s at $24\,^{o}\mathrm{C}$, the minimum power output of 0.85 W at $19\,^{o}\mathrm{C}$ and maximum of 1.58 W at $24\,^{o}\mathrm{C}$ for average $\dot{m}_{ws}$=0.0098 l/s.

It can be seen that more steam is produced than power output produced by the turbine. The work done by the turbine for both $\mathrm{values\ of}\ \dot{m}_{ws}$ generally increases with an increasing temperature change, δt. The turbine uses steam's energy to do work, and thus there is an observable temperature drop across the turbine that leads to an enthalpy drop.

4.5.3. ENTHALPY AND WORK OUTPUT

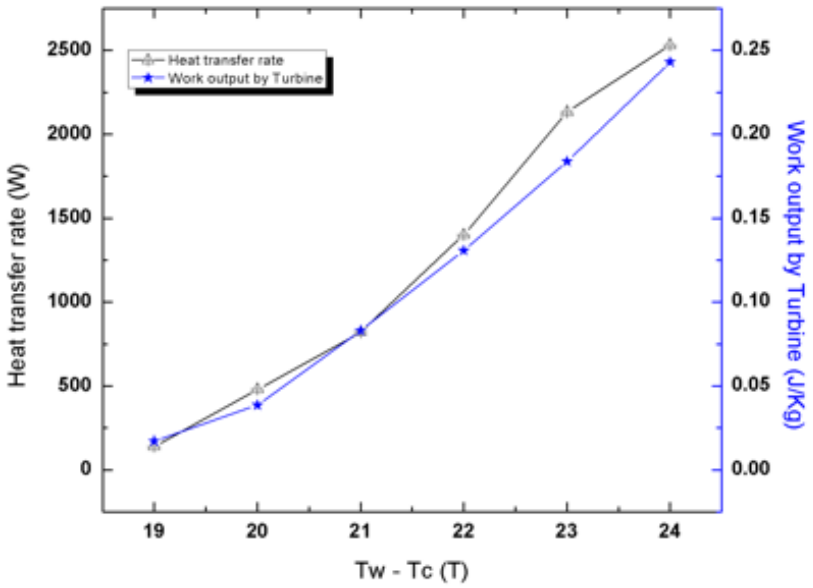

Figure 92: Enthalpy and work output of the system against operating temperature difference, for average of $\dot{m}_{ws}$=0.0372l/s.

A minimum enthalpy of 0.02 J/kg at $19\,^{o}C$ and maximum of 0.24 kJ/kg at $24\,^{o}C$ was observed in Fig 92. Fig. 92 establishes the minimum entropy of 130 KJ/kg at $19\,^{o}C$ and upper limit of 2500 KJ/kg at $20\,^{o}C$. Fig. 10 shows minimum work done of 0.125 kJ/kg at $19\,^{o}C$ and maximum of 0.72 kJ/kg at $24\,^{o}C$.

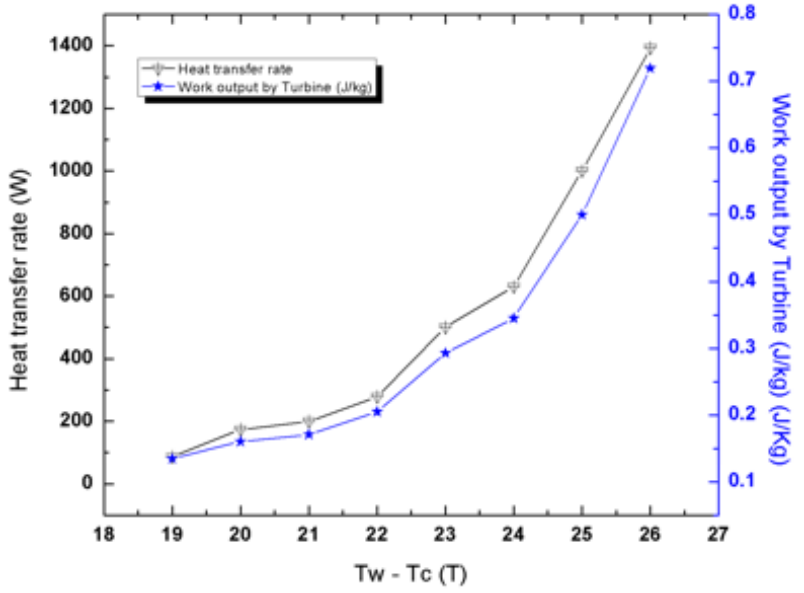

Figure 93: Enthalpy and work output of the system against operating temperature difference, for average of $\dot{m}_{ws}$=0.0098l/s.

Fig. 93 shows minimum work done 0.15 kJ/kg at $19^{o}C$ and maximum of 0.73 kJ/kg at $24\,^{o}C$. It is seen that as more energy is required to heat up water to produce steam, there is more work done with regards to the output produced by the turbine.

The work done by the turbine for both $\text{values of } \dot{m}_{ws}$ generally increases with the increasing δt and enthalpy. Steam is a source of energy used by the turbine to do work, hence there is a pressure drop across the turbine leading to lower enthalpy.

TABLE 20: EXPERIMENT RESULT OF OC OTEC PLANT.

Pressure (kPa)	Volume flowrate (l/s)	Cold water (°C)	Warm water (^{0}C)	∆ (°C)	Specific heat capacity (kJ/kgK)	Volume flowrate (l/s)	Power (W)	Work output by Turbine (J/kg)	Enthalpy at turbine inlet {h1} (J/kg)	Enthalpy at turbine outlet {h2} (J/kg)	Time (s)	Mass flow rate (kg/s)	Heat transfer rate (W)	Steam (kg/s)
5	0,022	5	29	24	4,18	0,001	4,101	0,0171	25460	2546059,9	15	1,386	139,08	0,056
7	0,019	5	28	23	4,18	0,005	2,616	0,2431	25442	2544259,7	13	4,991	479,83	0,196
6	0,014	5	28	23	4,18	0,008	2,222	0,1838	25442	2544259,8	11	8,318	799,72	0,326
6	0,013	5	28	23	4,18	0,011	2,134	0,1308	25442	2544259,8	8	11,09	1066,2	0,435
2	0,002	5	28	23	4,18	0,022	1,386	0,0229	25442	2544259,9	8	22,18	2132,5	0,871
1.5	0,004	5	28	23	4,18	0,026	1,530	0,0186	25442	2544259,9	6	26,34	2532,4	1,034

Fig. 94 shows the indirect condenser of the OC-OTEC. This system is utilised to generate fresh water.

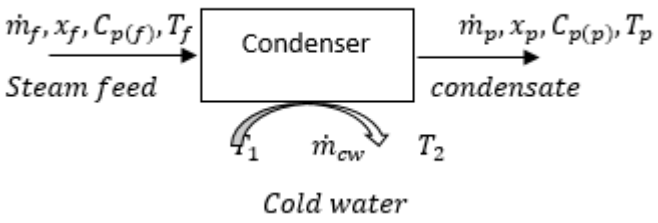

Figure 94: Indirect condenser.

$\dot{m}, x, C_p, T$: Mass flow rate, solids fraction, specific heat, temperature resp. Subscripts: (f) for feed; (p) for product; (1) for inlet water; (2) for outlet water. The overall mass balance is $\dot{m}_f = \dot{m}_p$ and the solids balance is $\dot{m}_f x_f = \dot{m}_p x_{p,} \quad thus, x_p = x_f$.

The energy balance is $\dot{m}_f C_{p(f)} T_f + \dot{m}_{cw} C_{p(1)} T_1 = \dot{m}_{cw} C_{p(2)} T_2 + \dot{m}_p C_{p(p)} T_p$, $C_{p(1)}$ and $C_{p(2)}$ are determined from tables containing the properties of water at temperatures. T_1 and T_2 respectively. When approximation are used, $C_{p(1)} = C_{p(2)} = 4180\ kJ/kg\,K$. The rejected heat within the turbine is $q_{out} = h_2 - h_3$, $h_2 = 2461.4435\ kJ/kg$; $h_3 = 75.169\ kJ/kg$.

$$q_{out} = h_2 - h_3$$
$$= 130.459 - 75.169$$
$$= 55.29\ kJ/kg$$
$$\dot{m}_{cw} C_{p(cw)} \Delta T_{cw} = \dot{m}_p q_{p(out)}$$
$$\dot{m}_{cw} = \frac{0.75 \times 55.297}{4.18(10-5)}$$
$$= 1.984\ kg/s$$

6.4.1. Energy Balance

$$\dot{m}_f C_{p(f)} T_f + \dot{m}_{cw} C_{p(1)} T_1 = \dot{m}_{cw} C_{p(2)} T_2 + \dot{m}_p C_{p(p)} T_p$$
$$0.75 \times 4.2(18) + 1.984 \times 4.2 \times 5 = 1.984 \times 4.2 \times 10 + \dot{m}_p \times 4.2 \times 13$$
$$\dot{m}_p = \frac{98.364 - 83.328}{4.2 \times 13}$$
$$\dot{m}_p = 0.356\ kg/s$$

Figs. 95 and 96 show steam, fresh water mass flowrate and power output of the system against volume flowrate. It seen that as condensation begins in the condenser, the steam at the inlet of the condenser is cooled by cold water at a temperature of $5^{o}C$ and the steam changes phase from steam to liquid. The fresh water that is produced is less than the amount of steam being cooled.

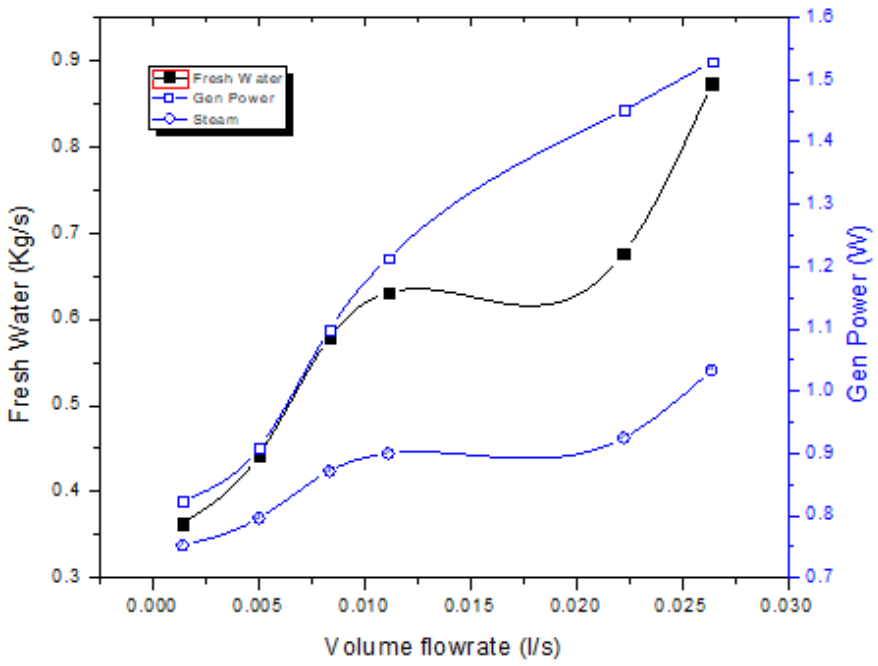

Figure 95: Steam, fresh water mass flowrate and power output of the system against volume flowrate.

As the system produces more steam, there is more power output from the turbine and more fresh water after the condenser. There is then more power output produced by the turbine.

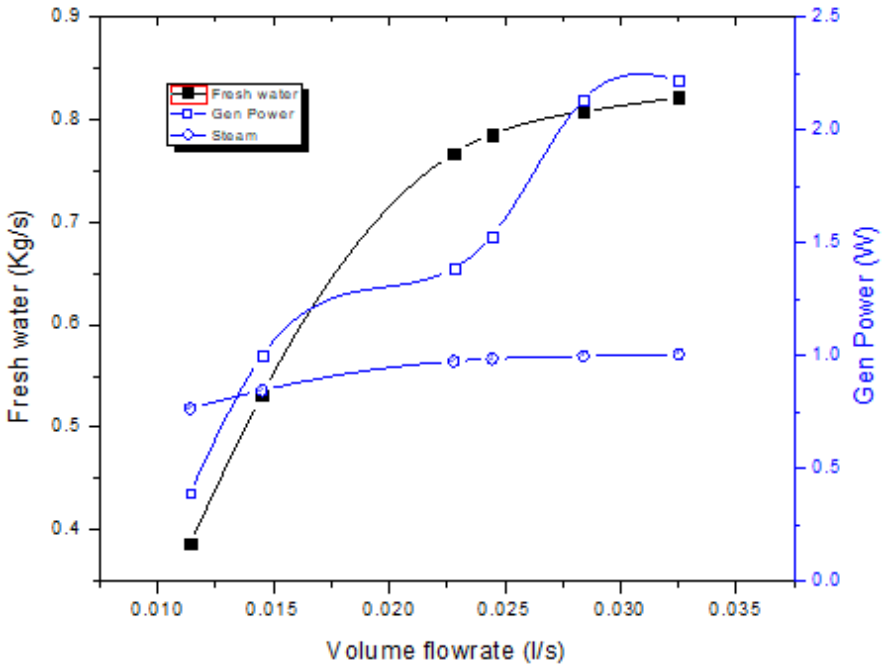

Figure 96: Steam, fresh water mass flowrate and power output of the system against volume flowrate.

The work done by the turbine for both $\dot{m}_{ws}$ generally increases with increasing operating temperature difference and more fresh water as by-product. The turbine uses the energy from the steam to do work, and as a result there is an observable drop across the turbine that leads to an enthalpy change.

Although the efficiencies are low (of the order of < 1%.) the system works in principle and can be adapted for a larger plant.

4.6. DESIGN OF 206.18KW OC-OTEC PILOT SYSTEM

The steam turbine and generator was designed for an output of 200 kW operating with warm water at 26ºC with a corresponding net power of 98kW (98.186) and a production of 0.5l/sec (43 200 l/day) of desalinated water.

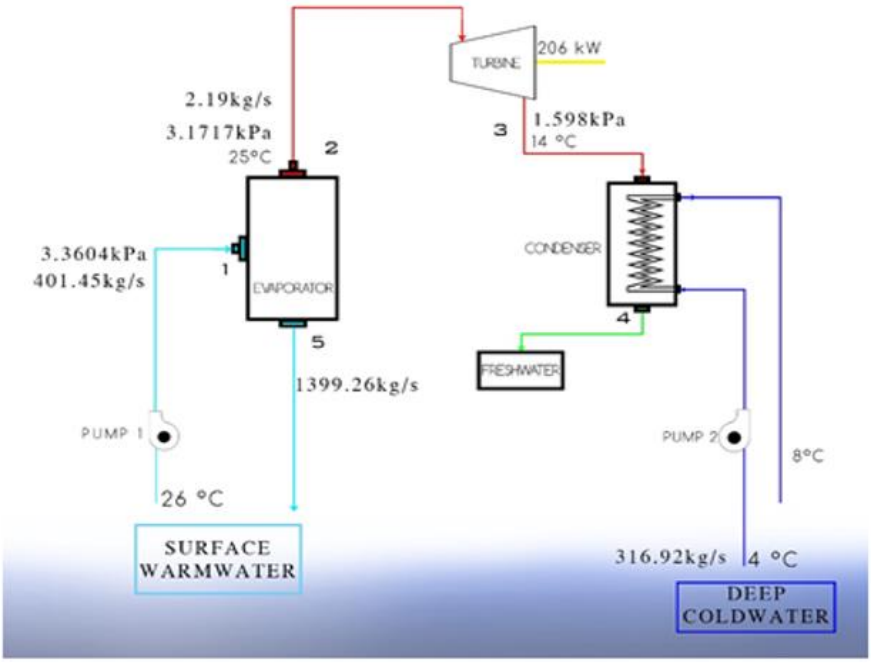

Figure 97: 206.186kW O-C OTEC process diagram.

4.6.1. ASSUMPTIONS

The model design for this project was optimised for approximately 98.186kW Net power. During this research there were numerous important mechanisms that have a substantial influence on the produced net power.

TABLE 21: 98.186KW NET AND 206,186 KW GROSS POWER PROCESS.

Symbol	Quantity	SI [a]
T_{WW}	temperature of warm water	26 ^{O}C
T_{CW}	temperature of cold water	4 ^{O}C
M_G	net power output	98.186kW
η_G	generator efficiency	97 %
T_{st} in	steam temperature	25 ^{O}C
T_{st} out	steam temperature	14 ^{O}C
Cp	specific capacity of water	4.18 kJ/kgK /kg
η_p	seawater pump efficiency moment	85%

Following are brief calculations for the design of 206.186kW process of Open-Cycle OTEC plant.

4.6.1.1. SYSTEM POWER ENERGY

The total system energy power was compensating for the mechanical, electrical and turbine losses. Consequently, the total power energy to be generated by the turbine can be calculated as: Turbine power output is $M_T = 206.186\text{kW}$.

$$M_{Gross} = \frac{\text{Net Power}}{\text{Generator Efficiency}} = \frac{M_{net}}{\eta_G}$$

$$= \frac{200\text{kW}}{0.97}$$

$$= 206.186\ \text{kW}$$

4.6.1.2. TURBINE ANALYSIS

A. State 2 – 3 process

Steam Table is used for identifying, Temperature, Pressure, Enthalpy and Entropy; etc. see below the table 22 and 23.

TABLE 22: APPARATUS FOR SATE 2.

Symbol	Quantity	SI
T_2	temperature	25 ^{O}C
P_2	pressure	3.1717 kPa
h_2	enthalpy	2547.855KJ/Kg
S_2	entropy	8.55975KJ/Kg

TABLE 23:APPARATUS FOR SATE 3.

Symbol	Quantity	SI
T_2	temperature	14 ^{O}C
P_2	pressure	1.5985 kPa
h_2	enthalpy	2453.8403 KJ/Kg
S_2	entropy	8.55975KJ/Kg

$$S_2 = S_3 = 8.55975\ \text{kJ/kgK}$$

$$S_3 = S_{f_3} + x_3 S_{fg_3}$$

$$8.55975 = 0.2098 + x_3 \times 8.5969$$

$$= 0.97 = 97\%$$

$$h_3 = h_{f_3} + x_3 h_{fg_3}$$
$$= 59.2401 + 0.97 \times 2468.66$$
$$= 2453.8403 \text{ kJ/kg}$$

4.6.1.3. TURBINE WORK OUTPUT W_T

To calculate the mass flowrate of steam to be received by the turbine, inlet and outlet conditions for the turbines can be utilised as shown below:

$$W_T = \dot{m}_{st}(h_3 - h_2)$$
$$206.186 = \dot{m}_{st}(2453.8403 - 2547.855\ )$$
$$\dot{m}_{st} = 2.19 \text{ kg/s}$$

4.6.1.4. EVAPORATOR ANALYSIS

State 1 – 2 – 5 process

The mass flowrate of surface warm ocean water can be calculated by heat balancing the evaporator with respect to the inlet and outlet conditions of Steam and warm water. Heat energy required to generate the steam at a temperature of 25℃.

$$\dot{m}_{st} = \frac{q_w}{h_{fg}}$$
$$2.19 = \frac{q_w}{2442.845}$$
$$q_w = 5349.83055 \text{ kJ/kg}$$

The amount of water required at the evaporator $\dot{m}_{ww}$

$$\dot{m}_{ww} = \frac{\dot{m}_{st} q_w}{Cp_{ww} \Delta T_{ww}}$$
$$= \frac{2.19 \times 5349.83055}{4.18(26-24)}$$
$$= 1401.450826 \text{ kg/s}$$

The warm water mass flowrate leaving the evaporator at temperature 24°C is discharged back to the ocean.

$$\dot{M}_{out} = \dot{m}_{ww} - \dot{m}_{st}$$
$$= 1401.450826 - 2.19$$

$$= 1399.260826 \frac{\text{kg}}{\text{s}}$$

4.6.1.5. THERMAL ENERGY DIFFERENCE WITHIN THE EVAPORATOR

$$\Delta Q_{ww} = Cp_{ww}\left(T_{in}\dot{m}_{ww} - T_{out}\dot{M}_{out}\right)$$
$$= 4.18(26 \times 1401.450826 - 24 \times 1399.260826)$$
$$= 11935.82971 \text{ kJ/kg}$$

A. Evaporator heat transfer area $\mathbf{A_h}$

Uv is a quantity of heat exchanger performance consisting of overall heat transfer coefficient (U-value).

TABLE 24: 98.186KW NET POWER, UV VALUE.

Symbol	Quantity	SI
E_V	evaporator	0.16W/m^{o}C

B. Evaporator

$$\Delta T_1 = T_{wwin} - T_{wwst}$$
$$= 26 - 14 = 12℃$$

$$\Delta T_2 = T_{wwin} - T_{wwout}$$
$$= 26 - 24 = 2℃$$

$$\Delta T_{LM} = \frac{\Delta T_1 + \Delta T_2}{\ln\left(\frac{\Delta T_1}{\Delta T_2}\right)}$$
$$= \frac{12+2}{\ln\left(\frac{12}{2}\right)}$$
$$= 7.81℃$$

$$A_{hE} = \frac{t_h q_w}{U_{stainless}\Delta T_{LM}}$$
$$= \frac{1\times10^{-3}\times5349.83055}{0.16\times7.81}$$
$$= 4.28 \text{ m}^2$$

4.6.1.6. CONDENSER ANALYSIS

A. State 3 – 4 process

The thermal energy output rejected at the condenser is Q_{out}

$$Q_{out} = \dot{m}_{st}(h_3 - h_4)$$
$$= 2.19(2453.8403 - 34.2606)$$
$$= 5298.88\ kJ/kg$$

B. Heat energy rejected into seawater

$$q_c = \dot{m}_{cw} Cp_{cw}(T_{cwo} - T_{cwi})$$
$$5298.88 = \dot{m}_{cw} \times 4.18(8 - 4)$$
$$\dot{m}_{cw} = 316.919\ kg/s$$

Therefore, the mass flowrate of Coldwater is, $\dot{m}_{cw} = 316.919\ kg/s$.

TABLE 25: 98.186KW NET POWER, UV VALUE.

Symbol	Quantity	SI
E_V	evaporator	0.16W/m^{o}C

$$\Delta T_1 = T_{icon} - T_{cwout}$$
$$= 14 - 8 = 6℃$$
$$\Delta T_2 = T_{0con} - T_{cwin}$$
$$= 6 - 4 = 2℃$$

$$\Delta T_{LM} = \frac{\Delta T_1 + \Delta T_2}{\ln\left(\frac{\Delta T_1}{\Delta T_2}\right)}$$
$$= \frac{6+2}{\ln\left(\frac{6}{2}\right)}$$
$$= 7.28℃$$

$$A_{hE} = \frac{t_h Q_{out}}{U_{stainless} \Delta T_{LM}}$$
$$= \frac{1 \times 10^{-3} \times 5298.88}{0.16 \times 7.28}$$
$$= 4.55\ m^2$$

4.6.1.7. CONDENSER ANALYSIS

A. State 3 – 4 process

The thermal energy output rejected at the condenser is Q_{out}

$$Q_{out} = \dot{m}_{st}(h_3 - h_4)$$
$$= 2.19(2453.8403 - 34.2606)$$
$$= 5298.88\ \text{kJ/kg}$$

B. Heat energy rejected into seawater

$$q_c = \dot{m}_{cw} Cp_{cw}(T_{cwo} - T_{cwi})$$
$$5298.88 = \dot{m}_{cw} \times 4.18(8 - 4)$$
$$\dot{m}_{cw} = 316.919\ \text{kg/s}$$

4.6.1.8. FIXED LOSS FACTORS

The L_{fixed} is calculated as the cold water intake power loss, condenser and distribution forcing loss, evaporator and delivery pushing loss within the process.

A. Pump Loss factor

$$\text{Pump Loss Factor} = \frac{\dot{m}_{wwg}}{\eta}$$
$$= \frac{1401.45 \times 9.81}{0.85}$$
$$= 16.17\text{kW/m}$$

B. Circulation Pumping Loss and Evaporator

This secure loss is estimated created on assumptions for 98.186 kW Net Power. The consistent Head Loss would be roughly 3.49m. the 3.49m of head accounts for the loss transversely consumption and discharge of evaporator.

$$\text{Evaporator and Distibution Pumping Loss} = \frac{\dot{m}_{ww} g h_{ww}}{\eta}$$
$$\text{Warmwater Mass Flowrate } \dot{m}_{ww} = 1401.450826\ \text{kg/s}$$
$$\text{Warm Water Head Loss } h_{ww} = 3.5\text{m}$$
$$\text{Seawater Pump Efficiency } \eta = 85\%$$
$$\text{Evaporator and Distibution Pumping Loss} = \frac{\dot{m}_{ww} g h_{ww}}{\eta}$$
$$= \frac{1401.450826 \times 9.81 \times 3.5}{0.85}$$

$= 56.61\text{kW}$

C. Coldwater Consumption Power Loss

This immobile loss is estimated built on water velocity and an identified factor for a bulging pipe entering, which is expected for cold-water inlet.

$$\text{Minor Head Loss(h)} = \frac{CV^2}{2g}, \text{where } V = \frac{Q}{A} = \frac{4\dot{m}}{\pi\rho D^2}$$

$\text{Head Loss Coefficient for Protruding pipe Entrance (C)} = 0.8$

$\text{Nominal seawater density } (\rho) = 998.2\text{kg/m}^3$

$\text{Coldwater pipe internal diameter (ID)} = 2\text{m}$

$\text{Mass Flowrate of Cold Water } (\dot{m}_{cw}) = 316.919\ \text{kg/s}$

4.6.1.9. PUMP LOSS FACTOR

$$\text{Pump Loss Factor} = \frac{\dot{m}_{cw} g}{\eta}$$

$$= \frac{316.919 \times 9.81}{0.85} = 3.66\text{kW/m}$$

$$V = \frac{4\dot{m}}{\pi\rho D^2}$$

$$= \frac{4 \times 316.919}{\pi \times 998.2 \times 2^2} = 0.101\ \text{m/s}$$

$\text{Intake Head Loss } (h_{intake})$

$$= \frac{0.8 \times (0.101)^2}{2 \times 9.81}$$

$$= 0.00042\text{m}$$

Cold Water Intake Power Loss

$= P_{LF} \text{ x } I_{HL}$

$= \times 0.00042$

$= 1.54\text{W}$

The C_w consumption power loss was calculated as drop in power loss. The arrival may be rounded formed to decrease losses. The 0.8 coefficient is used for

this characteristic bulging pipe' entry since the filter elements are unknown for this design.

A. Condenser and Feeding Pumping Loss

The static loss is estimated assumptions losses across the condenser and distribution pipe. The consistent Head Loss would be roughly 4.39m. the 4.39m of head accounts for the loss across intake and discharge of the condenser.

$= \text{Pump Loss Factor} \times \text{Assumed Head}$

$= 3.66 \times 4.5 = 16.47\text{kW}$

B. Cold Water Pipe (CWP) Friction Loss

This variable loss is dependent upon the length of the Cold-Water Pipe (CWP), the pipe diameter and the inside surface. The factor is established by estimating pipe wall friction based on the smoothness of the pipe, pipe diameter and water velocity.

$$\text{Head Loss due to Friction } (h_f) = \frac{fLV^2}{2Dg}$$

$$\text{Head Loss due to Friction per unit Length } \left(\frac{h_f}{L}\right) = \frac{fLV^2}{2DgL} = \frac{fV^2}{2Dg} \quad (4.1)$$

$$\text{Hydraulic Pipe Diameter } (D) = 2\text{m}$$

$$\text{Velocity in pipe } (V) = \frac{\dot{m}_{cw}}{\rho A}$$

$$= \frac{316.919}{1000 \times \frac{\pi(2)^2}{4}} = 0.1\text{m/s}$$

Colebrook Equation for Friction Factor (f)

$$: \frac{1}{\sqrt{f}} = -2\log_{10}\left(\frac{\frac{\epsilon}{D}}{3.7} + \frac{2.51}{Re\sqrt{f}}\right) \quad (4.2)$$

$$\text{Pipe Rougness Coeffient } (\epsilon) = 0.0000$$

$$\text{Reynold's Number } (Re) = \frac{DV\rho}{\mu}$$

$$\text{Absolute Viscosity } (\mu) = 1.573\text{Pa.s}$$

$$\text{Reynold's Number } (Re) = \frac{2\times0.1\times1000}{1.573} = 127.1455$$

$$\frac{1}{\sqrt{f}} = -2\log_{10}\left(\frac{\frac{0.00005}{2}}{3.7} + \frac{2.51}{127.145\sqrt{f}}\right) \therefore f = 0.1497$$

$$\text{Head Loss due to Friction per unit Length } \left(\frac{h_f}{L}\right)$$

$$= \frac{0.1497 \times (0.1)^2}{2 \times 2 \times 9.81} = 0.0381 \times 10^{-3}$$

$$\text{Pipe Friction Loss} = \frac{h_f}{L} \times \text{Pump Loss Factor} \quad (4.3)$$

$$= 0.0381 \times 10^{-3} \times 3.66 = \frac{0.1396W}{m}$$

The flow rate of warm seawater -$1401.450826\ kg/s$ at 26 °C is brought thru a 2.5 m ID FRP pipe. The pipe has an intake depth of 25 m and is 130 m long. The turbine propeller pump supplies the evaporator with warm seawater mass flowrate of $1401.450826\ kg/s$.

The pumping system puts the fluid into the chamber at the head of 3.5m from mean sea level (MSL). One submersible propeller-type pump brings $316.919\ kg/s$ of cold seawater through a 2m pipe from a depth of 1000 m. The length of the pipe is 2590 m.

The evaporator spout flashes the warm water through into the evaporation chamber at a pressure of 3.3604 kPa. The slight amount portion ($2.19\ kg/s$) of supply water is changed into steam and the rest is discharged into the ocean at a temperature of 24°C. Steam ($2.19\ kg/s$) from the evaporator enters the turbine at 3.1717 kPa and leaves the turbine diffuser system at 1.5985 kPa. The OTEC generator system generate the gross output of $206.186kW$. the exhausted steam from the OTEC turbine go in the condenser. The condenser collects $316.919\ kg/s$ of cold seawater at 4 °C and condenses $2.19\ kg/s$ of the incoming steam.

TABLE 26: SEA WATER PUMPS RATES.

Function	Warm water supply	Cold water supply	Warm water discharge	Cold water discharge
Flow rate (kg/s)	401.45	316.92	399	247
Total head (m)	1.4	3.6	3.2	5.4
Efficiency (%)	85	85	85	85

The function of the compressor on the system it pressurised all the particle that are not require on the system such as residual water and all gases that were dissolved on the solution.

TABLE 27: VACUUM PUMP RATES.

Symbol	Quantity	SI
F_{IN}	Inlet flow rate	6.9 m^3/s
P_{IN}	Inlet pressure	1.2 kPa
D_P	Discharge pressure	101 kPa
P_M	Maximum power	40 kW

For the purpose of this project a generic calculation of net power was considered as per the concept calculated below. The net power generated is from OTEC plant is 98.186kW achieved subsequently deducting $108\ \text{kW}$ for cold water supply pumping; $40\ \text{kW}$ for warm water supply pumping; $38\ \text{kW}$ for compressor; and $30\ \text{kW}$ for fresh water pumping from the gross power generated. Table 28 below present the out power produced see below.

$$\boxed{\boldsymbol{NET\ POWER}} = \boxed{Gross\ Power} - \{(Cold\ Sea\ Water\ Pump - Vacuum\ Pump - Warm\ Water\ Pump)\}$$

$$\boldsymbol{NET\ POWER} = 206.186 - 40 - 30 - 38 = \boldsymbol{98.186\ kW} \tag{4.4}$$

TABLE 28: CALCULATION DATA OF OC-OTEC 206.186KW PLANT PROPOSED.

Parameters	**Power** 206.186kW
Warm Water Temperature T_{ww}	26^oC
Cold Water Temperature T_{cw}	4^oC
Generator Gross Output Power	$206.186\ \text{kW}$
Net Power Output M_G	98.186kW
Generator Efficiency η_G	0,97
Steam Temperature T_{st} in	25^oC
Steam Temperature T_{st} out	14^oC
Specific capacity of water Cp	4.18 kJ/kgK
Seawater Pump Efficiency	85%
Mass flow rate of steam $\dot{m}_{st}$	$2.19\ \text{kg/s}$
Thermal Energy Difference within the evaporator	$11935.82971\ \text{kJ/kg}$
Evaporator heat transfer area A_h	$4.28\ m^2$

Thermal energy output rejected at the condenser is Q_{out}	$5298.88\ kJ/kg$
Heat energy rejected into seawater $\dot{m}_{cw}$	$316.919\ kg/s$
Condenser heat transfer area A_h	$4.55\ m^2$
Pump Loss factor	$16.17kW/m$
Evaporator and distribution pumping loss	$56.61kW$
Condenser and distribution pumping loss	$16.47kW$

CHAPTER 5

5. CONCLUSIONS AND RECOMMENDATIONS

This thesis focuses on the prospect of OC-OTEC in South Africa and possible locations suitable for this technology.

- This project it unique because it has never been implemented in Southern Africa.
- It is also a unique application because it generates electric power and simultaneously harvests fresh water. It is, in effect a self-powered desalination plant.

During this research the following points were undertaken:

- The feasible site for placing an OC-OTEC plant was investigated.
- Aspen software was used to design and simulate a small scale model OC-OTEC.
- The laboratory experiment model was designed and built at DUT.
- And a 200kW OC-OTEC model plant was designed.

South Africa is generally a water scarce country. This is particularly so on the South Coast of KwaZulu-Natal. In addition, the present problems faced by Eskom are mitigating against power hungry solutions such as r o desalination.

This paper proposes a solution to this problem by employing OC-OTEC to generate a self-powered solution for the provision of fresh water. It is shown that a 200kW pilot plant could generate up to about 100kW of electricity and also able to supply about 43000l of fresh water per day. Further work needs to be done to solve the large, low speed generator required but rapid advances are being made in this field and this problem will soon be overcome.

The simulation results from aspen and the small scale model plant were compared. The results obtained were presented against the temperature difference, since this is an important parameter in selecting an actual plant location. Potential sites, system design of Open-Cycle OTEC and its performance was experimentally

studied with the help of temperature and pressure readings before and after each component.

During the experiment the thermal efficiency and the power output increase with increasing temperature difference was noted. The power output is produced when the total temperature difference is sufficient to allow heat transfer within the evaporator and provide a pressure drop across the turbine. The efficiencies for the average of $\dot{m}_{ws} = 0.0372\,l/s$ are approximately equal to the efficiencies of the average of $\dot{m}_{ws} = 0.0098\,l/s$. The work done by the turbine for both $\dot{m}_{ws}$ increases with increasing operating temperature difference. The turbine uses the energy from the steam to do work, and as a result there is an observable drop across the turbine that leads to an enthalpy drop. it is also noted that the thermal efficiencies increase with increasing pressure across the turbine. An increase in pressure drop leads to a power output increase.

Throughout the research results it is felt that the Port Edward area is suited to the placement of an OC-OTEC plant owing to the nature of the ocean bathymetry off the coast with the continental shelf close to the shore giving a steep drop off to 3000m. The Port Edward area has a high possibility of utilising OTEC to extract freshwater water from the ocean. In addition to electricity generation, an OC-OTEC plant produces freshwater as a by-product of the power generation process.

Solar and wind power energy are good choice as ~~a~~ renewable energy sources, but ~~it~~ need~~s~~ massive funding, which would strain the economy and only provide peaking power as opposed to the base load power required in South Africa. Other ocean technologies were also briefly discussed and were seen, apart from ocean current harvesting, not to be suitable for the KZN region. OC-OTEC might have a significant initial cost, but in the long run it pays off the investment. according to calculation, within four years before a profit from the OC-OTEC system can be generated.

OC-OTEC power systems satisfy the criteria for suitable energy systems for South Africa, and if the suggestions introduced in this thesis are executed, it would be a giant leap toward solving the present energy and water crisis of the country.

REFERENCES

[1]. Kahrl, William L. Water and power: The conflict over Los Angeles water supply in the Owens Valley. University of California Press, 1983.

[2]. Weedy, Birron Mathew, et al. Electric power systems. John Wiley & Sons, 2012.

[3]. Hossain, Abrar, et al. Ocean thermal energy conversion: The promise of a clean future. Clean Energy and Technology (CEAT), 2013 IEEE Conference on. IEEE, 2013.

[4]. Kobayashi, Hiroki, Sadayuki Jitsuhara, and Haruo Uehara. The present status and features of OTEC and recent aspects of thermal energy conversion technologies. 24th Meeting of the UJNR Marine Facilities Panel, Honolulu, HI, November. 2001.

[5]. Bouwer, Herman. Integrated water management for the 21st century: problems and solutions. Journal of Irrigation and Drainage Engineering 128.4 (2002).

[6]. McMichael, Anthony J., et al. Food, livestock production, energy, climate change, and health. The lancet 370.9594 (2007).

[7]. Magesh, R. OTEC technology–a world of clean energy and water. World Congress on Engineering (WCE). 2010.

[8]. Botkin, Daniel B., Edward A. Keller, and Dorothy B. Rosenthal. Environmental science. Wiley, 2012.

[9]. Demirbas, Ayhan. Potential applications of renewable energy sources, biomass combustion problems in boiler power systems and combustion related environmental issues. Progress in energy and combustion science31.2 (2005).

[10]. Dessne, P., Fachina, V., Golmen, L. G., Miller, A. K., Panchal, C. B., Hammar, L., & Baird, J. (2015). OTEC matters 2015.

[11]. Goosen, Mattheus, Hacene Mahmoudi, and Noreddine Ghaffour. Overview of renewable energy technologies for freshwater production. Renewable energy applications for freshwater production (2012).

[12]. Edenhofer, Ottmar, et al. IPCC special report on renewable energy sources and climate change mitigation. Prepared by Working Group III of the Intergovernmental Panel on Climate Change, Cambridge University Press, Cambridge, UK (2011).

[13]. Semiat, Raphael. Present and future. Water International 25.1 (2000).

[14]. http://www.sabc.co.za/news/a/ee713e804a2bfdde8691cfa53d9712f0/Thousands-affected-by-drought-in-KZN-20151110, Thousands affected by drought in KZN, Sunday 11 October 2015.

[15]. Finney, Karen Anne. Ocean thermal energy conversion. Guelph Engineering Journal 1 (2008): 17-23.

[16]. Alkhalidi, A., M. Qandil, and H. Qandil. Analysis of Ocean Thermal Energy Conversion Power Plant using Isobutane as the Working Fluid. Int. J. of Thermal & Environmental Engineering 7.1 (2014): 25-32.

[17]. Althof, J. A. Direct-Contact Condensers for Open-Cycle OTEC Applications. (1988).

[18]. Vega, L.A. and Michaelis, D., 2010, January. First generation 50 MW OTEC plantship for the production of electricity and desalinated water. In Offshore technology conference. Offshore Technology Conference.

[19]. Yousefi, H., Mortazavi, S.M., Noorollahi, Y., Mortazavi, S.M. and Ranjbaran, P., 2017, February. A Review of Solar-geothermal Hybrid Systems for Water Desalination. In Proceedings, Workshop on Geothermal Reservoir Engineering Stanford University, Stanford, California (pp. 1-9).

[20]. Jadhav, M.S. and Kale, M.R., 2005. Ocean thermal energy conversion. Alternative Energy Sources, 90(12), pp.69-75.

[21]. Muralidharan, S., 2012. Assessment of ocean thermal energy conversion (Doctoral dissertation, Massachusetts Institute of Technology).

[22]. Mario, R., 2001. Ocean Thermal Energy Conversion and the Pacific Islands. Enery Unit, South Pacific Applied Geoscience Commission.

[23]. Khalid, S.S., Liang, Z. and Shah, N., 2012. Harnessing tidal energy using vertical axis tidal turbine. Research Journal of Applied Sciences, Engineering and Technology, 5(1), pp.239-252.

[24]. Ooi, B.J., Chew, B.C. and Khay, C.C., 2012. Managing the Transition of Fossil Fuels to Renewable Energy: Application of Ocean Thermal Energy Conversion at Sabah. (2012).

[25]. Rauchenstein, L.T., Van Zwieten, J.H. and Hanson, H.P., 2011, June. Model-based global assessment of OTEC resources with data validation off Southeast Florida. In OCEANS, 2011 IEEE-Spain (pp. 1-5). IEEE.

[26]. Hammar, L., Ehnberg, J., Mavume, A., Cuamba, B.C. and Molander, S., 2012. Renewable ocean energy in the Western Indian Ocean. Renewable and Sustainable Energy Reviews, 16(7), pp.4938-4950.

[27]. Faizal, M. and Rafiuddin Ahmed, M., 2011. On the ocean heat budget and ocean thermal energy conversion. International Journal of Energy Research, 35(13), pp.1119-1144.

[28]. Nihous, G.C., 2007. A preliminary assessment of ocean thermal energy conversion resources. Journal of Energy Resources Technology, 129(1), pp.10-17.

[29]. Finney, K.A., 2008. Ocean thermal energy conversion. Guelph Engineering Journal, 1, pp.17-23.

[30]. Ascari, M.B., Hanson, H.P., Rauchenstein, L., Van Zwieten, J., Bharathan, D., Heimiller, D., Langle, N., Scott, G.N., Potemra, J., Nagurny, N.J. and Jansen, E., 2012. Ocean Thermal Extractable Energy Visualization-Final Technical Report on Award DE-EE0002664. October 28, 2012 (No. DOE/EE0002664-1). Lockheed Martin Mission Systems and Sensors.

[31]. Ascari, M., 2012. Ocean Thermal Extractable Energy Visualization (No. DE--0002664). Lockheed Martin Corporation, Bethesda, MD (United States).

[32]. Vega, L.A., 2002. Ocean thermal energy conversion primer. Marine Technology Society Journal, 36(4), pp.25-35.

[33]. Harris, T.F.W., 1978. Review of coastal currents in southern African waters. National Scientific Programmes Unit: CSIR.

[34]. Lutjeharms, J.R., 2006. The coastal oceans of south-eastern Africa (15, W). The sea, 14, pp.783-834.

[35]. Barnes, D.K., Fuentes, V., Clarke, A., Schloss, I.R. and Wallace, M.I., 2006. Spatial and temporal variation in shallow seawater temperatures around Antarctica. Deep Sea Research Part II: Topical Studies in Oceanography, 53(8-10), pp.853-865.

[36]. Smit, A.J., Roberts, M., Anderson, R.J., Dufois, F., Dudley, S.F., Bornman, T.G., Olbers, J. and Bolton, J.J., 2013. A coastal seawater temperature dataset for biogeographical studies: large biases between in situ and remotely-sensed data sets around the coast of South Africa. PLoS One, 8(12), p.81944.

[37]. Schlegel, R.W. and Smit, A.J., 2016. Climate change in coastal waters: time series properties affecting trend estimation. Journal of Climate, 29(24), pp.9113-9124.

[38]. Hammar, L., Ehnberg, J., Mavume, A., Cuamba, B.C. and Molander, S., 2012. Renewable ocean energy in the Western Indian Ocean. Renewable and Sustainable Energy Reviews, 16(7), pp.4938-4950.

[39]. Eskom KwaZulu-Natal, Our Journey, our story. 1923 to 2012.

[40]. Eskom Transmission Development Plan 2016-2025, Eskom Transmission Group.

[41]. Nihous, G.C., 2007. An estimate of Atlantic Ocean thermal energy conversion (OTEC) resources. Ocean Engineering, 34(17-18), pp.2210-2221.

[42]. Nihous, G.C., 1989. Conceptual Design of a Small Open-Cycle OTEC Plant for the Production of Electricity and Fresh Water in a Pacific Island. In Proc. of Int. Conf. on Ocean Energy Recovery.

[43]. Harrison, S., 2010. Ocean thermal energy conversion. Submitted as coursework for Physics, 240, pp.1-6.

[44]. Avery, W.H. and Wu, C., 1994. Renewable energy from the ocean: a guide to OTEC. Oxford University Press.

[45]. National Renewable Energy Laboratory. Desalinated Water Date Unknown. 15 Apr. 2005 http://www.nrel.gov/otec/desalination.html.

[46]. Patel, H.K., Ram, A., Jatav, N. and Xaxa, M., 2015. A review of Ocean thermal energy conversion technique and its Economical consideration. International Journal of Research, 2(5), pp.668-675.

[47]. Rupeni, M., 2001. Ocean thermal energy conversion and the Pacific Islands. SOPAC miscellaneous report, 417.

[48]. Quoilin, S., Van Den Broek, M., Declaye, S., Dewallef, P. and Lemort, V., 2013. Techno-economic survey of Organic Rankine Cycle (ORC) systems. Renewable and Sustainable Energy Reviews, 22, pp.168-186.

[49]. Ooi, B.J., Chew, B.C. and Khay, C.C., 2012. Managing the Transition of Fossil Fuels to Renewable Energy: Application of Ocean Thermal Energy Conversion At Sabah.

[50]. Meisen, P. and Loiseau, A., 2009. Ocean energy technologies for renewable energy generation. Global Energy Network Institute.

[51]. Toossi, R., 2009. Energy and the environment: Sources, technologies, and impacts. Verve Publishers.

[52]. Tooke, M., 2005. Oil Peak–A Summary. April Retrieved, 2.

[53]. Szpunar, C.B. and Gillette, J.L., 1993. Environmental externalities: Applying the concept to Asian coal-based power generation (No. ANL/EAIS/TM--90). Argonne National Lab.

[54]. Hall, D.O. and House, J., 1995. Biomass: an environmentally acceptable fuel for the future. Proceedings of the Institution of Mechanical Engineers, Part A: Journal of Power and Energy, 209(3), pp.203-213.

[55]. Hansen, U., 1998. Technological options for power generation. The Energy Journal, pp.63-87.

[56]. Twidell, J. and Weir, T., 2015. Renewable energy resources. Routledge.

[57]. Dincer, I., 2000. Renewable energy and sustainable development: a crucial review. Renewable and sustainable energy reviews, 4(2), pp.157-175.

[58]. Charlier, R.H., 2007. Forty candles for the Rance River TPP tides provide renewable and sustainable power generation. Renewable and Sustainable Energy Reviews, 11(9), pp.2032-2057.

[59]. Terray, E.A., Donelan, M.A., Agrawal, Y.C., Drennan, W.M., Kahma, K.K., Williams, A.J., Hwang, P.A. and Kitaigorodskii, S.A., 1996. Estimates of kinetic energy dissipation under breaking waves. Journal of Physical Oceanography, 26(5), pp.792-807.

[60]. Wiedemann, H.O., Airbus Defence and Space GmbH, 1979. Apparatus for utilizing natural energies. U.S. Patent 4,159,427.

[61]. Fein, G.S. and Merritt, E., Genedics LLC, 2008. System and Method for Desalinating Water Using Alternative Energy. U.S. Patent Application 11/829,603.

[62]. Hagerman, George and Polagye, Brian. Methodology for estimating tidal energy resource and power production by Tidal In-Stream Energy Conversion (TISEC) devices. EPRI, September 2000.

[63]. McCormick, Michael E. Ocean wave energy conversion. Courier Corporation, 2013.

[64]. P. Clark, R. Klossner, L. Kologe, Tidal Energy, final project, November 2003.

[65]. Finney, Karen Anne. Ocean thermal energy conversion. Guelph Engineering Journal 1 (2008): 17-23.

[66]. Magesh, R. OTEC technology–a world of clean energy and water. World Congress on Engineering (WCE). 2010.

[67]. Buigues, G., et al. Sea energy conversion: problems and possibilities. International Conference on Renewable Energies and Power Quality (ICREPQ'06), 8p. 2006.

[68]. Hossain, Abrar, et al. Ocean thermal energy conversion: The promise of a clean future. Clean Energy and Technology (CEAT), 2013 IEEE Conference on. IEEE, 2013.

[69]. Straatman, Paul JT, and Wilfried GJHM van Sark. A new hybrid ocean thermal energy conversion–Offshore solar pond (OTEC–OSP) design: A cost optimization approach. Solar Energy 82.6 (2008): 520-527.

[70]. Pelc, Robin, and Rod M. Fujita. Renewable energy from the ocean. Marine Policy 26.6 (2002): 471-479.

[71]. Asou, Hiroyuki, Takeshi Yasunaga, and Yasuyuki Ikegami. Comparison between Kalina Cycle and Conventional OTEC System using Ammonia-Water Mixtures as Working Fluid. The

Seventeenth International Offshore and Polar Engineering Conference. International Society of Offshore and Polar Engineers, 2007.
[72]. Goto, Satoru, et al. Remote operation system including simulator function for OTEC plant. SICE Annual Conference (SICE), 2011 Proceedings of. IEEE, 2011.
[73]. Farret, Felix A., and Marcelo G. SimÃµes. Integration of alternative sources of energy. John Wiley & Sons, 2006.
[74]. Vega, Luis A. Ocean thermal energy conversion primer. Marine Technology Society Journal 36.4 (2002): 25-35.
[75]. Haven, Kendall F. Green Electricity: 25 Green Technologies that Will Electrify Your Future. ABC-CLIO, 2011.
[76]. Cohen, Robert. An overview of ocean thermal energy technology, potential market applications, and technical challenges. Offshore Technology Conference. Offshore Technology Conference, 2009.
[77]. Plant in Korea. The Twenty-fifth International Offshore and Polar Engineering Conference. International Society of Offshore and Polar Engineers, 2015.
[78]. Winter, CJ., Rudolf L. Sizmann, and Lorin L. Vant-Hull, Solar power plants: fundamentals, technology, systems, economics. Springer Science & Business Media, 2012.
[79]. Ahmadi, Pouria, Ibrahim Dincer, and Marc A. Rosen. Multi-objective optimization of an ocean thermal energy conversion system for hydrogen production. International Journal of Hydrogen Energy 40.24 (2015): 7601-7608.
[80]. Ahmadi, Pouria, Ibrahim Dincer, and Marc A. Rosen. Performance Evaluation of Integrated Energy Systems. Progress in Sustainable Energy Technologies: Generating Renewable Energy. Springer International Publishing, 2014. 103-147.
[81]. Kreith, Frank, and Ron West. Fallacies of a hydrogen economy: a critical analysis of hydrogen production and utilization. Journal of Energy Resources Technology 126.4 (2004): 249-257.
[82]. Long, George. Hydrogen reacted with carbon source to produce a usable hydrocarbon fuel. U.S. Patent No. 4,189,925. 26 Feb. 1980.
[83]. Awad, A. H., and T. Nejat Veziroğlu. Hydrogen versus synthetic fossil fuels. International journal of hydrogen energy 9.5 (1984): 355-366.
[84]. Ahmadi, Pouria, Ibrahim Dincer, and Marc A. Rosen. Energy and exergy analyses of hydrogen production via solar-boosted ocean thermal energy conversion and PEM electrolysis. International Journal of Hydrogen Energy38.4 (2013): 1795-1805.
[85]. Hoffert, Martin I., et al. Advanced technology paths to global climate stability: energy for a greenhouse planet. Science 298.5595 (2002): 981-987.
[86]. Wang, Dongxiang, Xiang Ling, and Hao Peng. Performance analysis of double organic Rankine cycle for discontinuous low temperature waste heat recovery. Applied Thermal Engineering 48 (2012): 63-71.
[87]. Huang, JOSEPH C., Hans J. Krock, and STEPHEN K. Oney. Revisit ocean thermal energy conversion system. Mitigation and Adaptation Strategies for Global Change 8.2 (2003): 157-175.

[88]. Uehara, H., et al. The experimental research on ocean thermal energy conversion using the Uehara cycle. Proceedings of International OTEC/DOWA Conference, Imari, Japan. 1999.
[89]. Daniel, Thomas. Ocean thermal energy conversion and the Natural Energy Laboratory of Hawaii. OTEC Aquaculture in Hawaii 5 (1988).
[90]. Vega, Luis A. Ocean thermal energy conversion primer. Marine Technology Society Journal 36.4 (2002): 25-35.
[91]. Huang, JOSEPH C., Hans J. Krock, and STEPHEN K. Oney. Revisit ocean thermal energy conversion system. Mitigation and Adaptation Strategies for Global Change 8.2 (2003): 157-175.
[100]. Vega, Luis A. Ocean ocean/oceanic Thermal Energy Conversion ocean/oceanic thermal energy conversion (OTEC). Renewable Energy Systems. Springer New York, 2013. 1273-1305.
[101]. Vega, Luis A. Ocean Thermal Energy Conversion (OTEC). Renewable Energy Systems. Springer New York, 2013. 1273-1305.
[102]. Vega, Luis A. Economics of ocean thermal energy conversion (OTEC): an update. Offshore Technology Conference. Offshore Technology Conference, 2010.
[103]. Vega, L. A., and Renewable Energy OTEC. Your in-depth source of information for Ocean Thermal Energy Conversion.
[104]. Avery, William H., and Chih Wu. Renewable energy from the ocean: a guide to OTEC. Oxford University Press, 1994.
[105]. Nihous, Gérard C. A preliminary assessment of ocean thermal energy conversion resources. Journal of Energy Resources Technology 129.1 (2007): 10-17.
[106]. Jagusztyn, Tadeusz F., and Marie Reny. Natural Cold Water District Cooling Plants Enabled by Directional Drilling. Road to Climate Friendly Chillers UNEP–ASHRAE Conference Sept. 2010.
[107]. Tomayko, James E. Solar Sea Power: Over a Century of Invention. ASME 2005 International Solar Energy Conference. American Society of Mechanical Engineers, 2005.
[108]. Panchal, C. B., and K. J. Bell. Simultaneous production of desalinated water and power using a hybrid-cycle OTEC plant. Journal of solar energy engineering 109.2 (1987): 156-160.
[109]. Yeh, Rong-Hua, Tar-Zen Su, and Min-Shong Yang. Maximum output of an OTEC power plant. Ocean Engineering (2005): 685-700.
[110]. Vega, Luis A., and Dominic Michaelis. First generation 50 MW OTEC plantship for the production of electricity and desalinated water. Offshore Technology Conference. Offshore Technology Conference, 2010.
[111]. Nihous, G. C., M. A. Syed, and L. A. Vega. Conceptual design of an open-cycle OTEC plant for the production of electricity and fresh water in a Pacific island. Ocean Energy Recovery. ASCE, 1990.
[112]. Kishore, Shalinee, Larry Snyder, and Parth Pradhan. Electricity from ocean wave energy: Technologies, opportunities and challenges. Newsletter (2013).
[113]. Constans, Jacques. Marine Sources of Energy: Pergamon Policy Studies on Energy and Environment. Vol. 53. Elsevier, 2013.

[114]. Gritton, Eugene C., et al. A Quantitative Evaluation of Closed-Cycle Ocean Thermal Energy Conversion (OTEC) Technology in Central Station Applications. Rand Corporation Report R-2595-DOE. 1980.
[115]. Ravindran, Muthukamatchi, and Raju Abraham. Ocean Thermal Energy Conversion. Springer Handbook of Ocean Engineering. Springer International Publishing, 2016. 1245-1266.
[116]. Lohani, Bindu, and Luis A. Vega. Wave Energy Conversion and Ocean Thermal Energy Conversion Potential in Developing Member Countries. (2014).
[117]. Dessne, Petter, et al. OTEC matters 2015. (2015).
[118]. Lohani, Bindu, and Luis A. Vega. Wave Energy Conversion and Ocean Thermal Energy Conversion Potential in Developing Member Countries. (2014).
[119]. Vega, Luis A. Ocean ocean/oceanic Thermal Energy Conversion ocean/oceanic thermal energy conversion (OTEC). Renewable Energy Systems. Springer New York, 2013. 1273-1305.
[120]. Lohani, Bindu, and Luis A. Vega. Wave Energy Conversion and Ocean Thermal Energy Conversion Potential in Developing Member Countries. (2014).
[121]. Vögler, Arne, and Vengatesan Venugopal. Observations on Shallow Water Wave Distributions at an Ocean Energy Site. ASME 2015 34th International Conference on Ocean, Offshore and Arctic Engineering. American Society of Mechanical Engineers, 2015.
[122]. Avery, William H., and Chih Wu. Renewable energy from the ocean: a guide to OTEC. Oxford University Press, 1994.
[123]. Avery, W. H., and G. L. Dugger. Contribution of ocean thermal energy conversion to world energy needs. International Journal of Ambient Energy1.3 (1980): 177-190.
[124]. Masutani, Stephen M., and Patrick K. Takahashi. Ocean thermal energy conversion. Wiley Encyclopedia of Electrical and Electronics Engineering (1999).
[125]. Vollenweider, R. A., et al. Characterization of the trophic conditions of marine coastal waters, with special reference to the NW Adriatic Sea: proposal for a trophic scale, turbidity and generalized water quality index. Environmetrics 9.3 (1998): 329-357.
[126]. Nebot, E., et al. Model for fouling deposition on power plant steam condensers cooled with seawater: Effect of water velocity and tube material. International Journal of Heat and Mass Transfer 50.17 (2007): 3351-3358.
[127]. Parsons, Brian K. Potential of Proposed Open-Cycle OTEC Experiments to Achieve Net Power Harold F. Link. Conference Record. Vol. 1. IEEE, 1986.
[128]. Link, H., and B. Parsons. Potential of Proposed Open-Cycle OTEC Experiments to Achieve Net Power. OCEANS'86. IEEE, 1986.
[129]. Rogers, L. J., et al. A Status Assessment of OTEC Technology. Ocean Resources. Springer Netherlands, 1990. 213-231.
[130]. Panchal, C. B., and K. J. Bell. Simultaneous production of desalinated water and power using a hybrid-cycle OTEC plant. Journal of solar energy engineering 109.2 (1987): 156-160.
[131]. Latteman, Sabine. Development of an environmental impact assessment and decision support system for seawater desalination plants. CRC press, 2010.

[132]. Friesth, Kevin Lee. Quintuple-Effect Generation Multi-Cycle Hybrid Renewable Energy System with Integrated Energy Provisioning, Storage Facilities and Amalgamated Control System Cross-Reference to Related Applications. U.S. Patent Application No. 14/613,994.
[133]. Bharathan, D. Direct-Contact Evaporation. Direct-Contact Heat Transfer. Springer Berlin Heidelberg, 1988. 203-222.
[134]. CRAVEN, JOHN P. Tropical Energy for North Temperate Zone Port Cities. Coastal Ocean Space Utilization (2002): 306.
[135]. Miguel, A. F., and M. Aydin. Ocean exergy and energy conversion systems. International Journal of Exergy 10.4 (2012): 454-470.
[136]. Berkovsky, B. Ocean Thermal Energy-Prospective Renewable Source of Power. Natural resources forum. Vol. 2. No. 4. Blackwell Publishing Ltd, 1978.
[137]. Parsons, Brian, Desikan Bharathan, and Jay Althof. Open cycle OTEC thermal-hydraulic systems analysis and parametric studies. OCEANS 1984. IEEE, 1984.
[138]. Masutani, Stephen M., and Patrick K. Takahashi. Ocean thermal energy conversion. Wiley Encyclopedia of Electrical and Electronics Engineering (1999).
[139]. Delgado Martín, Anna. Water Footprint of Electric Power Generation: Modelling its use and analysing options for a water-scarce future. Diss. Massachusetts Institute of Technology, 2012.
[140]. Smith Jr, Calvin Schwartz. Production of energy by direct contact of water immiscible working fluid with hot or warm water to vaporize liquid working fluid, utilization of vapor to produce mechanical energy and direct contact of spent vapor with cold or cool water to condense same. U.S. Patent No. 4,009,082. 22 Feb. 1977.
[141]. Bao, Junjiang, and Li Zhao. A review of working fluid and expander selections for organic Rankine cycle. Renewable and Sustainable Energy Reviews 24 (2013): 325-342.
[142]. Kalina, Alexander I. Generation of energy by means of a working fluid, and regeneration of a working fluid. U.S. Patent No. 4,346,561. 31 Aug. 1982.
[143]. Ravindran, Muthukamatchi, and Raju Abraham. Ocean Thermal Energy Conversion. Springer Handbook of Ocean Engineering. Springer International Publishing, 2016. 1245-1266.
[145]. Nihous, Gérard C. Ocean Thermal Energy Conversion (OTEC) and derivative technologies: Status of development and prospects. Global Status and Critical Developments in Ocean Energy (2008): 31.
[146]. Huang, JOSEPH C., Hans J. Krock, and STEPHEN K. Oney. Revisit ocean thermal energy conversion system. Mitigation and Adaptation Strategies for Global Change 8.2 (2003): 157-175.
[147]. Thomas, Anthony, and David L. Hillis. First production of potable water by OTEC and its potential applications. OCEANS'88. A Partnership of Marine Interests. Proceedings. IEEE, 1988.
[148]. Avery, William H., and Chih Wu. Renewable energy from the ocean: a guide to OTEC. Oxford University Press, 1994.
[149]. Giannotti, J., and J. Vadus. Ocean Thermal Energy Conversion (OTEC): Ocean Engineering Technology Development. OCEANS 81. IEEE, 1981.
[150]. Daniel, Thomas. Ocean thermal energy conversion and the Natural Energy Laboratory of Hawaii. OTEC Aquaculture in Hawaii 5 (1988).

[151]. Parsons, J. M., and F. Zangrando. US Department of Energy. (1990).
[152]. Orhan, Mehmet Fatih. Conceptual design, analysis and optimization of nuclear-based hydrogen production via copper-chlorine thermochemical cycles. Diss. University of Ontario Institute of Technology, 2011.
[153]. Kalogirou, Soteris A. Seawater desalination using renewable energy sources. Progress in energy and combustion science 31.3 (2005): 242-281.
[154]. Veerapaneni, Srinivas Vasu, et al. Reducing energy consumption for seawater desalination. American Water Works Association. Journal 99.6 (2007): 95.
[155]. Cohen, Robert, et al. Energy from the Ocean [and Discussion]. Philosophical Transactions of the Royal Society of London A: Mathematical, Physical and Engineering Sciences 307.1499 (1982): 405-437.
[156]. Link, H., and B. Parsons. Potential of Proposed Open-Cycle OTEC Experiments to Achieve Net Power. OCEANS'86. IEEE, 1986.
[157]. Hunt, D. F., et al. Commercialization of Solar Systems Through Standards, Evaluation, Inspection and Redress: A Joint Effort. Solar Energy & Conservation 1 Symposium-Workshop. 1978.
[158]. Penney, T., et al. An Assessment of Technology for a Small-Scale, Shore-Based, Open-Cycle Ocean Thermal Energy Conversion System-A Design Case Study for an Integrated Research Facility. Solar Energy Research Institute, SERI-TR-252-2184, Golden, CO: May (1984).
[159]. Watt, Arthur D., F. S. Mathews, and R. E. Hathaway. Open cycle ocean thermal energy conversion: a preliminary engineering evaluation. Final report. No. ALO-3723-76/3. Colorado School of Mines, Golden (USA). Dept. of Engineering Physics, 1977.
[160]. Parsons, Brian K. Potential of Proposed Open-Cycle OTEC Experiments to Achieve Net Power Harold F. Link. Conference Record. Vol. 1. IEEE, 1986.
[161]. Kim, Albert S., et al. Dual-use open cycle ocean thermal energy conversion (OC-OTEC) using multiple condensers for adjustable power generation and seawater desalination. Renewable Energy 85 (2016): 344-358.
[162]. Althof, J. A. Direct-Contact Condensers for Open-Cycle OTEC Applications. (1988).
[163]. Prochazka, T. Framework for Developing Innovation Systems in Small Island Developing States: Roadmap for turning Curaçao into the OTEC Centre of Excellence. Diss. TU Delft, Delft University of Technology, 2012.
[164]. Mario, Rupeni, et al. Pacific Islands Applied Geoscience Commission (SOPAC), Fiji.
[165]. Bharathan, Desikan, et al. Conceptual design of an open-cycle ocean thermal energy conversion net power-producing experiment (OC-OTEC NPPE). No. SERI/TP-253-3616. Solar Energy Research Inst., Golden, CO (USA), 1990.
[166]. Energy Island Ltd. URL http://www.energyisland.com/technologies.html.
[167]. Jackson, W. D., et al. Considerations in the Development of Open Cycle MHD Systems for Commercial Service. CONF-750601-P5 VOL. V-LATE PAPERS TIP. 1975.
[168]. McDonald, Colin F. The Closed-Cycle Turbine: Present and Future Prospective for Fossil and Nuclear Heat Sources. ASME 1978 International Gas Turbine Conference and Products Show. American Society of Mechanical Engineers, 1978.

[169]. Kuo, Tsai-C., Samuel H. Huang, and Hong-C. Zhang. Design for manufacture and design for 'X': concepts, applications, and perspectives. Computers & Industrial Engineering 41.3 (2001): 241-260.

[170]. Jackson, W. D., et al. Considerations in the Development of Open Cycle MHD Systems for Commercial Service. CONF-750601-P5 VOL. V-LATE PAPERS TIP. 1975.

[171]. Zabihian, Farshid, and Alan Fung. Advanced Power Generation Technologies: Fuel Cells. INTECH Open Access Publisher, 2010.

[172]. ELECTIVE-II, ELECTIVE-I. Proposed Structure and Syllab.

[173]. El-Dessouky, H., and H. Ettouney. Ocean thermal energy conversion. (2001).

[174]. Mitsumori, Tomohiro, Yasuyuki Ikegami, and Haruo Uehara. Comparison of OTEC power plant using plate type heat exchanger and one using double fluted tube type. The Eighth International Offshore and Polar Engineering Conference. International Society of Offshore and Polar Engineers, 1998.

[175]. Takazawa, Hiroyuki, Masatsugu Amano, and Tadayoshi Tanaka. Performance characteristics of barometric-type open-cycle OTEC system. Heat Transfer-Japanese Research 25.4 (1996): 226-237.

[176]. Nelson, J. S., et al. Simulations of the performance of open cycle desiccant systems using solar energy. Solar Energy 21.4 (1978): 273-278.

[177]. Gordon, J. M., and Mahmoud Huleihil. General performance characteristics of real heat engines. Journal of Applied Physics 72.3 (1992): 829-837.

[178]. Raja, A. K. Power plant engineering. New Age International, 2006.

[179]. Abdalla Hanafi, Desalination using renewable energy sources, Desalination, 97, pp. 339-352, 1994.

[180]. Warfel, C.G., Manwell, J.F., McGowan, J.G., Techno-economic study of autonomous wind driven reverse osmosis desalination systems, Solar & Wind Technology, Vol. 5, No. 5, pp. 549-561, 1988.

[181]. Towards the Large Scale Development of Decentralised Water Desalination, PRODESAL Final Report, EEC, DG XII, APAS, RENA CT94-0005, 1996.

[182]. Decision Support System for the Integration of Renewable Energies into Water Desalination Systems, REDES Final Report, EEC, DG XII, APAS, RENA CT94-0058, 1996.

[183].The European Renewable Energy Study, EEC, DG XVII, 1994.

[184]. Magal B.S, Solar power engineering, McGraw-Hill, New Delhi, 1990.

[185]. Twidell J, Weir T, Renewable energy sources, University Press, Cambridge, 1986.

[186]. Stone L. S., Photovoltaics: Unlimited electrical energy from Sun, reprinted from Physics Today http://www.nrel.gov/research/pv/dpcs/pvpaper.html (1993).

[187]. Rados, K.G., Assimacopoulos, D., Zervos, A., Application Possibilities of Wind - Reverse Osmosis desalination plants in Greek islands, Proc. MED Conference, Santorini, 1996.

[188]. European Commission, Joule-Thermie Programme, Desalination Guide Using Renewable Energies, (1998).

[189]. Mathioulakis, E., V. Belessiotis, and E. Delyannis. Desalination by using alternative energy: Review and state-of-the-art. Desalination 203.1 (2007): 346-365.
[190]. Van Santen, Rutger, Djan Khoe, and Bram Vermeer. 2030: Technology that will change the World. Oxford University Press, 2010.
[191]. Rischard, Jean-Francois. High noon: Twenty global problems, twenty years to solve them. Basic Books, 2002.
[192]. Burgi, Philip H. Water challenges in the 21st century. Water Engineering and Management through Time-Learning from History. E. Cabrera and F. Arregui. AK Leiden, CRC Press/Balkema (2010): 303-334.
[193]. Shiklomanov, Igor A. World water resources. A new appraisal and assessment for the 21st century (1998).
[194]. Miller, James E. Review of water resources and desalination technologies. Sandia national labs unlimited release report SAND-2003-0800 (2003).
[195]. Corcoran, Emily, ed. Sick water the central role of wastewater management in sustainable development: a rapid response assessment. UNEP/Earthprint, 2010.
[196]. Epstein, T. Scarlett, and David Jezeph. Development—There Is Another Way: A Rural–Urban Partnership Development Paradigm. World Development 29.8 (2001): 1443-1454.
[197]. Liu, Xiaohua, et al. Thermal and economic analyses of solar desalination system with evacuated tube collectors. Solar Energy 93 (2013): 144-150.
[198]. Liu, Xiaohua, et al. The research on thermal and economic performance of solar desalination system with salinity-gradient solar pond. Desalination and Water Treatment 51.19-21 (2013): 3735-3742.
[199]. Supply, Water. FR/R0013. (2011).
[200]. Awerbuch, L. Future Directions in Integration of Desalination. Energy and the Environment. International Desalination Association Seminar, Boston, Feb 23rd. 2009.
[201]. Shackleton, Charlie M., et al. The importance of dry woodlands and forests in rural livelihoods and poverty alleviation in South Africa. Forest policy and economics 9.5 (2007): 558-577.
[202]. Lockhat, Rafiq, and Ashley Van Niekerk. South African children: A history of adversity, violence and trauma. Ethnicity and Health 5.3-4 (2000): 291-302.
[203]. Brichieri-Colombi, Stephen. The world water crisis: The failures of resource management. Vol. 14. IB Tauris, 2008.
[204]. Gupta, Joyeeta, and Pieter van der Zaag. Interbasin water transfers and integrated water resources management: Where engineering, science and politics interlock. Physics and Chemistry of the Earth, Parts A/B/C 33.1 (2008): 28-40.
[205]. Jury, William A., and Henry Vaux. The role of science in solving the world's emerging water problems. Proceedings of the national academy of sciences of the United States of America 102.44 (2005): 15715-15720.
[206]. Fischer, Günther, and Gerhard K. Heilig. Population momentum and the demand on land and water resources. Philosophical Transactions of the Royal Society of London B: Biological Sciences 352.1356 (1997): 869-889.

[207]. Li, Norman N., et al., eds. Advanced membrane technology and applications. John Wiley & Sons, 2011.
[208]. Ghaffour, Noreddine, et al. Renewable energy-driven desalination technologies: A comprehensive review on challenges and potential applications of integrated systems. Desalination 356 (2015): 94-114.
[209]. Jeppesen, T., et al. Metal recovery from reverse osmosis concentrate. Journal of Cleaner Production 17.7 (2009): 703-707.
[210]. Bamaga, O. A., et al. Hybrid FO/RO desalination system: Preliminary assessment of osmotic energy recovery and designs of new FO membrane module configurations. Desalination 268.1 (2011): 163-169.
[211]. Merten, Ulrich. Desalination by reverse osmosis. The MIT Press, 1966.
[212]. Mulder, J. Basic principles of membrane technology. Springer Science & Business Media, 2012.
[213]. Baker, Richard W. Membrane technology. John Wiley & Sons, Inc., 2000.
[214]. Evans, Annette, Vladimir Strezov, and Tim J. Evans. Assessment of sustainability indicators for renewable energy technologies. Renewable and sustainable energy reviews 13.5 (2009): 1082-1088.
[215]. Xie, Ming, et al. A forward osmosis–membrane distillation hybrid process for direct sewer mining: system performance and limitations. Environmental science & technology 47.23 (2013): 13486-13493.
[216]. Judd, Simon. The MBR book: principles and applications of membrane bioreactors for water and wastewater treatment. Elsevier, 2010.
[217]. Le My, Dinh. Membrane Distillation Application in Purification and Process Intensification. Diss. Asian Institute of Technology, 2015.
[218]. Ali, Muhammad Tauha, Hassan ES Fath, and Peter R. Armstrong. A comprehensive techno-economic review of indirect solar desalination. Renewable and Sustainable Energy Reviews 15.8 (2011): 4187-4199.
[219]. Mulder, J. Basic principles of membrane technology. Springer Science & Business Media, 2012.
[220]. Lockeed Martin (2013), Covenant Lockeed Martin, Reignwood Group, signed on13April2013,www.lockheedmartin.co.uk/us/news/pressreleases/2013/october/131030-mst-otec-lockheed-martin-and-reignwood-group-sign-contract-to develooceanthermal-energy-conversion-power-plant.html.
[221]. Vega, L.A., (2007), OTEC Economics, Offshore Infrastructure Associations, 22 August 2007.
[222]. Vega, L.A., (2010), Economics of Ocean Thermal Energy Conversion (OTEC): An Update, Offshore Technology Conference 2010, OTC 21016, Houston, Texas, 3-6 May, http://hinmrec.hnei.hawaii.edu/wp-content/uploads/2010/01/OTEC-Economics-2010. pdf.
[223]. Vega, L.A., (2012), Ocean Thermal Energy Conversion, Encyclopedia of Sustainability Science and Technology, Springer, pp. 7296-7328, http://hinmrec

[224]. Muralidharan, S. (2012), Assessment of Ocean Thermal Energy Conversion, MSc thesis System Design and Management Program, Massachusetts Institute of Technology,February,http://dspace.mit.edu/handle/1721.1/76927hnei.hawaii.edu/wpcontent/uploads/2010/01/OTEC-Summary-Aug-2012.pdf.

[225]. Lewis, A., et al. (2011), Ocean Energy, In O. Edenhofer et al. (Eds.) IPCC Special Report on Renewable Energy Sources and Climate Change Mitigation, Cambridge University Press, Cambridge, and New York, http://srren.ipcc-wg3.de/report/IPCC_SRREN_Ch06. pdf.

[226]. Cussler, Edward Lansing. Diffusion: mass transfer in fluid systems. Cambridge university press, 2009.

[227]. Simon, Albert. Diffusion of like particles across a magnetic field. Physical Review 100.6 (1955): 1557.

[228]. Diamantoudis, A. T, and G. N. Labeas. Stress intensity factors of semi-elliptical surface cracks in pressure vessels by global-local finite element methodology. Engineering Fracture Mechanics 72.9 (2005): 1299-1312.

[229]. Murphy, James C. Flanged diffuser and air cell retainer for pressure vessel. U.S. Patent No. 5,388,720. 14 Feb. 1995.

[230]. Leckie, F. A., and D. J. Payne. Some observations on the design of spherical pressure vessels with flash cylindrical nozzles. Proceedings of the Institution of Mechanical Engineers 180.1 (1965): 497-512.

[231]. Xue, M. D., et al. A reinforcement design method based on analysis of large openings in cylindrical pressure vessels. Journal of pressure vessel technology 118.4 (1996): 502-506.

[232]. Powers, John R., et al. Method for obtaining commercial feed juices having a more hand-squeezed character. U.S. Patent No. 4,889,739. 26 Dec. 1989.

[233]. MacGregor, James Grierson, et al. Reinforced concrete: mechanics and design. Vol. 3. Upper Saddle River, NJ: Prentice Hall, 1997.

[234]. Mohee, Romeela, and Ackmez Mudhoo. Analysis of the physical properties of an in-vessel composting matrix. Powder Technology 155.1 (2005): 92-99.

[235]. Kim, Albert S., et al. Dual-use open cycle ocean thermal energy conversion (OC-OTEC) using multiple condensers for adjustable power generation and seawater desalination. Renewable Energy 85 (2016): 344-358.

[236] Rogers, G.F.C., and Y.R. Mayhew. Heat transfer and pressure loss in helically coiled tubes with turbulent flow. International Journal of Heat and Mass Transfer 7.11 (1964): 1207-1216.

[237] Mori, Y., and W. Nakayama. Study of forced connective heat transfer in curved pipes (2nd report, turbulent region). International Journal of Heat and Mass Transfer 10.1 (1967): 37-59.

[236]. Janssen, L. A. M., and C. J. Hoogendoorn. Laminar convective heat transfers in helical coiled tubes. International Journal of Heat and Mass Transfer 21.9 (1978): 1197-1206.

[237]. Lei, Yong-Gang, et al. Effects of baffle inclination angle on flow and heat transfer of a heat exchanger with helical baffles. Chemical Engineering and Processing: Process Intensification 47.12 (2008): 2336-2345.

[238]. Salimpour, M. R. Heat transfer coefficients of shell and coiled tube heat exchangers. Experimental thermal and fluid science 33.2 (2009): 203-207.
[239]. Simon, N. J., E. S. Drexler, and Richard Palmer Reed. Properties of copper and copper alloys at cryogenic temperatures. US National Institute of Standards and Technology (USA), (1992): 850.
[240]. Naphon, Paisarn. Thermal performance and pressure drop of the helical-coil heat exchangers with and without helically crimped fins. International Communications in Heat and Mass Transfer 34.3 (2007): 321-330.
[241]. Salimpour, M. R. Heat transfer coefficients of shell and coiled tube heat exchangers. Experimental thermal and fluid science 33.2 (2009): 203-207.
[242]. Seban, R. A., and E. F. McLaughlin. Heat transfer in tube coils with laminar and turbulent flow. International Journal of Heat and Mass Transfer 6.5 (1963): 387-395.
[243]. Richards, Mark S., and Shannon B. Copeland. Fluid separation apparatus. U.S. Patent No. 3,931,011. 6 Jan. 1976.
[244]. Kumar, Sudarshan, Kaoru Maruta, and S. Minaev. On the formation of multiple rotating Pelton-like flame structures in radial microchannels with lean methane–air mixtures. Proceedings of the Combustion Institute 31.2 (2007): 3261-3268.
[245]. Dixon, S. Larry, and Cesare Hall. Fluid mechanics and thermodynamics of turbo machinery. Butterworth-Heinemann, 2013.
[246]. Alhazmy, M. M., and Y. S. H. Najjar. Augmentation of gas turbine performance using air coolers. Applied Thermal Engineering 24.2 (2004): 415-429.
[247]. Kotas, Tadeusz Jozef. The exergy method of thermal plant analysis. Elsevier, 2013.
[248]. Robinson, Douglas M., and Eckhard A. Groll. Efficiencies of transcritical CO_2 cycles with and without an expansion turbine: Rendement de cycles transcritiques au CO_2 avec et sans turbine d'expansion. International Journal of Refrigeration 21.7 (1998): 577-589.
[249]. Chen, Huijuan, D. Yogi Goswami, and Elias K. Stefanakos. A review of thermodynamic cycles and working fluids for the conversion of low-grade heat. Renewable and sustainable energy reviews 14.9 (2010): 3059-3067.
[250]. Bernad, Sandor, et al. Flow investigations in Achard turbine. Proc. the Romanian Academy 9.2 (2008): 1-12.
[251]. Schuermans, Bruno, et al. Thermoacoustic analysis of gas turbine combustion systems using unsteady CFD. ASME Turbo Expo 2005: Power for Land, Sea, and Air. American Society of Mechanical Engineers, 2005.
[252]. Mansfield, Donald H., Douglas W. Boyce, and William G. Pacelli. Guidelines for Specifying and Evaluating the Rerating and Reapplication of Steam Turbines. Proceedings of the 35th Turbomachinery Symposium. 2006.
[253]. Bloch, Heinz P. A practical guide to compressor technology. John Wiley & Sons, 2006.
[254]. Bloch, Heinz P., and Murari Singh. Steam Turbines: Design, Application, and Re-Rating. McGraw Hill Professional, 2008.
[255]. Nussbaumer, Thomas, and J. E. Hustad. Overview of biomass combustion. Developments in thermochemical biomass conversion. Springer Netherlands, 1997. 1229-1243.

[256]. Havakechian, S., and R. Greim. Aerodynamic design of 50 per cent reaction steam turbines. Proceedings of the Institution of Mechanical Engineers, Part C: Journal of Mechanical Engineering Science 213.1 (1999): 1-25.

[257]. Austin, Gary Nin. Sodium injection for advanced steam turbines. U.S. Patent Application No. 12/151,610.

[258]. Dowson, Phillip, Stephen L. Ross, and Carl Schuster. The investigation of suitability of abradable seal materials for application in centrifugal compressors and steam turbines. Proceedings of the twentieth turbomachinery symposium. 1991.

[259]. Seban, R. A., and McLaughlin, E. F., 1963, Heat transfer in tube coils with laminar and turbulent flow, Int. J Heat Mass Transfer, 6, 387-495.

[260]. Singh, Bharat Raj, and Onkar Singh. A Study on Sustainable Energy Sources and its Conversion Systems Towards Development of an Efficient Zero Pollution Novel Air Turbine to Use as Prime-Mover to the Light Vehicle.ASME 2008 International Mechanical Engineering Congress and Exposition. American Society of Mechanical Engineers, 2008.

[261]. Filonenko, G. K. Hydraulic resistance in pipes. (1954): 40-44.

[262]. Seban, R. A., and McLaughlin, E. F., 1963, Heat transfer in tube coils with laminar and turbulent flow, Int. J Heat Mass Transfer, 6, 387-495.

[263]. Singh, Bharat Raj, and Onkar Singh. A Study on Sustainable Energy Sources and its Conversion Systems Towards Development of an Efficient Zero Pollution Novel Air Turbine to Use as Prime-Mover to the Light Vehicle. ASME 2008 International Mechanical Engineering Congress and Exposition. American Society of Mechanical Engineers, 2008.

APPENDIX A

DESIGN CALCULATION OF THE EXPERIMENT PROTOTYPE OF OC-OTEC PLANT

$$Q_{ww} = Av$$

$$0.000583 = \frac{\pi}{4}\left(0.02^2\right)v \qquad \text{…A1}$$

$$\therefore v = 1.857\,\text{m/s}$$

MASS FLOWRATE OF WARM WATER $\dot{M}_{in}$;

$$\dot{M}_{in} = \rho Av$$

$$= 983.13 \times \frac{\pi}{4}(0.02)^2 \times 1.857 \qquad \text{…A2}$$

$$= 0.573\,\text{kg/s}$$

STEAM MASS FLOWRATE, $\dot{m}_{st}$;

$$f_{st} = \frac{\dot{m}_{st}}{\dot{M}_{in}}$$

$$= 0.00565 = \frac{\dot{m}_{st}}{0.573_{st}} \qquad \text{…A3}$$

$$\therefore \dot{m}_{st} = 0.003238\,\text{kg/s}$$

THE MASS FLOWRATE BALANCE

$$\dot{M}_{out} = \dot{M}_{in} - \dot{m}_{st}$$

$$= 0.573 - 0.003238 \qquad \text{…A4}$$

$$= 0.5698\,\text{kg/s}$$

VELOCITY OF DISCHARGED WATER

$$\dot{M}_{out} = \rho Av$$

$$= 0.5698 = 983.13 \times \frac{\pi}{4}(0.02)^2\, v \qquad \text{…A5}$$

$$\therefore v = 1.845\,\text{m/s}$$

FLOWRATE OF DISCHARGED WATER

$$Q_{ww} = Av$$
$$= \frac{\pi}{4}(0.02)^2 \times 1.845 \quad \text{…A6}$$
$$= 0.00058\,m^3/s$$
$$\therefore v = 1.857\,m/s$$

Thermal energy difference between the intake and discharged warm water

$$\Delta Q_{ww} = C_{cp}\left(T_{in}\ \dot{M}_{in} - T_{out}\ \dot{M}_{out}\right)$$
$$= 4182(303.15 \times 0.573 - 293.15 \times 0.5698) \quad \text{…A7}$$
$$= 27.88\,kW$$

LATENT HEAT (SPECIFIC HEAT OF EVAPORATOR)

$$\Delta Q_{ww} = \dot{m}_{st} L_{h,ev}$$
$$27934 = 0.003238\,L_{h,ev} \quad \text{…A8}$$
$$L_{h,ev} = 8627.22\,kJ/kg$$

Calculated steam temperature by interpolation:

$$\frac{28.96 - 24.08}{4 - 3}$$
$$= \frac{T_{st} - 24.08}{3.5 - 3} \quad \text{…A9}$$
$$T_{st} = 26.52^0\,C = 299.67\,K$$

THE FLASH STEAM GENERATED %

$$\text{Flashgenerated}\,\% = \frac{h_{f,in} - h_{f,out}}{h_{fg,st}}$$
$$= \frac{125.811 - 84.2043}{2439.248} \quad \text{…A10}$$
$$= 0.017 = 1.7\%$$

CONDENSATE VOLUME

$$V_{cond} = (1 - \mathit{flashgenerated}\%) \cdot c_v$$
$$= (1 - 0.017) \cdot 0.001004 \qquad \text{...A11}$$
$$= 0.00099\,\mathrm{m}^3/\mathrm{kg}$$

STEAM VOLUME

$$V_{steam} = (\mathrm{flashgenerated}\%)\,c_v$$
$$= 0.017 \times 45.9 \qquad \text{...A12}$$
$$= 0.78\,\mathrm{m}^3/\mathrm{Kg}$$

CALCULATION STEAM SPEED INSIDE A PIPE

$$\dot{m}_{st} = \rho A v$$

$$0.003238 = 1.12083 \times \frac{\pi}{4}(0.02)^2\ v$$

$$\therefore v = 9.2\,\mathrm{m/s}^{-1}$$

$$Q_{ww} = Av$$
$$= \frac{\pi}{4}(0.02)^2 \times 9.2 \qquad \text{...A13}$$
$$= 0.00299\,\mathrm{m}^3/\mathrm{s}^{-1}$$

APPENDIX B

OTEC DESIGN FRAME

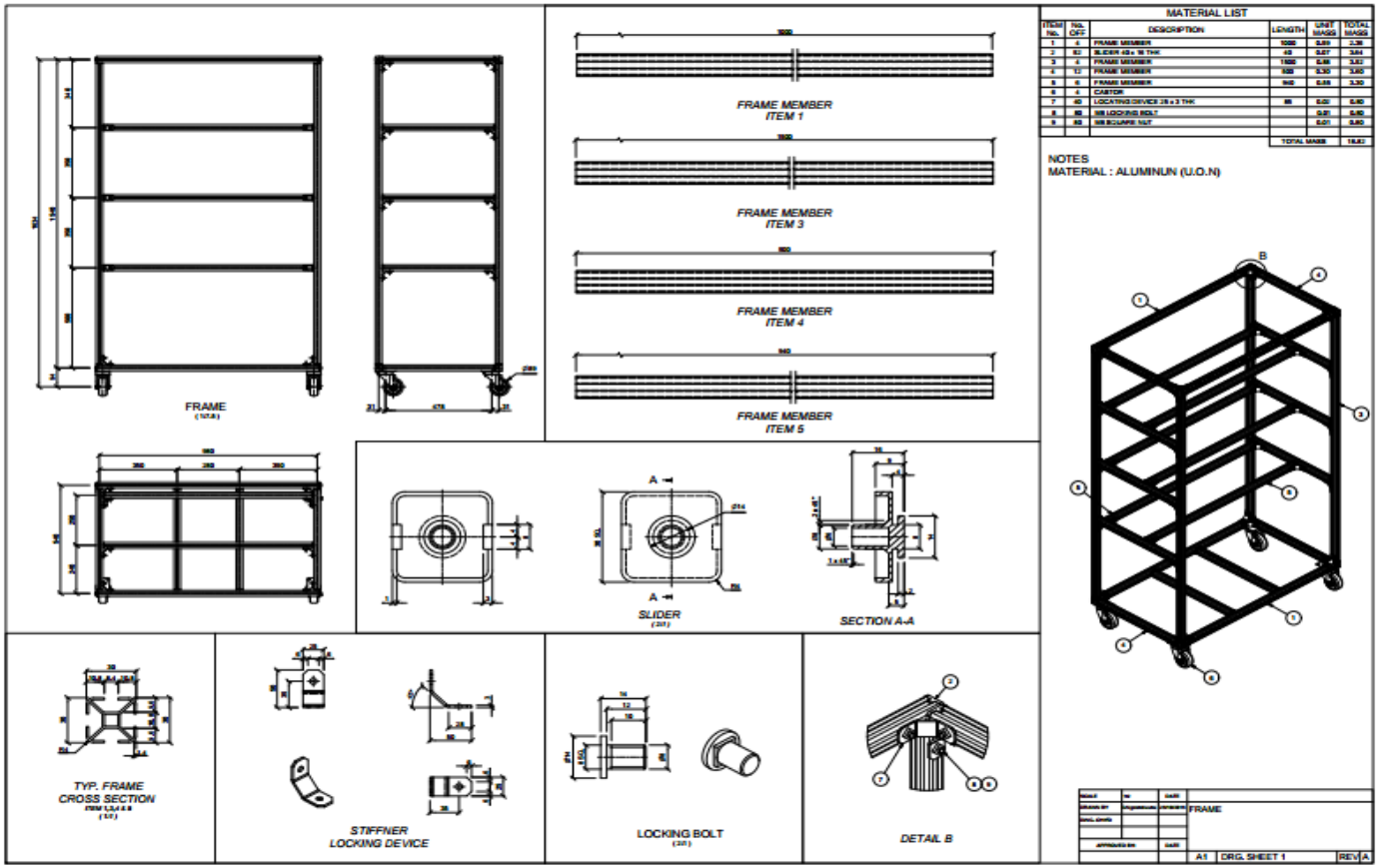

APPENDIX C

OTEC DESIGN FLASH EVAPORATOR

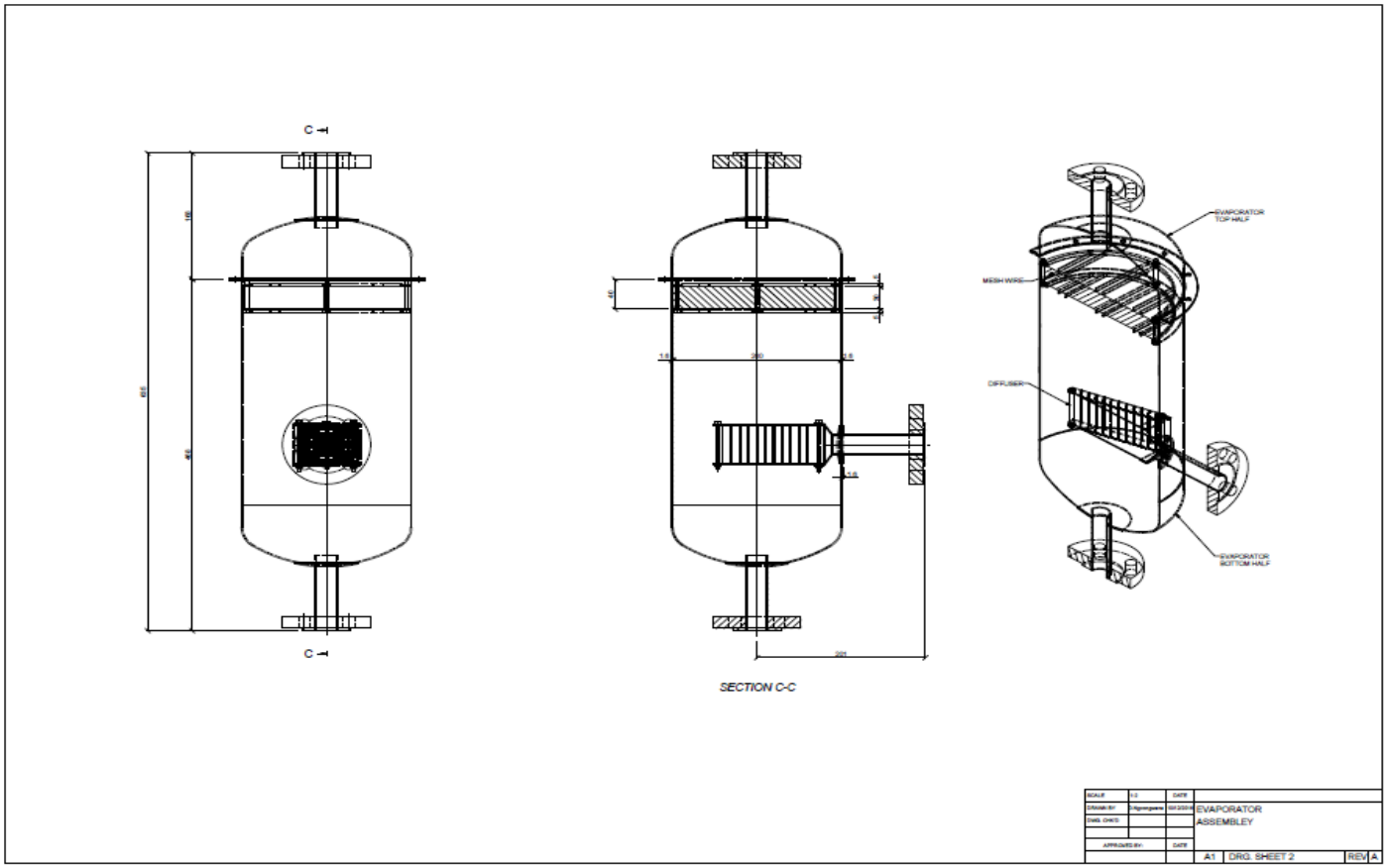

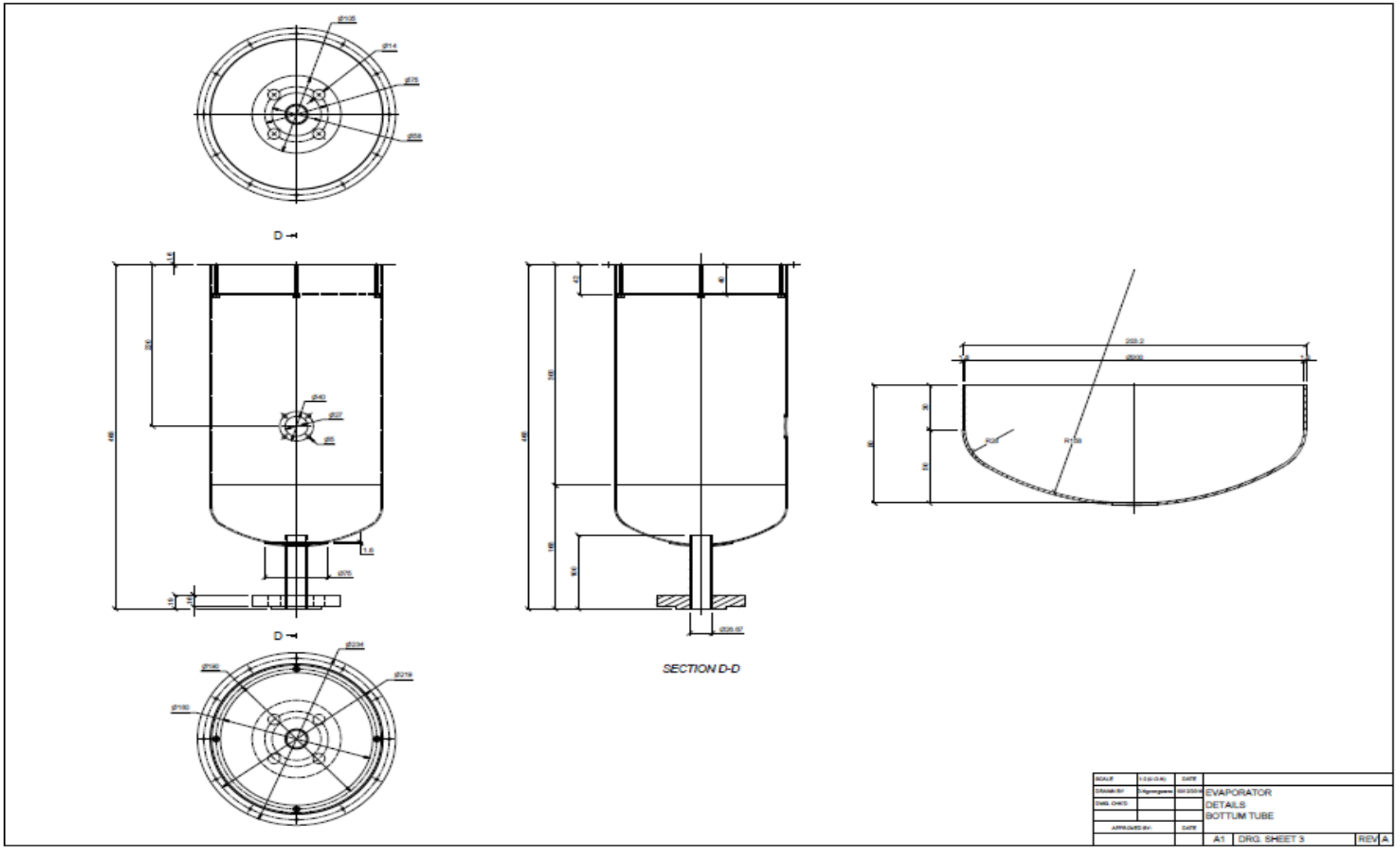
D
D
SECTION D-D
EVAPORATOR
DETAILS
BOTTUM TUBE
A1
DRG. SHEET 3
REV A

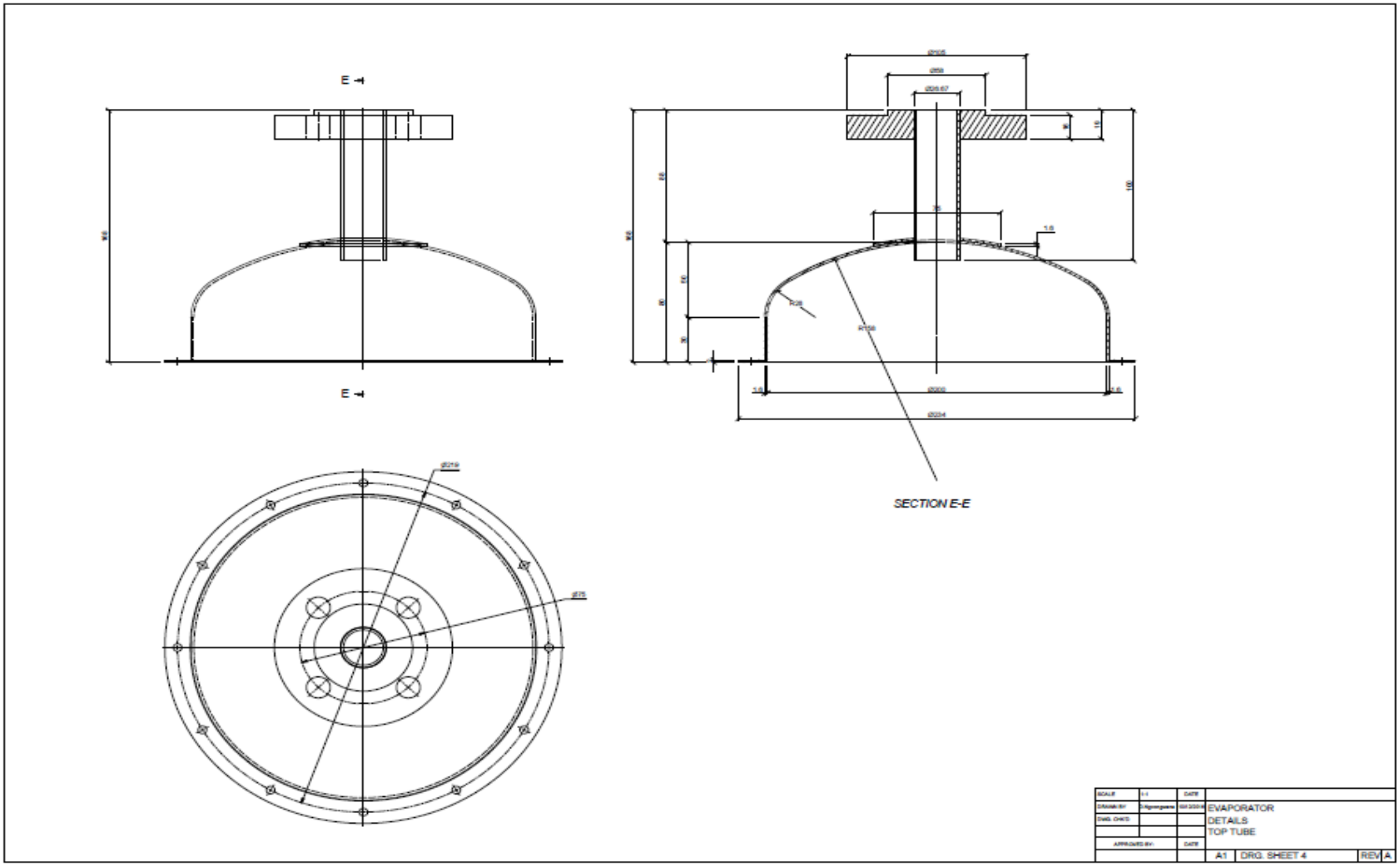
E
E
SECTION E-E
EVAPORATOR
DETAILS
TOP TUBE
A1
DRG. SHEET 4
REV A

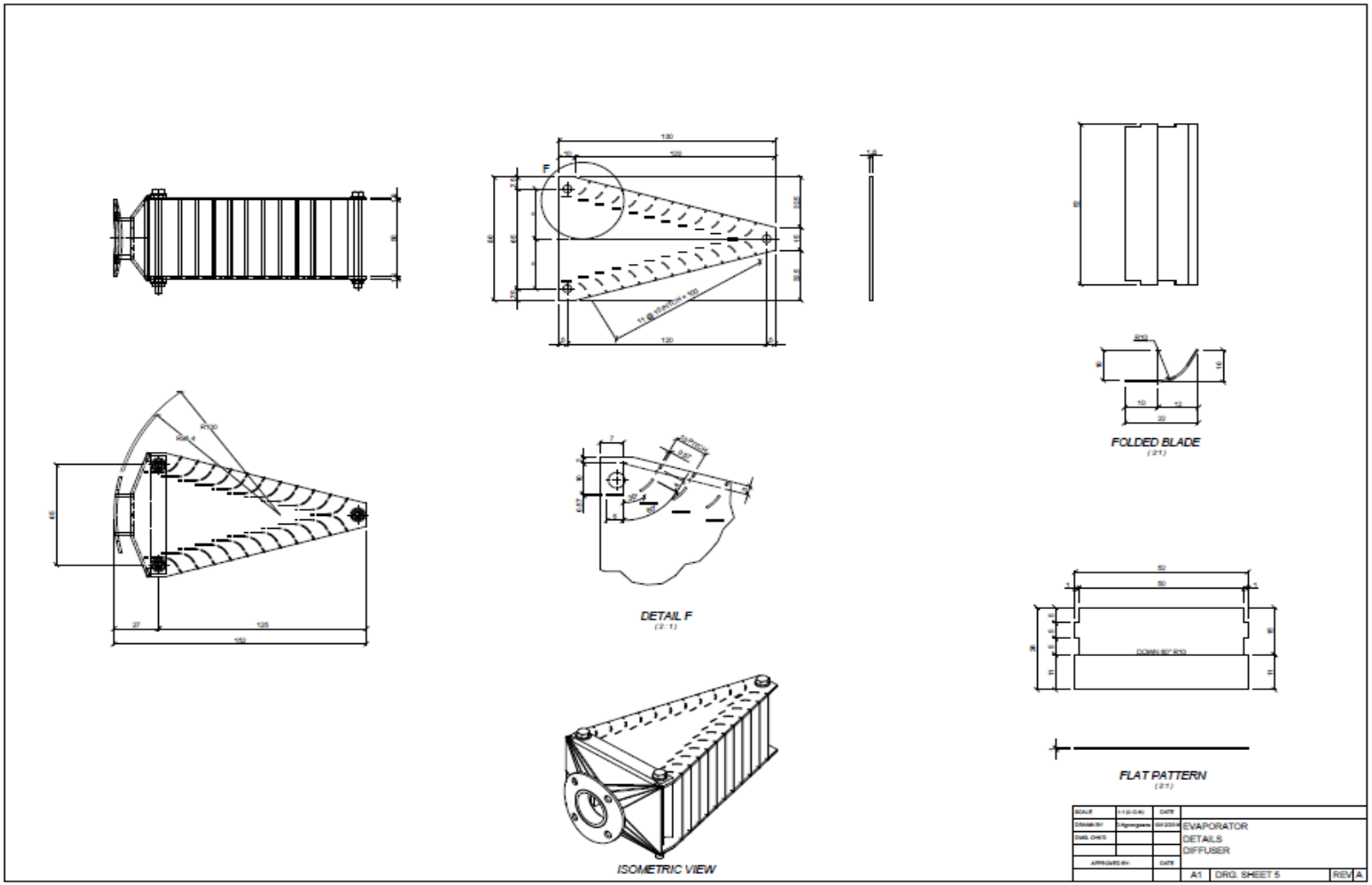
F
DETAIL F
(2 : 1)
FOLDED BLADE
(21)
ISOMETRIC VIEW
FLAT PATTERN
(21)
EVAPORATOR
DETAILS
DIFFUSER
A1
DRG. SHEET 5
REV A

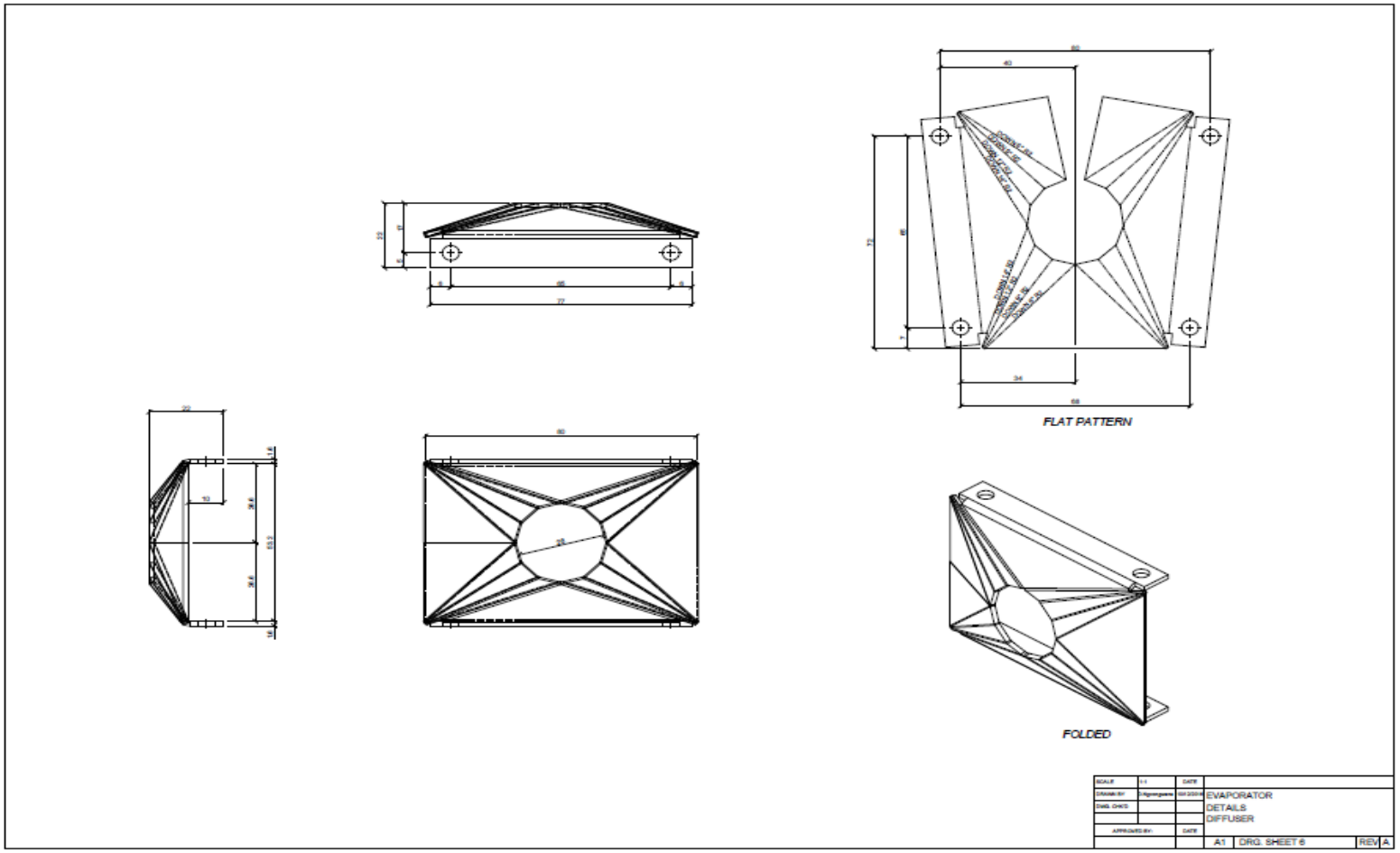
FLAT PATTERN
FOLDED
EVAPORATOR
DETAILS
DIFFUSER
A1
DRG. SHEET 6
REV A

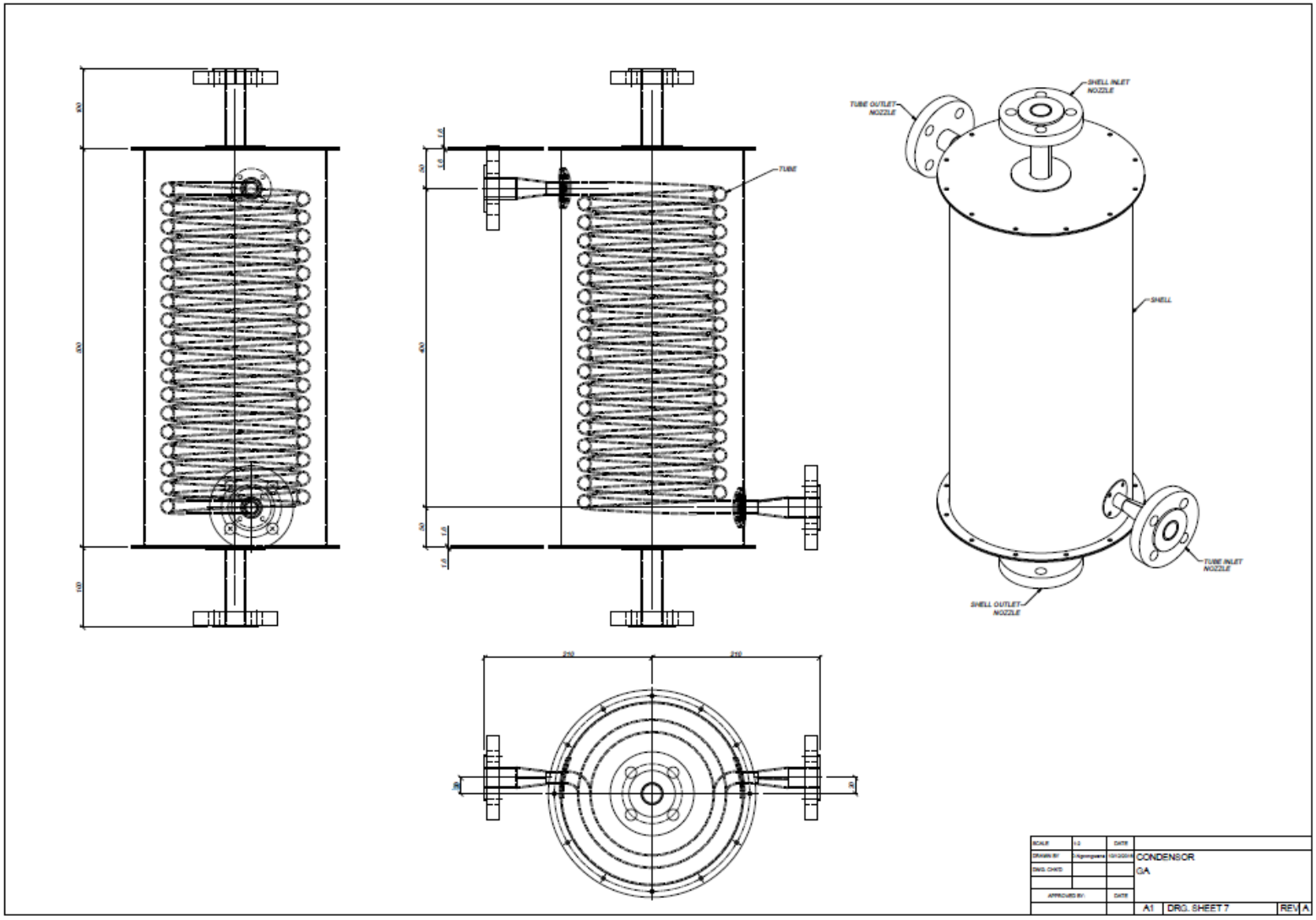
TUBE
SHELL INLET NOZZLE
TUBE OUTLET NOZZLE
SHELL
TUBE INLET NOZZLE
SHELL OUTLET NOZZLE
210
210
CONDENSOR
GA
A1
DRG. SHEET 7
REV A

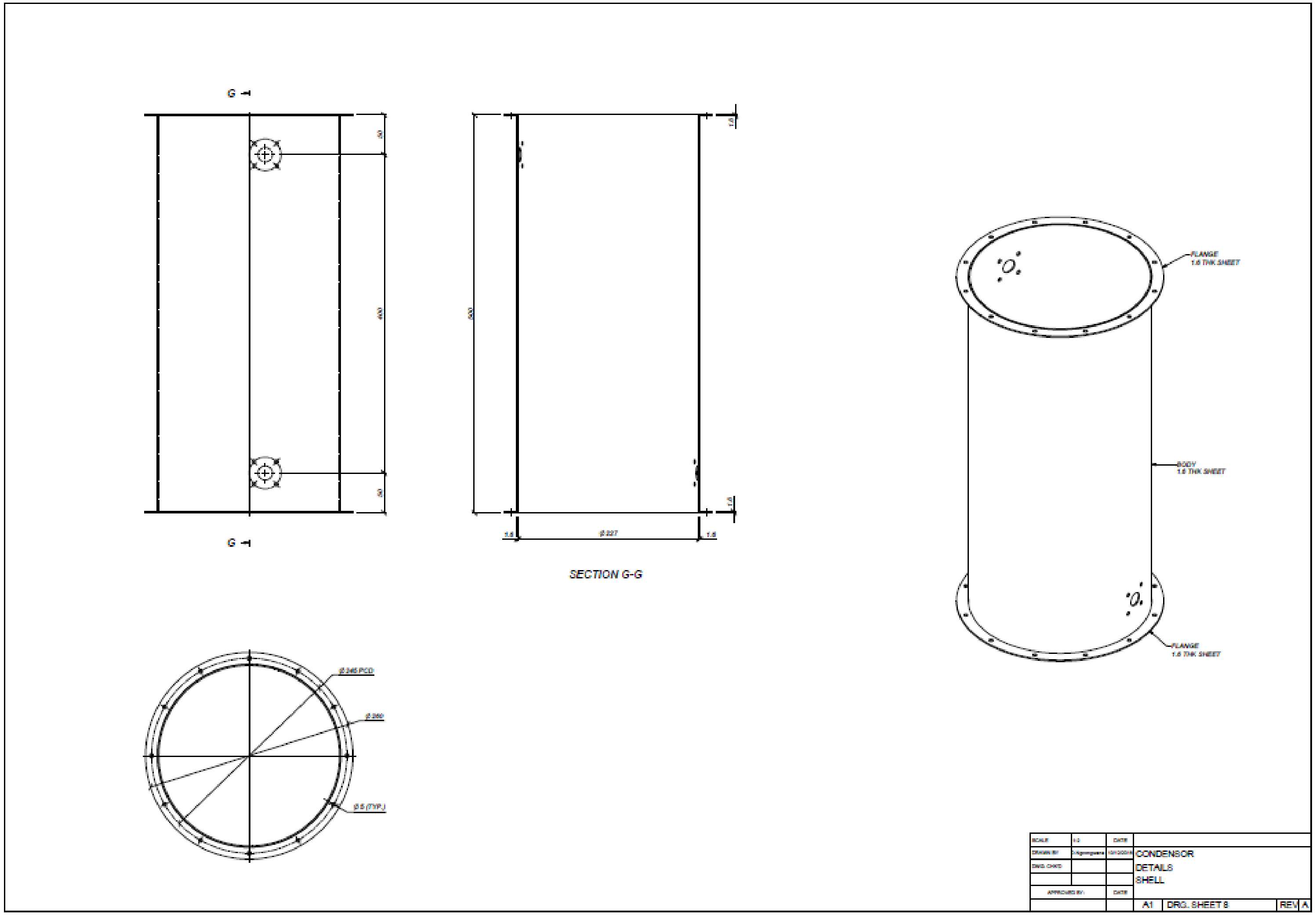
G
G
SECTION G-G
FLANGE 1.6 THK SHEET
BODY 1.6 THK SHEET
FLANGE 1.6 THK SHEET
CONDENSOR
DETAILS
SHELL
A1
DRG. SHEET 8
REV
A

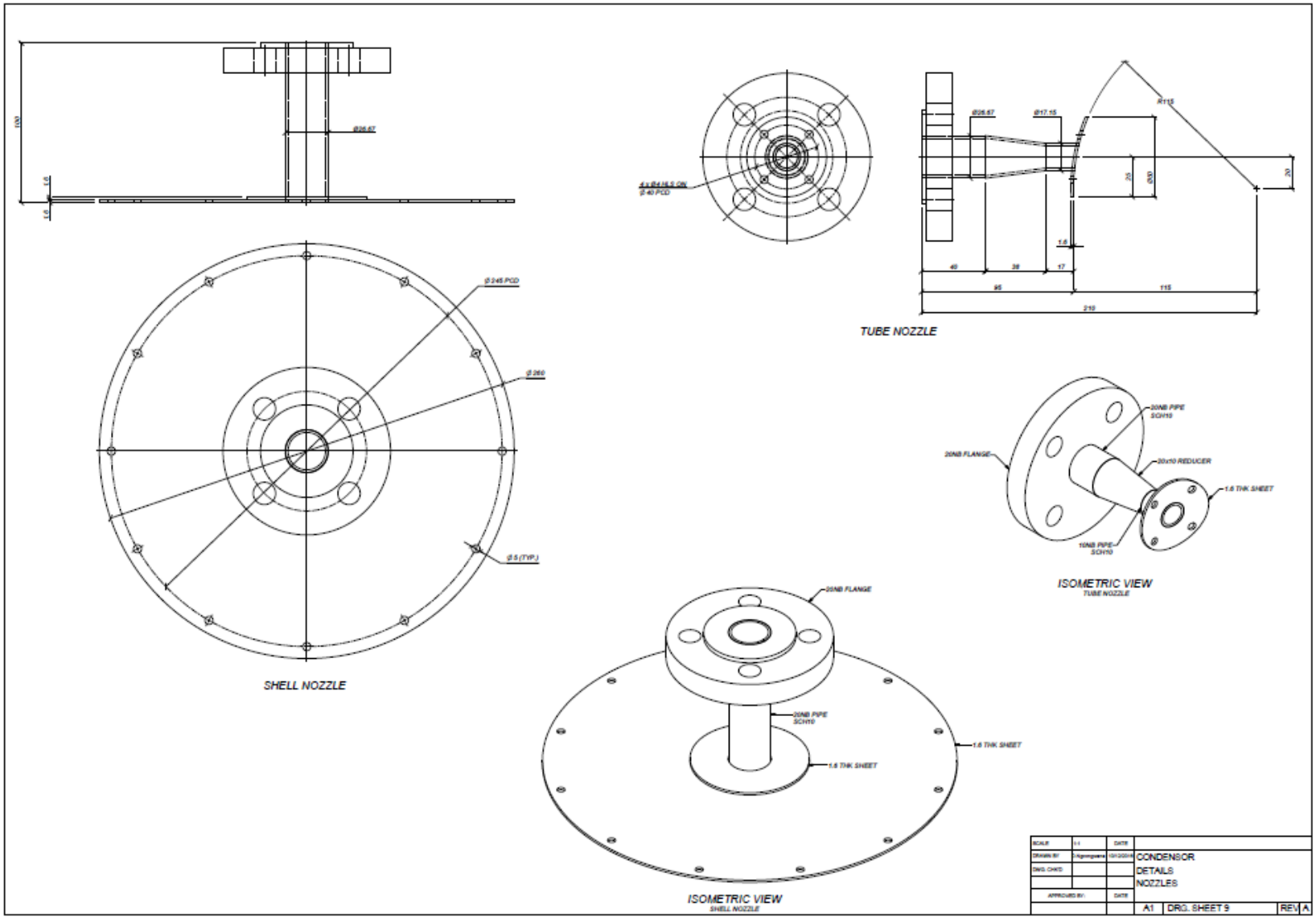
Ø26.67
1.6
1.6
4 x Ø4 (6.5 DP)
Ø 40 PCD
Ø26.67
Ø17.15
R115
25
Ø30
20
1.6
40
38
17
95
115
210
TUBE NOZZLE
Ø 245 PCD
Ø 260
Ø 5 (TYP.)
SHELL NOZZLE
20NB PIPE
SCH10
20NB FLANGE
20x10 REDUCER
1.6 THK SHEET
10NB PIPE
SCH10
ISOMETRIC VIEW
TUBE NOZZLE
20NB FLANGE
20NB PIPE
SCH10
1.6 THK SHEET
1.6 THK SHEET
ISOMETRIC VIEW
SHELL NOZZLE
SCALE
1:1
DATE
Drawn BY
Ngongoara
CONDENSOR
DETAILS
NOZZLES
DRG. CHKD
APPROVED BY:
DATE
A1
DRG. SHEET 9
REV
A

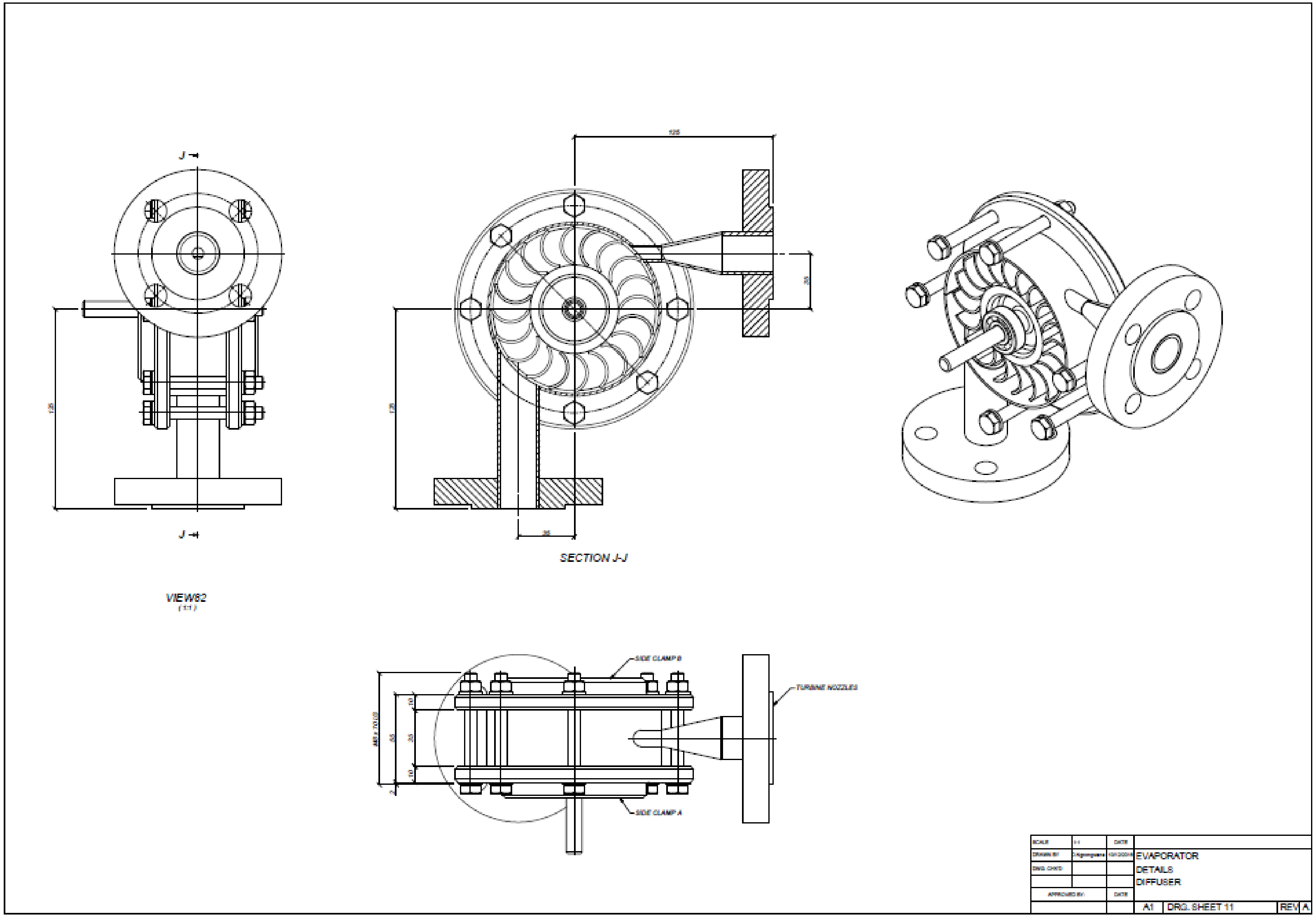
SECTION J-J
VIEW82
SIDE CLAMP B
SIDE CLAMP A
TURBINE NOZZLES
EVAPORATOR
DETAILS
DIFFUSER
A1
DRG. SHEET 11
REV
A

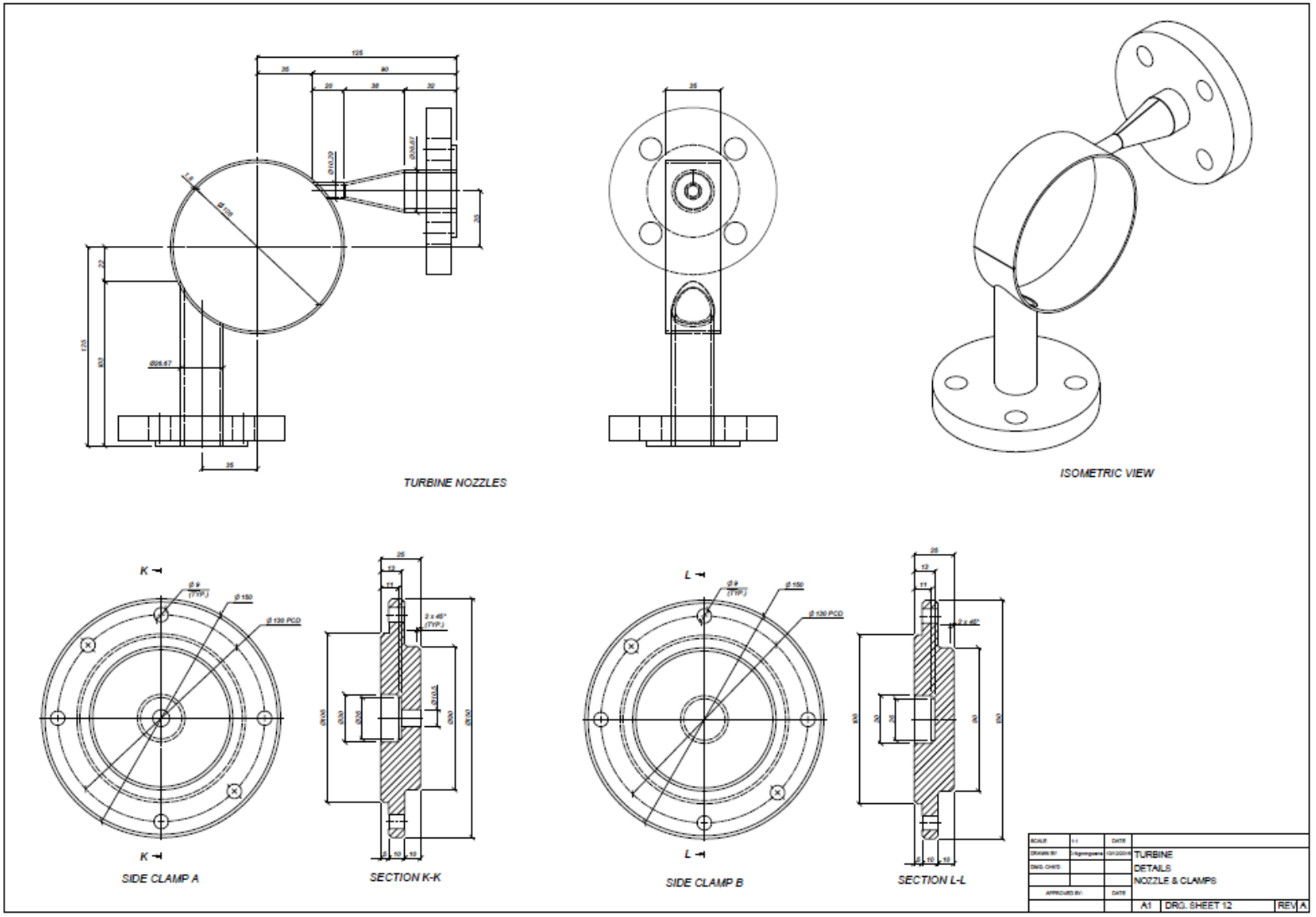
TURBINE NOZZLES
ISOMETRIC VIEW
SIDE CLAMP A
SECTION K-K
SIDE CLAMP B
SECTION L-L
TURBINE
DETAILS
NOZZLE & CLAMPS
A1
DRG. SHEET 12
REV A

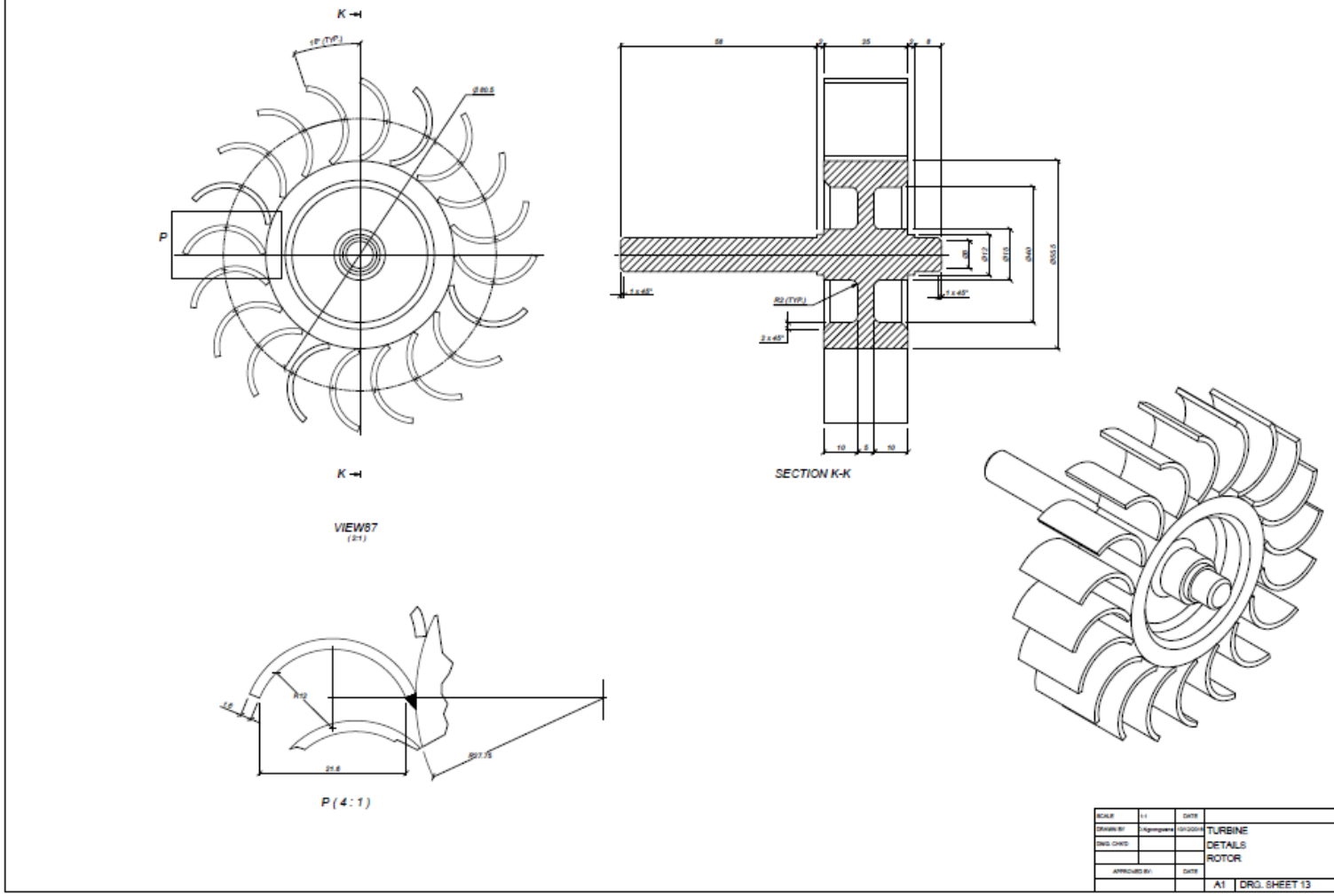
K
P
K
VIEW67
(2:1)
SECTION K-K
P (4 : 1)
TURBINE
DETAILS
ROTOR
A1
DRG. SHEET 13
REV. A

APPENDIX D

PAPER AND PUBLICATION

Experimental Design of Possible Open Cycle-OTEC Plant in KwaZulu Natal-South Coast

Gunnede M. Author, *Member, SAIEE, ECSA* and D'Almaine F. Author, *Member, SAIEE, SAIETE, SAARET*

***Abstract*— This article demonstrates an experimental model of an Open cycle - Ocean thermal energy conversion (OC-OTEC) plant. OC-OTEC plant uses the temperature difference between warm surface water and deep cold water of the ocean to drive a turbine engine to produce electrical energy. The exhaust steam from the turbine is condensed to form fresh water. This research is mainly laboratory based concentrating on design, calculations, modelling and simulation of OC-OTEC. The thermodynamic fluid calculations were undertaken with a view to design the main mechanical components of an OC-OTEC system, i.e. flash evaporator, condenser and steam turbine. An OC-OTEC demonstration plant was designed and constructed in an Electrical Power Laboratory at DUT. The investigational research was carried out on the demonstration plant with consideration given to water temperature, mass flow rate of fluid, and pressure. The measurements were taken before and after each component. The results obtained were compared.**

***Index Terms*— Ocean Thermal Energy Conversion, Open Cycle.**

I. Introduction

It is a well-known fact that South Africa is under resourced regarding fresh drinkable water. It is also well known that certain areas such as the South Coast of KwaZulu-Natal suffer more from lack of water than other areas.

A steady and reliable supply of power and water is important for modern human life. Presently a large majority of all the energy consumed in South Africa and indeed worldwide is provided by fossil fuels and nuclear power [1], [2]. As the world population grow exponentially, so does the requirement for power and water [3]. This increase will result in future straining of finite resources of coal, oil, gas, uranium etc. thus alternatives to these resources will need to be identified [4][5].

An unwanted side effect of burning fossil fuels to generate power is the air pollution caused by the pumping of CO_2 and NO_x into the atmosphere resulting in raised global temperatures (global warming) [6].

It is therefore imperative to explore all alternative forms of energy production of which OTEC is one. OTEC is a carbon neutral, environmentally friendly and semi-permanent energy source. Which is suited to an area such as port Shepstone where the offshore continental shelf is close inshore providing the possibility of cold water from the depths and warm surface water to give the required temperature difference for this technology.

It must be noted that a constant output from an OTEC system is difficult to maintain owing to daily and seasonal variations in water temperature [8]. Therefore, the thermal efficiency of OTEC is slightly low (5-6%) compared with commercial thermal plants (40-50%) [7]. This is, however offset by the lack of a fuel requirement.

Interest shown by the UGu Municipality in Southern KwaZulu-Natal in sourcing fresh water and electric power has prompted a novel design of an OC OTEC plant to fulfill these needs and the optimum site selection in this region. Fig. 1 indicates the relative contribution by renewable energy to global primary energy consumption.

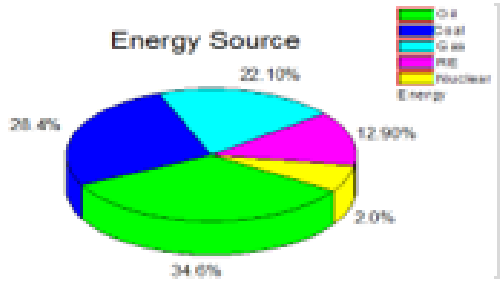

Fig 1. Share of energy sources in total global primary energy supply.

II. Open Cycle (Otec) Overview

Open cycle was initiated in 1930 by George Claude, student of d'Arsonval [10]. The system utilised steam along the other evaporated straight from the seawater to power a turbine. Subsequently the seawater temperature was not as much of than the normal boiling point at atmospheric pressure was sub atmospheric. The previous research led by the Florida Solar Energy Center (FSEC) over the previous half dozen years has saved data and advances that were lately functional to a new systematic study of the open-cycle technology [11]. FSEC presented that all the major expectations done in the initial feasibility investigation had remained unadventurous. So, open-cycle OTEC (Fig. 2) is even more auspicious than first planned. Their outcomes proposed that smaller plants (5-15 MW), are approximately as reasonable to construct as greater systems [11].

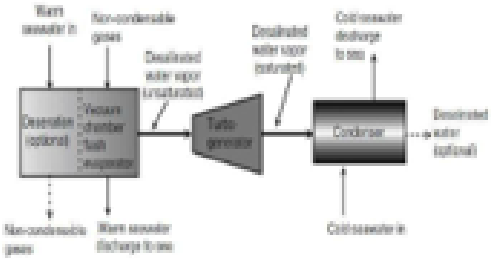

Fig 1: OC-OTEC Plant [12].

III. Oc-Otec: Efficiency

Entire efficiency of OC-OTEC system is given by the following equation:

$$\eta = \frac{P_n}{\dot{Q}_{in}}$$

where P_n is the net power and $\dot{Q}_{in}$ is the rate of heat transfer into the system [20]. The potential efficiency of an OC-OTEC is higher since a greater portion of the temperature change is available to produce power. In addition, it can also be used to provide drinking water. According to system analysis done in 1985, the condenser surface area of a plant produce 2 MWe of net power can generate approximately 4300 cubic meters of purified water each day [21].

Whereas OC-OTEC does have a higher efficiency potential, the technology aforementioned is not yet established.

IV. Oc-Otec Experimental System And Procedure

A study was carried out on a newly designed OC-OTEC laboratory demonstration system where temperature, mass flowrate and pressure readings were taken before and after each component. The flash evaporator was used in this plant to produce low pressure steam for the steam turbine. The exhausted steam from the turbine was lead to the condenser. Fig. 2 shows a photograph of the OC-OTEC experimental setup.

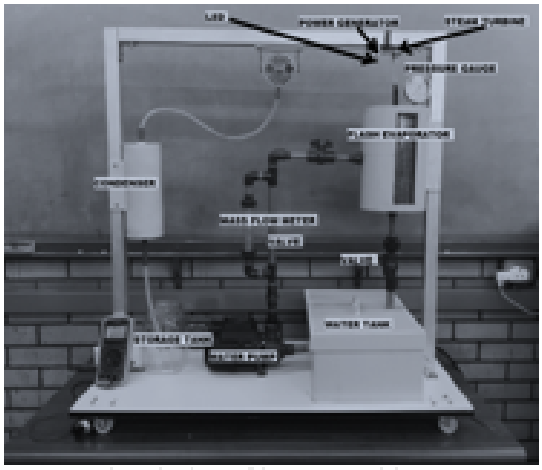

Fig 2: The picture of the OC-OTEC trial setup.

Outside diameter of the flash evaporator, D_o has a wall thickness 91,5 mm, with an inside diameter of 20mm and height (H) of 300mm. The design pressure is 3,5kPa and allowable stress σ_s. Mini turbine steam engine, is designed with two universal brass connecting rods with micro power generator. The length is 90mm, width 45mm, high 40mm, and inlet diameter. The Bourdon tube pressure gauge filled with liquid is utilised, with nominal size of 63mm and scale range is 0 – 60kPa. It also contains plastic flow meters for gases & liquids, using trogamid and polysulfone technology. Scaled directly in l/h, m3/h, %.

The temperatures reach up to 60°C trogamid, and 90°C polysulfone. Pressures goes up to 15 bars. The output is 4-20 mA.

V. Result And Discussions Oc-Otec: Efficiency

In this section, we compare performance of an OC - OTEC system by controlling the mass flow rates of inlet warm water and inlet cold water. Two cases are considered for ultimate studies: power generated by the steam turbine and desalinated water produced in the condenser. The efficiency and power output of an OC-Cycle plant is calculated using the enthalpy values.

The properties to be calculated are saturation temperature, and fresh water generated.

The power output is then calculated using the enthalpy drop across the turbine $(h_1 - h_2)$ multiplied by the steam flowrate.

The thermal efficiency is calculated by dividing the enthalpy drop across the turbine by the enthalpy difference between the output and inlet of the evaporator.

Figs. 3 and 4 show the thermal efficiency and power output of the system plotted against δt (the temperature difference of between the warm and cold water). The thermal efficiency and the power output can be seen to increase with increasing δt. The power output is produced when the total temperature difference is large enough to

allow heat transfer within the evaporator and provide a pressure drop across the turbine.

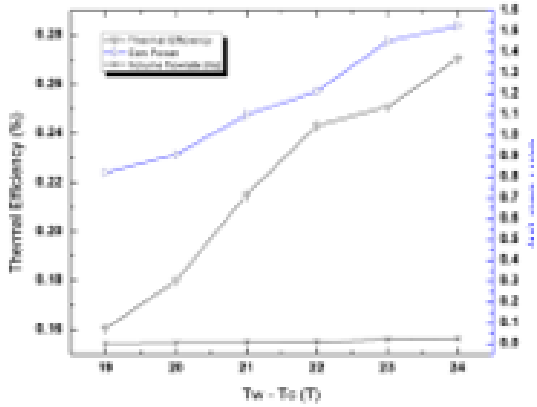

Fig 3: Thermal efficiency and power output of the system against operating temperature difference, for average of $\dot{m}$ ' $_{WH}$=0.0372 l/s.

Heat transfer (steam produced) in the evaporator increases when the flow rate is constant as energy loss in the process is minimized therefore providing the turbine with a better constant power output.

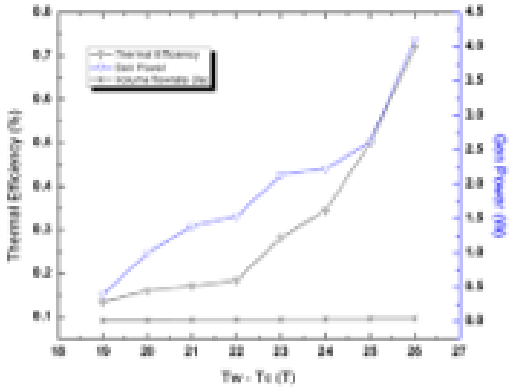

Fig 4: Thermal efficiency and power output of the system plotted against δt, for average $\dot{m}_{WH}$=0.0098 l/s.

The efficiencies for the average of $\dot{m}_{WH} = 0.0372\ l/s$ are approximately equal to the efficiencies of the average of $\dot{m}_{WH} = 0.0098\ l/s$. The work done by the turbine for both values of $\dot{m}_{WH}$ increases with increasing operating δt. The turbine uses the energy from the steam to do work, and as a result there is an observable temperature drop across the turbine that leads to an enthalpy drop.

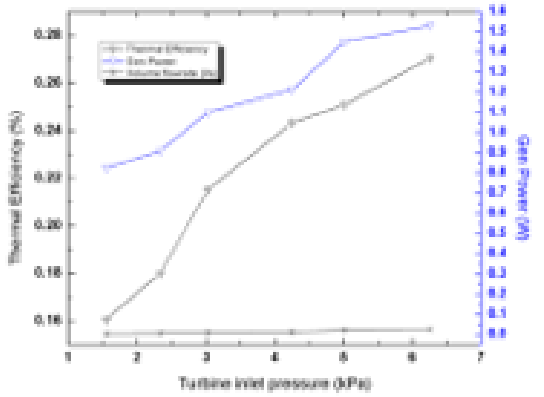

Fig 5: Thermal efficiency and power output of the system against the pressure drop across the turbine, for average of $\dot{m}_{WH}$=0.0372l/s.

Fig. 5 indicates the thermal efficiencies and power output of the turbine vs the pressure drop across the turbine for an average of $\dot{m}_{WH} = 0.0372\ l/s$. The pressure drops acquired from this experiment are between 1.5 and 6.5 kPa. According to the graph, it can be shown that the thermal efficiencies increase with increasing pressure drop across the turbine. The pressure drops increase thus leads to the power output increase.

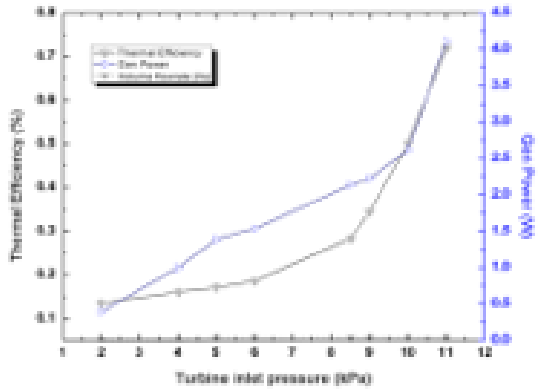

Fig 6: Power output and thermal efficiency of the system against the pressure drop across the turbine, for average of $\dot{m}_{WH}$=0.0098l/s.

Figs. 6 and 7 show minimum efficiency of 0.16 % and power output of 0.83 W, at 19°C and 1.5 kPa. The maximum efficiency is 0.26 % with power output of 1.55 W, at 24°C and 6.25 kPa for both. Fig. 6 shows the thermal efficiencies and power output vs the pressure drop across the turbine for the average of $\dot{m}_{WH} = 0.0098\ l/s$. The pressure drops obtained from this experiment are between 2 and 11 kPa.

According to the graph, it can be shown that the thermal efficiencies increase with increased pressure drop across the turbine. An increase in pressure drop leads to a power output increase. Comparing Figs. 7 and 8, it is clear to see

that power output of Fig. 7 is influenced by the increase in pressure up to 11 kPa, thus increasing the thermal efficiency.

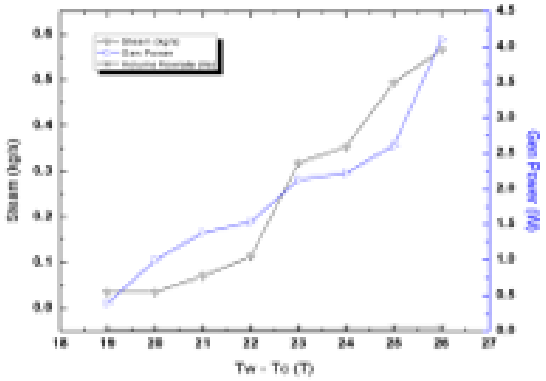

Fig 7: Steam and power energy generated of the system compared to operative temperature variance, for average of $\dot{m}_{wv}$=0.03721/s.

Fig. 8 shows the steam and power output vs the pressure drop across the turbine for the average of $\dot{m}_{wv} = 0.0372\ l/s$.

Fig. 9 shows the steam and power output vs the pressure drop across the turbine for the average of $\dot{m}_{wv} = 0.0098\ l/s$. Minimum steam mass flow rate of 0.05 kg/s at $19°C$ and maximum of 1.3 kg/s at $24°C$.

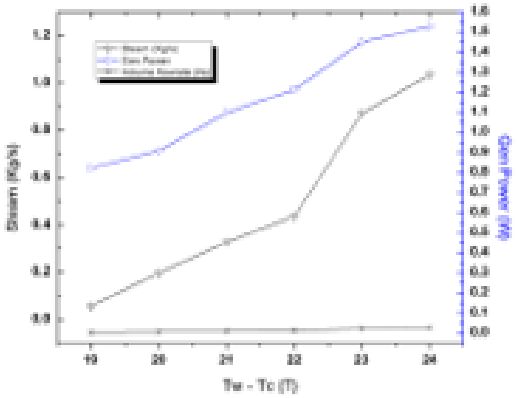

Fig 8: Steam and power produced from generator of the system compared to working temperature variance, for average of $\dot{m}_{wv}$=0.00981/s.

Fig. 9 shows the minimum power output of 0.85 W at $19°C$ and maximum of 1.58 W at 24°C. It can be seen that more steam is produced than power output produced by the turbine. The work done by the turbine for both values of $\dot{m}_{wv}$ generally increases with an increasing operating δt. The turbine uses the energy from the steam to do work, and as a result there is an observable drop across the turbine that leads to an enthalpy drop.

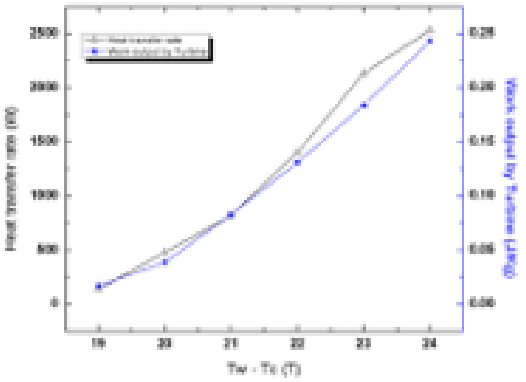

Fig 9: Enthalpy and work production of the plan compared to working temperature difference, for average of $\dot{m}_{wv}$=0.03721/s.

Figs. 8 and 9 show the enthalpy and work done by turbine against the operating temperature across the turbine from the average of $\dot{m}_{wv} = 0.0372\ l/s$ and $\dot{m}_{wv} = 0.0098\ l/s$. Fig. 10 establishes the minimum entropy of 130 KJ/kg at 19°C and upper limit of 2500 KJ/kg at 20°C. Fig. 110 shows minimum work done of 0.023 kJ/kg at 19°C and maximum of 0.24 kJ/kg at 24°C. Figs. 8 shows minimum enthalpy of 140 kJ/kg at 19°C and maximum of 680 kJ/kg at 24°C.

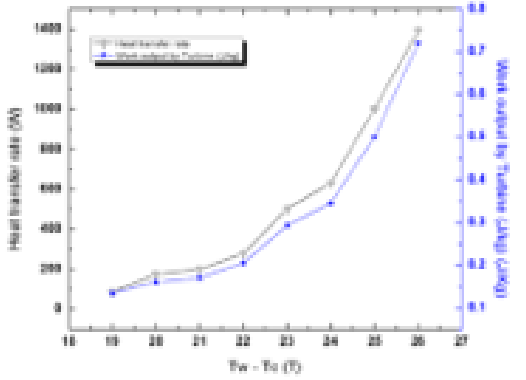

Fig 10: Enthalpy and work output of the system compared to working temperature variance, for average of $\dot{m}_{wv}$=0.00981/s.

Fig. 10 shows minimum work done 0.023 kJ/kg at 19°C and maximum of 0.35 kJ/kg at 24°C. It is seen that as more energy is required to heat up water to produce steam, there is more work done with regards to the output produced by the turbine. The work done by the turbine for both values of $\dot{m}_{wv}$ generally increases with the increasing δt and enthalpy. The turbine uses the energy from the steam to do work and as a result, there is a pressure drop across the turbine that leads to an enthalpy drop.

Fig. 11 shows condenser of OC-OTEC. This system is utilised to generate fresh water.

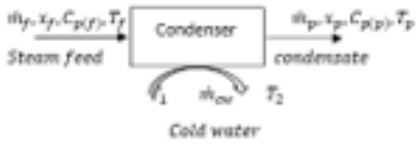

Fig 11: Indirect condenser.

$\dot{m}, x, C_p, T$: Mass flow rate, solids fraction, specific heat, temperature resp. Subscripts: (f) for feed; (p) for product; (1) for inlet water; (2) for outlet water. The overall mass balance is $\dot{m}_f = \dot{m}_p$ and the solids balance is $\dot{m}_f x_f = \dot{m}_p x_p$, $thus, x_p = x_f$.

The energy balance is $\dot{m}_f C_{p(f)} T_f + \dot{m}_{cw} C_{p(1)} T_1 = \dot{m}_{cw} C_{p(2)} T_2 + \dot{m}_p C_{p(p)} T_p$, $C_{p(1)}$ and $C_{p(2)}$ are determined from tables containing the properties of water at temperatures. T_1 and T_2 respectively. When approximation are used, $C_{p(1)} = C_{p(2)} = 4180\ kJ/kg\,K$. The rejected heat within the turbine is $q_{out} = h_2 - h_3$, $h_2 = 2461.4435\ kJ/kg$; $h_3 = 75.169\ kJ/kg$.

$$q_{out} = h_2 - h_3$$

$$= 130.459 - 75.169$$

$$= 55.29\ \text{kJ/kg}$$

$$\dot{m}_{cw} C_{p(cw)} \Delta T_{cw} = \dot{m}_p q_{p(out)}$$

$$\dot{m}_{cw} = \frac{0.75 \times 55.297}{4.18(10-5)}$$

$$= 1.984\ \text{kg/s}$$

A. Energy balance

$$\dot{m}_f C_{p(f)} T_f + \dot{m}_{cw} C_{p(1)} T_1 = \dot{m}_{cw} C_{p(2)} T_2 + \dot{m}_p C_{p(p)} T_p$$

$$0.75 \times 4.2(18) + 1.984 \times 4.2 \times 5 = 1.984 \times 4.2 \times 10 + \dot{m}_p \times 4.2 \times 13$$

$$\dot{m}_p = \frac{98.364 - 83.328}{4.2 \times 13}$$

$$\dot{m}_p = 0.356\ \text{kg/s}$$

Figs. 11 and 12 show steam, fresh water mass flowrate and power output of the system against volume flowrate. It is understood that as condensation begins in the condenser, the steam at the intake of the condenser is cooled by cold water at a temperature of 5°C and the steam changes phase from steam to liquid The fresh water that is produced is less than the amount of steam being cooled.

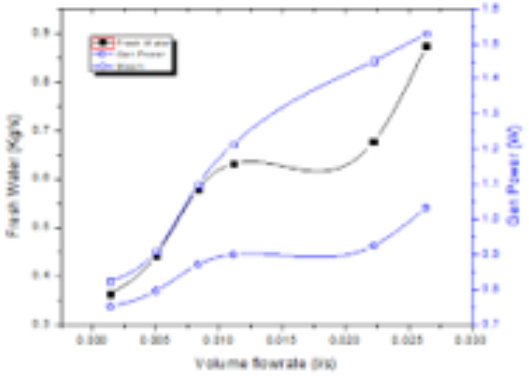

Fig 12: Steam, fresh water mass flowrate and power output of the system against volume flowrate.

As a system produces more steam, there is more power output from the turbine and more fresh water after the condenser. There is then more power output produced by the turbine.

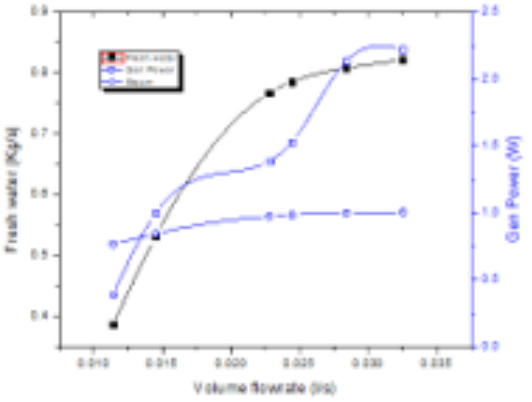

Fig 13. Steam, fresh water mass flowrate and power generated of the plant compared to volume flowrate.

work done by the turbine for together $\dot{m}_{wg}$ usually rises by with cumulative operative temperature variance and more fresh water as by-product. The turbine uses the energy from the steam to do work, and as a result there is an observable drip thru the turbine that results to an enthalpy variation. Although efficiencies are low (of the order of < 1%.) the system works in principle and can be adapted for a larger plant.

VI. Conclusion

The selection of a good process modelling, and simulation tool was of extreme importance for the success of this work. Throughout the measurements, it was found that the thermal efficiency (%) and the power output increased with increasing temperature difference δt = tw - tc. The power output was produced when the δt was large enough to allow heat transfer within the evaporator and provide a pressure drop across the turbine.

There was more heat transfer (steam produced) in the flash evaporator at a constant flow rate because the warm water continuously supplied heat energy to the evaporator without losing much energy through the process, therefore continuous feed to the turbine improved constant power output. The thermal efficiencies were increased with increasing pressure across the turbine. The increase of pressure drops across the steam turbine caused the output power to increase. The larger flow rates of the warm water lead to higher amounts fresh water produced from the condenser.

VII. Biography

Gumede M. Author was born in Durban, South Africa on December 25, 1987. He graduates with a MEng Degree in Electrical Engineering from Durban University of Technology, Durban, South Africa in 2015. Since January 2017 is a student at Durban University of Technology pursuing DEng in Electrical Engineering. He is currently working for ZLM Project Engineering Pty, Ltd under Electricity Department as Managing Director. His main interests are in the area of renewable energy, especially ocean energy such as OC-OTEC, offshore wind and ocean current. He has published number of paper from international and national journal Mr. Gumede is a member of Engineering Council of South Africa (ECSA) and South African Institute of Electrical Engineers (SAIEE).

D'Almaine G.F Author was born in Durban, South Africa on May 30, 1950 was Senior Director in the Department of Power Engineering at the Durban University of Technology. He specializes in ocean energy and power systems both on grid and off grid, and is a director of the Real Time Power System Simulator at the university. Mr F. D'Almaine was a former SAIETE Member and past local Chairman SAARET.

VIII. References

1. Kahrl, William L. *Water and power: the conflict over Los Angeles water supply in the Owens Valley*. University of California Press, 1983.
2. Weedy, Ramon Mathew, et al. *Electric power systems*. John Wiley & Sons, 2012.
3. Hossain, Abear, et al. "Ocean thermal energy conversion: The promise of a clean future." *Clean Energy and Technology (CEAT), 2013 IEEE Conference on*. IEEE, 2013.
4. Kobayashi, Hiroki, Sadayuki Jitsuhara, and Hanso Uehara. "The present status and features of OTEC and recent aspects of thermal energy conversion technologies." *34th Meeting of the UJNR Marine Facilities Panel, Honolulu, HI, November*. 2001.
5. Bouwer, Herman. "Integrated water management for the 21st century: problems and solutions." *Journal of Irrigation and Drainage Engineering* 128.4 (2002): 193-202.
6. McMichael, Anthony J., et al. "Food, livestock production, energy, climate change, and health." *The lancet* 370.9594 (2007): 1253-1263.
7. LUIS A. VEGA, "Ocean Thermal Energy Conversion" Encyclopedia of Sustainability Science and Technology, Springer, August 2012 pp. 7296-7328
8. Vega, Luis A. "Ocean thermal energy conversion primer." Marine Technology Society Journal 36.4 (2002): 25-35.
9. Jeffs, Eric. Greener Energy Systems: Energy Production Technologies with Minimum Environmental Impact. CRC Press, 2012.
10. Dabestani, Maryam. "Energy Generation Using Ocean Thermal energy." *American Journal of Life Science Researches ISSN 2332-0206* 3.3 (2015).
11. Link, Harold F., and Brian K. Parsons. "Potential of Proposed Open-Cycle OTEC Experiments to Achieve Net Power." *OCEANS'86*. IEEE, 1986.
12. Kim, Nam Jin, Kim Choon Ng, and Wongee Chun. "Using the condenser effluent from a nuclear power plant for Ocean Thermal Energy Conversion (OTEC)." *International Communications in Heat and Mass Transfer* 36.10 (2009): 1008-1013.
13. Althof, J. A. "Direct-Contact Condensers for Open-Cycle OTEC Applications." (1988).
14. Bin Jian, Ooi, Chew Boon Cheong, and Khay Chaong Chien. "Managing the transition of fossil fuels to renewable energy: application of ocean thermal energy conversion at Sabah." (2015).
15. Sea surface temperature around the world. (Available at:http://www.ospo.noaa.gov/data/sst/fields/FS_km10000.gif).
16. Lockheed Martin Mission Systems & Sensors (MS2), Ocean Thermal Extractable Energy Visualization, Lockheed Martin Corporation, DE-0002684, October 28, 2012.
17. Harrison, Sara. "Ocean Thermal Energy Conversion." Submitted as coursework for Physics 240, Stanford University, and November 28, 2010.
18. Da Rosa, Aldo Vieira. *Fundamentals of renewable energy processes*. Academic Press, 2012.
19. Khalid, Syed Shah, Zhang Liang, and Nazia Shah. "Harnessing tidal energy using vertical axis tidal turbine." *Research Journal of Applied Sciences, Engineering and Technology* 5.1 (2012): 230-252.
20. Avery, William H., and Chih Wu. Renewable Energy from the Ocean: A Guide to OTEC. New York: Oxford UP, 1994.
21. National Renewable Energy Laboratory. Desalinated Water Date Unknown. 15 Apr. 2005 http://www.nrel.gov/otec/desalination.html.
22. T Taniguchi, "The Future of Ocean Thermal Energy Conversion" Physics 80. 5/5/05 http://www.physics.hmc.edu/~saeta/courses/p80/oldwiki/files/25811.doc 120 321

Application and Design Calculation of 200kW OC- OTEC Plant in KwaZulu Natal (KZN) - South Coast

Gumede M. Author, *Member, SAIEE, ECSA* and D'Almaine F. Author, *Member, SAIEE, SAIETE, SAARET*

***Abstract*— This paper is based around assessing the Port Shepstone area for its suitability for establishing an open cycle ocean thermal energy plant.**
A novel application of this plant is demonstrated with its primary function being the production of fresh water and the secondary function being the production of electric power. This forms the basis of a self-powered desalination system with extra power generated being available for insertion into the grid.
The key components of a 200kW pilot plant were designed, sized, modelled and simulated in the laboratory using Simulink software and the fresh water output of such a plant has been calculated.

***Index Terms*— Open Cycle - Ocean Thermal Energy Conversion (OC-OTEC).**

I. Introduction

IT is a well-known fact that South Africa is under resourced regarding fresh drinkable water. It is also well known that certain areas such as the South Coast of KwaZulu-Natal suffer more from lack of water than other areas.
A steady and reliable supply of power and water is important for modern human life. Presently a large majority of all the energy consumed in South Africa and indeed worldwide is provided by fossil fuels and nuclear power [1], [2]. There is a directly proportional relationship between population growth and the need for water and power [3]. This will result in future straining of finite resources of coal, oil, gas, uranium etc. thus alternatives to these resources will need to be identified [4][5]. An unwanted side effect of burning fossil fuels to generate power is the air pollution caused by the pumping of CO_2 and NO_x into the atmosphere resulting in raised global temperatures (global warming) [6].

It is therefore imperative to explore all alternative forms of energy production of which OTEC is one. OTEC is a carbon neutral, environmentally friendly and semi-permanent energy source. Which is suited to an area such as port Shepstone where the offshore continental shelf is close inshore providing cold ocean bottom water and warm ocean surface water thus giving the temperature difference required for this technology.

It must be noted that a constant output from an OTEC system is difficult to maintain owing to daily and seasonal variations in water temperature [8]. Therefore, the thermal efficiency of OTEC is relatively low (5-6%) compared with commercial thermal plants (40-50%) [7]. This is, however, offset by the lack of a fuel requirement.
Interest shown by the UGu Municipality in Southern KwaZulu-Natal in sourcing fresh water and electric power has prompted a novel design of an OC OTEC plant to fulfil these needs and the optimum site selection in this region.
Fig. 1 indicates the relative contribution by renewable energy to global primary energy consumption.

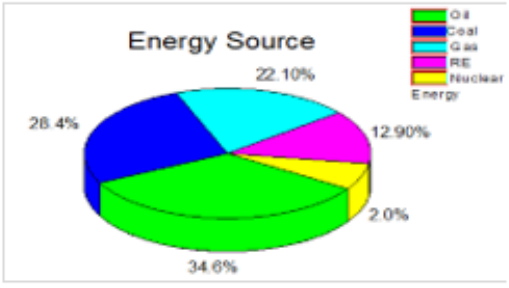

Fig 1. Breakdown of global primary energy sources.

II. Open Cycle Ocean Thermal Energy Conversion (OC-OTEC) Overview

Open cycle thermal energy conversion initiated in 1930 by George Claude [10]. This system utilized steam evaporated directly from seawater to power a turbine. Since the seawater pressure was sub atmospheric, the steam temperature was less than the normal boiling point at atmospheric pressure. Research conducted by Florida Solar Energy Center (FSEC) has delivered data and approaches used in a recent system study of OC-OTEC [11].

Fig 2. OC-OTEC Plant [12].

Open cycle OTEC has a distinct advantage over closed cycle OTEC systems provided by the use of a direct contact (flash) evaporator which is cheaper, smaller and more efficient

than the conventional or surface evaporator required for closed cycle systems.

If fresh water is not a requirement, then direct contact condensers can also be used [13].

If fresh water is a requirement, then a surface condenser can be used in this system since the evaporator act as a distillation unit. In this case studies have shown that the value of fresh water produced could offset the extra cost and possible performance degradation associated with its use.

Studies have shown that the most cost-effective operation utilizes a direct contact condenser in the system shown below in fig 3 [13].

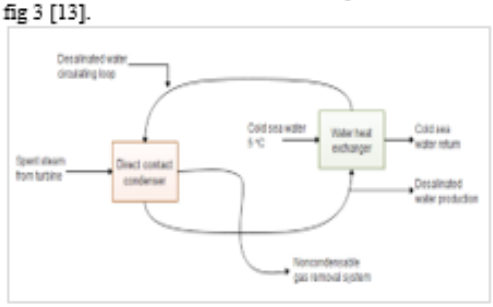

Fig 3. Purified water production scheme using condenser [13].

I. Research Developments

A suitable location for an OTEC plant location should be in a stable environment with suitable parameters for effective operation. The most important parameter is the temperature difference at the location which has to be Δt minimum of 20 °C between the sea surface and the sea bed. Even if the surface temperature is very warm. OTEC might not be viable if there is a lack of a cold water heat sink.

The most suitable resources can be found in the area between 30° South and 30° North, i.e. in tropical oceans [14]. Fig 3 indicates the Δt between water at depths of 20 m and 1km, and the locations with a temperature gradient of more than 20° C. The data presented below is for global assessments of potential OTEC resources mapped the global distribution of ΔT using data archived at the National Oceanographic Data Center. From this it is shown that the east coast of South Africa could be suitable for such a plant.

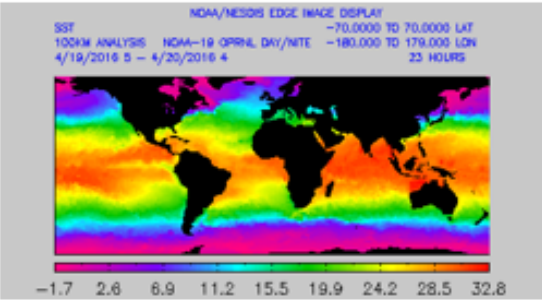

Fig 4. Global sea surface temperatures SST (Available at:http://www.ospo.noaa.gov/data/sst/fields/FS_km10000.gif. [15].

7. Available Ocean Power Along The KZN South Coast

The proposed site in KwaZulu natal (Port Shepstone to Port Edward) is naturally suited for the establishment of alternate energy collection sources such as OTEC. Since Port Shepstone is located at the coast of KZN just below the southern Tropic the two elements required: near constant sunlight and the Δt needed are present, hence its selection for this study.

OTEC sites are abundant in the southern parts of the case-study region. Off the coast of Southern KwaZulu Natal, the continental shelf is fairly close to the shore, approaching to within a few km in some places. Further, the shelf is steep dropping to a depth up to 3000 metres making this area suitable for investigation for OTEC in KZN. Maritime maps of the coast of KZN indicate possible sites where the continental shelf is suitably close the shore.

The University of Hawaii has tested this technology and obtained a significant volume of desalinated water [18] which can help the countries that have a problem with water such as South Africa. The figure below shows the proposed site for Open Cycle OTEC.

Fig 5. The propose site for Open Cycle OTEC.

8. Ocean Thermal Energy Converison Research Methodology

In order to meet the objective of this research, the following steps have been undertaken:

- A site suitable for OTEC has been broadly identified.
- Surface and sub-surface temperatures at this site will be measured over a period.
- A computer model of a suitable OTEC plant has been developed and simulated at DUT.
- A physical small-scale model has been built in the DUT laboratory and measurements have been compared with the simulation. A next step will be a pilot plant near Port Shepstone.

9. OC-OTEC: Efficiency

The overall efficiency of an OC-OTEC system is given by the following equation:

$$\eta = \frac{P_n}{\dot{Q}_{in}}$$

where P_n is the net power and $\dot{Q}_{in}$ is the rate of heat transfer into the system [20]. The potential efficiency of an OC-OTEC is higher than close cycle since a greater portion of

the temperature change is available to produce power. In addition, it can also be used to provide drinking water. According to a system analysis done in 1985, the condenser surface area of a plant produce 2 MWe of net power can generate approximately 4300 cubic meters of purified water each day [21].

Whereas OC-OTEC does have a higher efficiency potential, the technology required is not yet established. That is, OC-OTEC systems are not yet economically feasible. Todd Taniguchi reported that the Research and Development of OC-OTEC systems have been stalled because of foreseeable problems with developing the technology on a commercial scale. As mentioned above, no OC-OTEC system has been designed or built because of the large turbine sizes [22]. This project mitigates against these constraints by concentration mainly on water production this reducing the size of generator required if used for pure energy production.

7. Design Of 206.18kw Oc-Otec Pilot System

The steam turbine and generator was designed for an output of 200 kW operating with warm water at 26°C with a corresponding net power of 98kW (98.186) and a production of 0.5l/sec (43 200 l/day) of desalinated water.

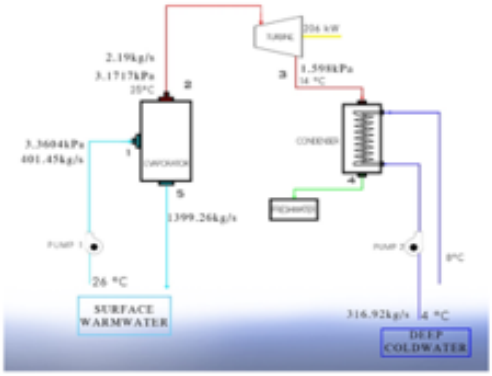

Fig 6. 206.186kW O-C OTEC process diagram.

8. *Assumptions*

The model design for this project was optimised for approximately 98.186kW Net power. During this research there were numerous important mechanisms that have a substantial influence on the produced net power.

TABLE 1
98.186kw Net And 206,186 Kw Gross Power Process.

Symbol	Quantity	Conversion from Gaussian to SI *
T_{ww}	temperature of warm water	26 °C
T_{cw}	temperature of cold water	4 °C
M_n	net power output	98.186kW
η_G	generator efficiency	97 %
$T_{st\ in}$	steam temperature	25 °C
$T_{st\ out}$	steam temperature	14 °C
C_p	specific capacity of water	4.18 kJ/kgK /kg
η_p	seawater pump efficiency moment	85%

Following are brief calculations for the design of 206.186kW process of Open-Cycle OTEC plant.

9. Gross Power Energy

$$M_{Gross} = \frac{\text{Net Power}}{\text{Generator Efficiency}} = \frac{M_{net}}{\eta_G}$$
$$= \frac{200kW}{0.97}$$
$$= 206.186\ kW$$

The total system energy power was compensating for the mechanical, electrical and turbine losses. Consequently, the total power energy to be generated by the turbine can be calculated as: Turbine power output is $M_T = 206.186kW$.

10. Turbine Analysis

B. State 2 – 3 process

Steam Table is used for identifying, Temperature, Pressure, Enthalpy and Entropy; etc. see below the table.

TABLE 2
APPARATUS FOR SATE 2.

Symbol	Quantity	SI
T_2	temperature	25 °C
P_2	pressure	3.1717 kPa
k_2	enthalpy	2547.855KJ/Kg
S_2	entropy	8.55975KJ/Kg

TABLE 3
APPARATUS FOR SATE 3.

Symbol	Quantity	SI
T_2	temperature	14 °C
P_2	pressure	1.5985 kPa
k_2	enthalpy	2453.8403 KJ/Kg
S_2	entropy	8.55975KJ/Kg

$$S_2 = S_3 = 8.55975\ kJ/kgK$$
$$S_3 = S_{f_3} + x_3 S_{fg_3}$$
$$8.55975 = 0.2098 + x_3 \times 8.5969$$
$$= 0.97 = 97\%$$

$$h_3 = h_{f_3} + x_3 h_{fg_3}$$
$$= 59.2401 + 0.97 \times 2468.66$$
$$= 2453.8403\ kJ/kg$$

11. Turbine Work Output W_T

To calculate the mass flowrate of steam to be received by the turbine, inlet and outlet conditions for the turbines can be utilised as shown below:

$$W_T = \dot{m}_{st}(h_3 - h_2)$$
$$206.186 = \dot{m}_{st}(2453.8403 - 2547.855)$$
$$\dot{m}_{st} = 2.19\ kg/s$$

12. Evaporator Analysis

2) State 1 – 2 – 5 process

The mass flowrate of surface warm ocean water can be calculated by heat balancing the evaporator with respect to the inlet and outlet conditions of Steam and warm water. Heat

energy required to generate the steam at a temperature of 25°C.

$$\dot{m}_{st} = \frac{q_w}{h_{fg}}$$
$$2.19 = \frac{q_w}{2442.845}$$
$$q_w = 5349.83055 \text{ kJ/kg}$$

The amount of water required at the evaporator $\dot{m}_{ww}$

$$\dot{m}_{ww} = \frac{\dot{m}_{st} q_w}{Cp_{ww}\Delta T_{ww}} = \frac{2.19 \times 5349.83055}{4.18(26-24)} = 1401.450826 \text{ kg/s}$$

The warm water mass flowrate leaving the evaporator at temperature 24°C is discharged back to the ocean.

$$\dot{M}_{out} = \dot{m}_{ww} - \dot{m}_{st} = 1401.450826 - 2.19 = 1399.260826 \frac{kg}{s}$$

7. Thermal Energy Difference Within The Evaporator

$$\Delta Q_{ww} = Cp_{ww}(T_{in}\dot{m}_{ww} - T_{out}\dot{M}_{out}) = 4.18(26 \times 1401.450826 - 24 \times 1399.260826) = 11935.82971 \text{ kJ/kg}$$

C. *Evaporator heat transfer area A_h*

Uv is a quantity of heat exchanger performance consisting of overall heat transfer coefficient (U-value).

TABLE 4
98.186KW NET POWER, UV VALUE.

Symbol	Quantity	SI
E_T	evaporator	0.16W/m°C

D. *Evaporator*

$$\Delta T_1 = T_{wwin} - T_{wwst} = 26 - 14 = 12°C$$

$$\Delta T_2 = T_{wwin} - T_{wwout} = 26 - 24 = 2°C$$

$$\Delta T_{LM} = \frac{\Delta T_1 + \Delta T_2}{\ln\left(\frac{\Delta T_1}{\Delta T_2}\right)} = \frac{12+2}{\ln\left(\frac{12}{2}\right)} = 7.81°C$$

$$A_{hE} = \frac{t_h q_w}{U_{stainless}\Delta T_{LM}} = \frac{1\times10^{-3}\times5349.83055}{0.16\times7.81} = 4.28 \text{ m}^2$$

8. Condenser Analysis

C. *State 3 – 4 process*

The thermal energy output rejected at the condenser is Q_{out}

$$Q_{out} = \dot{m}_{st}(h_3 - h_4) = 2.19(2453.8403 - 34.2606) = 5298.88 \text{ kJ/kg}$$

D. *Heat energy rejected into seawater*

$$q_c = \dot{m}_{cw}Cp_{cw}(T_{cwo} - T_{cwi})$$
$$5298.88 = \dot{m}_{cw} \times 4.18(8-4)$$
$$\dot{m}_{cw} = 316.919 \text{ kg/s}$$

Therefore, the mass flowrate of Coldwater is, $\dot{m}_{cw}$ = 316.919 kg/s.

TABLE 6
98.186KW NET POWER, UV VALUE.

Symbol	Quantity	SI
E_T	evaporator	0.16W/m°C

$$\Delta T_1 = T_{icon} - T_{cwout} = 14 - 8 = 6°C$$
$$\Delta T_2 = T_{0con} - T_{cwin} = 6 - 4 = 2°C$$

$$\Delta T_{LM} = \frac{\Delta T_1 + \Delta T_2}{\ln\left(\frac{\Delta T_1}{\Delta T_2}\right)} = \frac{6+2}{\ln\left(\frac{6}{2}\right)} = 7.28°C$$

$$A_{hE} = \frac{t_h Q_{out}}{U_{stainless}\Delta T_{LM}} = \frac{1\times10^{-3}\times5298.88}{0.16\times7.28} = 4.55 \text{ m}^2$$

9. Condenser Analysis

C. *State 3 – 4 process*

The thermal energy output rejected at the condenser is Q_{out}

$$Q_{out} = \dot{m}_{st}(h_3 - h_4) = 2.19(2453.8403 - 34.2606) = 5298.88 \text{ kJ/kg}$$

D. *Heat energy rejected into seawater*

$$q_c = \dot{m}_{cw}Cp_{cw}(T_{cwo} - T_{cwi})$$
$$5298.88 = \dot{m}_{cw} \times 4.18(8-4)$$
$$\dot{m}_{cw} = 316.919 \text{ kg/s}$$

10. Fixed Loss Factors

The L_{fixed} is calculated as the cold water intake power loss, condenser and distribution forcing loss, evaporator and delivery pushing loss within the process.

D. *Pump Loss factor*

$$\text{Pump Loss Factor} = \frac{\dot{m}_{wwll}}{\eta}$$

183

$$= \frac{1401.45 \times 9.81}{0.85}$$
$$= 16.17\text{kW/m}$$

D. Circulation Pumping Loss and Evaporator

This secure loss is estimated created on assumptions for 98.186 kW Net Power. The consistent Head Loss would be roughly 3.49m. the 3.49m of head accounts for the loss transversely consumption and discharge of evaporator.

$$\text{Evaporator and Distibution Pumping Loss} = \frac{\dot{m}_{ww} g h_{ww}}{\eta}$$

Warmwater Mass Flowrate $m_{ww} = 1401.450826$ kg/s
Warm Water Head Loss $h_{ww} = 3.5$m
Seawater Pump Efficiency $\eta = 85\%$

$$\text{Evaporator and Distibution Pumping Loss} = \frac{\dot{m}_{ww} g h_{ww}}{\eta}$$
$$= \frac{1401.450826 \times 9.81 \times 3.5}{0.85}$$
$$= 56.61\text{kW}$$

E. Coldwater Consumption Power Loss

This immobile loss is estimated built on water velocity and an identified factor for a bulging pipe entering, which is expected for cold-water inlet.

$$\text{Minor Head Loss(h)} = \frac{CV^2}{2g}, \text{where } V = \frac{Q}{A} = \frac{4\dot{m}}{\pi \rho D^2}$$

Head Loss Coefficient for Protruding pipe Entrance (C) $= 0.8$
Nominal seawater density (ρ) $= 998.2\text{kg/m}^3$
Coldwater pipe internal diameter (ID) $= 2$m
Mass Flowrate of Cold Water ($\dot{m}_{cw}$) $= 316.919$ kg/s

7. PUMP LOSS FACTOR

$$\text{Pump Loss Factor} = \frac{\dot{m}_{cw} g}{\eta}$$
$$= \frac{316.919 \times 9.81}{0.85} = 3.66\text{kW/m}$$
$$V = \frac{4\dot{m}}{\pi \rho D^2}$$
$$= \frac{4 \times 316.919}{\pi \times 998.2 \times 2^2} = 0.101 \text{ m/s}$$

$$\text{Intake Head Loss } (h_{intake})$$
$$= \frac{0.8 \times (0.101)^2}{2 \times 9.81}$$
$$= 0.00042\text{m}$$

Cold Water Intake Power Loss
$= P_{LF} \times I_{HL}$
$= \times 0.00042$
$= 1.54\text{W}$

The C_w consumption power loss was calculated as drop in power loss. The arrival may be rounded formed to decrease losses. The 0.8 coefficient is used for this characteristic bulging pipe' entry since the filter elements are unknown for this design.

C. Condenser and Feeding Pumping Loss

The static loss is estimated assumptions losses across the condenser and distribution pipe. The consistent Head Loss would be roughly 4.39m. the 4.39m of head accounts for the loss across intake and discharge of the condenser.
= Pump Loss Factor × Assumed Head
$= 3.66 \times 4.5 = 16.47\text{kW}$

D. Cold Water Pipe (CWP) Friction Loss

This variable loss is dependent upon the length of the Cold-Water Pipe (CWP), the pipe diameter and the inside surface. The factor is established by estimating pipe wall friction based on the smoothness of the pipe, pipe diameter and water velocity.

$$\text{Head Loss due to Friction } (h_f) = \frac{fLV^2}{2Dg}$$

$$\text{Head Loss due to Friction per unit Length } \left(\frac{h_f}{L}\right) = \frac{fLV^2}{2DgL}$$
$$= \frac{fV^2}{2Dg}$$

Hydraulic Pipe Diameter (D) $= 2$m
Velocity in pipe (V) $= \frac{\dot{m}_{cw}}{\rho A}$

$$= \frac{316.919}{1000 \times \frac{\pi(2)^2}{4}} = 0.1\text{m/s}$$

Colebrook Equation for Friction Factor (f)

$$\therefore \frac{1}{\sqrt{f}} = -2\log_{10}\left(\frac{\frac{\epsilon}{D}}{3.7} + \frac{2.51}{Re\sqrt{f}}\right)$$

Pipe Rougness Coeffient (ϵ) $= 0.0000$
Reynold'sNumber (Re) $= \frac{DV\rho}{\mu}$
Absolute Viscosity (μ) $= 1.573$Pa. s
Reynold'sNumber (Re) $= \frac{2 \times 0.1 \times 1000}{1.573} = 127.1455$

$$\frac{1}{\sqrt{f}} = -2\log_{10}\left(\frac{\frac{0.00005}{2}}{3.7} + \frac{2.51}{127.145\sqrt{f}}\right) \therefore f = 0.1497$$

$$\text{Head Loss due to Friction per unit Length } \left(\frac{h_f}{L}\right)$$
$$= \frac{0.1497 \times (0.1)^2}{2 \times 2 \times 9.81} = 0.0381 \times 10^{-3}$$

$$\text{Pipe Friction Loss} = \frac{h_f}{L} \times \text{Pump Loss Factor}$$
$$= 0.0381 \times 10^{-3} \times 3.66 = \frac{0.1396\text{W}}{\text{m}}$$

The heat and mass balance produced is shown on Figure 115. The flow rate of warm seawater -1401.450826 kg/s at 26 °C is brought thru a 2.5 m ID FRP pipe. The pipe has an intake depth of 25 m and is 130 m long. The turbine propeller pump supplies the evaporator with warm seawater mass flowrate of 1401.450826 kg/s. The pumping system puts the fluid into the chamber at the head of 3.5m from mean sea level (MSL). One submersible propeller-type pump brings 316.919 kg/s of cold seawater through a 2m pipe from a depth of 1000 m. The length of the pipe is 2590 m.
The evaporator spout flashes the warm water through into the evaporation chamber at a pressure of 3.3604 kPa. The slight amount portion (2.19 kg/s) of supply water is changed into

steam and the rest is discharged into the ocean at a temperature of 24°C. Steam (2.19 kg/s) from the evaporator enters the turbine at 3.1717 kPa and leaves the turbine diffuser system at 1.5985 kPa. The OTEC generator system generate the gross output of 206.186kW. the exhausted steam from the OTEC turbine go in the condenser. The condenser collects 316.919 kg/s of cold seawater at 4 °C and condenses 2.19 kg/s of the incoming steam.

TABLE 7.
SEA WATER PUMPS RATES.

Function	Warm water supply	Cold water supply	Warm water discharge	Cold water discharge
Flow rate (kg/s)	401.45	316.92	399	247
Total head (m)	1.4	3.6	3.2	5.4
Efficiency (%)	85	85	85	85

The function of the compressor on the system it pressurised all the particle that are not require on the system such as residual water and all gases that were dissolved on the solution.

TABLE 8.
VACUUM PUMP RATES.

Symbol	Quantity	SI
F_{cr}	Inlet flow rate	6.9 m^3/s
P_{cr}	Inlet pressure	1.2 kPa
D_p	Discharge pressure	101 kPa
P_{st}	Maximum power	40 kW

For the purpose of this project a generic calculation of net power was considered as per the concept calculated below. The net power generated is from OTEC plant is 98.186kW achieved subsequently deducting 108 kW for cold water supply pumping; 40 kW for warm water supply pumping; 38 kW for compressor; and 30 kW for fresh water pumping from the gross power generated. Table below present the out power produced.

$$NET\ POWER = Gross\ Power - ((Cold\ Sea\ Water\ Pump - Vacuum\ Pump - Warm\ Water\ Pump))$$

$$NET\ POWER = 206.186 - 40 - 30 - 38 = \mathbf{98.186\ kW}$$

7. CONCLUSION

South Africa is generally a water scarce country. This is particularly so on the South Coast of KwaZulu-Natal. In addition, the present problems faced by Eskom are mitigating against power hungry solutions such as r o desalination.
This paper proposes a solution to this problem by employing OC-OTEC to generate a self-powered solution.
for the provision of fresh water
It is shown that a 200kW pilot plant could generate up to about 100kW of electricity and also supply about 43000l of fresh water per day
Further work needs to be done to solve the large, low speed generator required but rapid advances are being made in this field and this problem will soon be overcome.

XVI. REFERENCES

[1]. Kahrl, William L. *Water and power: the conflict over Los Angeles water supply in the Owens Valley*. Univ of California Press, 1983.
[2]. Weedy, Birron Mathew, et al. *Electric power systems*. John Wiley & Sons, 2012.
[3]. Hossain, Abrar, et al. "Ocean thermal energy conversion: The promise of a clean future." *Clean Energy and Technology (CEAT), 2013 IEEE Conference on*. IEEE, 2013.
[4]. Kobayashi, Hiroki, Sadayuki Jitsuhara, and Haruo Uehara. "The present status and features of OTEC and recent aspects of thermal energy conversion technologies." *24th Meeting of the UJNR Marine Facilities Panel, Honolulu, HI, November*. 2001.
[5]. Bouwer, Herman. "Integrated water management for the 21st century: problems and solutions." *Journal of Irrigation and Drainage Engineering* 128.4 (2002): 193-202.
[6]. McMichael, Anthony J., et al. "Food, livestock production, energy, climate change, and health." *The lancet* 370.9594 (2007): 1253-1263.
[7]. LUIS A. VEGA, "Ocean Thermal Energy Conversion" Encyclopedia of Sustainability Science and Technology, Springer, August 2012 pp. 7296-7328
[8]. Vega, Luis A. "Ocean thermal energy conversion primer." Marine Technology Society Journal 36.4 (2002): 25-35.
[9]. Jeffs, Eric. Greener Energy Systems: Energy Production Technologies with Minimum Environmental Impact. CRC Press, 2012.
[10]. Dabestani, Maryam. "Energy Generation Using Ocean Thermal energy." *American Journal of Life Science Researches ISSN 2332-0206* 3.3 (2015).
[11]. Link, Harold F., and Brian K. Parsons. "Potential of Proposed Open-Cycle OTEC Experiments to Achieve Net Power." *OCEANS'86*. IEEE, 1986.
[12]. Kim, Nam Jin, Kim Choon Ng, and Wongee Chun. "Using the condenser effluent from a nuclear power plant for Ocean Thermal Energy Conversion (OTEC)." *International Communications in Heat and Mass Transfer* 36.10 (2009): 1008-1013.
[13]. Althof, J. A. "Direct-Contact Condensers for Open-Cycle OTEC Applications." (1988).
[14]. Bun Jian, Ooi, Chew Boon Cheong, and Khay Choong Chien. "Managing the transition of fossil fuels to renewable energy: application of ocean thermal energy conversion at Sabah." (2015).
[15]. Sea surface temperature around the world. (Available at: http://www.ospo.noaa.gov/data/sst/fields/FS_km10000.gif)
[16]. Lockheed Martin Mission Systems & Sensors (MS2), Ocean Thermal Extractable Energy Visualization, Lockheed Martin Corporation, DE-0002664, October 28, 2012.
[17]. Harrison, Sara. "Ocean Thermal Energy Conversion." Submitted as coursework for Physics 240, Stanford University, and November 28, 2010.
[18]. Da Rosa, Aldo Vieira. *Fundamentals of renewable energy processes*. Academic Press, 2012.

Gumede M. Author was born in Durban, South Africa on December 25, 1987. He graduates with a MEng Degree in Electrical Engineering from Durban University of Technology, Durban, South Africa in 2015. Since January 2017 is a student at Durban University of Technology pursuing DEng in Electrical Engineering. He is currently working for ZLM Project Engineering Pty, Ltd under Electricity Department as Managing Director. His main interests are in the area of renewable energy, especially ocean energy such as OC-OTEC, offshore wind and ocean current. He has published number of paper from international and national journal Mr. Gumede is a member of Engineering Council of South Africa (ECSA) and South African Institute of Electrical Engineers (SAIEE).

D'Almaine G.F was born in Durban, South Africa on May 30, 1950 was Senior Director in the Department of Power Engineering at the Durban University of Technology. He specializes in ocean energy and power systems both on grid and off grid, and is a director of the Real Time Power System Simulator at the university. Mr F. D'Almaine was a former SAIETE Member and past local Chairman SAARET.

186

The Extraction of Power and Fresh Water from the Ocean off the Coast of KZN utilizing Ocean Thermal Energy Conversion (OTEC) Techniques

M. Gumede*[1] and F. D'Almaine*[2].
[1]Durban University of Technology, Durban, 4001, South Africa
*Email: makhosonkegumede32@gmail.com
*Email: dalmaine@dut.ac.za

mailto:makhosonkegumede32@gmail.com

Abstract: This paper investigates the available data on thermal energy resource around KZN south coast region (Port Edward) which ultimately can be used for generation of electrical power and fresh water. The geographical location of this region is very suited to the development of renewable energy (Ocean thermal electrical conversion). OTEC is a promising renewable energy technology and has other applications such as the production of freshwater, seawater air-conditioning, marine culture and chilled-soil agriculture. The site of Port Edward is naturally suited for the establishment of alternate energy collection sources like OTEC. Since Port Shepstone lies just beneath the tropic of cancer and on the shore of the Indian ocean, the two important elements: constant sunlight and large coastal areas needed for OTEC can easily be found in this region, hence by experimental design we want to prepare an OTEC site for a new and original development.

Keywords: OTEC and open cycle

1. INTRODUCTION

The new technologies for the extraction of valuable ocean resources have become significant following the increased scarcity of other relatively cheap sources i.e. oil [1], [2]. Furthermore global warming has shown the disadvantage of using other fossil fuels such as coal [3], [4], [5]. Any alternative to coal fired power station in South Africa would lead to a large saving in carbon based pollution. Replacing the energy supply with a renewable energy source, such as OTEC, eliminates the pollution caused by fossil fuels and other problems associated with the use of fossil fuels to produce potable water.

A white paper emanating from the Department of Minerals and Energy indicates that the South African Government is committed to ensuring that renewable energy including wind, solar and ocean energy becomes a significant part of its energy portfolio. Considering the above and further categorizing ocean energy into its component parts viz. ocean currents, tidal currents, wave energy, thermal energy and energy derived from differences in salinity this paper examiners the ocean thermal resource.

According to L.A. Vega (2003), the amount of solar energy absorbed by the oceans in a year is equivalent to at least 4000 times the amount currently consumed on earth. For an OTEC efficiency of 3%, in converting ocean thermal energy to electricity, we would need less than 1% of this renewable energy to satisfy the world demand [6]. The aim of this research is to identify an optimum site (or sites) off the coast of KwaZulu natal suitable for developing OTEC generating station on the shore.

2. BACKGROUND

OTEC technology was developed and started in the 1880s. In 1881, Jacques Arsene D'Arsonval was the first proposed the harnessing of the stored thermal solar energy in the seas in France [7]. In 1930, Georges Claude's student of D'Arsonval tried to build the first OTEC plant open-cycle shore at Matanzas Bay-Cuba [8]-[9]. The system generated 22-kilowatt (gross) of electricity with a low pressure steam turbine [7]. In 1956, French researchers designed a 3 MW plant for Abidjan on Africa's west coast [7], [10]-[11]. The plant was never completed because of competition with low-cost hydroelectric power. In 1979, the Natural Energy Laboratory of Hawaii Authority (NELHA), start closed-cycle floating OTEC experimental plant. The system was producing 53 kW of gross power and 18 of net power. Hilbert Anderson and James (1962) they focused on increasing component efficiency. In 1967, these guys were originated their new close-cycle. In 1982, Toshiba and TEPC (Japans) contribute to the development of the technology [12].

NELHA (1993) installed an open-cycle OTEC plant at Kea hole Point, Hawaii, producing 50 kW of net power, surpassing the record set by the Japanese system (1982) [13]-[14]. A 210 kW (gross) open cycle shore based OTEC plant facility off the island of Hawaii was designed built and run successfully by NELHA (US) for a period of 6 years (1993-1998) by the US Government with a net power production of 100 kW [15]-[16]. This OTEC plant would also provide 1.25 Millions of Gallons per day of potable water to the base [8], [15], [17]. A private U.S. company has proposed to build a 10 MW OTEC plant at Guam. Lockheed Martin's

Alternative Energy Development team is currently in the final design phase of a 10 MW closed cycle OTEC pilot system which will become operational in Hawaii by 2012-2013 [18],[8]. This system is being designed to expand to 100MW commercial systems in the near future.

Table 1: OTEC Background theory

Year	Task	Year	Task
1881	D'Arsonval (France) conceived of OTEC	1982	Kyushu Electric Power Co. succeeded with 50KW of power at Kagoshima, Japan
1926	Claude (France) began research for commercial use	1985	Saga University completed 75KW of power plant
1933	Claude built power generating ship (1200KW)	1988	Inauguration of Organization of OTEC Study (Japan
1964	Anderson's proposal for a power generation in the sea	1989	Agency of Science and Technology (Japan) began study of utilization of Deep Sea Water (DSW) off Toyama in Japan Sea
1970	OTEC research results examined by the board of investigation into new power generation methods (Japan)	1990	IOA (international OTEC Association) was organized by Taiwan, USA and Japan)
1973	Saga University, Japan, commenced research study on OTEC technology-power generation	1993	210KW open cycle system completed in Hawaii
1974	OTEC research commenced as part of Sunshine project plan (Japan)	1994	Saga University constructed a new cycle plant
1974	ERDA project (USA) commenced	1995	Saga University started on testing new 4.5KW cycle plant (Kalina cycle, Uehara cycle)
1974	First international OTEC conference (USA)	1997	Signing of collaboration memorandum with National Institute of Ocean Technology (NIOT), India, on OTEC study
1977	Saga University succeeded with 1kw of power	2003	Saga University Completed 30KW multipurpose OTEC Plant in Imari, Saga, Japan
1979	Mini-OTEC (USA) succeeded with 50KW of power	2005	OPOTEC (Organization for the Promotion of the Ocean Thermal Energy Conversion) established in Saga, Japan
1980	Saga University performed experiments on the sea, off Shimane in Japan Sea	2013	A 1.25 MW OTEC power plant was built in Japan's Kumejima Island, which supplies 10% of the island's total electricity consumption
1981	Tokyo Electric Power Co., succeeded with 120KW of power on Nauru		

1. OCEAN THERMAL ENERGY CONVERSION SUMMARY

The ocean is world's largest solar collector. In tropical seas, temperature differences of about 20 °C- 25 °C may occur between the warm, solar-absorbing near-surface water and the cooler 500–1000 m depth 'deep' water at and below the thermocline [19]. Subject to the laws and practicalities of thermodynamics, heat engines can operate from this temperature difference across this huge heat store. The word ocean thermal energy conversion (OTEC) refers to the conversion of some of this thermal energy into convenient work for electricity generation. Specified sufficient scale of efficient equipment, electricity power generation could be sustained day and night at 200 kW_e from access to about 1 km^2 of tropical sea, equivalent to 0.07% of the solar input. Pumping rates are about 6 $m^3 s^{-1}$ of water per MW_e electricity production [20].

OTEC uses natural energy, CO2 and NOx are not exhausted and the control of the green energy house gas can be expected. Furthermore, OTEC is environment-friendly and semi-permanent energy source. On the other hand, a steady output is difficult to be obtained because of the change in water temperature through the season and a day [21]. Therefore, the thermal efficiency of the OTEC is rather low (about 5-6%) compared with commercial thermal plants (about 40-50%) [22].

The technology for energy mining is similar efficiency improvement in industry with superior flows of heated discharge, but on a much large scale. The attractiveness of OTEC is the seemingly infinite energy of the hotter surface water in relation to the colder deep water and its potential for constant, base load, extraction. However, the temperature difference is very small and so the efficiency of any device for transforming this thermal energy to mechanical power will also be very small. Even for heating, warm seawater cannot be spilt on land due to its high salt content. Moreover, large volumes of seawater need to be pumped, so reducing the net energy generated and requiring large pipes and heat exchangers. The following table below describe OTEC operation.

Table 2: OTEC operation theory

Resource	Transfer Function	Product
ΔT (0C)	Public Domain	kWh; H2O, AC
Ocean Volume	24/7	

AC= air conditioning, H2O = water, kWh = kilowatt-hour, m = meter, T = temperature.

The Open cycle (OC) OTEC controls vacuum pressure in the flash evaporator to vaporize warm surface seawater, rotates a turbine using the steam that is produced, and condenses the vapor at the same rate as the flash evaporation. A by-product of OC-OTEC is desalinated water, which is about 0.5-0.6% by volume of the input warm surface seawater [23].

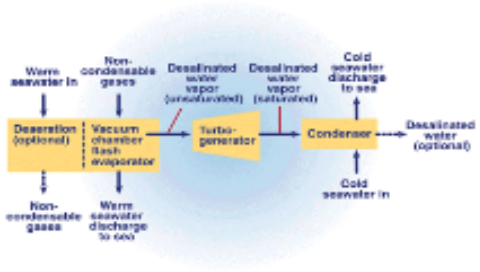

Figure 1: OC-OTEC Plant [6].

In 2012, Cornelia et al have done comparison study for the renewable energy supply options in the oceans, and the conclusion was that the OTEC route is the best fit for a scenario of high energy and carbon prices. Such expectations may afford competitive economic performance indicators in locations with no access to hydropower, or with high fuel costs for thermal power plants or fresh water demand [24].

2. RESEARCH DEVELOPMENT

OTEC has least environment impact and is capable enough to provide thousands of megawatt which are urgently required in developing countries [25]. OTEC usually incorporates a low- temperature Rankine cycle engine which boils a working fluid such as ammonia to generate a vapour which turns the turbine to generate electricity, and then is condensed back into a liquid in a continuous process.

Compared to other ocean energy technologies, OTEC has some advantages. It can provide continuous base-load power, and it can also provide fresh water for irrigation or drinking water and cold water for refrigeration. Resources for ocean thermal energy conversion are larger than for any other type of ocean energy. It is estimated that between 30000 and 90000 TWh/year of power are

extractable without having negative impacts on the thermal characteristics of the oceans [26], [27], and [28]. Main resources can be found in the area between 30° S and 30° N, which means in tropical seas. Figure 2.1 shows the temperature difference between water depths of 20 m and 1000 m, and the potential of areas showing a temperature gradient of more than 20° C.

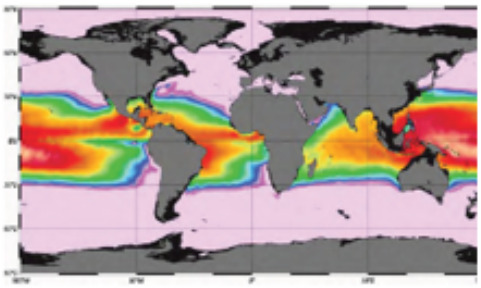

Figure 2.: Worldwide Average Ocean Temperature Differences between 20m- and 1,000-Meter Depths [29].

As the peoples of the world grown more prosperous, there will be a demand for higher quality food. Industry agriculture and commerce will require more fresh water. It is possible to use this resource to produce fresh water instead of producing electric power if there is a large ask for fresh water. The fresh water appearances when the cold water is put into contact with the vapour from the warm water stream in a large tank.

The vapours condense on the secondary heat exchangers, leaving the salt behind the warm water stream. The yield of fresh water from a 100-megawatt power plant would be approximately 33,000,000 cubic meter per year, comparable to a flow of a medium-sized river [30]. This is enough to support the city of Port Edward with water during a whole year. This water is completely salt-free, suitable for all agricultural, commercial, industrial and domestic uses.

3. AVAILABLE OCEAN POWER IN KZN SOUTH COST

The site of KwaZulu natal (Port Shepstone) is naturally suited for the establishment of alternate energy collection sources like OTEC. Since Port Shepstone lies just beneath the tropic of cancer and on the shore of the Indian ocean, the two vital elements: constant sunlight and large coastal areas needed for OTEC can easily be found in this region, hence by experimental design we want to prepare an OTEC site for a new and original development.

OTEC are abundant in southern parts of the case-study region that southern parts. The coast of KwaZulu Natal, the continental shelf is relatively close to the shoreline, approaching to within 3km in some places. More importantly, the steep drop in water depth up to 3000 metres can makes this worthy of research for ocean thermal energy conversion. Maritime maps of the coast of KZN indicate possible site where continental shelf is suitable close the shore. The University of Hawaii has tested this technology and a significant by-product of this process is fresh water [31] which could be interesting to a water-stressed country such as South Africa. Although

OTEC might be viable for KZN, it is known to be very expensive.

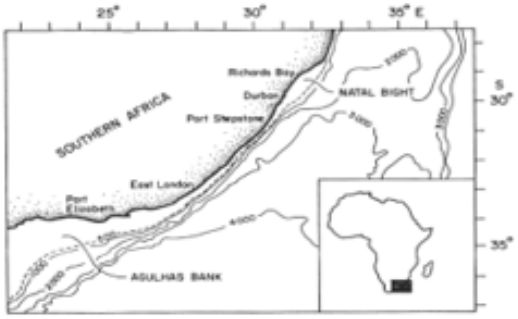

Figure 3: Map of Northern KZN coastline showing vicinity of 3000m depth contours to shore.

Surface waters are a combination of Tropical Surface Water from the South Equatorial Current, and Subtropical Surface Water from the mid-latitude Indian Ocean which regularly enters the Agulhas Current from the east at depths of between 150 m and 300 m. The surface waters are warmer than 20° C and of a lower salinity than the South Indian Ocean, Equatorial Indian Ocean and Central water masses present below. Conversely, the characteristics of surface water do vary due to isolation and mixing (Schumann, 1998). Water temperatures along the East Coast vary seasonally, and in relation to the distance offshore. The temperature increases offshore towards the centre of the Agulhas Current.

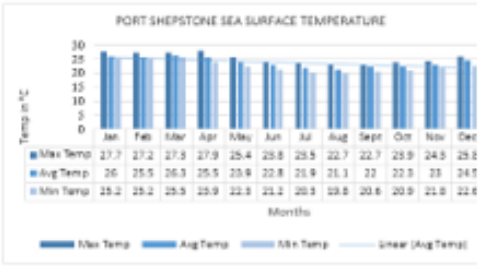

Figure 4: Port Shepstone sea surface temperature.

Gründlingh reported that seasonal variation (warmest in the Southern Hemisphere summer and coldest in winter) only occurs in the upper 50 m of the water column, with only insignificant variations occurring deeper down [32]. According to Schumann (1998), water temperatures within the Agulhas Current may exceed 25° C in summer and 21° C in winter, and are enduringly warmer than the water inshore and offshore of the Current. [33] Water temperatures also decrease with depth, with temperatures at 50 m below the surface being 4° C cooler than the surface in summer, and 1° C cooler in winter. Water under the current is, however, significantly cooler.

4. EFFICIENCY IN OTEC PLANT SITE

Equation 3 (Carnot's equation) was utilised to get an idea about the efficiency of OTEC. It is worth noting that while the temperature difference between the topmost and bottommost layers in tropical regions of the ocean is appreciable when compared with other ocean environments, it is still quite small. The ideal Carnot efficiency (η) for a heat engine operated with a heat source [34], [35].

$$\text{Carnot equation: } w = \frac{T - To}{T} \cdot Q \quad (3)$$

Here,
W - Work obtained (energy)
T - Surface water temperature (K)
To - The deep water temperature (K)
Q - Thermal value
Typical example for tropical climate:
T - 25 °C
To - 4 °C

$$w = \frac{(273 + 25) - (273 + 4)}{(273 + 25)} \cdot Q = \frac{21}{298} \cdot Q$$
$$= 7.\% \cdot Q$$

5. PRINCIPLE OF OTEC

OTEC is a heat engine with a low boiling point 'working fluid', e.g. ammonia, operating between the 'Cold' temperature *Tc* of the water pumped up from substantial depth and the 'hot' temperature,

$$Th = Tc + \Delta T_{water} \quad (1)$$

, of the surface

The working fluid circulates in a closed cycle, accepting heat from the warm water and discharging it to the cold water through heat exchangers. As the fluid expands, it drives a turbine, which in turn drives an electrical generator. The working fluid is cooled by the cold water, and the cycle continues.

Alternative 'open cycle' systems have seawater as the working fluid, but this is not recycled but condensed, perhaps for distilled 'fresh' water; the thermodynamic principles of the open cycle are similar to the closed cycle. In an idealized system with perfect heat exchangers, volume flow *Q* of warm water passes into the system at temperature *Th* and leaves at *Tc* (the cold water temperature of lower depths). The power given up from the warm water in such an ideal system is [36]:

$$P_e = pcQ\Delta T \quad (2)$$

6. OTEC ECONOMICS

The OTEC electrical power will be cost effective if the unit cost of power is comparable with other power plants such as wave, hydro and diesel [37]. Conversely, it is imperative that all capital costs and continuing maintenance or service costs are included so that the individual technologies are compared on a level playing field. Work carried out by [38] and his team in Hawaii has shown that for plants of the 1 MW range, the unit cost is considered comparable, see graph below.

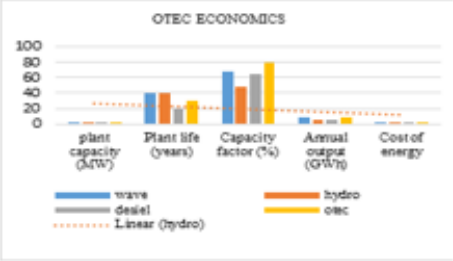

Figure 5: OTEC economics.

7. RESEARCH METHODOLOGY

In order to meet the objective of this research, the following technical approach will be evaluated:

- A site suitable for OTEC will be identified.
- Surface and sub-surface temperatures at this site will be measured over a period.
- A model of a suitable OTEC plant will be developed and simulated at DUT.

A physical small scale model will be built in the DUT laboratory and measurements will be compared with the simulation. A further step will be a pilot plant near Port Shepstone.

8. CONCLUSION

Fossil fuels will dry up in the near future, thus alternative energy sources have to be identified. OTEC power sources are gaining popularity across the world due to the demand of renewable energy. This report is aimed at presenting the proposal of OTEC on the KZN South Coast. Off the south coast of KwaZulu Natal, the continental shelf is relatively close to the shoreline, approaching to within 3km in some places. More importantly, the steep drop in water depth up to 3000 metres can makes this worthy of research for ocean thermal energy conversion.

9. REFERENCES

[1] Toossi, Reza. Energy and the Environment: Resources, Technologies, and Impacts. Verve Publishers, 2009.

[2] Tooke, Mike. Oil Peak–A Summary. April Retrieved 2 (2005).

[3] Szpunar, Carole Bryda, and Jerry L. Gillette. Environmental externalities: Applying the concept to Asian coal-based power generation. Argonne National Laboratory, Environmental Assessment and Information Sciences Division, 1993.

[4] Hall, D. O., and J. House. Biomass: an environmentally acceptable fuel for the future. Proceedings of the Institution of Mechanical Engineers, Part A: Journal of Power and Energy 209.3 (1995): 203-213.

[5] Hansen, Ulf. Technological options for power generation. The Energy Journal (1998): 63-87.

[6] Kobayashi, Hiroki, Sadayuki Jitsuhara, and Haruo Uehara. The present status and features of OTEC and recent aspects of thermal energy conversion technologies. *24th Meeting of the UJNR Marine Facilities Panel, Honolulu, HI, November.* 2001.

[7] Mario, Rupeni. *Ocean Thermal Energy Conversion and the Pacific Islands*. Energy Unit, South Pacific Applied Geoscience Commission, 2001.

[8] Khalid, Syed Shah, Zhang Liang, and Nazia Shah. Harnessing tidal energy using vertical axis tidal turbine. *Research Journal of Applied Sciences, Engineering and Technology* 5.1 (2012): 239-252.

[9] Ooi, Bun Jian, and Boon Cheong Chew. Managing the transition of fossil fuels to renewable energy: application of ocean thermal energy conversion at Sabah. (2012).

[10] Soerensen, Hans Chr, and Alla Weinstein. Ocean energy: position paper for IPCC. *IPCC Scoping Meeting on Renewable Energy Sources–Proceedings*. 2008.

[11] El-Dessouky, H., and H. Ettouney. Ocean thermal energy conversion. (2001).

[12] World Energy Council, Ocean Thermal Conversion, survey of energy resources 2004, chapter 16, 419-432, Elsevier.

[13] Harrison, Sara. Ocean Thermal Energy Conversion. Submitted as coursework for Physics 240, Stanford University, November 28, 2010

[14] Hurwood, David L. Ocean thermal energy: Potentials and pitfalls. *Ocean Development & International Law* 10.1-2 (1981): 13-40.

[15] Worzyk, Thomas. *Submarine power cables: design, installation, repair, environmental aspects*. Springer Science & Business Media, 2009.

[16] Vega, L. A., and Renewable Energy OTEC. Your in-depth source of information for Ocean Thermal Energy Conversion.

[18] Choby, Adam, et al. Graphite Foam Heat Exchangers for OTEC.

[19] Bose, Debajyoti. The Renewable Curiosity: A Review.

[20] Da Rosa, Aldo Vieira. *Fundamentals of renewable energy processes*. Academic Press, 2012.

[21] Nawaz, I., and G. N. Tiwari. Comparative analysis of conventional and renewable energy sources for a typical Indian village. *International Journal of Ambient Energy* 28.1 (2007): 3-14.

[22] TAHIR, Musthafah BIN MOHD, and Noboru YAMADA. Characteristics of small ORC system for low temperature waste heat recovery. *Journal of Environment and Engineering* 4.2 (2009): 375-385.

[23] Kim, Albert S., et al. Dual-use open cycle ocean thermal energy conversion (OC-OTEC) using multiple condensers for adjustable power generation and seawater desalination. *Renewable Energy* 85 (2016): 344-358.

[24] Vicente Fachina, Petrobras, Brazil Fresh Water from Ocean Thermal Energy OTEC matters: 2015

[29] LUIS A. VEGA, Ocean Thermal Energy Conversion Encyclopedia of Sustainability Science and Technology, Springer, August 2012 pp. 7296-7328

[30]Maria Bechtel and Erik Netz, Ocean Thermal Energy Conversion

[25] Winter, C-J., Rudolf L. Sizmann, and Lorin L. Vant-Hull, eds. *solar power plants: fundamentals, technology, systems, economics*. Springer Science & Business Media, 2012.

[26] Mario, Rupeni. *Ocean Thermal Energy Conversion and the Pacific Islands*. Energy Unit, South Pacific Applied Geoscience Commission, 2001.

[27] Khalid, Syed Shah, Zhang Liang, and Nazia Shah. Harnessing tidal energy using vertical axis tidal turbine. *Research Journal of Applied Sciences, Engineering and Technology* 5.1 (2012): 239-252.

[28] Ooi, Bun Jian, and Boon Cheong Chew. Managing the transition of fossil fuels to renewable energy: application of ocean thermal energy conversion at Sabah. (2012).

[31] Vega, Luis A. Ocean thermal energy conversion primer. *Marine Technology Society Journal* 36.4 (2002): 25-35.

[32] Harris, Thomas Frank Wyndham. *Review of coastal currents in Southern African waters*. National Scientific Programmes Unit: CSIR, 1978.

[33] Lutjeharms, JOHANN RE. The coastal oceans of south-eastern Africa (15, W). *The sea* 14 (2006): 783-834.

[34] Leff, Harvey S. Thermal efficiency at maximum work output: new results for old heat engines. *Am. J. Phys* 55.7 (1987): 602-610.

[35] Ceperley, Peter H. Gain and efficiency of a short traveling wave heat engine. *The Journal of the Acoustical Society of America* 77.3 (1985): 1239-1244.

[36] Gauthier, M.L. Golmen and D. Lennard 2001: Ocean thermal energy conversion (OTEC) and Deep Ocean water applications (DOWA). Market opportunities for European industry. IOA Newsletter Vol. 12, No. 1-2001, 1-5.

[37] Twidell, John, and Tony Weir. *Renewable energy resources*. Routledge, 2015.

[38] Mario, Rupeni. *Ocean Thermal Energy Conversion and the Pacific Islands*. Energy Unit, South Pacific Applied Geoscience Commission, 2001.

2016

ENGINEERING CONFERENCE

PROCEEDINGS

19-20 SEPTEMBER 2016 | **BOET TROSKE HALL**

BLOEMFONTEIN, SOUTH AFRICA

The Conference hosted jointly by the Department Electrical Electronic and Computer Engineering from the Central University of Technology, Free State, South African Institute of Electrical Engineers and Eskom is bringing together technicians, technologists, engineers and researchers in the field of Electrical Engineering to exchange ideas on research, latest innovations and developments in the field.

"Engineering for a better future:
Utilising our engineering innovations to solve the earth's challenges"

CONTACT PERSONS

Dr Ben Kotze: bkotze@cut.ac.za
Dr Frik Grobler: GroblerFA@eskom.co.za

Proposal of Open Cycle-Ocean Thermal Energy Conversion (OTEC) Plant from Ocean off The Coast of KZN

M. Gumede*[1] and F. D'Almaine[2].
[1]Durban University of Technology, Durban, 4001, South Africa
*Email: makhosonkegumede32@gmail.com
Email: dalmaine@dut.ac.za

Abstract: This paper investigates the available data on thermal energy resource around KwaZulu Natal, south coast region (Port Shepstone) which ultimately can be used for extraction of electrical power and fresh water. The geographical location of this region is very suited to the development of renewable energy Ocean thermal electrical conversion (OTEC). OTEC is a promising renewable energy technology and has other applications such as the production of freshwater, seawater air-conditioning, marine culture and chilled-soil agriculture. The site of Port Shepstone is naturally suited for the establishment of alternate energy collection sources like OTEC. Port Shepstone lies just beneath the tropic of cancer and on the shore of the Indian Ocean, the two important elements: constant sunlight and large coastal areas needed for OTEC can easily be found in this region. More importantly, the steep drop in water depth up to 3000 metres can makes this worthy of research for ocean thermal energy conversion in KwaZulu Natal (Port Shepstone). Hence by experimental design we want to prepare an OTEC (Open Cycle) site for a new and original development.

Keywords: Ocean Thermal Energy Conversion (Open Cycle).

ISSN: 2301-3656
IJOEE
International Journal of Electrical Energy
HTTP://WWW.IJOEE.ORG; EMAIL: IJOEE@EJOURNAL.NET

IJOEE Notification of Acceptance

http://www.ijoee.org/

Paper ID: JOE0060

Paper Title: Proposal of Open Cycle-Ocean Thermal Energy Conversion (OTEC) Plant from Ocean off The Coast of KZN

Dear M. Gumede and F. D'Almaine,

Sincere congratulations to you. It is a great pleasure to inform you that your paper listed above has successfully got through the peer-review, and the final revised paper will be published in IJOEE. Kindly note that this is subject to the receipt of Final Paper & Filled Copyright Form before March 30th, 2017.

IJOEE (International Journal of Electrical Energy) aims to provide a high profile, leading edge forum for academic researchers, industrial professionals, engineers, consultants, managers, educators and policy makers working in the field to contribute and disseminate innovative new work on Electrical Energy. All papers will be blind reviewed and accepted papers will be published quarterly by the IJOEE which is available online (free access) and in printed version.

IJOEE published papers will be indexed by several world class databases, such as EI (INSPEC, IET), Google Scholar, ET Library, Crossref, JournalSeek, *etc*. For more information, please visit the website http://www.ijoee.org/.

Please finish the following steps on time to guarantee your paper published on IJOEE successfully.

1. Revise your paper according to the review comments carefully.
2. Format your paper by following the Paper Template.
3. Fill out the Copyright Form. (Handwritten signature required)

The author's company or institution will be requested to pay a flat publication fee of USD 300 for an accepted manuscript regardless of the length of the paper. 250 USD for students, and 200 USD for reviewers of IJOEE. The publication charges are mandatory. In addition, translation paper undergoes professional language checking will be charged USD 20 per page (full paper).

Payment Terms

Credit Card Online Payment (VISA and Master card ONLY. No handling fees):

http://meeting.5upay.com/web/main.action?meetingId=188

(Please fill in the Journal Name "IJOEE" in the conference title and other important information, to make sure your registration is successful. Make sure you have VISA or Mastered Credit Card before clicking this link.

and you should also calculate the right amount and pay.)

IJOEE is an Open Access journal and all full texts of published articles are available online free of charge for everyone. Anyone who are interested in hardcopy subscription, please send us email if any further inquiries are needed.

Yours sincerely,

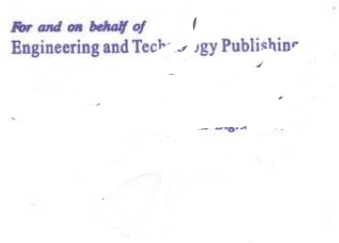

IJOEE Editorial Board